UNIVERSITY OF SOUTHAMPTON

FACULTY OF ENGINEERING AND THE ENVIRONEMENT

National Centre for Advanced Tribology at Southampton (nCATS)

Understanding the role of tribology in maintaining oral hygiene

by

Mahdiyyah Baig

Thesis submitted for the degree of Doctor of Philosophy

September 2018

UNIVERSITY OF SOUTHAMPTON

ABSTRACT

FACULTY OF ENGINEERING & THE ENVIRONEMNT

UNDERSTANDING THE ROLE OF TRIBOLOGY IN MAINTAINING ORAL HYGIENE

Thesis for the Degree of Doctor of Philosophy

by Mahdiyyah Baig

The importance of maintaining good oral hygiene is vital to a healthy body and aesthetically attractive smile. However, cleaning your teeth comes with a drawback. Toothpastes contain abrasive particles that have the potential to harm the tooth enamel resulting in wear. The aim of this project is to develop an understanding on the behaviour of abrasive particles in a toothpaste and how their impact and performance affect enamel wear. An integrated approach is employed in this study to investigate the delivery of abrasive particles to a tooth surface, using a Nylon toothbrush or ball, to understand how a polished surface with minimal tooth wear can be achieved.

To understand the interface of the tooth and the toothbrush, the microstructure, composition and mechanical properties of bovine enamel were visualised using Scanning Electron Microscopy (SEM) and nanoindentation. The filament properties such as tuft size and shape were analysed by metallographic preparation, SEM and optical microscopy respectively.

For a better understanding of the effects of tribology, tests on the TE77 high speed reciprocating tribometer were undertaken, using a load of 5N and a frequency of 4Hz. Wear depth, roughness data, groove width analysis and high speed friction was recorded using profilometric and measurement analysis. Tests were carried out with alumina, silica, spherical silica and control saliva slurries. The wear mechanism identified was 2-body grooving formed by microchipping, by abrasive particles embedded around the filament tips. Results showed that spherical silica produced the smoother surface (R_a 0.22µm) with the least amount of enamel wear. There was no measurable wear with the saliva test indicating the particles are causing damage. A higher coefficient of friction was reported for the saliva control slurry test compared to the particle tests. This could be due to the higher friction between hydrated enamel and the filaments as compared to hydrated enamel and the particles. The groove analysis of the 2-body wear scars showed grooves in the size range of the filaments and particles (12- 130µm). This indicated agglomeration on the filaments should be avoided to minimise wear on the enamel surface.

The relationship between the combined effects of particle shape/size and load on the volume loss, wear rates and wear mechanisms of enamel on the TE66 microabrasion rig were reported. A nylon ball was used and volume concentrations of 5% – 20% alumina, silica and spherical silica abrasives. Post experimental surface analysis was performed to analyse the wear scar morphology and groove analysis. Mono-sized particles as compared to bimodal. appeared to give the best outcome and least wear of enamel. The synergistic effects of bimodal particles vs. mono sized particles in toothpastes were quantified. A positive synergy existed for the alumina and silica synergy tests, indicating the bimodal particles were causing more wear than the mono-sized particles and contributing to the increased volume loss of enamel. The synergistic mechanisms were a combination of crushing and fracture of the enamel rods, followed by micro-chipping and removal of enamel. The magnitude and the distribution of the particle sizes is the most dominant factor in determining the levels of wear, with smaller particles and narrow distributions of the particle size reducing the magnitude of wear. The shape of the particles is another factor influencing wear, with the spherical tests generating lower wear rates than the angular tests. Load is an important variable

along with slurry concentration affecting the load per particle, with higher loads per particle resulting in greater wear. The factor which influences wear the least is the composition of the slurry.

Table of contents

List of tables

Table of figures

Declaration of Authorship

I, Mahdiyyah Baig

Hereby declare that the thesis entitled

UNDERSTANDING THE ROLE OF TRIBOLOGY IN MAINTAINING ORAL HYGIENE

and the work presented in the thesis are my own, and have been generated by me as the result of my own original research.

I confirm that:

1. This work was done wholly or mainly while in candidature for a research degree at this University;
2. Where any part of this thesis has previously been submitted for a degree or any other qualification at this University or any other institution, this has been clearly stated;
3. Where I have consulted the published work of others, this is always clearly attributed;
4. Where I have quoted from the work of others, the source is always given. With the exception of such quotations, this thesis is entirely my own work;
5. I have acknowledged all main sources of help;
6. Where the thesis is based on work done by myself jointly with others, I have made clear exactly what was done by others and what I have contributed myself;
7. Parts of this work has been published as:
    - Baig, M., Wood, R. J. K., Cook, R. B., Pratten, J, Gee, M, (2017) "Understanding the role of tribology in maintaining oral hygiene" BSODR.

Signature: Date:

Acknowledgements

بِسْمِ اللهِ الرَّحْمٰنِ الرَّحِيْمِ

First and foremost ٱلْحَمْدُ للهِ

Coming from a dental background into the world of engineering has been quite a journey!

I would like to sincerely thank and express a special appreciation to my supervisors Professor Robert Wood and Dr Richard Cook. I would like to thank you for your support, encouragement and guidance throughout my PhD, which has really helped me through. I am also thankful for the multiple revisions of my thesis. Robert, your hard work ethic (even on weekends) really inspired and motivated me during my PhD. Thank you for sending me useful articles and always getting the best out of me. For this, I am really grateful. Thank you for your perseverance and patience with me and for making the best analogies of my work. Your unique analogies really helped me perform better during the challenging times. It has been an honour and privilege to be one of your PhD students!

Thank you to my industrial sponsors, GSK and NPL. I would like to thank GSK for their financial support throughout the duration of my studies. Thank you to Dr Jonathan Pratten for your support in assisting the project and always being so jolly and a breath of fresh air in our meetings. You have always been willing to advise on all aspects of my project. It has been a pleasure to have you on board. Thank you for organising the industrial placement at GSK and giving me an insight into the industrial aspect of my project. A thank you also goes to Simon King who supervised me during my time at GSK and Lisa Glover who provided me with the spherical silica data. Thank you for organising inductions and talks with other GSK colleagues. Thank you to Professor Mark Gee and Dr John Nunn for my time spent at NPL and allowing me access to the NPL facilities.

A special thank you goes to Dr Terry Harvey for assisting me in the practical aspects of my project and for giving me good suggestions. I also would like to extend my thanks to Dr Liam Goodes and Dr Simon Dennington, it was sad to see you leave the supervisory team, but thank you for your invaluable input during my first two years. Thank you to Dr Rob Lucas at GSK for his input into the project and insightful chats during the first stages of my PhD and also to Dr Andrew Gant from NPL.

A thank you goes to the following people at the University of Southampton; Dr JB for help with micro-abrasion, Dr Timothy Kamps for his guidance on the TE77 rig and all the staff in the nCATS research group for their help and assistance during my project.

I thank all my family for all their duas. Without your duas, I would have never achieved this.

Southampton, you have truly been amazing. These four years have been the most happiest and testing times of my life. You will truly be missed!

Finally, my dadajee and dadijan, the light of my eyes. I know you would have been proud.

Nomenclature

Definitions and abbreviations

2-body	Abrasive wear mechanism. Observed as grooving.
3-body	Abrasive wear mechanism. Observed as rolling.
ASTM	American society for Testing and Materials (standard organisation)
B.D	Brushing direction
BSI	British Standard Institution (standard organisation)
CEJ	Cemento-enamel junction
CMC	Carboxymethyl cellulose
COF	Coefficient of friction
DEJ	Dentino-enamel junction (junction between enamel and dentine)
Enamel rods	Also known as enamel prisms. Primary unit of the enamel structure.
Erosion	Acid softening of enamel (not cavitation, sand/ rain erosion).
FFT	Fast Fourier Transform
FIB	Focused ion beam
GMP	Good manufacturing practice
GSK	GlaxoSmithKline
HA	Hydroxyapatite (coating)
HV	Vickers hardness
ISO	International standards organisation (standard organisation)
Mixed-mode	Abrasive wear mechanism. Observed as grooving and rolling.
Mohs scale	Hardness scale
NPD	New product development
NPL	National physical laboratory
RDA	Relative dentine abrasivity
REA	Relative enamel abrasivity
RMS	Root mean square

S.D	Sliding diirection
SEM	Scanning electron microscopy
SWR	Specific wear rate
TEM	Transition electron microscopy
PCR	Pellicle cleaning ratio
PEG	Polyethylene glycol
PMMA	Polymethyl methacrylate

Symbols

Degrees Celsius	$^{\circ}C$	$^{\circ}$C
Area	A	m^2
Diameter of the wear scar	b	m
Youngs modulus	E	GPa
Reduced Youngs modulus	Er	GPa
Frictional force	F	N
Hardness	H	GPa
Specific wear rate	K	m^3/Nm
Sliding distance	L	m
Density	ρ	g/cm^3
Arithmetic mean roughness	R_a	µm
Root mean square roughness	R_q	µm
Maximum profile valley depth	R_v	µm
Maximum roughness	R_z	µm
Synergy	S	%
Severity of contact	S_c	-
Time	t	s
Radius	r	m
Wear volume loss	V	mm^3
Volume per volume	v/v	m^3
Volume fraction of abrasives	υ	v/v

Units

µm	Micrometre
cm	Centimetre
g	Gram
GPa	Giga-Pascal
Hz	Hertz
m	Metre
mm	Millimetre
MPa	Mega-Pascal
ms^{-1}	Millisecond
N	Newton
nm	Nanometre
s	Second

1. Introduction

1.1 Background

Having clean teeth is an important aspect of health and attractive appearance. The most common method for maintenance of oral hygiene is tooth brushing using a toothpaste. Tooth brushing is used to disrupt bacterial biofilm on the surfaces of teeth and try to avoid the formation of advanced plaque. Dental plaque is a biofilm; it is a sticky colourless film that develops naturally on teeth and in-between teeth. Dental plaque is formed by colonising bacteria trying to attach themselves to the tooth's smooth surface. There is nothing that can be done to stop the growth of dental plaque. Daily brushing with toothpaste that contain abrasive particles is recommended to remove the build-up, Figure 1.1. If plaque is left alone it forms a hard yellow substance called tartar by mineralization. This substance can not be removed with regular brushing; it must be scraped away using special dental equipment.

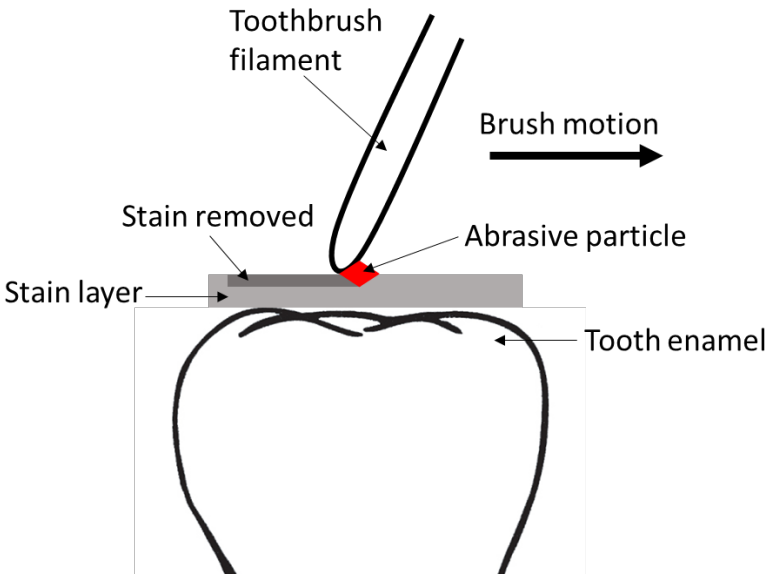

Figure 1.1: Stain removal on a tooth surface with abrasive particle

Many types of toothpastes contain abrasive particles that are harmful to the delicate tissues of the teeth. Wear produced in the mouth is a complex phenomenon with many underlying processes. In a toothpaste the abrasive particles in the slurry are free to rotate and translate between two surfaces in sliding contact. This is known as three-body abrasion. Brushing can also give two-body grooving abrasion, where the particles get trapped in the filaments and result in a two-body action [1].

Studies focusing on the wear of enamel are often avoided due to the hard nature of enamel and more attention is given to the wear of dentine. Previously, there have been investigations looking into different aspects of tooth brushing habits with toothpaste, however many of these tests do not successfully simulate the mechanical action of tooth brushing, or focus on enamel wear, rather dentine wear, due to the soft nature of dentine and ease in accounting for wear.

One of the main factors of importance to patients is the appearance of their teeth, such as the colour. 28% of UK adults were dissatisfied with the appearance of their teeth and 50% professed to discoloration issues. Extrinsic stains can form on the tooth surfaces and often appear yellow, black or brown on the tooth surface. Poor oral hygiene or the ability to control stain removal and the prevention of stain by a toothpaste can influence extrinsic stains [2].

The most commonly used abrasives in toothpastes are alumina and silica [3]. The main role of an abrasive agent is to remove extrinsic stains from tooth surfaces. A salivary pellicle layer, which is formed from proteins, is readily formed on the tooth surface after tooth cleaning. The pellide provides protection to the tooth surface against acid damage. However, a highly abrasive paste can remove the pellicle layer and expose the enamel surface. The ability of the filaments to trap abrasive particles, keeping them in contact with the tooth surface, will determine the extent to which tooth material is removed, as well as having an effect on the abrasive nature of the toothpaste. Factors such as particle size, particle shape, filament geometry, load and brushing technique all influence the ability of a particle to be trapped [2]. The enamel surface is easily abraded when hard particles with large asperities or sharp edges contact the surface under load [3]. The influence of acids also increases wear rates of the tooth structure [4]. Acid removal in dentistry is known as erosive wear [4]. Enamel exposure to acid results in softening of the outer enamel surface making it more susceptible to abrasive wear. Saliva is also an important factor to consider as it lowers the friction between contacting surfaces reducing wear of teeth [5]. During tooth brushing, these hard particles can cause the tooth surface to wear and be abraded.

1.1.1 GSK Spherical Silica

For the current project, GSK have provided a spherical version of silica. This version has been reported to reduce abrasion and show good performance when incorporated in toothpastes. The aim of the spherical silica being introduced into toothpastes is to reduce the abrasivity of the toothpaste, without compromising the cleaning ability. A small concentration of the abrasive is required to give a high cleaning effect, compared to a higher concentration of other morphologies of silica abrasive particles. Clinical in- house studies carried out by GSK show these results. Figure 1.2 shows the spherical silica cleaning performance. Pronamel and Pronamel Gentle Whitening are formulated GSK toothpastes. The Pronamel with 0.5% of the spherical silica (NP-30) shows an increased pellicle cleaning ratio (PCR), which is noted by the two asterisks. The spherical silica formulation with no abrasive shows that a relative dentine abrasivity (RDA) is achievable (noted by asterisk) [5].

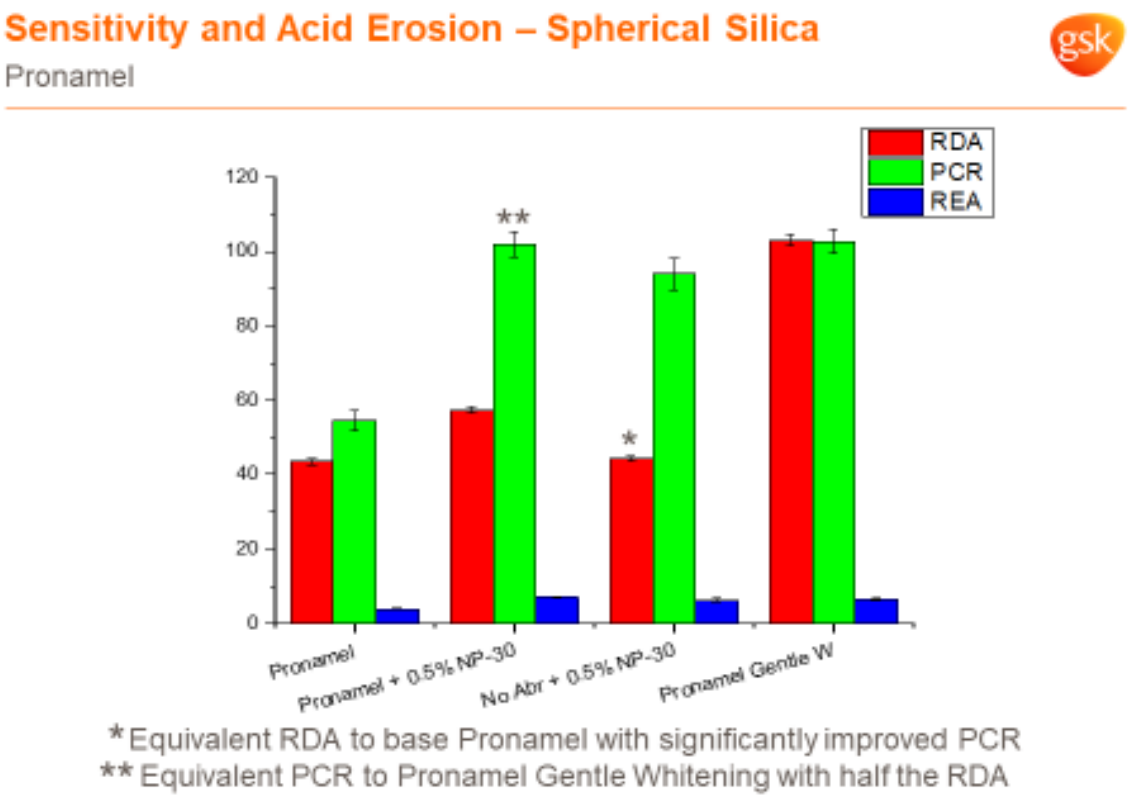

Figure 1.2: Abrasivity and cleaning performance of spherical silica formulation (based on Pronamel). Where RDA is the relative dentine abrasivity, PCR is the pellicle cleaning ratio and REA, is the relative enamel abrasivity [5].

A study carried out by Lewis et al. [6] focusing on the interaction between toothbrush and toothpaste particles during simulated abrasive cleaning, used a model process to visualise tooth cleaning. The abrasive used was calcite particles and PMMA was used as the test surface. Photography was used to study the process by which the toothbrush trapped the abrasive particles. It was concluded that a few filaments in the toothbrush caused the abrasive action of wear on a tooth surface [6].

A later study carried out by Lewis et al. [7] on particle motion and stain removal, analysed scratch patterns on a glass slide, using a linear reciprocating test rig. Loads in the region of 10 – 300g were used for loading and perlite particles incorporated in a water solution were used as the abrasive. It was concluded that perlite particles caused little counter-face damage [7].

A degree of abrasivity is required by a toothpaste to prevent and reduce the formation of extrinsic stains. This is due to the inability to remove stains by a low or non-abrasive toothpaste. However to prevent the removal of enamel, the abrasivity of a toothpastes should be moderated. Thus, toothpastes that maximize cleaning whilst minimizing hard tissue damage are being formulated by manufacturers [2].

To polish a tooth surface and create a lustre, a shine has to be given to the enamel. To achieve this, the abrasive agents in toothpaste have to be harder than the enamel surface. Biofilm has low hardness (HV) similar to that of dentine (~70 HV) [8] and can easily be removed with less abrasive agents contained in a toothpaste. However, many toothpastes contain harder abrasives such as alumina with a hardness of 2500 HV and silica with a hardness of 1200 HV to give a polished appearance to the enamel surface [1, 2]. The toothbrush also plays an important part in the wear process. The toothbrush acts as a carrier vehicle and can modulate or influence the abrasivity of the dentifrice. This, however, depends on characteristics of the toothbrush, such as the filament tip shape, the stiffness of the filaments, the type of toothbrush, the brushing method and the way the toothbrush is used.

One of the main concerns with enamel tooth wear is gingival recession and hypersensitivity of dentine [25]. Toothpastes have the potential to damage the hard tissues of the teeth, by the degree of abrasivity, which has also been recognised by the International Standard Organisation (ISO). The ISO published dental abrasivity standards, to design upper limits of abrasivity for toothpastes to avoid the enamel from wearing away [9].

The clinical treatment of oral hard tissues could be aided by understanding the tribological behaviours in the mouth. Few efforts have been made to understand the behaviours of oral tribology and dental wear. Many studies have been carried out of enamel after erosive attack and on dental restorative materials such as composites, however studies on friction and wear behaviour of human teeth are few. The wear mechanisms of teeth have a lack of understanding associated with them and this hinders the knowledge on the subject [10]. A very important point is that a conscious effort has to be made to simulate the oral environment and conditions as closely as possible in the mouth, otherwise the problem arises with in-vitro and in-vivo test results having a lack of correlation. For this reason, the apparatus used should be wear test machines which best replicate the conditions in the mouth [10].

It would really help the depth of knowledge if there was an universally accepted, reliable and efficient in-vitro tribological test method that would develop oral tribology, which this thesis addresses [10].

There is a demanding need and expectation from consumers for new toothpastes. The appeal to develop new toothpastes, to provide and improve the efficiency of the existing products is at an all-time high [2].

1.2 Aim

The aim of this PhD project is to investigate the interfacial science and the effects of delivering abrasive particles to a tooth surface.

1.3 Objectives and scope of research

The primary objective of this PhD is to develop a systematic understanding of enamel wear and combine factors such as the abrasive nature of particles, to help determine the most favourable conditions which result in a clean enamel surface, with minimal tooth wear.

The development of new and novel capabilities will make a significant contribution to the body of knowledge on enamel wear.

In order to achieve this, the interaction between the tooth, toothbrush and toothpaste has been investigated in detail. Characterisation of the bovine enamel, toothbrush filaments and abrasive particles has been established, Figure 1.3.

The main sub-objectives of this research are as follows:

- Obtain a better understanding of the science behind the interface of the tooth, toothbrush and toothpaste.

- To characterise the mechanical properties, hardness and Youngs modulus of the enamel, abrasive particles and toothbrush filaments.

- Use of the TE66 micro-abrasion rig to understand the systematic effect of particle shape and size on the wear mechanisms and volume loss of enamel.

- Understand the influence of load using three loads of 0.1N, 0.2N and 0.5N on the wear rate of enamel. To study the effects of a change in load on the wear transitions of enamel from grooving to rolling abrasion. Interpret wear maps and the severity of contact.

- Study the wear of enamel using slurries containing, alumina, silica, spherical silica and saliva. Undertake profilometric and scanning electron microscopy (SEM) analysis on the worn bovine enamel to understand the wear mechanisms and to quantify the roughness changes. Understand the influence of abrasive particles on the friction and wear characteristics of enamel.

- Investigate the mode of performance of abrasive particles in a toothpaste and the conditions of the abradant such as the size, composition and concentration that give a high polish to the enamel surface with minimal wear.

- Understand and attempt to quantify synergy between the mono-sized particles and the bimodal particles.

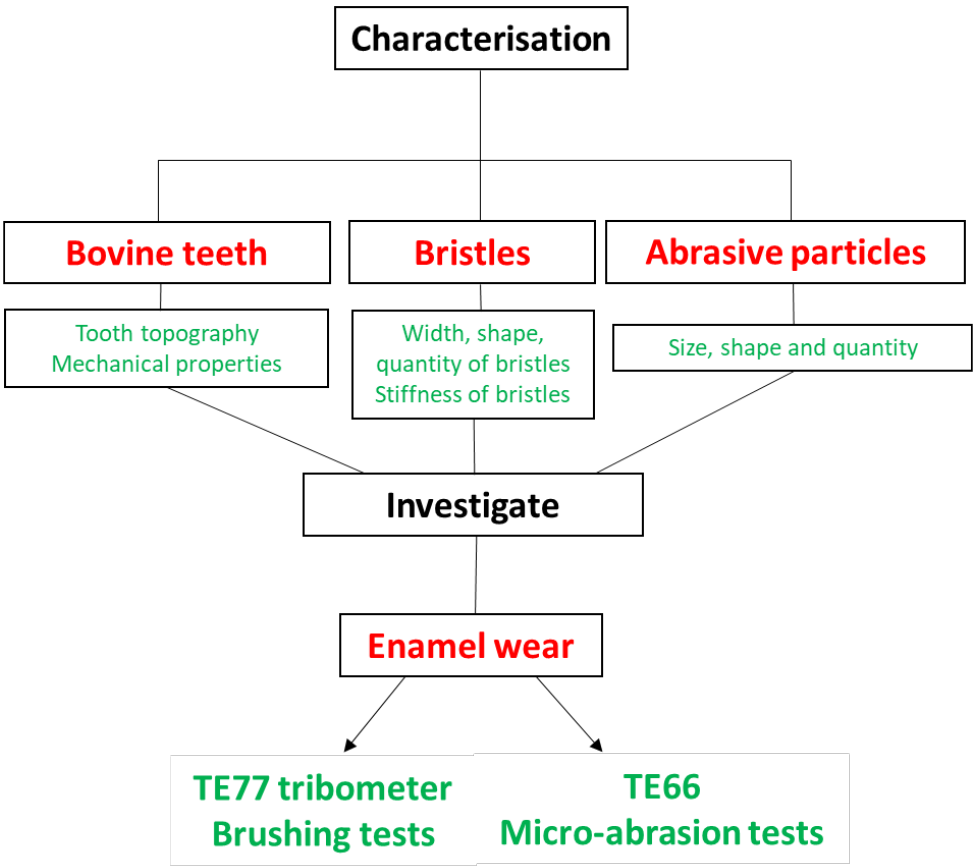

Figure 1.3: Main approaches taken in this thesis to develop an integrated understanding of tooth wear.

1.4 Thesis structure

Chapter 1 briefly outlines the background to the subject area, the concept of wear of enamel and the problems faced when the enamel is worn away. The aim and objective of the research project is laid out. This chapter also includes specific objectives of the current work and structure of the thesis.

Chapter 2 provides a thorough literature review where the relevant subject areas and the state of the art of the field are reviewed. The structure of a tooth, the different cleaning mechanisms of teeth, biofilm and plaque, the role of a toothbrush and toothpaste in tooth cleaning and the tribological processes involved in the mechanical action of tooth brushing are outlined. It also provides an evaluation of previous studies that have been carried out.

A description of the materials and the experimental techniques are presented in chapter three. The characterisation of the tooth topography, filament tip geometry and the abrasive particle sizes are illustrated in this chapter.

The experimental results obtained in this work are covered in chapters 4, 5, 6, 7 and 8. The first section of chapter 4 describes the microstructural characterisation and mechanical properties of the bovine enamel discs and the Tek Pro® firm filaments.

Chapter 5 presents the first of the micro-abrasion tests understanding the influence of particle shape and size on the volume loss of enamel. Mono-sized and bimodal sized particles will be studied. The effects of synergy were analysed.

Chapter 6 studies the effect of load on the specific wear rate of enamel using loads of 0.1N, 0.2N and 0.5N. Results were compared and the severity of contact was studied in detail. The wear was observed by optical and SEM microscopy and the groove sizes were measured.

Chapter 7 presents the TE77 high speed reciprocating tests and details the results of the brushing tests with abrasive slurries. Roughness data was reported. High speed friction data was analysed and the groove widths were reported. In depth investigation of the wear scar was carried out.

Chapter 8 will discuss the main findings from this study and combine all the factors contributing to enamel wear. The chapter will bring together aspects of the TE66 micro-abrasion tests and the TE77 brushing tests. An analysis of the groove width will take place and synergy will be discussed in detail. All the results will be correlated and similarities between the tests will be reported.

Chapter 9 summarises the main conclusions from this study and the novel contributions added to the existing body of knowledge. The last section of chapter 9 will be dedicated to describe the future work plans.

1.5 List of publications and work presented

Below are a list of publications, oral presentations and posters presented as part of the research:

List of publications:

- Baig, M., Wood, R. J. K., Cook, R. B., Pratten, J, (2018) "The effect of micro-abrasion on enamel using abrasive slurries" (pending submission BioTribology Elsevier journal)

- Baig, M., Wood, R. J. K., Cook, R. B., Pratten, J, Gee, M, (2018) "Wear of enamel during simulated tooth brushing using alumina and silica abrasive slurries" (pending submission)

- Baig, M., Wood, R. J. K., Cook, R. B., Pratten, J, Gee, M, (2017) "Understanding the role of tribology in maintaining oral hygiene" BSODR.

Oral presentations:

- 4th International conference on BioTribology, Montreal. Canada, 26-29 September 2018.

- 73rd STLE annual meeting and exhibition, Minnesota, U.S.A., 20 – 24 May 2018.

- 26th Mission of Tribology Research, IMechE, London, U.K., 14 December 2017.

- BSODR, British Society for Oral and Dental Research annual meeting, Plymouth, U.K., 6 – 8 September 2017.

- GSK Science Symposium, annual meeting, Weybridge, U.K., 11 – 12 October 2017.

- GSK Science Symposium, annual meeting, Weybridge, U.K., 12 – 13 October 2016.

Poster presentations:

- "The effect of micro-abrasion on enamel using abrasive slurries" 96th General Session and Exhibition 'International Association of Dental Research (IADR)', London, U.K., 25 – 28 August 2018. *Richard Cook presenting on my behalf.

- "The effects of toothbrusing on the wear of dental tissues" 13th Tribo –UK conference 'Tribology in the next decade', University of Leeds, Leeds, U.K., 14-15 April 2016.

- "The effects of toothbrusing on the wear of dental tissues" GSK science symposium, Weybridge, U.K., 30-1 September/October 2015.

- "Tribology of teeth cleaning" Tribo-UK conference, Loughborough University, Loughborough, U.K., 16-17 April 2015.

Industry internship:

- GSK, Weybridge, U.K., 18– 27 September 2017.
  Toothpaste formulation (batches created for testing), marketing insight, formulation laboratory training, Good Manufacturing Practice (GMP) induction, New Product Development (NPD) induction and tour.

2. Literature review

2.1 Structure of a tooth

The tooth comprises two major areas; the crown and the root. Enamel covers the crown and cementum covers the root portion. The cemento- enamel junction (CEJ) joins the crown and root together. The gum tissue which is referred to as the gingiva only covers the cervical third of the crown, Figure 2.1 [11]. There are four tooth tissues that make up the tooth. These are the enamel, dentine, cementum and the dental pulp, Figure 2.1. The hard tissues are enamel, dentine and cementum. The pulp is composed of soft tissue [11]. The root is part of the tooth which is below the gum line. The root is not visible, although it can be exposed by overzealous tooth brushing and toothbrush abrasion. The alveolar bone firmly holds the tooth in place in the jaw, Figure 2.1 [11].

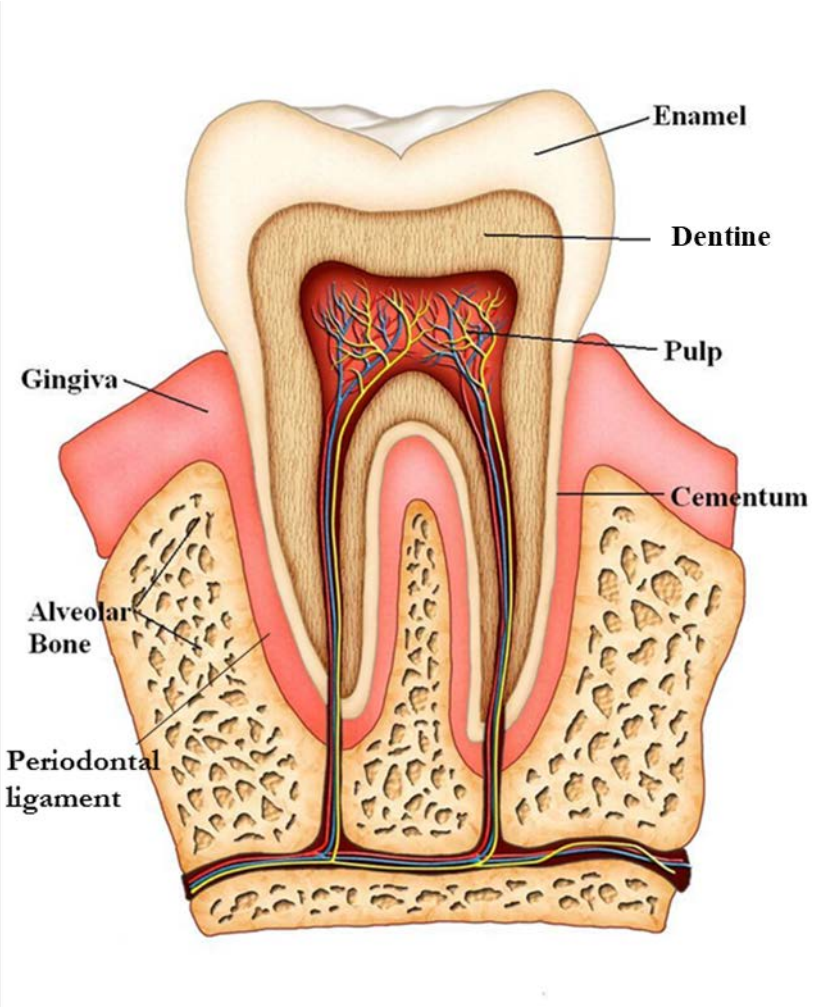

Figure 2.1: The structure of a tooth [12].

Enamel is the hardest tissue in the human body and is formed by epithelial cells called ameloblasts. It is composed of 96% organic material and 4% inorganic material. The microstructure of enamel is anisotropic and its mechanical properties are influenced by the orientation (location and arrangement) of the rods. Enamel is composed of rods (also referred to as prisms), which are the primary unit of the enamel structure. The enamel rods lie perpendicular to the tooth surface and have a length of 6-8 microns and a width of 5µm. The enamel rod is made up of a head and a tail which resembles a key-hole shape. Hydroxyapatite crystals make up each rod, Figure 2.2. The chemical formula of the hydroxyapatite crystals is: $Ca_{10}(PO_4)_6.(OH)_2$. The hydroxyapatite crystals are fibre-like structures which are 100nm – 500nm in length, 60nm in width and 30nm in thickness [13]. The hydroxyapatite crystals are aligned parallel to the long axis of the rods. The rods are perpendicular to the dentinoenamel junction (DEJ) and run from the dentinoenamel junction to the surface of the tooth.

Debate has arisen on the formation of the enamel rod. However, it has been reported that 3-4 ameloblasts form one rod. Fibres and a matrix are laid down by the ameloblasts and the matrix is deposited with hydroxyapatite crystals. The early deposit of hydroxyapatite crystals in the rod is referred to as the mineralisation stage of the enamel rod. The maturation stage is the second stage of calcification of the enamel rod and this is when the hydroxyapatite crystals grow and form a tightly packed structure [11].

An organic interspace is present between the enamel rods, which is called the rod sheath [14]. The rod sheath, is a thin layer of protein made up of 1% – 2% organic matter which surrounds and cements each rod [14]. The rod sheath is also referred to as an *interrod substance* or interrod enamel [11]. The thickness of enamel is in the region of 2.5mm.

A study conducted by Cuy et al. [15] reported the mechanical properties of enamel are influenced by the chemical composition, mineralisation and the location/ arrangement of the rods. The highest hardness of enamel was observed at the surface of enamel, with a hardness of 4.6GPa and a modulus of 91.9Gpa respectively. Moving away from the DEJ, this decreased to 3.4GPa for the hardness and 66.2GPa for the modulus. This finding was confirmed by Roy et al. [16] who reported a hardness value of enamel to be 3.5GPa at the surface and a drop in hardness to 2GPa – 2.5GPa, 100µm – 600µm away from the DEJ.

Nano-indentation was carried out on the rods of enamel. A number of studies [17-20] reported the head of the rod to differ in hardness to the tail. The head of the rod had a hardness of 5GPa – 7GPa compared to 4 GPa for the tail of the rods [19].

Age of the tooth is another contributing factor to the difference in mechanical properties of enamel. It was found by Park et al. [21] that a higher hardness and elastic modulus of enamel was reported for an old permanent tooth compared to a young tooth. An explanation for this could be the reduced organic content and increased mineral content with age of tooth.

Zhou et al. [20] carried out nano-scratch tests on a longitudinal section of human enamel. The scratch tests were carried out on the parallel and vertical axis of the enamel rod, at loads of 20mN, 50mN and 100mN to investigate the orientation effects of the enamel hydroxyapatite crystals. At a load of 5mN no pile up of enamel was observed. Increasing the load to 20mN resulted in slight pile up of enamel and at 50mN there was evidence of pile-up at the sides of the enamel scratch. The hardness and elastic modulus of interrod enamel, was found to be lower than the hardness and elastic modulus of the enamel rod and thus showed a lower wear resistance. The tests showed scratching the enamel surface caused the hydroxyapatite crystals to be broken into smaller crystals [20].

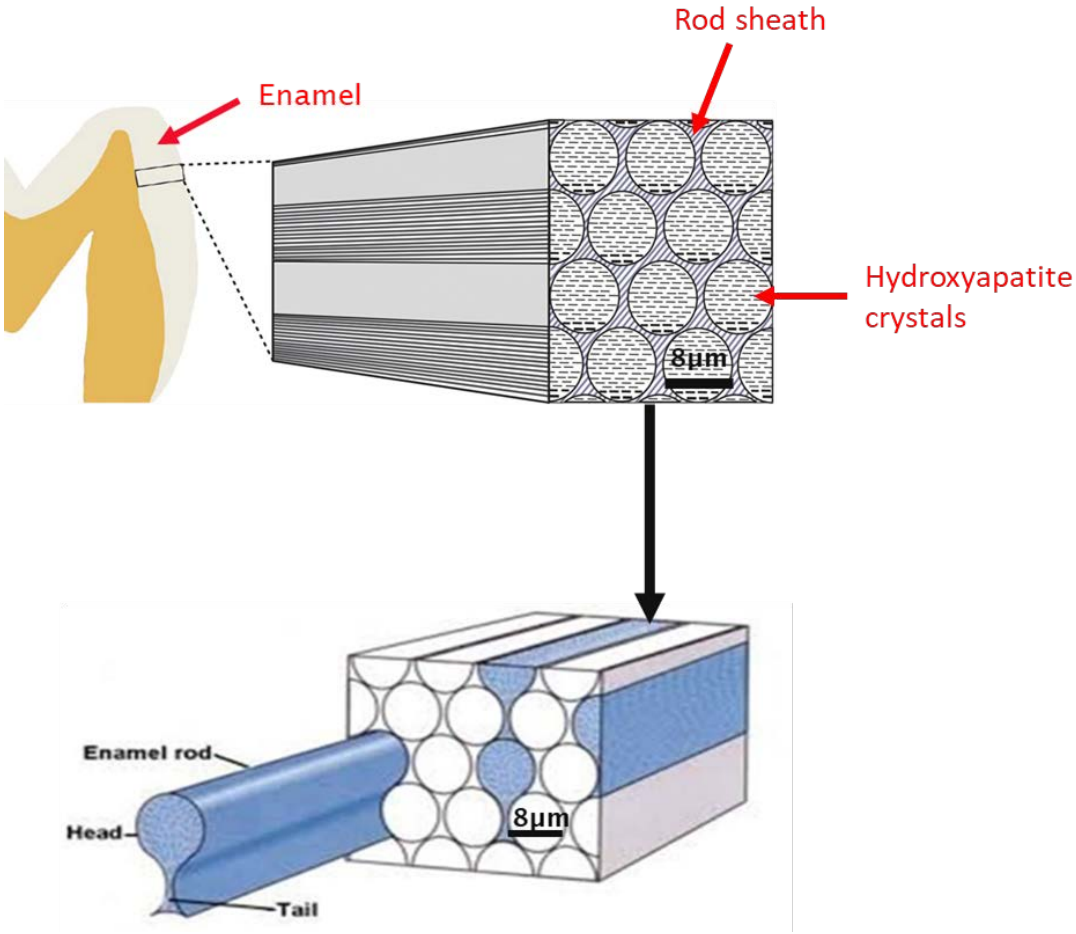

Figure 2.2: Schematic of enamel rods. Adapted from [22, 23].

The mechanical properties and structure of enamel and dentine are shown in Table 2.1 and Table 2.2.

Underlying the enamel, a dense, protein-rich layer called dentine exists. Dentine is softer than enamel and it is formed by odontoblast cells [14]. It is composed of 70% inorganic material and 30% organic material. The inorganic material contains hydroxyapatite crystals, which measure 20nm in length and 3nm in width. Dentine contains tubules which run to the pulp of the tooth. The tubules are filled with dentinal fluid, which provides nutrients to the pulp [11].

Table 2.1: Mechanical properties of tooth tissues.

	Enamel	**Dentine**
Density / kg/m³	2500 [1, 24, 25]	2900 [1, 25, 26]
Young's modulus / GPa	62.7 - 98.3 GPa [1, 25, 27]	24.8 GPa [1, 25, 27]
Compressive strength / GPa	0.095 – 0.386 [1, 25]	0.249 – 0.315 [1, 25]
Tensile strength / GPa	0.030 – 0.035 [1, 25]	0.040- 0.276 [1, 25]
Poisson's ratio	0.29 [1, 25]	0.11 [1, 25]
Hardness	283- 374 HV [1, 28]	53 – 63 HV [1, 28]

Table 2.2: Tooth structure information.

Dental tissue	**Enamel**	**Dentine**
Composition	96% inorganic material 4% organic material and water [1]	70% inorganic material 30% collagen and water [1]
Microstructure	Enamel rods, enamel rod sheath [12]	Dentine tubules, peritubular dentine, intertubular dentine [12]

2.1.1 Demineralisation of enamel

Organic acids are produced when bacteria metabolise fermentable carbohydrates and sugars in plaque formation, which cause the dissolution rate of hydroxyapatite to increase. Demineralisation of enamel takes place following the formation of H^+ ions by dissociation of acids. This can result in a reduction of pH to below 5.5. Calcium and phosphate from the tooth surface are dissolved during the demineralisation process, Figure 2.3 [29]. The subsurface of enamel undergoes a process where the hydroxyapatite crystals are dissolved, leading to tooth decay. The process of demineralisation can be reversed, providing that neutralisation of the acidic biofilm takes place.

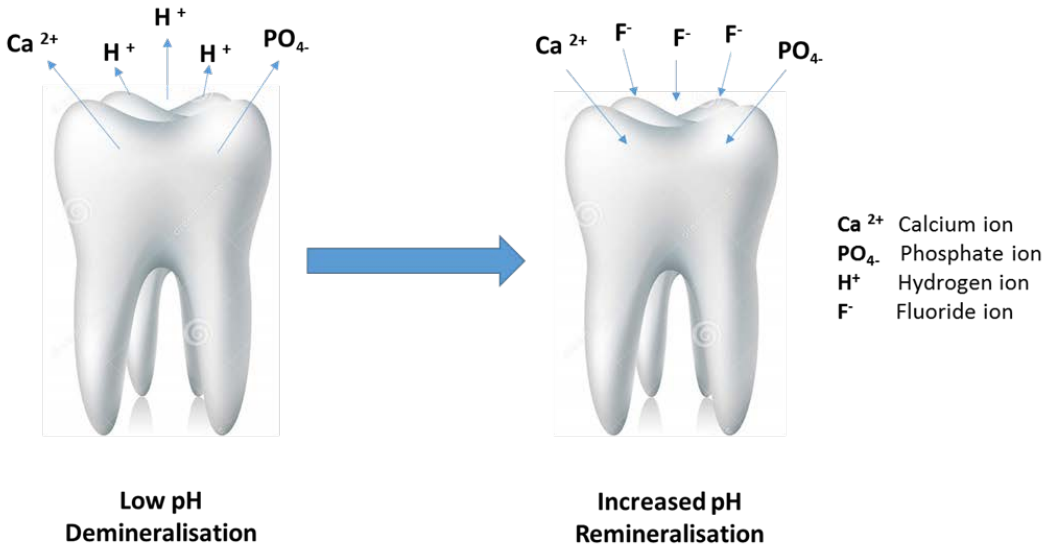

Figure 2.3: Demineralisation and remineralisation process of a tooth. Adapted from [30].

The tooth surface can undergo a natural repair process which relies on calcium and phosphate ions from the saliva; this is called remineralisation, Figure 2.3.

Saliva is crucial in restoring a neutral pH to the biofilm; it provides calcium and phosphate to the enamel surface and also acts as a buffering agent. To maintain a healthy body, a supply of saliva is needed. Saliva serves many functions of the body such as aiding mastication, protecting the tooth enamel, preventing decay caused by biofilms, and minimising wear of the tooth surfaces by providing a thin film of lubrication. Human saliva consists of approximately 99% water with the remaining 1% being proteins in the form of electrolytes (potassium, calcium, sodium), enzymes, white blood cells, mucus, immunoglobulins and antimicrobial agents [31].

Using artificial saliva substitutes is acceptable for wear tests, as the interaction of artificial saliva with the bovine tooth tissues, is that which would normally take place in the mouth, however it must not be overlooked that human saliva is very difficult to reproduce and serves many complicated biological processes in the mouth. Many wear tests carried out [32-35] have used artificial saliva as a substitute for their tests and it has proved very successful. The main artificial saliva substitute that has been used is one complying with Fusayama- Meyers method. There are many adaptions to this method, however an updated method by Licausi et al., which uses Fusayama's as a base closely resembles human saliva, Table 2.3 [32].

Table 2.3: Adaption of Fusayama – Meyer's artificial saliva. Composition of artificial saliva, which closely resembles natural saliva [33].

NaCl Sodium chloride	0.4g
KCl Potassium chloride	0.4g
$CaCl_2$ Calcium chloride	0.6g
$Na_2HPO4.12H2O$ Sodium dihydrogen phosphate dodecahydrate	0.58g
CH_4N_2O Urea	1g
H_2O Distilled water	1L
pH	6.5

A fluorinated dentifrice (toothpaste) can also be used to remineralise the tooth surface. Due to fluoride being highly reactive, it can react with the dissolved enamel crystallites resulting in crystallite re-growth. Fluoride can react with dissolved calcium and phosphate to remineralise acid softened enamel with fluoroapatite, which is less soluble than calcium hydroxyapatite [36]. For remineralisation to take place a pH of 7.5 – 8.5 has to exist in the oral cavity. A new surface is rebuilt on the enamel crystal structure. The new remineralised crystals are tougher and are less prone to acid attacks [37].

Under erosive conditions, acids act on the enamel surface. The outermost enamel surface undergoes mineral dissolving. This is called erosive demineralisation. Bulk tissue loss can occur when the mineral is dissolved layer by layer [38]. Physical impacts such as biting on hard objects (bottle caps, nails) will affect the enamel surface due to the loss of mineral on the enamel surface. This will result in a loss of micro hardness, depending on the severity of the erosive attack. Physical impacts will wear enamel more easily [38]. For example, the action of tooth brushing and the abrasives in dentifrices can cause abrasion to the eroded enamel surface. Table 2.4 shows the operating environment conditions which cause abrasion. The erosive agent can cause the crystallites of enamel to become weak. Abrasion can be observed on the oral hard tissues by friction. This occurrence poses a problem during toothbrusing using an abrasive dentifrice.

Finke, et al. [39] investigated the effects of 250ml of orange juice on the hardness of human enamel over 10 minute periods at selected time intervals, using nano-indentation. It was found the hardness of enamel decreased from 3.02GPa to 1.21GPa after exposure to orange juice [39].

Another study carried out by Attin et al. [40] investigated the effect of carbonated drinks on bovine enamel. Bovine enamel samples were immersed in 10ml of the drink for 1 minute, 5 minutes and 15 minutes. It was found that the hardness of the samples decreased with an increase in exposure time, with a 30% reduction in hardness value after 15 minutes of exposure to the drink. There was a change in hardness from 3.05GPa to 2.12GPa after the 15 minute treatment time [40].

Wongkhantee et al. [41] determined the effect of acidic drinks on enamel. The enamel samples were immersed in 32.5ml of acid and artificial saliva for a total soaking time of 100s. After the acidic treatment there was a change in hardness from 2.71GPa to 1.72GPa. The acid softened the enamel and reduced the surface hardness [41].

Table 2.4: Operating environment conditions which cause tooth wear.

	Operating environment	
	Bio-environment	**Mechanical**
Source	• Sweet, sugary foods, candy, sweet drinks • Acidic foods (oranges) and carbonated drinks [42]	• Tooth brushing • Grinding Using teeth to: • Remove bottle tops • Remove hard nails • Hold pins [42]
Consequences	• Acid produced by bacteria – decay, demineralisation, loss of enamel [43]. • Acid (not from a bacterial source) – erosion, loss of tooth structure.	• Abrasion. Loss of tooth structure • V- shaped notches at the cervical region of teeth [44].

2.2 Biofilm

2.2.1 Development and build up

A biofilm can be defined as a community of microbial cells in the oral cavity, which are embedded in an extracellular polymeric matrix [45]. An important role is played by the accumulation of dental plaque biofilms in the development of gingivitis, caries and periodontitis. Dental biofilms contain many species of bacteria such as streptococci bacteria, including S. mutans, S. oralis, S. sanguis, S. mitis, and Actionomyces israelis and Corynebacterium species. They reside in a microenvironment which is influenced by the ecological relationships that exist between microorganisms. Nutrients within the oral environment are utilized by biofilms, predominantly external dietary carbohydrates from ingested food [45] .

Tooth enamel is made up of 96% hydroxyapatite, which is a mineral. The dissolution rate of the hydroxyapatite is increased when bacteria release acids, resulting in low acidic levels in the oral cavity [46]. The inorganic component of enamel is hydroxyapatite, and the acid decalcification of this material initiates dental caries formation. As this process occurs, the enamel protein is degraded by an enzymatic degradation process. The enamel and dentine of the tooth are destroyed by cariogenic bacteria which invade the tooth and result in cavitation [47]. The development of caries is accelerated by the low acidity in the oral environment. This in turn causes an increased

rate of demineralisation of enamel. The fermentation of dietary sugars causes acid production and allows aerobic and anaerobic niches to form and thus develops the biofilm ecosystem progressively and may further reduce the pH in anaerobic areas.

The role of plaque accumulation is well established. Dental plaque is a type of biofilm that forms on teeth, Figure 2 4. Bacteria in the presence of a natural aqueous environment such as saliva adhere to surfaces of teeth to form biofilms. When plaque builds up on teeth, the acid released can cause the tooth surface such as enamel to break down. Once the enamel is broken down and cavities have formed, the acid can then target dentine [37].

Plaque accumulates on teeth and gums, which can lead to serious health complications like periodontal diseases, as well as dental caries. Biofilm removal is the basis of prevention and treatment of dental disease. Tooth brushing is the most widely used method for biofilm removal and control: a good standard of regular oral hygiene needs to be practised, in order to control the formation and progression of dental plaque biofilms. The type of toothbrush, dentifrice, and conditions used have an effect on plaque removal rates, as will be explored in the remainder of this literature review [48].

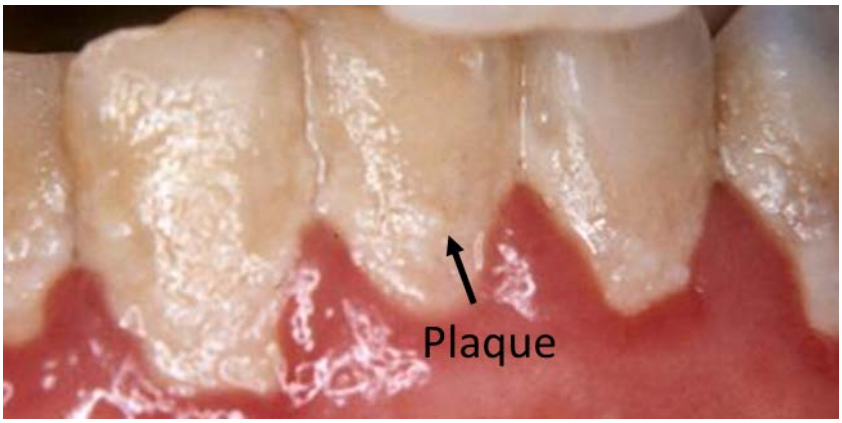

Figure 2 4: Accumulation of dental plaque on teeth [49].

Dental caries, periodontitis and gingivitis are caused by oral biofilms, which are very complex in nature. Salivary phosphoproteins are the first to attach to teeth, within seconds of cleaning the teeth. The clean tooth is bacteria-free, although proteins and bacteria remaining within the oral cavity will immediately adhere to the surface, Figure 2.5. This is due to the high affinity of bacteria to hydroxyapatite [45]. Organic molecules are transported faster to the tooth surface than bacterial

cells. The conditioning film on tooth surfaces precedes the formation of biofilm. Another term used for the thin conditioning film is the 'acquired enamel pellicle'. The acquired pellicle's formation is governed by van der Waals forces, hydrophobic interactions and ionic interactions. The properties of the tooth surface are influenced by the pellicle. It assists in the interactions between the surface of the tooth and the bacteria and oral fluids [45, 50].

The initiation of dental plaque biofilms is caused by an early coloniser of the surface of the tooth, Streptococcus mutans, which is gram positive and anaerobic [38]. S. mutans causes tooth damage by producing acid in the presence of sugars and carbohydrates as a by-product of the fermentation process [51].

Adhesion–receptor interactions allow bacteria to adhere to the pellicle. Co-aggregation and quorum sensing, the process by which bacterial communities communicate and determine optimal adhesion sites, allow the plaque to mature, Figure 2.5. The increasing species diversity of bacteria plays a part in the maturation process of dental plaque [8]. If the bacteria is left to develop, the plaque eventually turns into a hard yellow substance called tartar, Figure 2.6 [50]. Tartar has a hardness of 0.20 – 0.40 GPa [52].

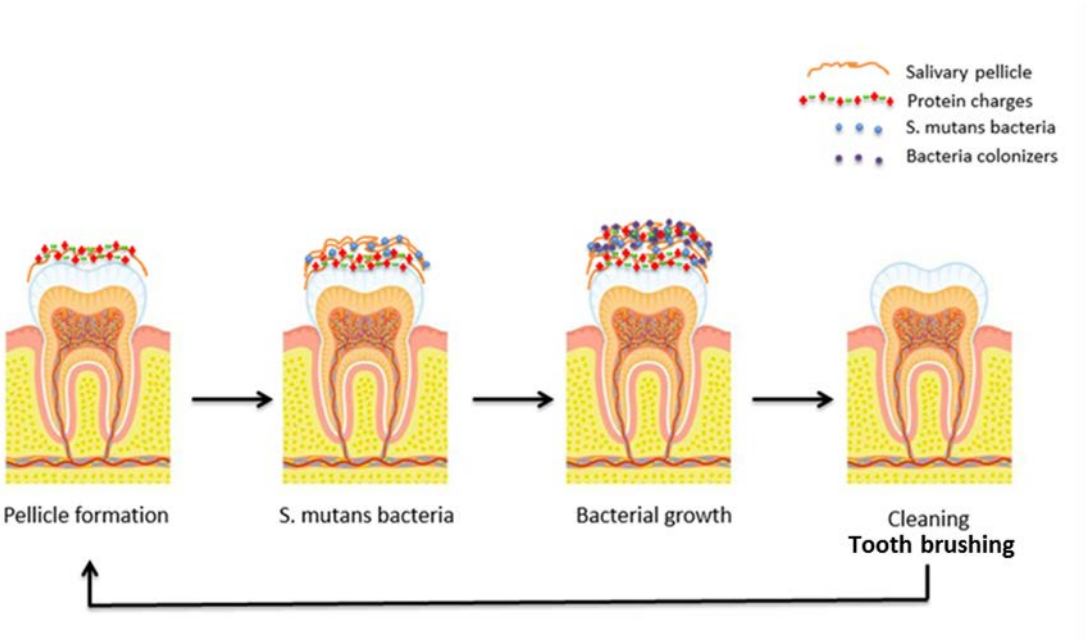

Figure 2.5: Process of dental plaque formation on a tooth surface. Adapted from [12].

Figure 2.6: Plaque build-up resulting in the formation of tartar surfaces of teeth [50].

2.2.2 Effects

The accumulation of pathogenic bacteria in the oral cavity forms dental plaque [45].

Plaque that is naturally formed is harmless if removed regularly and benefits the oral environment by preventing harmful microorganisms attacking the teeth. Hardened plaque that is left to form due to poor oral hygiene develops into a layer that is thick and hard to remove [53].

The advanced form of dental plaque is called calculus or tartar. Brushing of teeth can remove plaque, but tartar requires removal by a dentist using specialised scale and polish instruments [53]. When plaque is left to mature, it can cause damage to the periodontal ligament which is the bone supporting the teeth and gums.

Continued plaque accumulation can lead to gingivitis and periodontitis [54]. Supra gingival plaque (above the gum line) can cause damage and irritation to the gums which over time can lead to gum disease, which is also known as gingivitis [54]. Sub-gingival plaque, which accumulates below the gum line, eventually forms tartar and can cause the gum tissue to be irritated and inflamed, Figure 2.7 [55].

Figure 2.7: Red, sore inflamed gums [56].

Dental plaque can also cause subsurface porosities, which appear as white spot lesions. These white spot lesions result from demineralisation of the tooth surface. The process of the demineralisation starts when plaque on the teeth release acids, which results in mineral loss of the enamel surface resulting in white marks, Figure 2.8 on the tooth surface [57].

Figure 2.8: Demineralisation of teeth resulting in white marks [57].

Gingivitis can be controlled by progressive tooth bushing, flossing and with regular visits to the dentist. If left untreated, the formation of pockets between gums and teeth allow easy access of bacteria, which result in periodontitis. Peritonitis can damage the supporting bone structure which holds the teeth in place, which will eventually lead to tooth loss [58].

2.2.3 Removal

The formation of dental plaque biofilms needs to be prevented and the first step in achieving this is to prevent the existence of biofilm. This can be achieved by the use of oral hygiene procedures.

Two minutes of tooth brushing twice a day, allows for a maximum of 5 seconds of contact on a particular tooth surface if the effort is evenly distributed [59].

The most conventional and convenient method to disrupt dental plaque bacterial biofilms is by the mechanical action of tooth brushing, whereby compressive and shear forces are applied to the biofilm from different directions in a reciprocating motion, to detach the biofilm from the tooth surface [32]. The brushing technique also plays an important part in removing biofilm. Varying brushing motions can affect the level of plaque removal. The choice of toothbrush is another factor which can also contribute to the efficiency of plaque removal [60]. One of the most effective ways to remove consolidated plaque biofilm is scaling, which requires a dentist to carry out. For optimal oral health, interdental cleaning is beneficial [54, 61]. The removal of dental plaque biofilm can be controlled by brushing twice a day and maintaining a high level of oral hygiene. Flossing and using mouthwash also helps the build-up of plaque and tartar [53]. The prevention of plaque hardening into tartar can be controlled by using a dentifrice [55].

2.3 Advantages and disadvantages of tooth cleaning

The oral health sector is one of the most rapidly growing hygiene product sectors [62]. The need for healthy and aesthetically attractive teeth is consumed by the world we live in, with people becoming more conscious about teeth. Discolorations or stains on teeth can cause issues for people's self-esteem. The appearance of teeth is a very important aspect for the majority of people, since teeth are one of the main focal points which attract people's sight. The market for oral care supplements is fast growing and it is driven by consumers wanting the appearance of their teeth to be cosmetically attractive .

Tribology plays a big element in the oral hygiene procedure. An example of this is waking up in the morning and brushing your teeth with toothpaste containing abrasive particles [63]. Brushing teeth daily is very important, as it removes the plaque build-up on teeth which can develop and cause tooth decay and gum disease [42, 64].

A hostile environment can be created in the mouth by the chemical nature of food and beverages that are consumed. Discoloration of tooth surfaces and physiological damage to tooth surfaces and gums can be caused by bacterial plaque growth enhanced by acids and sugars [65]. This can be mitigated and controlled if regular cleaning of teeth is practised; saliva irrigation alone will not be enough.

There are many health benefits of tooth brushing. Cleaning teeth daily can protect the teeth against tooth decay resulting in a decreased chance of developing cavities [64]. Good practice of oral care can prevent gingivitis which is caused by plaque build-up on teeth. Prolonged gingivitis will eventually develop into periodontitis, which will cause loss of alveolar bone which holds the teeth in place, eventually leading to loss of teeth.

One of the ports of entry for infections in the body is through the mouth. If teeth are brushed daily it will reduce the chances of infections developing and affecting the rest of the body. Bacteria in the mouth can get into the blood stream and cause health complications such as dementia, diabetes and pneumonia [67, 68].

However, tooth brushing is not without its drawbacks. Damage can be caused to the gums by vigorous brushing. This can lead to an increased likelihood of gum recession. In addition, toothbrush abrasion can be caused by overzealous brushing with stiff filaments which results in v-shaped notches in the enamel. This can lead to receding and sensitive gums and teeth. Receding gums can

cause other dental complications such as root cavities and periodontal disease, which will require dental treatment [67, 68]. Severe wear of enamel resulting from over-brushing can lead to the sensitive root area of the tooth being exposed.

2.4 Cleaning mechanisms of teeth through history

2.4.1 History of dentifrices

A dentifrice can be defined as, a substance used for the hygiene of teeth and tissues, prepared for the public [38]. Most commonly, dentifrices are toothpastes in the form of a paste or a gel and are formed from the preparation of a semi-solid dentifrice [61].

Dentifrices came into use when it was found that brushes were able to clean the softer deposits from teeth, but the removal of harder deposits and stains was not able to be achieved solely using a toothbrush [59].

The earliest established example of a dentifrice was a paste containing soot and gum Arabic, which was used around 5000 BC by the Egyptians to clean their teeth [69].

Toothpastes were also used by the ancient Greeks who used ingredients such as crushed bones and oyster shells to make highly abrasive toothpastes. One of the concerns which started the prevalence of toothpaste was to have a fresh smelling breath and keep the tooth surface clean. This is still relevant for toothpastes in today's era. Toothpastes created by the Romans also incorporated flavouring to help keep a fresh smell. Herbal mints and salt were some of the ingredients incorporated by the Chinese in toothpastes [69].

The 1800s saw the rise of the modern toothpaste using ingredients such as soap, chalk and ground charcoals, Figure 2.9. The majority of toothpastes before the 1850s were powders. The 1890s saw the first tube-based toothpaste, which was created by Colgate [69]. The onset of modern toothpastes was marked the addition of a range of different ingredients to combat and to help treat and prevent specific oral conditions and diseases, ranging from tooth sensitivity to decay. In 1914, fluoride was added to toothpaste to help combat tooth decay. Soap was incorporated in toothpastes until 1954 when it was replaced by sodium lauryl sulphate. The benefit of this incorporation was a smooth consistency of paste [69].

More recently, overzealous brushing is a problem that has been addressed by manufactures, by developing toothpastes with a lower abrasivity [69].

Today, the most common of teeth-cleaning practices is tooth brushing using modern dentifrices. Other cleaning procedures include the use of a mouth wash, flossing, and using an interdental aid. It is recommended that these additional cleaning practices should be applied in conjunction with tooth brushing. Dentifrices are discussed in more detail in section 2.5.

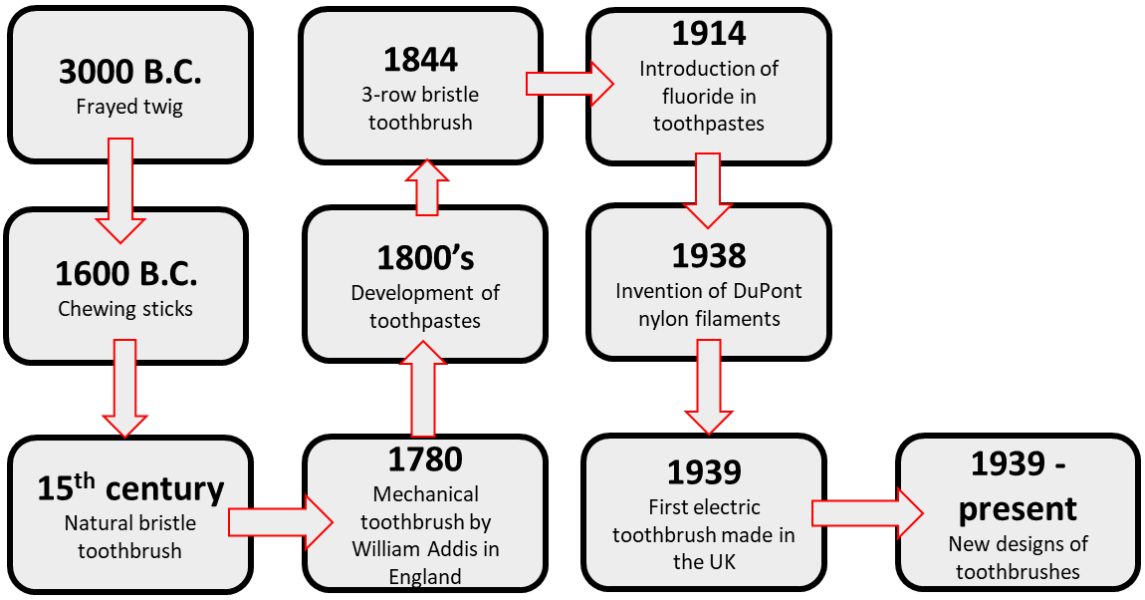

Figure 2.9: Historical timeline of a toothbrush and toothpaste. Data taken from [70].

2.4.2 History of the toothbrush

The first sort of brush was created by fraying the end of a twig. The earliest documented instance of this is attributed to the Babylonians and Egyptians dating back to 3500 – 3000 BC. Chewing sticks were then used by the Chinese around the era of 1600 BC. These were used to freshen breath and were made from aromatic tree twigs [69]. In the 15th century, the Chinese invented a toothbrush made from filaments from pigs' necks. Bone or bamboo handles were used to hold the filaments in place. This represented the earliest naturally-derived filament. A similar design was then adapted in Europe by using horsehairs which were softer. Feathers were also used in some European toothbrush designs [69].

In 1780, William Addis created the first modern toothbrush, using cattle bone as the handle and swine filaments for the toothbrush filaments [71]. A design for a three-rowed filament toothbrush was developed in 1844 [71]. The invention of nylon by DuPont resulted in nylon filaments which were a breakthrough; in 1938, a modern toothbrush using nylon filaments was created and by 1950 nylon filaments that were softer in texture were developed [72]. 1939 saw the development of the electric toothbrush in the UK, Figure 2.9 [71].

The toothbrush has come a long way. The modern toothbrush now consists of a plastic handle and nylon filaments. The filaments range in degree of different grades of synthetic fibres, from very soft to hard in texture. Toothbrush handles come in a variety of designs from straight to angled and curved. The various designs make it easier for people to hold and use a toothbrush. However, the design principles of a toothbrush have not changed from when it was first created. It still comprises a handle that is used to grip and filaments to clean the surface of the tooth. The modern toothbrush is a well-designed instrument that incorporates modern designs as well as being safe and beneficial for use.

A well designed toothbrush has to have the following features. The filaments of a toothbrush should be soft so that they do not damage the soft tissues of the teeth. For plaque removal in hard to reach areas in the mouth, a toothbrush with a small brush head is needed. The handle on a toothbrush should be easy to grip, even when wet and comfortable to use. Research has shown that a well-designed toothbrush can have flat trimmed or angled filaments. Angled filaments are designed to reach tooth contacts and provide more contact with tooth surfaces, which results in more plaque removal. A well designed toothbrush should be comfortable to the user, remove plaque and encourage the user to brush their teeth [73].

In 1938, the development of the modern toothbrush started, which stemmed from the invention of nylon. Prior to this, filaments were naturally-derived. Softer nylon filamentd toothbrushes were being widely commercially produced in the 1950s. The majority of modern toothbrush filaments are synthetic and the texture can range from very soft to hard [69]. Today's toothbrush filaments are fabricated from nylon or a blend of nylon-polyester [74].

2.5 Dentifrice

The most common method for maintenance of oral hygiene is tooth brushing using a dentifrice. The benefits of this include extrinsic stain control, removal of plaque, and delivery of therapeutic and preventative agents to the dental tissues [75, 76].

Evidence has shown from clinical and laboratory reports that abrasion of dental hard tissues, as well as gingival trauma and recession, may be caused by tooth brushing using a dentifrice. Many studies [75-77] have reported the negligible effect of the toothbrush alone to the hard tissues [75, 76].

Plaque and calculus deposits can be reduced on the tooth surfaces by the use of a dentifrice with a tooth brush. A dentifrice can also aid in the removal of stains and discolouration's [78]. The forms in which a dentifrice can be delivered are powder, pastes, foam and gel based combinations. Natural or synthetic ingredients can both be incorporated into a toothpaste [70]. There are no requirements in place by official bodies such as the American Dental Association (ADA) for the use of natural or artificial ingredients in a dentifrice [70].

2.5.1 BS EN ISO Standard for Dentifrices

The UK follows EU regulatory standards for dentifrices. Guidelines are outlined by the BS EN ISO 11609:2010 document, which outlines the tests methods such as determining the dentine and enamel abrasivity, stability as well as outlining the correct physical and chemical properties of dentifrices. The guidelines also cover packaging, labelling and marking of dentifrices [79].

Physical and chemical properties

The fluoride content of a dentifrice should not exceed 0.15% mass and the pH should be below 10.5.

The abrasivity levels for dentine cannot exceed 2.5x of calcium pyrophosphate, which is the calibrated reference material. if using the irradiation method and 2x that of calcium pyrophosphate, if the surface profile method is used.

For enamel, the abrasivity should not exceed 4x that of calcium pyrophosphate when using either the surface profile or irradiation method. The dentifrice should be stable so it does not deteriorate after 30 months at room temperature [79].

Test methods for abrasivity

There are two main methods to calculate the abrasivity of a dentifrice. The first method is according to the American Dental Association (ADA) procedure. The technique requires use of a brushing machine and a radioactivity detector to irradiate the tooth samples. The dentine and enamel samples are prepared by removing the crown and root tips. The teeth are radiated and mounted in resin. Nylon, flat cut filaments that measure 10mm in length are used for the tests [79].

The second method to test dentifrice abrasivity is the surface profile method, which makes use of a contact profilometer. The enamel and dentine samples are prepared by sectioning, polishing and embedding in epoxy resin. Two pieces of tape are placed parallel to the exposed section of enamel/ dentine. During the test procedure the specimens are kept hydrated. The procedure requires 10,000 brushing stokes and a load of 150g. Depending on the type of profilometer, profiles are taken from the taped area across the specimen. 3 profile scans at different points are taken across the exposed area and the mean abrasive depth is calculated for each of the specimens [79].

Abrasive slurry

To prepare the abrasive slurry for the brushing tests, the first step is making the stock paste. 0.5% CMC (Carboxy-methyl cellulose) solution is diluted in 10% glycerine. This formulation is used as the paste. The preparation stages for 1L of paste are as follows:

- 100 ml of glycerine (heat to 60°C) + 5g of CMC.
- Add 900ml of water.
- Allow to stand (overnight) to stabilise viscosity and allow for the mixture to cool down.
- 10g of abrasive is diluted in 50 ml of the paste.

The final step of the slurry requires mixing 25g of the abrasive paste and 40 ml of water. A mechanical stirrer should be used to avoid the abrasive particles from agglomerating and settling [79].

2.5.2 Relative Dentine Abrasivity (RDA)

To remove or prevent extrinsic stains from forming, a dentifrice requires a degree of abrasivity. To prevent the removal of any underlying enamel and exposed dentine the abrasivity of a dentifrice needs to be moderated. To minimise hard tissue wear and to maximise cleaning is the aim of dentifrice manufacturers. It is important to quantify the abrasivity of a dentifrice and many methods have been developed to measure this parameter [80]. Past methods include recording the gravitational changes in dental tissues and using irradiated teeth to record the radioactive calcium or phosphate released. Recent methods include scanning electron microscopy, surface profilometry, surface replication techniques and digital image analysis [81]. The abrasivity of the dentifrice is then inferred from the damage caused to the surfaces analysed.

The International Standards Organisation (ISO) describes the radiotracer method to measure toothpaste abrasivity. This method allows the toothpaste abrasivity to be calculated allowing values for the relative dentine abrasivity (RDA) or relative enamel abrasivity (REA) to be given. The first step involves placing human enamel and dentine samples in a neutron flux to make them radioactive. A brushing machine is used to brush the tooth samples using a slurry of test toothpaste, under set conditions. To determine the amount of tooth material that has been abraded, measurements are taken for the amount of radioactive material that is present in the slurry. Under the same conditions, a reference abrasive (calcium pyrophosphate) is tested. Calculations are made comparing the abrasivity of the test toothpaste to the reference abrasive [81]. The RDA is set to 100 for the reference abrasive standard, calcium pyrophosphate. To maintain teeth free from staining, a dentifrice with a RDA value of 60 – 100 is adequate [82]. The guidelines given by the BSI 2135 British Standard Institute state that the RDA value of a dentifrice must not exceed 250 [80]. Based on RDA values a range of 151- 250 would denote a highly abrasive dentifrice, a moderately abrasive dentifrice would be in the range of 70 – 150 and a low abrasive dentifrice would be below 70 RDA, Table 2.5.

Table 2.5: The RDA categorisation for dentifrices [70, 83].

Relative Dentine Abrasivity (RDA) Scale	
RDA Score	**Level**
0 – 70	**Low abrasive** Safe for cementum, dentine and enamel
71 - 100	**Medium abrasive** Safe for enamel Dangerous for cementum and dentine
101 – 150	**High abrasive** Dangerous for cementum, dentine and enamel
150 – 250	**Very high abrasive** Harmful limit Damaging to teeth
250 +	Not recommended

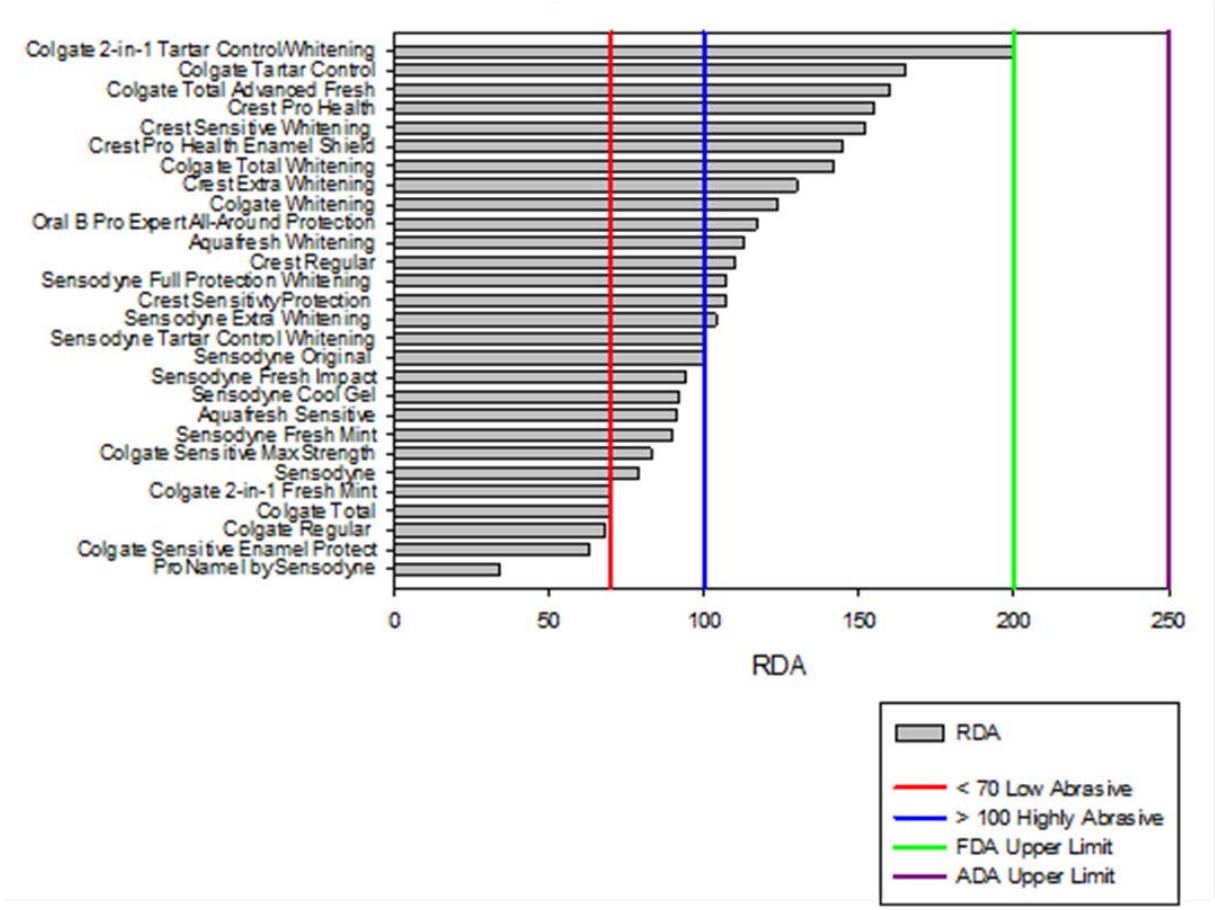

Figure 2.10: RDA values for commercial dentifrices represented in a graph. Data taken from [64].

To make a direct comparison between the abrasive nature of dentifrices is difficult, because each manufacturer uses different protocols and laboratory products. Research methodologies differ; no link exists between abrasivity scales [70]. As a result, the Foods and Drugs Administration Agency (FDA) in America requires dentifrices to have an independently-determined RDA value before they are approved. On the other hand, the UK has no set regulation and the abrasivity of dentifrices is not monitored. The FDA have their own limit of approval which is 200 whereas the American Dental Association (ADA) accept up to a limit of 250, Figure 2.10.

Johannsen et al. [80] recognises the importance of acknowledging the roughness of abraded material. since the RDA value does not give roughness values of the tooth surface after a dentifrice has been used. This finding is in agreement with a study carried out by Liljeborg et al. [84] which suggests that it is important to ascertain a roughness value (which is qualitative) and a volume loss value (which is quantitative) when rating a dentifrice for abrasivity and polishing effect [80].

The complex interactions in the oral environment prevent the RDA scale from being able to give true values of clinical abrasive wear. The RDA test does not accurately reproduce the complex multifactorial nature of the abrasive process of tooth brushing in the oral cavity. Caution should therefore be taken when relating the laboratory test results to clinical relevance. Nonetheless, RDA can be beneficial in determining the levels of abrasivity of dentifrices [85].

2.5.3 Use of a dentifrice

A dentifrice can be used to aid plaque removal and deliver therapeutic agents to the tooth surfaces, when used in combination with tooth brushing. A dentifrice is used primarily to clean the tooth surfaces from stains, food debris and dental plaque, whereas a toothpaste is designed to remove naturally occurring soft deposits from teeth; it is semi-aqueous in nature and used simultaneously with a toothbrush.

Dentifrices come in two forms. They can either be cosmetic or therapeutic. Cosmetic dentifrices remove plaque biofilm and food debris, and they help keep the teeth clean from stains and provide a polishing effect to increase the whiteness and lustre of the visible surface. The first use for a dentifrice was for cosmetic reasons [86]. Therapeutic dentifrices provide the tooth surface and the oral tissues with drug substances which help prevent or mitigate disease in the mouth. They can be used to reduce the incidence of caries and gingivitis, as well as stop the formation of calculus and help reduce tooth sensitivity. Triclosan is a common drug substance which is incorporated into dentifrices to reduce plaque growth and gingivitis on teeth. It works by making the membrane of bacteria permeable, which allows the agent to penetrate the bacteria and kill the microorganism [87].

2.5.4 Components

Preventing toothpaste from hardening can be achieved by using a humectant. A humectant retains the moisture of a toothpaste and prevents desiccation [50]. A humectant therefore ensures chemical and physical stability of the product and prolongs its shelf life, Table 2.6 [70].

Separation of liquid and solid phases of a dentifrice can cause problems; a binding agent is added to prevent this. During storage of a dentifrice the addition of a binder provides stable suspension, Table 2.6 [50]. They also can be used to thicken the dentifrice [70].

The foaming action of a dentifrice is caused by the addition of a detergent, which cleans the surfaces of a tooth, by lowering the surface tension which in turn loosens debris and staining matter, Table 2.6. A detergent penetrates and loosens plaque deposits on the surfaces of teeth.

Contamination of dentifrices needs to be controlled and this can be achieved by the addition of a preservative, which inhibits bacterial and mould growth. They also prolong the shelf life of dentifrice, Table 2.6 [70].

Unflavoured dentifrices often taste unpleasant; to mask the taste, ingredients that provide a refreshing flavour and taste are added. The taste of toothpaste has to be pleasant for it to be accepted by a consumer. A consumer's compliance to toothpaste and brushing recommendations increases if the colour, taste, smell and consistency is favourable, Table 2.6.

Table 2.6: The ingredients in a dentifrice and the functions they serve [70].

Function of Common Toothpaste Ingredients	
Ingredient	**Function**
Abrasive	Stain removal and polishing
Detergent (surfactant)	Foaming, stability, solubiliser, anti – microbial and plaque inhibitory
Binder (thickener)	Stability, consistency, appearance
Humectant	Maintain moisture and flow ability
Flavour	Taste and freshness
Colour	Appearance
Water	Solvent for some ingredients Promotes user compliance

For stain removal. whitening agents can be added to dentifrices. This action is achieved by the inclusion of small abrasives, or chemical agents such as hydrogen peroxide which remove or whiten intrinsic stains and also may prevent further stain formation .

Other ingredients can also be added to dentifrices for treatment, preventive care or for beneficial purposes. These ingredients can be used as therapeutic agents or medicinal ingredients. Examples include ingredients such as triclosan and pyrophosphate to treat gingivitis and plaque formation [70].

2.5.5 Composition

All dentifrices contain a flavouring agent, a detergent and an abrasive or a polishing agent. These are the basic ingredients of a dentifrice. Addition of other ingredients such as binding agents, humectant, therapeutic and cleansing agents as well as colouring agents are also added, Table 2.7. The abrasive or polishing agent is the most functional ingredient which has most importance. An abrasive agent should not cause any removal of the tooth tissues, but it should provide stain removal [78]. Figure 2.11 shows the percentage of components contained inside a dentifrice.

Table 2.7: The components and the agents that are contained in a dentifrice [70].

Components of Dentifrices		
Components	**Percentage**	**Examples**
Cleansing and polishing agents	10 – 40	Phosphate Calcium pyrophosphate, dicalcium phosphate dehydrate, anhydrous dicalcium phosphate Carbonates Calcium carbonate, sodium bicarbonate Silica Silicates, dehydrated silica gels, perlite Aluminium compounds Hydrated aluminium oxides, aluminium trihydrates, alumines, amorphous aluminium silicate
Humectants	20 – 70	Glycerine, sorbitol, mannitol, propylene glycol
Water	5 – 30	Distilled water, deionized water, spring water
Binders (gelling agents or thickeners)	1 - 2	Mineral colloids Natural gums Alginates, gum carrageenan Synthetic cellulose Carboxymethyl cellulose (CMC), hydroxyethyl cellulose ,ethyl cellulose Others Polyethylene glycol (PEG), glycerol carbomer
Detergents (surfactants or foaming agents)	1 - 3	Sodium lauryl sulphate (SLC), derivatives of sodium
Flavouring agents	1 – 2	Oils Menthol, vanilla, nutmeg, clove oil, spearmint, cinnamon
Preservatives	2 - 3	Alcohols, sodium benzoates, phenolics (methyl, ethyl, propyl)
Sweeteners	2 – 3	Noncariogenic artificial sweetener, sorbitol, glycerine, xylitol
Colouring agents	2 - 3	Titanium dioxide, sodium perborate, chlorophyll, magnesium peroxide
Therapeutic agents	0.1 – 0.5	Anti-caries agents Anti-gingivitis/ oral biofilm control Anti-calculus agents Pyrophosphates derivatives and zinc derivatives Anti-stain agents Abrasives Peroxides Hydrogen carbide

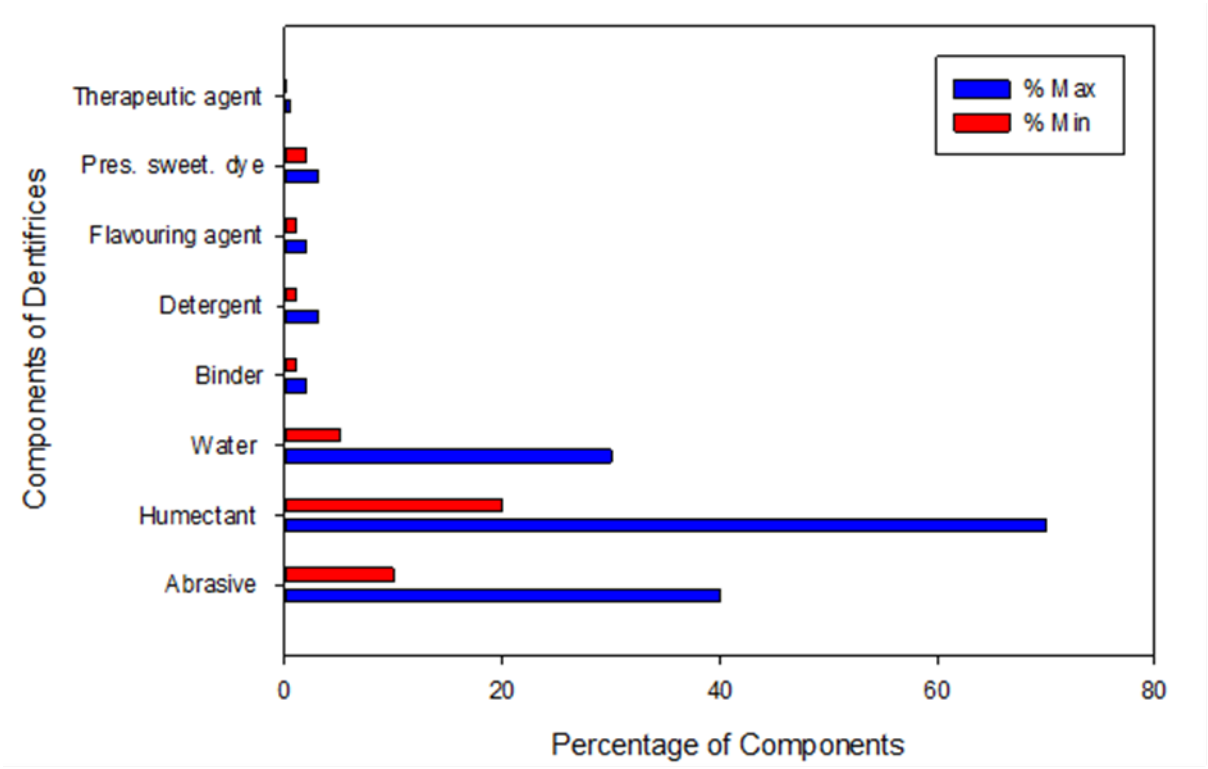

Figure 2.11: The maximum and minimum percentage of components that could be contained in a dentifrice. Data taken from [70].

2.5.6 Rheology

The main factors that influence rheology of a toothpaste are the:

- Humectant type/ composition
- Water content
- Abrasive

The main humectants which are most commonly used in toothpastes are glycerine, sorbitol (aqueous) and polyethylene glycols (PEG's). Glycerine and sorbitol are mixed with water. These ingredients add viscosity to the paste, whereas PEGs can change the viscosity. This is dependant upon the interaction of PEG with other compounds in the paste or the amount/ weight of the PEG used in the paste [88].

When a dentifrice is squeezed out of the tube a clean break should be achieved. The ratio of water/ polymer needs to be controlled to control the leanness of the paste, so that it still has the desired properties such as a good thickness [88].

Viscosity, low shear yield stress, pseudo-plasticity and thixotropy are the rheological characteristics of a dentifrice influencing its texture, performance and ease of use [53]. A dentifrice is a non-Newtonian fluid which exhibits elastic properties. A dentifrice will exhibit elasticity when subjected to a high shear rate [89]. The viscosity of a dentifrice ranges typically from 70,000 – 100,000 cP [90].

The desired texture of a dentifrice should have properties such as a low thixotropy and a good thickness (viscosity) and firmness [91]. To control or modify the rheology of a dentifrice in terms of viscosity, thixotropy and yield value, binders are needed which play a crucial role in influencing the sample texture [48]. By adjusting the binder content it allows control of the texture and consistency of a dentifrice as well as other properties such as the solid-liquid and water-humectant ratios. The concentration of binder necessary to achieve a desired viscosity of a dentifrice can be affected by the surface area and particle size of the abrasive agents. Thickening and binding agents' primary functions therefore include: to give acceptable rheology and texture during preparation; allow no separation or syneresis of phases; exhibit good stability, storage and utilisation [89].

The abrasive agent concentration is the most influential factor on the dentifrice structure. The size, shape and amount of abrasive particles contribute to the rheological behaviour [88]. To structure a dentifrice the main inorganic component which is used extensively is finely divided silica [88].

Finely divided amorphous silica particles have a high surface area and a high internal porosity; they can increase the viscosity from a lean solvent system dentifrice to provide the consistency of a gel or viscous paste. High loading of abrasives in a lean humectant system can produce a high viscosity dentifrice, however the three dimensional structure of a dentifrice has to be well ordered and plays an important part in stability. These findings are interesting as it highlights the fact that further research is needed in the rheology of silicas in dentifrices based on lean solvent systems, in order to understand the roles of an abrasive in a dentifrice formulation. A minor effect on rheological structure is seen with the type and amount of surfactant, however, there is little published work on this.

Rheological concerns must be addressed when choosing certain ingredients for a dentifrice. This is because the interactions could be strong, resulting in alteration to the properties of final dentifrice formulation [88].

2.5.7 Abrasiveness

Cleaning of debris and stains can be achieved through efficient cleaning using a dentifrice. Extrinsic stain is a form of stain developed from the acquired pellicle. A definite degree of abrasivity is required by a dentifrice to prevent and reduce extrinsic stains from forming; non-abrasive or low abrasive dentifrices are unable to remove extrinsic stains. To prevent the removal of enamel and dentine which are underlying minerals, the abrasivity of the dentifrice needs to be moderated. There are many factors such as the particle size, shape and hardness that can influence the dentifrice's abrasivity. Manufactures try to formulate dentifrices that minimise damage to the oral tissues but maximise cleaning [92].

The majority of studies conclude very little abrasion of enamel and only minor abrasion of dentine over normal tooth brushing during a course of a patient's lifetime; less than 1 mm of abrasion total [81].

Stained material on the enamel surface can be removed by abrasives using a number of means such as cutting, brittle cracking or by intersection of the grooves. The ploughing process allows the formation of shoulders; this is where the stained layer is pushed to the side of the groove [81]. Elastic distortion can take place on the surface of the pellicle or plastic deformation can occur below the surface. This is seen using softer particles or lightly loaded hard particles. Loss of the stained material from the pellicle surface can also occur by delamination. This event is caused by failure of the subsurface interface by fatigue after constant exposure to the abrasive particles [81].

When acid is present, toothpaste abrasion can become a major problem, although literature results are sometimes conflicting. A study conducted by Voronets et al. [93] reported increased enamel surface loss with increased abrasivity of toothpastes, whereas a study conducted by Turssi et al. [94] found when comparing whitening paste and regular toothpaste there was no difference seen in wear of acid-softened enamel. Softened enamel is easily abraded and very unstable [59]. Mild abrasive forces can easily wear softened enamel [81].

A study conducted by Kitchin and Robinson 1948 [95] found a link between the rate of dentine abrasion with the abrasive properties of dentifrices. Other studies comparing dentifrice performance with more emphasis on abrasive agents have been carried out by [95-97]. The tests to characterise the stain removal qualities of an abrasive dentifrice are run with one control group brushing with water only (or an abrasive free dentifrice) and the other group brushing with an abrasive dentifrice. These tests give a comparison on the performance of dentifrices and the ability

to remove stains. A study conducted by Bjorn and Lindhe 1966 [98] found that the primary factor which determined the rate of abrasion was the concentration of particles per area unit on the brushing surface.

A highly abrasive dentifrice can remove large amounts of oral biofilm. However, it can produce the pellicle faster than a less abrasive dentifrice. Proteins from saliva absorb and adhere to the clean tooth surface. Erosion of enamel can be avoided due to the fast formation of the acquired pellicle. Abrasion of exposed root surfaces increases with a highly abrasive dentifrice. This can also cause dental hypersensitivity [70].

Most studies have focused on wear of dentine [85]. The study carried out by Hunter et al. [92] acknowledges that dentine abrasion has been the main focus of research, whereas the wear of enamel has been relatively understudied [92]. Likewise, focus has mainly been on the mechanical action of tooth brushing using a dentifrice. Properties such as the hardness, shape and size of the abrasive particles are important in determining the abrasivity of a dentifrice .

Investigations into dentifrice abrasivity can be carried out in vitro, in vivo and in situ. In vitro methods use prepared human or bovine teeth, to record the amount of tooth tissue loss after being subjected to experimental conditions. In vivo methods focus on comparing tooth profiles over a certain period of time by taking dental impressions. The in situ method involves attaching a dental device to the natural dentition and allowing it to be exposed to the conditions of the oral environment [81]. To consider the worst case scenario for dentifrice abrasion the employment of an in vitro technique can be used; however, some techniques do not provide reliable results and poorly simulate the oral environment [92].

2.5.8 Abrasive agents

The main abrasives used in a dentifrice are phosphates, carbonates, silicas and alumina compounds, Table 2.8 [70].

The oldest components added to dentifrices are abrasives. Insoluble materials such as calcium carbonate, precipitated silica, calcium phosphates, perlite, aluminium oxide and pumice have been used for centuries. These components improve the cleaning characteristics of dentifrices. A dentifrice's abrasivity can depend on many factors such as the abrasive amount used, size of the abrasive particle, the particles' surface shape, as well as the other ingredients in the dentifrice that chemically influence the product.

The abrasives have the highest composition of particles in a dentifrice. The effect of the abrasive and polishing agents also depend on many factors such as the force applied during brushing, the technique used, the filament texture, the properties of the abrasive particle as well as the surface being polished [86]. Rapid tooth surface removal will take place the faster the abrasive is moved across the surface of the tooth and the harder the force used when brushing teeth [99]. A low capacity of abrasive agent is less effective in removing extrinsic stains, whereas increased abrasion can be seen with a high abrasive capacity. This is aggravated if the brushing forces are excessive [70].

Dentifrices that contain abrasive agents are primarily used for stain prevention. Salivary glycoproteins are part of the acquired pellicle which thickens and toughens over time. If the pellide is left undisrupted the thickness of the pellicle can range up to 10 µm. Frequent brushing of teeth removes the pellicle that starts to form after 24 hours, resulting in a build-up of visible films [65]. A discoloured pellicle can be removed by the addition of an abrasive agent. However, the texture of the abrasive can have an effect on the dental tissue, in areas along the gingival margin and along the gum line. On smooth surfaces of the tooth an abrasive agent can provide a whitening effect [86], although coarse abrasives which are used in whitening toothpastes can damage the oral hard and soft tissue.

In dentistry, abrasives are used in two different forms: bonded and loose. Bonded abrasives are enclosed within a matrix or binder; such as sand paper and grinding wheels where the abrasive material is contained in a binder material [100]. Loose abrasives are free to circulate between surfaces, such as the particles in a toothpaste or polishing paste. However, loose abrasives will get stuck in the filaments of the toothbrush and be dragged across the surface of the tooth causing them to act like bonded.

Table 2.8: The categorisation of abrasive agents in a dentifrice and the components [70].

Dentifrice Abrasives	Examples
Phosphates	Dicalcium phosphate dehydrate Calcium pyrophosphate Anhydrous dicalcium phosphate
Carbonates	Sodium bicarbonate (baking soda) Calcium carbonate (chalk)
Silicas	Pure silica Precipitated silica, fused silica, silica gel
Alumina and aluminium compounds	Aluminium trihydrate Alumina
Other	Clay Pumice Methacrylate

A dentifrice's abrasiveness can be increased with insoluble ingredients. Abrasives that are insoluble are silica and alumina.

A gentle dentifrice would have a low abrasive content and the level of insoluble materials would be below 20% [70].

Ingredients that are used in a dentifrice that contain no insoluble materials and have no abrasivity are water, hydrogen peroxide and sodium bicarbonate. A low level of abrasiveness is seen with sodium bicarbonate owing to its high solubility. However, the particles of sodium bicarbonate are irregular and if they are used dry, they can abrade dentine. To reduce the abrasive levels of a dentifrice, micronized abrasive particles can be used. If a material is high on the Mohs scale but the particle sizes are fine, it is less abrasive in terms of the linear wear caused [70].

The Mohs hardness scale gives a clear interpretation of the abrasiveness of cleaning and polishing agents relative to oral tissues [70]. Cementum and dentine can be exposed by gingival recession and have a hardness in the region of 2 – 4. To avoid tooth structure loss on exposed roots, it is recommended to use dentifrices with abrasives levels of 2 or less on the Mohs scale, Table 2.9 [70].

Certain abrasive agents are harder than the dental tissues, such as alumina compounds. To achieve stain removal with a dentifrice, alumina is an efficient abrasive agent. However, the hardness of alumina is higher than that of enamel and so there is a high risk of abrading the enamel surface [70].

These materials are highly abrasive and insoluble but may be employed in highly whitening mixtures. Table 2.9 shows some common abrasive agents and their hardness relative to the Mohs scale [70].

Table 2.9: The Mohs scale. The hardness of abrasive agents and tooth tissues. Data from [70].

	Mohs Scale	
Soft	Talc	1
	Gypsum	2
	Dentine	2 – 2.5
	Sodium bicarbonate	2.5
	Biofilm	2 – 3
	Calcite	3
	Calcium carbonate	3
	Fluorite	4
	Hydrated silica dioxide	2.5 - 5
	Apatite	5
	Dental enamel	5
	Calcium pyrophosphate	5
	Moonstone	6
	Pure silica	6 – 7
	Quartz	7
	Topaz	8
Hard	Alumina	9.25
	Diamond	10

Tooth tissues	
Abrasives	
Biofilm	

Table 2.10: Factors influencing the abrasiveness of a dentifrice [70].

Variables Influencing Dentifrice Abrasiveness	
Particle size	Larger the particles, the greater the wear depth on dental surfaces.
Particle shape	The more irregular the shape, the more the dental surfaces are worn and abraded. Round particles cause less tooth wear.
Particle hardness	The harder the particles, the more the dental surfaces abrade.
Concentration	The higher the concentration of abrasives, the greater the amount of tooth tissue removal.
pH level	The more acidic the dentifrice, an increased rate of tooth surface mineral loss.
Quantity of glycerine and water in dentifrice	The higher the level of glycerine in a dentifrice, the higher its level of abrasiveness. Glycerine reduces the dissolution of insoluble materials. The greater the amount of water in a dentifrice, the more soluble particles dissolve, resulting in a less abrasion on the dental surfaces, for specific abrasives like bicarbonate.

The greater the size of the abrasive particle the more stain material is removed resulting in the formation of deeper grooves, Table 2.10. The removal of stain layer will depend on the thickness of the stain layer and the size of the particles [81]. To achieve a shiny and smooth surface, it is preferable to use smaller abrasive particles. The method of abrasion, whether it is two or three body as well as the hardness and size of abrasive particles, determines the speed at which a lustrous surface is achieved, Table 2.10 [101]. An increase in size of the abrasive particles will decrease the efficiency of the filaments ability to trap and retain the particles at the tip. A study conducted by Lewis et al. [102] investigated how the abrasive particles in a toothpaste interact with the filaments. The study used silica particles which were 200 µm -300 µm in size, so that they were easy to observe.

Angular particles have a better scratch ability, cutting away more of the stain surface; however, the strength of angular particles needs to be high enough to avoid the particle breaking as a result of the high contact pressure owing to the small area of contact.

The filament-substrate interface becomes saturated by increasing the concentration of abrasive particles. An effective cleaning rate will be achieved if the abrasive particles does not exceed the particle threshold. However, exceeding the threshold will result in the filaments being extremely submerged causing inefficient stain removal [81].

The removal of asperities can be achieved by polishing a surface to optimise the reflection of light [81]. An indication of wear of a tooth surface is a highly polished surface or a highly roughened surface [78].

A trend of low abrasivity dentifrices with maintained cleaning performance is on the rise. This could be due to high performance abrasives such as hydrated silica which are being increasingly used in dentifrices [92].

2.5.9 Performance of abrasive particles with other particles in the slurry

A study conducted by Harte and Manly [103] evaluated factors that influenced tooth wear other than the abrasive agent [103]. Glycerine inhibited abrasion by 88%. Glycerine can minimise the abrasive agents erosive potential to a higher extent due to its viscosity, compared to saliva or a substitute diluent such as carboxymethyl cellulose (CMC). The abrasivity of a dentifrice can also be changed by detergents. When comparing the abrasion on a tooth surface by brushing with a water-based substance, dentifrice slurries and detergent slurries it was found that an increased loss of dentine was seen with brushing with detergent alone .

Issues have arisen with the chemical compatibility of the abrasive agent used and fluoride. Interaction between fluoride and abrasive agents causes a reduction in the anticaries activity as well as in solubilisation. To overcome this problem, sodium monofluorophosphate was used as a fluoride ion source, due to its low reactivity [104]. Low concentrations of hydrated amorphous silica can be used and serve as an alternative effective and compatible abrasive agent [88]. An in vitro study carried out by Moore et al. found that in the absence of the pellicle, the detergents in a toothpaste also abrade the dentine. The detergent agents remove the smear layer and cause dissolution of the collagen matrix [105].

A humectant agent present in dentifrices such as glycerine decreases abrasiveness. This is due to the action of lubrication it provides between the eroded tooth surface and the abrasive particles [106].

2.6 The role of the toothbrush in abrasion

A significant role is played by the toothbrush in the development of tooth wear. The abrasivity of a dentifrice affects the amount of abrasive wear that is produced on hard dental tissues. A toothbrush acts as a carrier vehicle and can modulate or influence the abrasivity of the system. This, however, depends on characteristics of the toothbrush such as the filament end rounding, stiffness, the type of toothbrush, tuft layout, filament angle and filament length [107].

Studies conducted by Harrington et al. [108] and Addy et al. [109] did not support the idea of a toothbrush causing abrasion, suggesting a negligible effect was produced by the toothbrush. It was found that the toothbrush was only used as a carrier vehicle to distribute the dentifrice across the surface of the tooth. However, these studies did not specify the forces and filament properties.

When studying the effects of toothbrush abrasion on tooth surfaces, many variables need to be taken into account. The size, nature and surface texture of the tooth surface should be defined. Consideration must also be given to the filament characteristics such as the width, end shape and length of the filaments, the size of the filament contact area with the tooth surface, as well as the shape of the contact area. The brushing force applied and the number and frequency of strokes are also factors that need to be controlled [110].

Many other studies have shown links between tooth brushing and wear rate. Tooth brushing factors play a part in the amount of abrasion that is caused [29]. For example, stain removal and prevention is very limited in the interdental areas, with no effect of the abrasivity of the dentifrice. This is due to the brushing technique.

When dentine is abraded or cut an artificial surface structure is formed, which is a smear layer. Collagen and hydroxyapatite from dentine make up the smear layer; it is 1µm in thickness. The underlying dentine and dentine tubules are covered by a smear layer. In the absence of acid, very little or no wear is seen on the dentine surface with tooth brushing using a dentifrice.

Addy and Hunter [111] found that the use of a toothbrush causes little or no damage to the teeth and using a dentifrice is the major cause of abrasion to hard tissues [75-77, 98, 111, 112] . An important element of this study is that it took into account variables that could influence toothbrush abrasion, such as force, time, frequency, brush type, filament end rounding and stiffness of filaments. Although the abrasion of hard dental tissues is caused by the dentifrice, the brush head design can modify the way it carries the toothpaste and effect the abrasivity of the

toothpaste. Hunter et al. [92] reported the difficulty in measuring the ability of a toothbrush to abrade the dental surfaces alone, as the action of tooth brushing is always performed together [92].

A study conducted by Hunter et al. [92] concluded that in vitro tooth brushing with the use of an abrasive agent can cause abrasion; however, using a toothbrush alone causes little damage. This study was supported by the findings from Moore and Addy, 2005 [113] who found that little or no effects were seen on the dental hard tissues by the use of a toothbrush alone.

Today, the designs of brushes are very complicated. Many materials are used for filaments; filaments are incorporated at various angles and cut at varying lengths, and different toothbrush head configurations exist. These are based on different arrangements and types of filaments. Toothbrush filaments can be made from different materials such as polyester or nylon and they can range in thickness, length, compactness as well as geometry of the tip. The carriage of a dentifrice over the surface of a tooth can be affected by the design of the toothbrush, and this can also affect abrasion [114].

Over the years, electric toothbrushes have become common and studies have revealed electric toothbrushes are effective at removing higher levels of plaque compared to manual toothbrushes [115]. However, with the correct brushing technique and habits, both types of toothbrush are a key foundation for promoting healthy oral care and are effective tools for removing oral plaque which can lead to disease. Much like manual toothbrushes, electric toothbrushes have many designs and range from oscillating to vibrating movements [73]. Some electric toothbrushes on the market have the addition of a pressure sensor and this can control the level of load applied to the teeth which can aid in reducing abrasion of the oral hard tissues [115].

To understand the abrasive process and what happens at the interface of a tooth, toothbrush and the abrasive particles, investigation is needed into how the abrasive particles in a dentifrice interact with toothbrush filaments [102].

2.6.1 Bristle characteristics

Filaments are characterised by their diameter and this determines whether they are soft, medium or hard, Figure 2.12. Commonly used filament diameters range from 0.2 – 0.4 mm; a soft brush typically has a diameter of 0.2 mm, a medium brush has a diameter of 0.3 mm and a hard brush has a diameter of 0.4 mm [116].

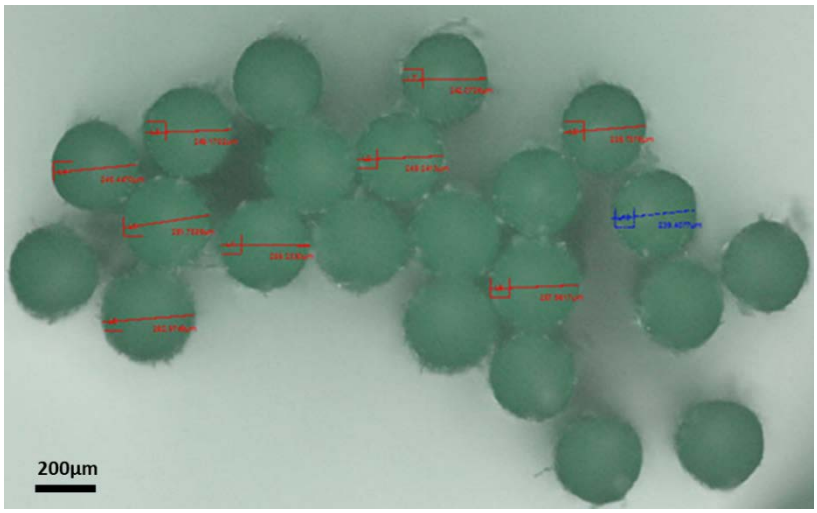

Figure 2.12: Measuring the filament diameter of a Tek Pro® firm toothbrush to determine the texture. Image taken from the optical microscope.

The most influence on abrasion is seen from soft-filament toothbrushes, which is most unanticipated. Dyer et al. [76] found that softer brushes caused a greater amount of abrasion on tooth surfaces than harder brushes. The deflection of soft filaments is increased with applied load, due to the ability of the soft bristles to flex. This can be explained by the ability of softer brushes to carry more paste: the small diameter filaments of soft toothbrushes hold the dentifrice better than hard filaments, since the contact area of the filaments with the tooth surface is increased due to the greater flexion of soft filaments under a specific load [81, 117, 118]. This allows an increased amount of dentifrice to move across the tooth surface [110]. This study was supported by Lewis et al. [102]. However, a study conducted by Niemi et al. [119] found hard toothbrushes to cause more gingival recession compared to soft toothbrushes [119]. A decrease in filament diameter of toothbrush filaments causes an increase in abrasive wear [118].

The effect of stiffness and the tip shape of filaments also plays a part in particle entrapment. Little deflection was seen on loading with a large tuft and stiff filaments. During particle entrapment, the particles stayed lodged in their original positions at the filament tip when they were trapped. This

was due to the stiffness of the toothbrush filaments. However, under the same applied load, more deflection and splay was seen with flexible filaments. When using flexible filaments, less trapping of particles occurred and the particles were able to pass through the filament tips [102].

Hard and soft graded toothbrushes differ in their potential removal rate of dental hard tissues. The stiffness of a toothbrush is affected by many factors, such as the modulus of elasticity of filaments, number of tufts, diameter of filaments, trim length of filaments and the number of filaments per unit area that are packaged within a tuft hole [110]. The majority of brush filaments function as a family of filaments and not as individual filaments. Moisture also affects filaments. When comparing nylon 612 (Tynex®) to nylon 6, dry nylon 6 is stiffer than Tynex®, however when hydrated Tynex® is stiffer [72].

The filament stiffness, filament configuration and the degree of splay of filaments on loading, dictates how long the particles will remain trapped and whether they are likely to be trapped. Stiff filaments that are packed in tight tufts deflect together on loading; they are able to trap particles more effectively, compared to tufts with flexible filaments which on loading splay out and obstruct the entry and exit of particles from the region of the tip [102]. However, a greater splay of toothbrush filaments allows the brush to enter the crevices and grooves in between teeth.

2.6.2 Filament tip characteristics

Toothbrush filament ends can be rounded using pumice. The filament end shape plays a big part in toothbrush abrasion; the incidence of gingival abrasion is affected by the way the filaments are end-rounded [120]. The form of the filament ends is a decisive factor in determining the extent to which the toothbrush aids in plaque removal or whether it damages the tooth surface and the gingiva. Sharp edged, cut filament ends lead to irreversible tooth defects and injure the gingiva.

To prevent mechanical damage to the soft dental tissues, end-rounded filaments are less damaging and preserve the integrity of dental soft and hard tissues, when compared to non-end rounded filaments which can damage the tooth structures up to two times as much [121-124]. Increased amounts of surface abrasion with zig zag and bi-level filament designs was reported [114]. A study conducted by Bass [123] described the end rounding of filaments as an important characteristic to optimise toothbrush design [121, 123]. This can be achieved after cutting the filament head and getting rid of sharp edges in production. In addition, the flat-ended filaments have been observed to trap fewer particles at the region of the filament tip, compared to rounded filament tips. This implies that a higher and more thorough cleaning efficiency is achieved with filaments with rounded

tips [102]. However, many toothbrushes on the market have non- rounded sharp edge filaments, due to the low cost in manufacturing non- rounded filaments [116, 121].

Toothbrushes with a high number of filaments retain a greater amount of abrasive agents, resulting in an increased amount of wear [38].

2.6.3 Brushing technique and parameters

The wear of teeth is influenced by the orientation of the toothbrush [125]. Brushing teeth using a horizontal motion results in v-shaped cervical lesions [126]. This was confirmed by early research [125]. However, it was noted that more research is needed into the formation of cervical lesions, to understand there primary cause [125]. When comparing horizontal brushing to vertical brushing, it was found that up to three times more wear was seen on tooth surfaces when brushing horizontally. This was observed by increased amount of scratches seen on replicas of teeth when brushing horizontally. The more contact between the filaments and the tooth surfaces resulted in more wear. The simple, routined motion of horizontal brushing can cause the brushing forces to become excessive, resulting in an increased amount of tooth wear [125].

Increasing particle motion at the filament-tooth interface is achieved by raising the brushing speed. When a sliding brushing technique is used, the accumulation of particles is around the edge of the filament contact and some particles are trapped in the contact region, Figure 2.13a [127]. A reciprocating brushing technique allows the filament tip contact to trap more particles compared to using a sliding brushing technique, Figure 2.13b. During sliding motions, build-up of particles occurs at the edge of the filament tip contact. These particles are then entrained in the contact. The geometry of the contact can be changed by increasing the load on the brush. This will lead to fewer particles remaining in the contact region of the tip [102]. When a low load is exerted on a toothbrush head, few particles enter the contact region and stay trapped amongst the filament tips. When a higher load is exerted, the filaments bend and particles wedge under the bend.

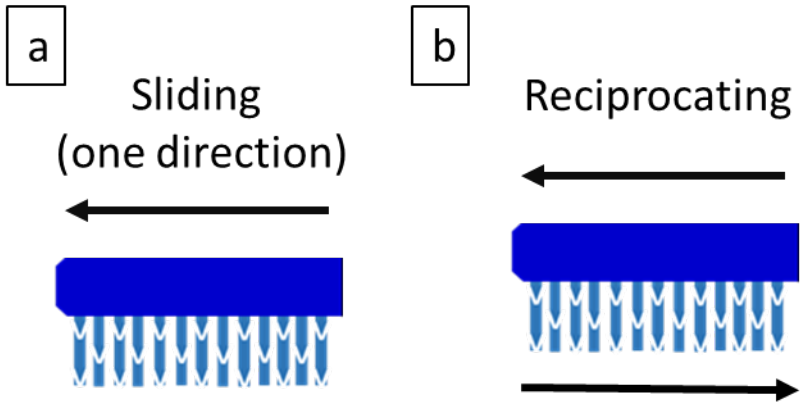

Figure 2.13: Brushing motions (a) sliding; (b) reciprocating.

The origin of damage to dental tissues is often due to brushing with excessive force. This has been supported by many clinical and experimental studies [119, 122, 128, 129]. Padbury and Ash [130], Alexander et al. [122] and Khocht et al. [131] found that the incidence of gingival lesions will increase relative to the force applied and time spent brushing. Brush wear will also increase with a higher applied load. Excessive deflection of brush filaments is achieved when the applied load is increased above a certain threshold, causing the rate of wear of a tooth surface to increase [102]. Using forces above 4 N results in a reduction in brushing efficiency with stiff filaments. This could be explained due to the filaments of the toothbrush bending to the side and no tip contact with the teeth. A high brushing force is classed as 3.5N or above whereas a brushing force of 1.5N is considered a regular brushing force [132]. Brushing with a force below 2N presented no brushing lesions, whereas acute lesions were formed when brushing above 2N [132].

A study conducted by Weigand et al. [110] found that the load used when brushing influenced the amount of abrasion on eroded enamel; however, for sound enamel the brushing load was seen to be of minor importance. This demonstrates a potential positive feedback cycle for tooth damage and abrasion, where initial defects are able to exacerbate subsequent erosive damage. This study takes into consideration that each tooth is subjected to 10-20 brushing strokes during a realistic level of daily brushing, irrespective of the loads applied [110]. An increased load during brushing (4.5 N) resulted in a large amount of acid-softened enamel loss, compared to brushing at 1.5 N [110].

2.7 Effects of abrasion on biological tissues

Functional. restorative and aesthetic problems are some of the problems faced with tooth wear [133]. Many clinical studies have proven brushing abrasion to be the foremost cause of cervical lesions in the mouth [81]. The impacts of toothbrush abrasion on the biological tissues can cause wear of enamel and dentine. Traumatising the gingival tissues by tooth brushing can over time lead to gingival recession, Figure 2.14b [124]. The effect of abrasion on the biological tissues can cause problems in the long run. Dentine is exposed by gingival recession. This leads to v-shaped notches in the cervical areas of the teeth and is most commonly associated with toothbrush wear, Figure 2.14a [81]. In addition, shear forces are used whilst tooth brushing and this action can have an impact on soft tissues of the mouth [134].

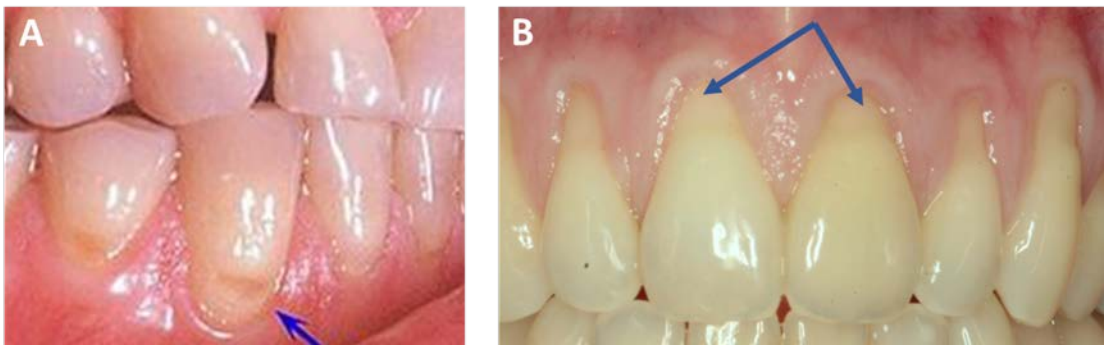

Figure 2.14: Wear on teeth (a) v-shaped notches on the cervical regions of the teeth [135]; (b) gingival recession leading to exposed roots [136].

Root surface exposure can be caused by tooth brushing, Figure 2.14b. The sequence starts with movement of the gingival margin. This results in exposure of the root surface of a tooth.

Using a vigorous tooth brushing action, extremely abrasive toothpaste or hard brush filaments with stiffer filaments can damage the gingiva to a greater extent and cause deeper lesions to form [134]. Less abrasion on the tooth surfaces can be achieved by end rounding the filament tips [134].

Dentine hypersensitivity has been linked to tooth brushing. Painful sensations as well as an increased sensitivity to hot and cold are linked to dentine hypersensitivity and are a result of cervical abrasion of the tooth surfaces [137].

Addy [109] demonstrated that the hard tissues of teeth may be more readily damaged as a result of the softening process from exposure to acids. This loss increases the susceptibility to wear of

enamel and dentine by tooth brushing. In enamel and dentine the softened zone can reach depths of several microns. This makes it problematic for tooth brushing using an abrasive dentifrice.

2.8 Tribology of teeth cleaning

2.8.1 Differences in terminology

The multi-disciplinary field of tribology integrates many different disciplines such as engineering, biology and dentistry [138]. Due to the enamel tissue structure; care needs to be taken with conventional tribology and engineering alloys. This is a common problem with biotribology as terms from engineering tribology do not simply translate to biotribology. This is due to the materials and conditions being very different.

Confusion has risen when terms such as dental abrasion, erosion, attrition and abfraction which are used in the dental field of research, have been used in tribology. The definition of the term erosion has a different meaning in each field. Erosion, which is used in dental literature and signifies tooth structure loss, is termed corrosion in the tribological field. Grippo et al. [139] suggested eliminating the term erosion from the dental dictionary and replacing it with corrosion. In engineering terms, erosion refers to material loss as a result of repeated impact of a solid or liquid matter [138]. The terminology used in engineering may not translate well to the oral situation.

In the present study, the dental term 'erosion' will be used to explain acid softening of enamel.

2.8.2 Abrasion

The most fundamental wear processes that are related to toothbrush abrasion are abrasive wear and erosive wear. Abrasive wear is caused by hard protuberances or by hard particles that are sliding in motion along a solid surface and are pushed against each other. This results in wear of a surface [81]. The process of abrasive wear, can be separated into two groups, namely, two-body wear and three-body wear [133, 140]. Figure 2.15 shows two-body abrasion and Figure 2.16 shows three-body abrasion. Two body abrasion is caused by hard protuberances or asperities on the material surface which slide over each other and cause wear. Three body abrasion is when there is

presence of particles as the third body. These abrasive particles are trapped between the surfaces, but are free to rotate and cause wear [141].

A study carried out by Harsha et al. [141] reported an order of magnitude lower rate of material removal for three body abrasion compared to two-body abrasion. An explanation for this was 90% of the time the abrasive particles in the three-body contact roll and during 10% of the time they abrade the solid surfaces. Three body wear affects many industrial equipment, whereas two-body wear is observed in operations which involve material removal. such as in impellers in pumps. One thing to note is wear is a dependant on the environment and system of the two surfaces [141].

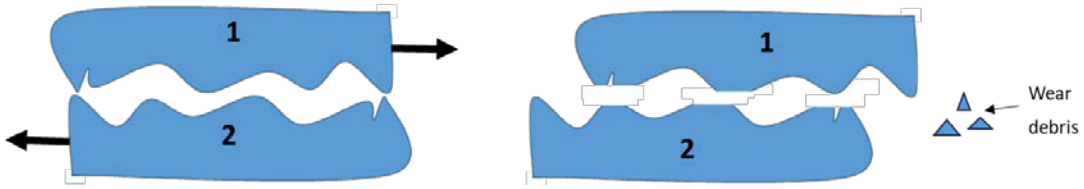

Figure 2.15: Schematic of two-body grooving.

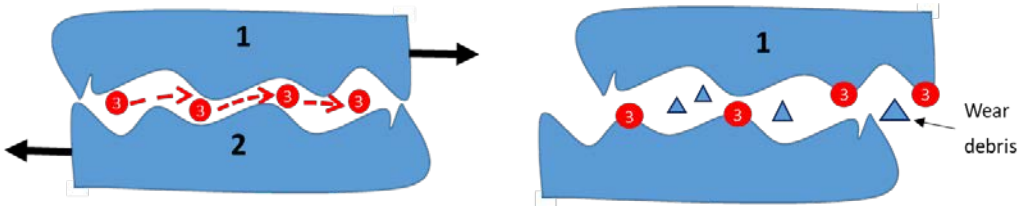

Figure 2.16: Schematic of three-body rolling.

For metals and alloys, the following terms can be used to describe the wear mechanisms. These terms are different to the terminology used to describe biological tissue wear (Figure 2.17) which will be explained in the next section. Different materials behave differently and this will affect their abrasion and deformation performance.

A soft surface which is cut by the action of a hard asperity or sharp grit, is termed cutting [142]. The material removed is wear debris, Figure 2.17a and Figure 2.18a [143].

If the material being abraded is brittle (ceramic) it fractures the surface. Cracks form on the surface of the material. Wear debris produced during fracture are a result of crack formation, Figure 2.17b [143].

When a grit abrades a ductile material (metal), the material is repeatedly deformed by ploughing of the grit; cutting cannot take place due to the materials ductile properties. Deformation of the surface takes place by repeated ploughing. The debris that are formed are a result of metal fatigue, Figure 2.17c and Figure 2.18b [143].

Ploughing causes grooves in a material. Material removal takes place and the formation of a groove is seen on the surface of the material. Ridges are created on the surface of the material. Figure 2.17b [144].

Grain detachment or pull-out occurs when detachment of a complete grain occurs and the detached grain is removed as wear debris, Figure 2.17d [143].

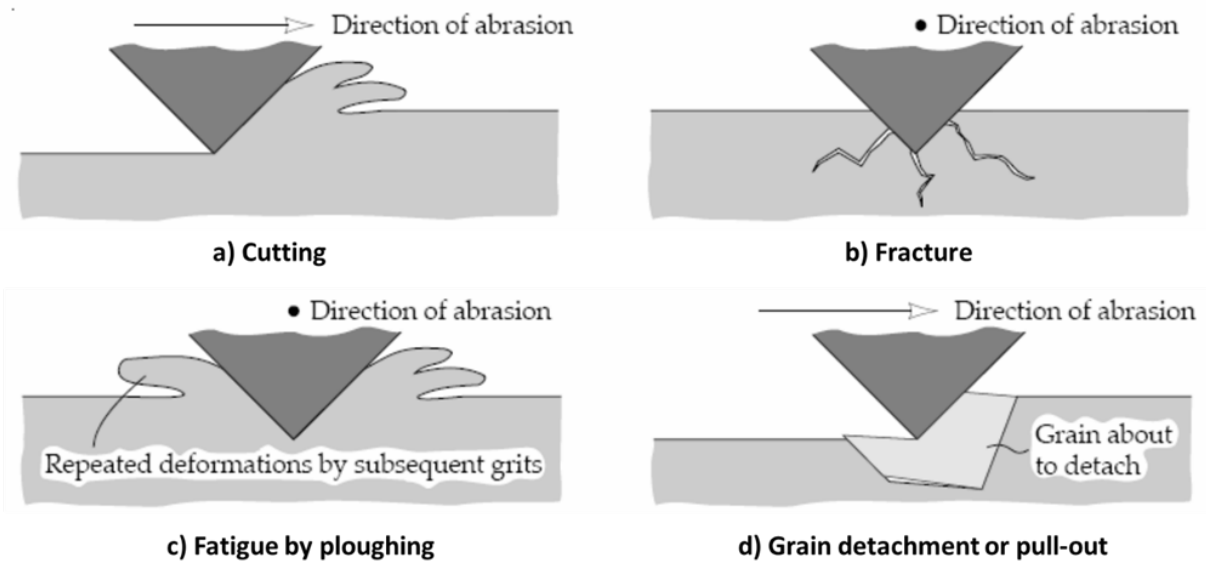

Figure 2.17: Mechanisms of abrasive wear [143].

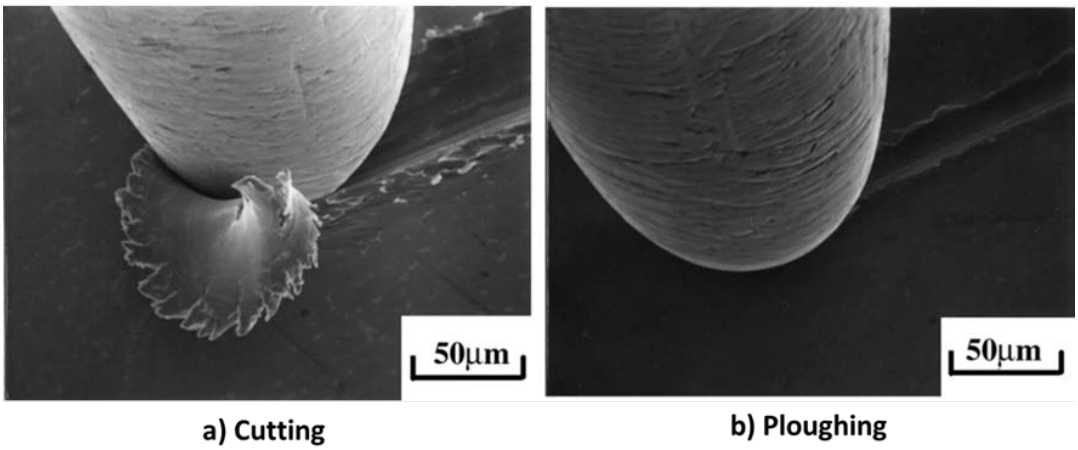

Figure 2.18: Modes of abrasive wear shown by a steel pin on a brass plate [145].

Two-body grooving wear

If two surfaces with asperities are in contact and a sliding action is present between them, removal of material is expected and this is termed two body abrasion [146]. The shape of the sharp protruding surface in two body abrasion is implemented into the softer surface [133].

With biological materials such as enamel, conventional terms used to describe metal and alloy wear are not used. Figure 2.19 shows a typical groove on enamel, caused by particles agglomerated to a nylon ball. As discussed earlier in section 2.1, enamel contains prisms, which are also known as rods. The agglomerated particles groove the enamel and fracture the enamel rods by a micro-chipping process [147].

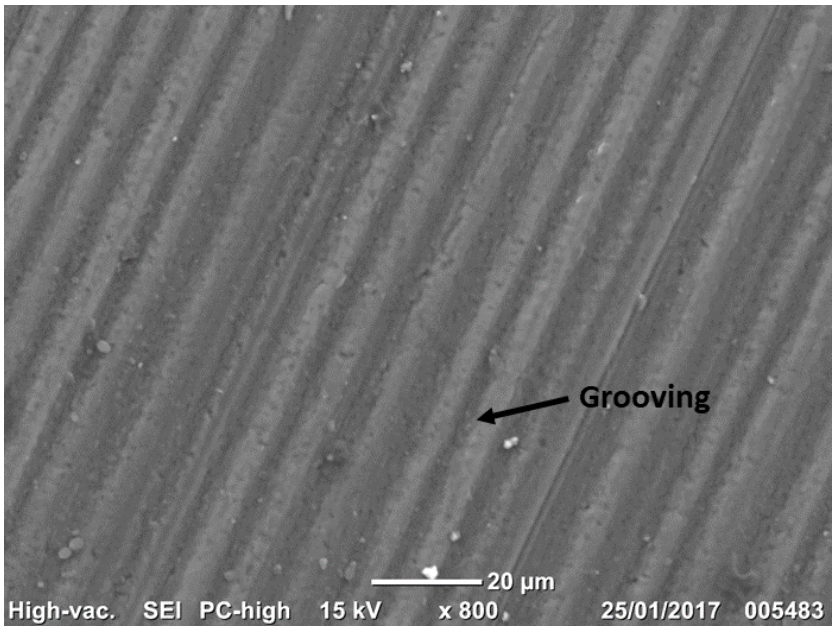

Figure 2.19: SEM of 2-body grooving on enamel.

Three- body rolling wear

In a dentifrice the abrasive particles in the slurry are free to rotate and translate between two surfaces in sliding contact. This is known as three-body abrasion. A slurry containing abrasive particles is the third body in three body abrasion [101, 133].

During three-body wear, the particles roll through the contact. If the softer surface contains sharp projections, these are cut away by the abrasive particles [133]. Figure 2.20 shows a typical three-body rolling wear scar on enamel. Abrasive particles are free to roll between the two surfaces forming multiple indents. Indenting is a result of densification of the enamel tissue, which causes enamel structure damage. After a number of loading cycles, this results in removal of enamel and breakup of the enamel prism surface [147].

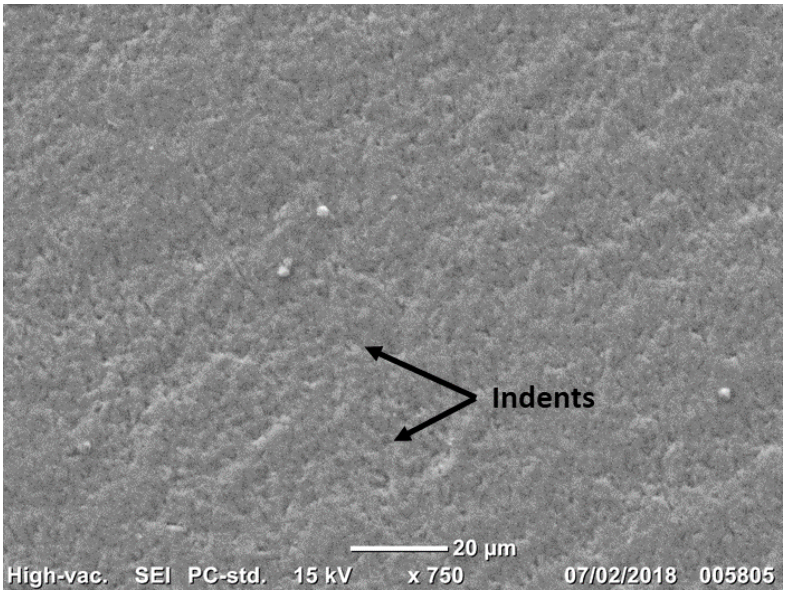

Figure 2.20: SEM of 3-body rolling on enamel.

Wear regimes and transitions

Studies carried out on the micro abrasion rig compared abrasion mechanisms. Adachi and Hutchings [148], mapped 2-body and 3- body wear. A change in wear mechanism was seen from 3-body rolling to 2-body grooving by decreasing the number of abrasives in the slurry solution. Increasing the load on the ball also caused the transitional change from 3-body to 2-body wear [148].

An extensive study carried out by Trezona et al. [149] found low loads and high concentrations of abrasives in the slurry caused a 3-body rolling mechanism, whereas a low volume of abrasives in the slurry and high loads dominated 2-body grooving. The change of transition from three-body abrasion to two-body abrasion was reported to be caused by a change of rolling to sliding particle motions in the sliding contact [148]. Adachi and Hutchings [148] reported the hardness ratio between the ball and the specimen dictate the transition from three-body rolling to two-body grooving. Two-body grooving wear is prominent when there is a high load per particle. A high load per particle can be achieved by high loads or low concentrations of abrasives in the slurry. In-between two-body grooving and three-body rolling there is a mixed-mode region, which shows signs of both grooving and rolling. Mixed mode abrasion is where 2-body grooving and 3-body

rolling occur simultaneously, Figure 2.22 [150]. Many studies ([148, 151], [152-156] have observed the mixed-mode wear transition.

Williams and Hyncica [157] proposed a 2-dimensional model for particle motion from three body rolling to two-body grooving wear. The proposal was based on the value of (D/h) lying above ~1.74 which is the critical value, where D is the particle diameter and h is the separation of the two surfaces, Figure 2.21 [148].

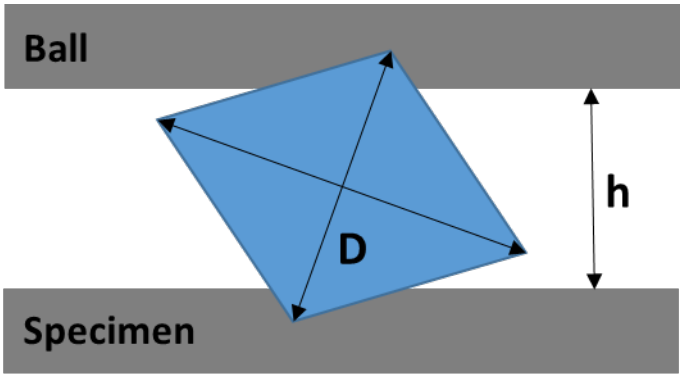

Figure 2.21: Two-dimensional D/h model.

The assumptions for the critical conditions are [148]:

1. The abrasive particles support the load and the load is distributed over the abrasive particles in the contact zone.
2. The abrasive particles remain un-deformed and are harder than the ball and the specimen.
3. The shape of the abrasive particles are spherical.
4. In the contact zone, the concentration of abrasive particles in the slurry is proportional to the volume fraction of abrasive.
5. The roughness of the ball and the specimen is low compared to the diameter of the particle.
6. The effects of hydrodynamics of the abrasive slurry is very small.

The transition from grooving to rolling motion at the critical condition of (D/h), occurs at the critical value of (W/AvH'). Where W is the load on the ball and specimen, H' is the ratio of the hardness between the ball and the specimen, v is the volume fraction of abrasives and A is the wear scar area. This group is dimensionless and is termed the severity of contact (S), Equation 2.1. The severity of contact can be calculated for the particles prior to testing without conducting an abrasion test. The quantities and values for this group are measurable by carrying out experiments [148]. The transitional condition can be written as [148]:

$$S = \frac{W}{AvH'} = S^* \quad \text{... Equation 2.1}$$

Where S exceeds the value of S* there is a change in wear mechanism from three-body rolling to two body grooving wear [148].

Figure 2.22 shows a typical mixed-mode wear scar on enamel. There are signs of grooving and rolling on the surface of enamel. The abrasive particles are adhered to the nylon ball and some are free to rotate which results in a mixed-mode wear scar. The particles groove the enamel and this causes fracture and crushing of the enamel rods, which results in a mixed-mode wear scar [147].

When particles roll in a contact, an increase in the separation of the surfaces of the ball and specimen is observed which leads to the value of (D/h) being decreased, and this can lead to a further increase rolling motion [148].

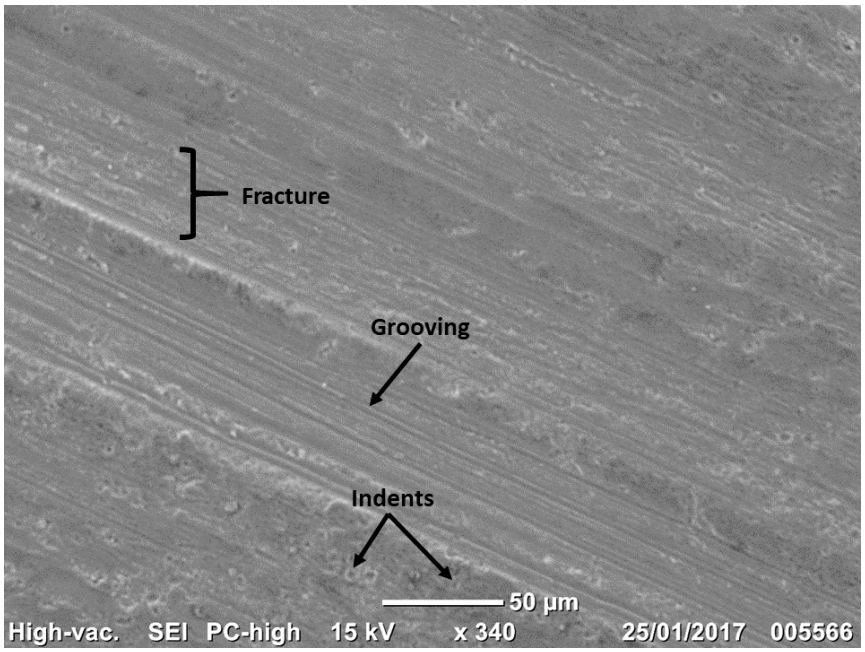

Figure 2.22: SEM of mixed- mode wear on enamel.

2.9 Test techniques

The wear behaviour of the enamel surface remains understudied, since the majority of studies have focused primarily on the effect of abrasion on dentine surfaces. This is partially due to the soft nature of dentine and wear results being more prominent and simpler to predict [1].

It should be noted that in-vitro tests can never simulate in vivo tooth brushing, due to the multifactorial process of wear in the oral cavity. Thus, the tests will attempt to simulate tooth brushing in the natural environment; a reliable test model will be devised giving greater standardisation.

Table 2.11 outlines the previous abrasion tests carried out to understand the tooth brushing action.

A study carried out by Lewis et al. [102] used optical equipment to visualise tooth cleaning. Large silica particles in the range of 200 µm – 3000 µm were used in the initial tests for ease of visualisation purposes, which were followed by 10µm silica particles. A standard flat (uniform filament length) nylon tipped brush head was used. The brushing load and speed was varied during the tests. The loads ranged from 2.4N – 8.8N and speeds from 30 mm/s – 150mm/s respectively.

The counterface material was a glass slide. It was found that the end rounding of the filament tips affected the trapping ability of abrasive particles. Round ended filaments trapped and entrained the particles better than flat ended filaments. At low loads, a few particles entered the filament tip contact and were trapped in the filament tips, whereas at high loads the flex in the filaments trapped the particles in the bend. Two brushing motions were analysed namely, sliding and reciprocating. The reciprocating motion trapped more particles that the sliding motion. With the small 10 µm silica particles, the sliding motion resulted in particles being trapped in and around the filament contact [102].

A later study by Lewis et al. [6] into friction and abrasion of toothpaste particles in a tooth cleaning contact used PMMA as the counterface surface. For the friction tests, 5 µm calcite particles were used with loads ranging from 1.8N – 3.7N. The increase in particle concentration did not have a large effect on the coefficient of friction value. Only a few particles are load carrying at any given time. An increase in coefficient of friction was observed with a low concertation of particles (0.2%) [6].

The abrasion test carried out by Lewis et al. [6] used 1µm diamond particles with loads ranging from 2.5N – 4.4N. The ability of the abrasive particles to scratch the PMMA surface was dependant on the trapping ability of abrasive particles by the filaments. Only a few particles were trapped by the filaments. To create a scratch, the filaments with the trapped particles were required to be load carrying. One thing to note is the particles have the ability to dislodge from the filaments, hence the scratches are caused by different particles. The abrasive action observed from the tests was two-body abrasion by a single particle in one directional pass of the filament. It has also been noted, that repeated scratches can be formed by a particle that is well adhered to the filament, resulting in scratches formed on the forwards and backwards action of the stroke.

A study carried out by Zhou et al. [158] used reciprocating apparatus and a titanium ball to study the friction and wear behaviour of enamel. Human enamel samples were used as the counterface material. It was found that the wear of enamel at high loads increased the wear rate, due to the microstructural properties of enamel such as its brittle nature. Low wear is observed on enamel at lower loads due to its high mineral content and the ability of enamel to resist wear [158].

Table 2.11: Previous literature on abrasion tests.

Author and year	Test performed	Abrasive slurry	Load, frequency, speed, and cycles	Brush details	Test material	Findings
Dyer et al. [76] 2000	Determine whether brushes vary in their ability to abrade a hard surface with a toothpaste.	Toothpaste containing a standardised fluoride product made with 5g toothpaste in 20ml water.	Load - 2N	Standard toothbrush. Multi-tufted flat trimmed design.	Optically clear methyl methacrylate	• Choice of hard, medium or soft toothbrush is of little relevance to hard tissue abrasion.
Zhou et al. [159] 2003	To obtain an understanding of the friction and wear behaviour of enamel and dentine against titanium using a reciprocating tribometer.	Artificial saliva according to Fusayma guidelines [31, 160].	Load - 10N, 20N and 40N. Frequency - 2Hz 2000 cycles	Titanium alloy used as a ball	Human teeth	• The wear condition dictates the friction and wear behaviour of human teeth. • Artificial saliva can act as a lubricant and reduce wear at low loads. • More wear of enamel is reported with increasing loads. • Micro-cracking action is reported.

Lewis et al. [102] 2004	Visualisation of simulated teeth cleaning contacts using optical apparatus.	Glycerol/ water particle fluid mixtures (1% mass). Coloured silica particles 200 – 300 µm 10µm silica particles	Load - 2.4 – 8.8N Frequency – 1 – 2Hz Speed – 30 to 150 mm/s	Electric toothbrush. Standard nylon flat equi-spaced tufts and filaments of same length. Flexible head design.	Glass slide	• Increase amount of particles are trapped in the filament tip contact with reciprocating motion. • At high loads, no particles are trapped in the filaments and are lodged between the bend of the filaments.
Lewis et al. [6] 2006	Model, visualise and simulate the teeth cleaning process. Study the behaviour of particles trapped in the filament tips.	<u>Friction testing</u> 5µm calcite particles. Liquid mixture is the same viscosity of toothpaste when diluted with saliva. <u>Abrasion testing</u> 1µm diamond particles mixed with glycerol	<u>Friction testing</u> Load – 1.8N – 3.7N Speed 3 – 15 cm/s <u>Abrasion testing</u> Load – 2.5 – 4.4N Frequency – 5Hz 50 and 4500 cycles	Standard nylon flat equi-spaced tuft toothbrush.	PMMA surface	<u>Friction testing</u> • No change in friction with increase in particle concentration. <u>Abrasion testing</u> • Few particles carry the load. • Filaments of a toothbrush cause little abrasion action. • Scratching on the PMMA surface is intermittent. • 2-body abrasion process by a single particle.
Joiner et al. [161] 2005	Using an in situ model with in-vivo brushing, determine the enamel and dentine wear by two whitening toothpastes	Calcium carbonate and perlite toothpaste Silica tooth whitening paste containing 3.3% pyrophosphate and sodium bicarbonate	Speed- 30 seconds per brushing period. 2x daily		Human enamel and dentine blocks	• Wear of enamel after 12 weeks was lower than dentine wear.

Zimmer et al. [162] 2005	Determine the loss of dentine during tooth cleaning	Four abrasive particles – calcium pyrophosphate, pumice, Hawe cleanic and nupro coarse	Load – 1.5N Speed – 80 seconds at 1600 rpm	Nylon brush	Dentine specimens	• Amount of dentine loss depends on the abrasive particle. • Smooth surface of dentine after the wear tests.
Lewis et al. [7] 2007	Visualise perlite particles using image capture (video camera) in a simulated teeth cleaning contact.	Silica 10µm particles and Perlite particles (1% concentration by mass)	Load – 225g Speed – 30mm/s	Standard nylon flat equi-spaced tuft toothbrush.	Glass disc	• Perlite particles produce less uniform scratches compared to the silica particles. • Perlite scratches shorter • Less stable trapping of perlite particles with the filaments. • Uniform stain removal with silica particles. • Rate of stain removal higher with silica particles.
Zhou et al. [158] 2007	Understand the friction and wear behaviour of human teeth.	Artificial saliva according to Fusaya's guidelines [31]	Loads – 10N, 20N and 40N Frequency- 2Hz 2000 cycles	Titanium alloy ball	Human teeth	• Enamel worn out at high load. • Increasing the load, wear more enamel. • High mineral content of enamel protects against wear at lower loads. • Due to the brittle nature of enamel, at high loads this could contribute to the higher wear rate.

Weigand et al. [110] 2008	The impact of toothpaste abrasivity and filament stiffness on the abrasion of eroded enamel	Control slurry + Toothpastes with different abrasivity	Load – 2.5N Frequency 4.5 strokes/s	Manual toothbrush with different stiffness- 0.15, 0.20 and 0.25mm	Eroded enamel samples + acrylic	• Abrasion of acid softened enamel influenced by abrasivity of paste. • High abrasion of acrylic with soft toothbrush. • Less abrasive toothpaste only abrade fragile crystals of softened enamel.

2.9.1 Wear mechanisms

Hard tissue wear is categorised into two methods. The first category is mechanical wear which includes, abrasion, abfraction and attrition. Abrasion is caused by physical damage and is the loss of dental hard tissue by the mechanical action of materials such as during toothbrusing. Abfraction can be described as the loss of hard tissue in the cervical area of the tooth, near the cemento- enamel junction [1]. This loss is caused by localised loads on the tooth from the flexure of teeth which result in shear stresses on the tooth. This results in weaker binds between the hydroxyapatite crystals of enamel [4]. This type of damage to the teeth has been a common prevalence in bruxist patients. Attrition is caused by the direct tooth- tooth contact with results in dental tissue loss. Attrition is also linked to tissue aging [4].

The second type of hard tissue loss is caused by the exposure of the tooth surface to acids which results in chemical dissolution of the tooth. This is termed dental erosion or otherwise dental corrosion [4].

Abrasion

One of the main causes of abrasion is due to physical damage of the teeth from the external environment. Substances such as food and actions such as toothbrusing using an abrasive dentifrice all are common causes for abrasive defects [4].

Abrasion is a common occurrence on the cervical area of teeth. In the posterior teeth abrasion is more common on the occlusal edges and the anterior teeth show signs of abrasion on the incisal edges [4].

Abfraction

The cervical areas of the tooth is prone to wear caused by abfraction by the occlusal forces of the teeth which cause compression/ tension in the enamel. This results in the tooth becoming more prone to erosive and abrasive damage. These lesions are most common in the cervical lesions and can also be referred to as cervical stress lesion [1]s. Chipping of the enamel can result due to the enamel hydroxyapatite crystals becoming weak due to the flexure of teeth. A number of habits can cause abfraction such as, grinding teeth, bruxism, premature tooth contacts and also occlusal barriers on the teeth [4]. The resulting effects of abfraction of teeth can be observed as V-shaped notches in the cervical third of the cemento-enamel junction. The main factor that causes the V-shaped notches are occlusal surface forces that occur on the teeth in the cervical region, along with improper brushing habits and the use of highly abrasive toothpastes and hard bristled toothbrushes [4].

Figure 2.23: V-shaped notches on teeth caused by abfraction [4].

Attrition

Attrition is referred to as the physical damage of teeth in functional contact areas which results in the mechanical abrasion of teeth attrition is classified as two-body wear and no participation by a third body takes place or any other substances during attrition [1]. Attrition is mostly commonly observed on the occlusal surfaces of the posterior teeth and the incisal edges of the anterior teeth. In the posterior teeth, the tooth cusps can reduce in height and also flattening of the occlusal surface can be observed. Attrition can occur on any tooth surface which has contact points with another tooth, such as in the case of malocclusion [4]. The most simple test rigs which have been used to simulate sliding movements in the mouth have been pin-on-disc sliding tests. Many of the tests which have employed pin-on-disks have studied two-body wear [34, 158, 163-165]. A study conducted by Condon et al. [166] studied abrasion and attrition using an uni-directional sliding test rig and an abrasive slurry. A stylus with an enamel tip was moved across a test material and the vertical load was increased and then released after each pass of the test. It must be noted that with any test rig used it is difficult to fully simulate the oral conditions and represent the reality of the oral environment.

Figure 2.24: Attrition on the upper and lower teeth [4].

Erosion

Loss of dental tissue results in chemical damage on teeth, which is caused by the action of acids on the tooth surface. This can be termed erosion. The acids which cause erosion can have an endogenous or an exogenous origin [4].

The endogenous acids can enter the oral cavity by vomiting, reflux or regurgitation and are gastric acids. These acids gradually soften the enamel surface by dissociating the hydronium cation and anion of the acid. A reaction takes place where the phosphate and carbonate anion react with the hydronium cation which leads to the softening of enamel [4].

The exogenous acids are found in drinks and foods, as well as certain medications, which can lead to loss of dental hard tissue. The chemical properties of the drinks and food such as the pH and the concentration of acids in the consumable, conditions the amount of tooth loss [4]. The first signs of erosion on the enamel appear as demineralisation. Excessive erosion leads to extensive loss of enamel and in a severe form, the exposure of dentine [4].

The difficulty in simulating in-vivo erosion tests, have been outlined, due to the harsh nature and risks of the erosion tests and the ability to lose sound enamel [59], however a number of in-vitro studies on abrasion and erosion have been carried out [167-169]. A study carried out by Wiegand et al.[169] used acid softened enamel and carried out abrasion tests on a brushing simulator. It was concluded that acid soften enamel was influenced by the brushing load. In enamel, erosion and abrasion act in synergy in the wear processes. A study carried out by Hooper et al. [59] used an in-situ approach to study the effects of an acid challenge on enamel and dentine. Enamel and dentine samples were placed on a denture appliance and worn by volunteers for a period of 10-

days. The results showed a loss in material for both the enamel and dentine overtime, with considerably higher loss for dentine [59].

Figure 2.25: Erosion of the central incisors, which leads to thinning of the teeth [170].

2.9.2 Abrasion testing

A range of test equipment has been developed and trialled to study the wear of teeth and how contributing variables also affect the levels of wear [1].

To test surface engineered materials, the ball cratering test equipment is a popular choice. There are many advantages of the ball cratering test such as the ability to test thin coatings and small volumes of material. It is a cheap and easy to use machine. The wear volume and volume loss can be generated from the TE66 micro abrasion test equipment. Standards have been described by Gee et al. [150] on how to use the machine [150].

The TE66 test is affected by variation in the test conditions. The condition of the test ball and load can affect the type of wear that is observed. Polished balls vs. worn in balls can also affect the results. To eliminate the problem, running-in to surface treat the ball has been suggested. Ridging can be observed with inconsistent wear scars; ill-defined craters can be formed if the test load is too high or due to poor slurry entrainment and contact pressures. A certain point to note is preliminary tests carried out on the TE66 micro-abrasion rig showed good repeatability and reproducibility in the results [150].

The ball material in the TE66 micro-abrasion tests can vary, with many studies ([150-152, 156, 171-175] using steel and zirconia balls, due to the high hardness of the balls. Polymer balls have received criticism for their ability to make slurry entrainment difficult [176]. With this said, polymer balls are still a popular choice amongst several studies, due to their chemical stability [177-180]. When comparing the wear rate of glass using a nylon ball and a polypropylene ball it was found that the nylon ball produced a higher wear rate, due to the higher stiffness of the nylon ball compared to the polypropylene ball. The nylon ball caused the abrasive particles to exert a higher force on the glass and indent the glass [181]. Buchanan et al. [177] compared nylon balls with steel balls and found nylon balls to produce less variance in the data and produce higher wear rates than a steel ball. There was no predominant particle embedment with the nylon ball compared to the steel ball, hence higher wear rates were observed with the nylon ball [177]. Nylon absorbs water and this can change the mechanical properties of Nylon [182]. Gant and Gee [178] have praised the nylon ball in producing repeatable results, due to less embedment of abrasive particles in the ball. Nylon balls were reported to produce low scatter [178].

Previous tests using the micro abrasion rig examined the effects of abrasion on dental composites, such as amalgam and porcelain [183]. A test carried out by Chan et al. [183] compared dental restorative material wear rates of enamel and found that enamel had undergone brittle delamination. A later study carried out by Antunes et al. [184] compared abrasion resistance of dental composites. Antunes et al. [184] came to the conclusion that micro abrasion tests were suitable for the study of dental materials [184].

Pena et al. [147] compared the wear on enamel and dental composites using the micro-abrasion rig and slurries containing SiC (silicon carbide) particles with either water or artificial saliva. It was reported that the micro-abrasive rig was a robust piece of equipment to obtain accurate wear performance measurements of dental composites and enamel. The wear performance and tribological behaviour of enamel compared to the dental composites was different when using the SiC-artificial saliva slurry. A reason for this was due to the compatibility of enamel and saliva. A thin film covered the enamel with the SiC-artificial saliva slurry which helped to decrease the wear rate and protect the enamel. A higher wear rate was reported with enamel compared to the dental composites due to the brittle nature and low organic content of enamel. The inorganic resistance of the dental composites resulted in better wear resistance than enamel, even though the dental composites exhibit a lower hardness than enamel. Scratch tests were performed on enamel at different directions and respect was given to the anisotropic properties of enamel and the difference in mechanical results in different enamel directions. In the occlusal section of enamel,

brittle delamination was observed at higher loads. At lower loads the enamel was shown to plastically deform [147].

A study carried out by Adachi and Hutchings [148] developed a theoretical model of evaluating wear and mapped wear mode regimes of engineering surfaces. This study is now used as a bench mark for comparing results with other studies and serves as the starting point for reference with future tests [148].

Due to the complexity of simulating oral conditions in the mouth, many attempts have been made to develop wear models that closely simulate the oral environment [1]. Wear test machines such as the pin- on disc and unidirectional sliding rigs have been previously used to study abrasion of tooth materials. Furthermore, simple models such as glass discs connected to toothbrushes using hydraulic actuators to represent the toothbrusing action have also been used to simulate the toothbrusing action [185, 186]. Many of the wear tests using the test rigs above, have assed wear on dental restorative materials to find restorative materials that would similarly replicate the mechanical and physical properties of the natural tooth structure [147].

The Phoenix reciprocating tribometer is a well-established research and development tool for the study of materials and lubricants. It has been used extensively for the development of coatings, metals, steels and ceramic composites. It has the ability to measure friction and wear properties, as well as high speed data acquisition for high and low frequencies <1KHz. It has an adjustable reciprocating arm which can be adapted for a variety of head designs. A shortcoming of the tribometer is the ability to only study reciprocating movements. Many conditions of the mouth can be matched using the TE77 reciprocating tribometer and it can represent the conditions in the mouth. It has a slurry feed which can represent the flow of saliva and toothpaste and a sample bath [187].

A study carried out by Lewis et al. [6] used a high frequency rig to look at the effect of abrasive particles on PMMA, during tooth brushing. The test models were praised and the results from the test were consistent with other research carried out on dental restorative materials [6].

Another study carried out by Popa et al. [188] used a simplified model of enamel and a toothbrush submerged in a slurry of silica, to reproduce the tooth cleaning motion. A novel tribometer was used to provide the reciprocating movements. Samples of glass were used to simulate human enamel [188].

To simulate the brushing conditions in the mouth and enable reliable predictions of wear on the enamel surface, a TE77 high frequency friction tribometer will be used, with a modified head design

to hold the toothbrush in place. An improved and superior rig developed by GSK and manufactured by Phoenix Tribology will later be used to replicate the brushing actions. This rig will enhance the test and allow reliable wear predictions to be made, improving on results from previous investigations.

2.9.3 Modelling of material removal

Modelling of material and stain removal can be challenging, due to the multi-factorial process of tooth wear. In the oral cavity, the stain layer can be attached to the acquired pellicle or the dental biofilm or directly to the dental enamel. Many test have been carried out in-vivo to investigate the removal of extrinsic stain on the tooth tissues by oral products. Many approaches have also been taken in-vitro to model stain removal. Many model stains such as wine, tea and coffee have all been used. A test that has been widely used is staining a polished and etched bovine tooth with either a stain of coffee or tea. The stained bovine disk is then brushed, using an abrasive dentifrice for a period of time using a brushing tester [189]. One of the limitations of the staining protocol is the bond strength between the stain and the substrate (such as bovine enamel). Weak bonding of the stain results in a stain layer which is not adequately bonded. Also, different cleaning regimes employed and the use of bleaching toothpastes and different abrasive toothpastes results in a lack of standardisation between the results obtained. Another issue is the application of a stain layer to the enamel surface. Applying a stain can take a prolonged amount of time to achieve the desired stain build- up. To provide results which have clinical significance it is important to model stain behaviours and interactions with natural enamel [189].

A study conducted by Wang et al. [189] developed an in vitro model for stain removal using bovine enamel and abrasive toothpastes. The stain used was ferric-tannate deposits due to the good stain retention and the easy preparation of the stain. The stain was also selected due to its ability to be sensitive to toothbrusing using an abrasive dentifrice. Commercially available toothpastes were used and the specimens were brushing on a tooth-brushing simulator. The stain was measured before and after the brushing tests using a spectrophotometer to study the specimen surface finish and the amount of stain removal. Comparisons were made between whitening toothpastes and non-whitening toothpastes. A 27% reduction in stain was obtained with the non-whitening pastes, compared to 59% stain removal with the whitening pastes after 1000 brushing strokes [189].

A model for stain removal has been developed by Lewis and Dwyer-Joyce [7]. The model uses silica particles in an abrasive cleaning approach for stain removal. To calculate the scratch depths and the amount of material removed, a theoretical model was used which looked at scratch depths

during particle indentation. To determine the number of scratches and the length of the scratch the scratch data was used. To validate the model, data collected from the literature was referred to [7].

A micro-indenter approach was assumed for the model via a particle being trapped by a filament tip. The silica particles used were assumed to be cubes. They were predicted to indent the specimen on one corner.

Many factors were considered such as the filament drag, the material loss/ displaced, elastic recovery in the scratch and the amount of trapped particles in the filaments that were cutting the specimen.

An equation was derived for the volume loss of material per brush stroke, V_b, Equation 2.2.

$$V_b = NbtA_sgfls \quad \text{...Equation 2.2}$$

N is defined as the total number of filaments, b is the number of filaments that contact the specimen, t is the proportion of the filaments that are in contact with the trapped particle, g is the cross-sectional area of the indentation, A_s is the elastic recovery and elastic deflection, f is the amount of material that has been lost as wear debris, l is the length of the brush stroke and s is the length of the scratch/ length of the brush stroke.

Scratch data was taken from a study on elastic deflection which was carried out by Jardret et al. [190] which obtained values for g and f.

The scratch area, A_P was also considered for the tests. the scratch area was calculated using the geometry and depth of the particle and the scratch width, w. With the assumption that the depth of the scratch is sufficient to penetrate through the stain layer, the stain removal area in one brush stroke, A_P, was calculated using Equation 2.3:

$$A_P = Nbtwls \quad \text{...Equation 2.3}$$

It must be noted that the amount of strain removal will not be the same per brushstroke as time progresses, as the level of stain will decrease during the test. With each brushing stroke, the amount of stain removal will be decreased. To accommodate this, the stain removal test was run for 15 second intervals. The amount of stain removal was calculated for the first test. For the second test the test result was multiplied by one minus the amount of stain removed in the first test [7].

The depths of material removal and scratch widths are dependent on the orientation and shape of the particles and the cutting of the particles. The model employed by Lewis and Dwyer- Joyce [7]

used silica particles that were shaped as cubes. it was noted that some filaments have no particles trapped in the filaments which results in stain removal by a small proportion of filaments [7].

2.10 Conclusions

In this chapter, a brief introduction on the structure of the tooth was presented. A review on the cleaning mechanisms of teeth were summarised and the fundamentals of biofilm formation and removal were discussed. Research on factors such as the composition, rheology and abrasive nature of the dentifrice was carried out. The interaction between the particles found in a dentifrice was described with special attention given to the abrasive nature of the particles. The role of the toothbrush in wear was detailed with factors such as the filament characteristics being highlighted. The main variables that lead to tooth wear have been discussed in detail. This serves as the foundation for the thesis and outlines the research progress in this fields.

The BS EN ISO 11609:2010 standards for dentifrices were summarised and methods for testing abrasivity of dentifrices were detailed [83].

An introduction to the topic of tribology of teeth cleaning was presented with wear mechanisms being discussed. It must be noted that enamel is a tissue and engineering approaches may differ for biomaterials. Many different disciplines need to be integrated to understand the science behind the interface of the tooth, toothbrush and toothpaste.

The various test rigs used in previous research, to measure wear rates of dental tissues were introduced and highlighted.

Each of these subjects is well established fundamentally. The oral cavity is a multifactorial complex environment and it is necessary to understand that many variables have the ability to affect tooth wear.

The addition of biofilms in abrasion testing has not been carried out intensively, due to the difficulty in applying and producing the biofilm on the enamel surface. It has been proven difficult to assess the wear damage with the addition of a biofilm and the amount of tissue removal. Another area that has not been researched extensively is the shape and profile of the tooth. A reason for this could be the difficult in obtaining certain teeth and the ethical approval for human teeth. Characteristics of a tooth such as the roughness has been understudied due to the lack of standardisation in roughness values and the difficulty in taking roughness measurements, due to the surface irregularities of the tooth [191].

The priority of this study is to investigate the most influential tooth brushing factors that affect enamel wear in the oral cavity.

From the literature review it was concluded that finite research has been carried out in the following areas:

- Understanding the abrasive nature of particles in a toothpaste and how factors such as the size, hardness and concentration of the abradant has an effect on wear rates of enamel.

- A study on the main variables influencing tooth wear has not been performed. Factors such as the filament tip shape, ability of the filament to carry the abrasive, texture of the filaments and the stiffness of the filaments needs to be investigated thoroughly.

- Investigating new methods to model and simulate enamel wear.

- Understanding the wear mechanism taking place during tooth brushing. More research is needed in understanding the role of the toothbrush during tooth brushing.

Therefore this PhD aims to bridge the gap between existing research and the research areas listed above, which are vital in understanding the science behind the interface of the tooth and toothbrush, lubricated by the abrasive slurry.

3. Materials and methodology

3.1 Introduction

This chapter describes the experimental methodology, including the sample materials used, the material preparation and characterisation, the rig design and modification, the test mechanisms used and the experimental procedures employed to understand the wear behaviour of enamel.

It also reviews additional techniques used for post-test analysis such as the Saturn DigiSizer for particle size analysis, Talysurf profilometer, micro-indentation, nano-indentation and various microscopic techniques such as the Alicona microscope and scanning electron microscopy (SEM).

3.2 Materials

3.2.1 Bovine teeth

The present study was approved by the research ethics committee for the University of Southampton – GlaxoSmithKline to use bovine teeth for the present research.

Using human teeth for in vitro studies has many drawbacks; gaining ethical approval by the research committee is difficult and can take a long duration of time. Human teeth are available in many different shapes and forms and it is difficult to standardise them. To obtain human teeth of the correct size for studies is difficult. For this reason many studies now employ using bovine teeth as a substitute for human teeth [192] .

Bovine teeth are readily available and can be acquired easily. They are an acceptable substitute for human teeth and are approved by the ethical board [193]. More control can be taken over the quality and age of bovine teeth when using them for studies. The size of bovine teeth allows them to be easily handled, unlike human teeth which are smaller in size [194].

Studies [192, 195-197] investigating fracture resistance, shear bond strength and microbiological properties have used bovine incisors as a substitute for human teeth and the results have been successful. Bovine teeth have been accepted as an industry standard [192].

Previous studies [198-201] found the enamel thickness, radio-density and the hardness of dentine is similar in both human and bovine teeth [192]. Bovine enamel discs, 25mm in length and 5mm thick, mounted in epoxy resin were supplied by GlaxoSmithKline. The enamel discs were prepared from central incisors of cattle aged between 5-6 years.

Table 3.1 shows the comparison of human and bovine teeth.

Table 3.1: Comparison of human and bovine teeth.

	Human teeth	**Bovine teeth**
General	Not readily available. Extracted due to extensive caries lesions or wisdom teeth. Ethical consent is required. Difficult to obtain sufficient quantity and good quality.	Readily available in large quantities. Accepted as industry standard.
Micro- morphology	Higher distribution of dentine [202]	More uniform composition Larger diameter of crystallites [203]
Chemical composition	Calcium by weight – 36.8 % [204]	Calcium by weight – 37.9 % Calcium distribution more homogeneous [204]
Physical properties	Small and curved surface	Relatively large flat surface [201] Higher radiographic density [205] Higher micro- hardness [201]
Dental abrasion	No difference in abrasion results [206-209]	

3.2.2 Toothbrush

The toothbrush being used for the study was the Tek Pro® firm toothbrush (Manufacturer – Dr Fresh, U.S.A, company- ProTek®), Figure 3.1 . This is a generic hard graded toothbrush, with a flat geometry (uniform filament length) and filament design. The choice of selection for this toothbrush was due to the flat filament design (geometry) of the brush, which would result in all the filaments contacting the bovine surface evenly at any one given time. The toothbrush head was cut off the handle prior to the wear tests. Figure 3.2 shows the deflection of the Tek Pro® firm filaments with load. No pre-soaking of the filaments was carried out before the wear tests.

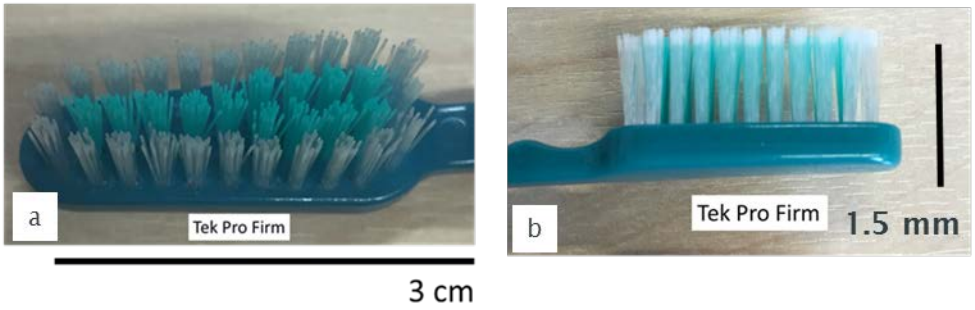

Figure 3.1: Tek Pro® firm toothbrush (a) top view; (b) side view.

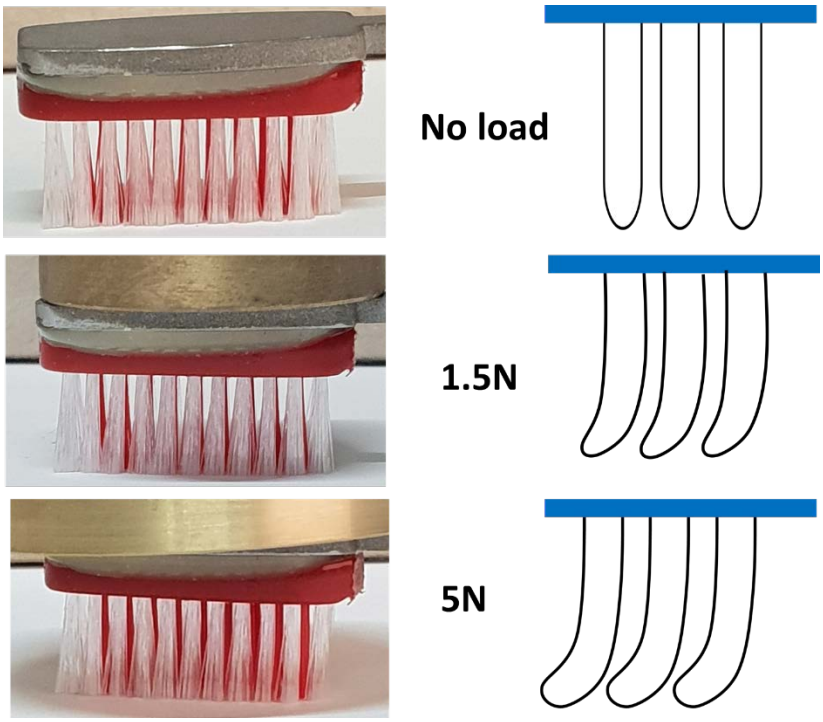

Figure 3.2: Deflection of filaments with load.

3.2.3 Abrasive particles

For the tests, nine types of abrasives with different sizes and size distributions have been used for this study. The specification and size range of the particles are shown in Table 3.2. The different sizes of the particles were used to look at the size effect of abrasive particles on the wear volume and wear rate of enamel. The particles selected for the tests where alumina and silica particles, which are the most commonly used abrasives found in toothpastes [210]. Spherical particles are often avoided to be incorporated into toothpastes, due to the spherical nature of the particles and the increased cost in including them in toothpastes. The average size of particles in toothpaste range from 4µm – 12µm. The particles were selected to cover the smallest and largest size of the particles in toothpastes.

The abrasive particles used in the wear test carried out by Adachi and Hutchings [148] were silicon carbide particles (SiC) that had a mean particle diameter of 4.3 microns [211]. Many tests, [171, 173, 178] have gone on to use silicon carbide as an abrasive in micro-abrasion tests [148]. A study carried out by Gee et al. [212] found that reproducibility and excellent test repeatability was given with these particles [212]. Table 3.2 shows the abrasive properties and suppliers for the particles.

Table 3.2: Specification of the abrasives used in this study.

Particle	Mean size and distribution/ µm	Maximum size /µm	Supplier
Alumina 1µm	1 ± 0.46	1.79	Logitech, UK
Alumina 5µm	5 ± 2.08	8.1	Logitech, UK
Alumina 9µm	9 ± 2.01	10.2	Logitech, UK
GSK 9µm alumina	9 ± 2.69	10.4	Almantis, USA
Silica 5µm	5 ± 8.26	23	US Research Nanomaterials, USA
Silica 10µm	10 ± 7.47	28	US Research Nanomaterials, USA
GSK 8µm silica	8 ± 2.67	9	Huber, Germany
5µm Spherical silica	5 ± 1.10	6.1	Sanyo Trading, Tokyo
GSK 6.5µm spherical silica	6.5 ± 1.25	8.8	Sanyo Trading, Tokyo

3.2.4 Artificial saliva solution

Using artificial saliva substitutes is acceptable for wear tests, as the interaction of artificial saliva with the bovine tooth tissues, is that which would normally take place in the mouth. However, it must not be overlooked that human saliva is very difficult to completely produce and serves many complicated biological processes in the mouth. Many wear tests carried out [32-34, 213] have used

artificial saliva as a substitute for their tests and it has proved a successful substitute for human saliva.

The artificial saliva solution was prepared according to the following recipe as described by Fusaya-Meyer, shown in Table 3.3 [160, 214]. This composition of artificial saliva, closely resembles natural saliva [31]. A pH meter was used to measure the pH three times to ascertain the repeatability. The artificial saliva was used as the base for micro abrasion tests.

Table 3.3: Composition of artificial saliva solution [160, 214].

Ingredients	**Quantity g/L**
NaCl Sodium chloride	0.40
KCl Potassium chloride	0.40
$CaCl_2$ Calcium chloride	0.60
$Na_2HPO_4.12H_2O$ Sodium dihydrogen phosphate dodecahydrate	0.58
CH_4N_2O Urea	1
$C_8H_{16}O_8$ Carboxymethyl cellulose (CMC)	5
$C_3H_8O_3$ Glycerol	50
Buffer **Phosphate buffer**	10
pH	6.5

3.3 Experimental techniques used

3.3.1 Preparation of bovine discs

A method of grinding and polishing that is identical for all the samples has been carefully applied. An automated Struers polishing machine (Tegra-pol 15, Struers Ltd, UK) was used to ensure consistency of results. The bovine discs were prepared according to the guidelines provided by Struers, Table 3.4. Struers advised in the preparation route and consumables needed to provide a mirror finish to the bovine discs. The quality and consistency of preparing bovine discs will determine the accuracy of the wear results.

To remove damaged/ deformed material from a surface grinding was carried out. The purpose of grinding was to achieve a planar surface. Plane grinding is the first process in the polishing procedure. It makes sure all the surfaces are similar in condition. This is then followed by fine grinding which results in a minimally deformed surface which can be removed via polishing. Fine abrasive particles are used for polishing. To remove the damage caused by grinding, polishing is carried out using fine abrasive particles. To achieve a plane surface and removal of material. diamond is employed as the abrasive.

Oxide polishing is the final step in achieving a deformation- free surface and can be used for soft, hard and ductile materials. This gives the best quality, scratch free surfaces. Oxide polishing is gentle and it has been reported that 0.04 µm colloidal silica gives the best results [215]. Smooth bovine enamel was used for the wear tests to allow comparisons of wear and roughness to be made before and after the wear tests. Smooth bovine enamel was used as a baseline. To ensure accuracy of the wear result measurements, the bovine disks were prepared to a smooth planar surface.

Figure 3.3 shows where the bovine tooth was cut to produce the enamel disc. The bovine enamel disc is shown in Figure 3.4 .

Before the wear tests, the bovine enamel discs were hydrated in artificial saliva solution for 24 hours, to reach maximum hydration.

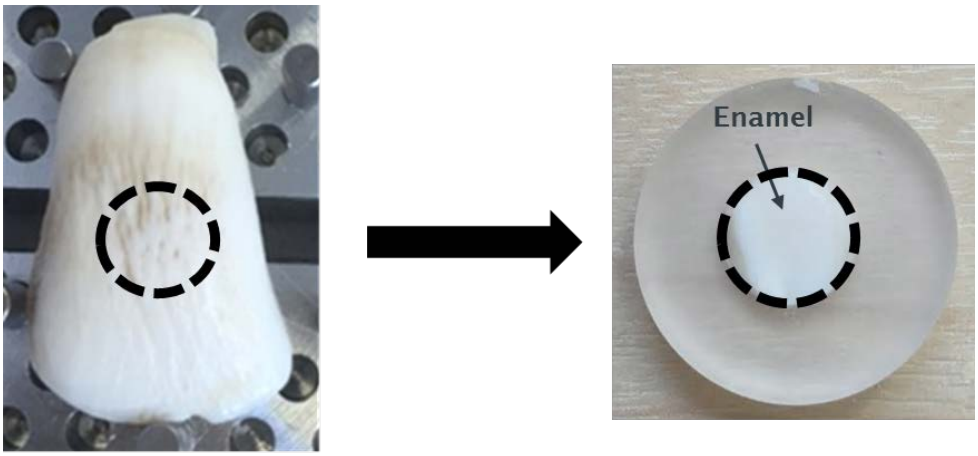

Figure 3.3: Position of bovine tooth cut for an enamel disc.

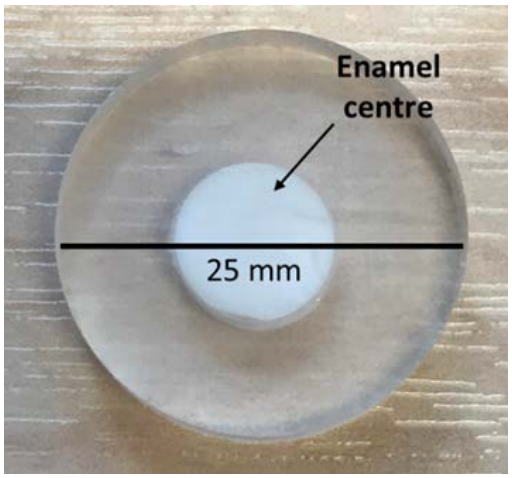

Figure 3.4: Bovine enamel disc mounted in epoxy resin supplied by GSK.

Table 3.4: Tailored preparation procedure provided by Struers for bovine teeth.

Grinding				
Step	**Plane grinding**	**Fine grinding 1**	**Fine grinding 2**	**Fine grinding 3**
Surface	SiC foil #320	SiC foil #500	SiC foil #1200	SiC foil #4000
Abrasive type	-	-	-	-
Lubricant type	Water	Water	Water	Water
Speed / rpm	150	150	150	150
Force / N	20	20	20	20
Holder direction	>>	>>	>>	>>
Time / minutes	01:29	02:59	02:59	02:59
Polishing				
Step	**Plane grinding**		**Fine grinding 2**	
Surface	MD- Nap		MD- Chem	
Abrasive type	DiaPro Nap R 1µm		OP- U, 0.04µm	
Lubricant type				
Speed / rpm	150		150	
Force / N	15		10	
Holder direction	>>		><	
Time / minutes	04:28		02:59	

The removal of scratches depends on the size of the scratch and the particle size of the abrasive papers, Table 3.5.

Table 3.5: Particle size of the abrasive papers.

Step	Abrasive paper	Particle size (µm)	Lubricant
Plane grinding (PG)	SiC #320	46	Water
Fine grinding (FG)	SiC #500	35	Water
Fine grinding (FG)	SiC #1200	18	Water
Fine grinding (FG)	SiC #4000	5	Water
Polishing (P)	Nap polishing cloth	1	Diamond paste
Oxide polishing (OP)	Chem cloth	0.04	Colloidal silica

3.3.2 Particle characterisation

Saturn DigiSizer

The particle sizes were analysed using the Saturn DigiSizer (Micromeritics®, USA V1.02). The Saturn DigiSizer can detect particle sizes ranging from 40 nm to 2.5 mm, making it an ideal choice of equipment to measure the abrasive particles. This instrument uses light scattering analysis to measure accurate particle sizes. This is coupled with three million detector elements, making it highly sensitive and enabling it to collect high-resolution data. The high resolution allows detection of differences in scattering patterns between the samples and therefore is able to detect subtle differences in particle size distributions. This allows greater in-depth knowledge about differences in size distributions.

A MasterTech 052 unit is connected to the Saturn DigiSizer and acts as an automatic sampling device. An ultrasonic probe was activated to avoid particle aggregation and assist in particle re-dispersion, before the sample was transferred into the Saturn DigiSizer for analysis [216].

3.3.3 Surface profilometry

Alicona Infinite Focus Microscopy

The Alicona G4 microscope (IFM 2.1, Infinite Focus, USA) is a 3D optical profilometer microscope used to measure surface form and roughness, by taking a series of images in the vertical axis and then applying a transform on adjacent images to determine the relative height location of features, thus building a 3D topology. It is equipped with 5 lenses (2.5x, 5x, 10x, 20x, 50x and 100x) and can measure 3D surface roughness, volume and surface profiles. The Alicona microscope was used to analyse the abrasive particles and scan the surfaces of the teeth before the wear tests. The Alicona was also used to examine toothbrush filaments and determine the thickness of enamel. The 2D measurement tool allowed the filament morphology to be studied in detail as well as to accurately measure the Vickers indents [217].

Scanning Electron Microscope (SEM)

A JOEL model JCM 6000PLUS benchtop scanning electron microscope (SEM) was used to investigate the topography of enamel, characterise the filament tips and abrasive particles. The SEM was also used to provide information on the wear mechanisms, after the wear tests. Gold coating was used to sputter on the bovine discs and toothbrush filaments to provide a thin layer of conductivity. The advantage of SEM over optical microscopy, is the large field depth which can image surfaces with high roughness and the high resolution (60, 000X). The SEM works by emitting electrons via a field emission gun at high energies (1 KeV and 30 KeV). The beam is collected by the electromagnetic condenser lens and focused using an objective lens. Deflection of the beam takes place by scanning coils over the sample surface. A cathode ray tube is scanned across the screen and this displays the image on the screen. The detector amplifies the current which modules the brightness of the SEM [218]. The microstructures were examined at an operating distance of 15Kv and a working distances of 10mm – 11mm.

Talysurf

The Talysurf (Taylor- Hobson Form Talysurf 120L) is a robust and precise contact surface profilometer that allows accurate surface profile measurements to be recorded. Figure 3.5 shows the Talysurf profilometer. The Talysurf Form 1202L consists of a stylus profilometer with a standard 2 µm radius diamond stylus. The stylus travels vertically across a sample and records surface measurements such as surface finish, form, roughness and contour. Calibration of the profilometer is carried out on a semi-sphere ball, Figure 3.6.

Figure 3.5: Talysurf contact surface profilometer.

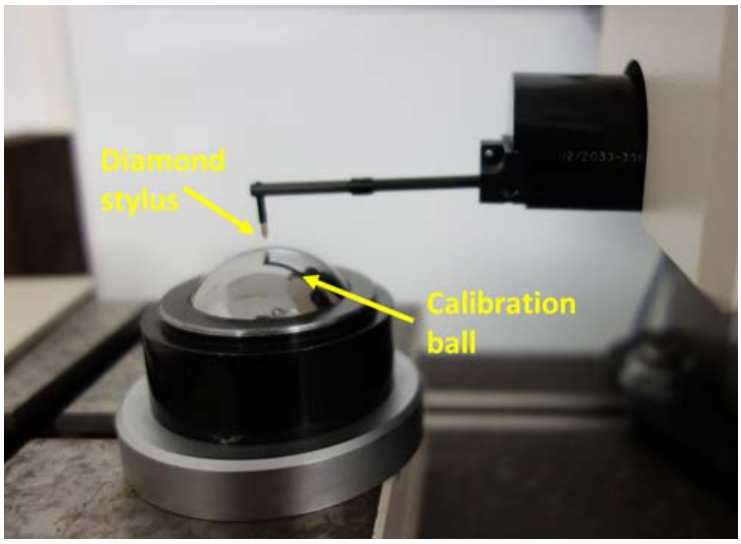

Figure 3.6: Calibration ball.

A profilometer can measure small surface variations in vertical stylus displacement as a function of position.

The Talysurf allowed the changes in topography to be recorded before and after the wear tests by measuring small surface variations (scratches) on the surface of the bovine discs. This allowed wear depth comparisons to be made and any deformation of the bovine surface to be measured. The baseline measurement (initial. 0hr) was taken after the hydration technique on the bovine discs and during the wear tests, profile measurements were taken at selected time intervals (2hr, 4hr and 6hr). For the present study all the profile measurements were taken using the same method. The Talysurf provides confidence for quantitative evaluation and comparison of the surface profiles before and after the wear tests.

The average wear depth was calculated by subtracting the wear after the test to the original start data. In order to calculate the mean and standard deviation values of roughness (Ra), skewness (Rsk), valley depth (Rv) and total height of profile (Rt), five profile measurements were taken in a perpendicular direction to the brushing direction, Figure 3.7. The data length was set to 4.8mm and lc (bandwidth) filter cut off length was selected according to the ISO 4288:1966 standard [219]. The vertical accuracy was 2nm.

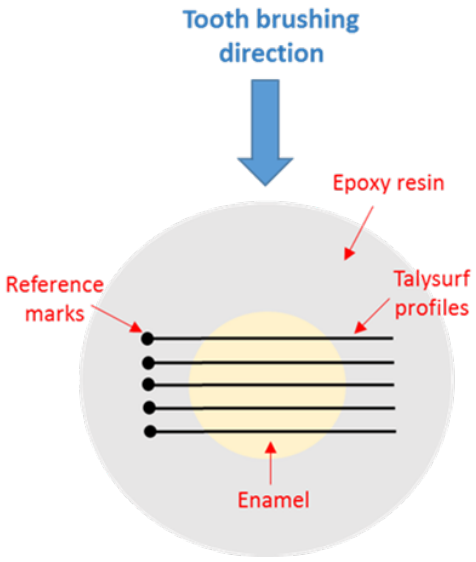

Figure 3.7: Talysurf profile measurement set-up.

3.3.4 Microstructural characterisation

Hardness testing

The nano-indenter was used to produce a hardness map of the tooth and to determine whether there was a significant difference in mechanical properties of the tooth tissues. A nano-indenter was used (NanoTest Vantage, MicroMaterials) with a diamond Berkovich (3-sided pyramid) indenter tip. The Berkovich indenter is the most commonly used indenter geometry in nanoindentation [15]. Table 3.6 shows the test parameters used for the depth controlled indentation.

Table 3.6: Parameters used for depth controlled indentation.

Parameters	
Initial load (mN)	0.05
Cut off load (mN)	0.05
Loading and unloading rate (mN/s^{-1})	5.0
Maximum depth (nm)	1000
Dwell time at maximum depth (s)	30
Number of indents	400
Spacing between each indent (µm)	50

The bovine tooth was sectioned so that three planes were visible; longitudinally, side-view and the top-view, Figure 3.8. A series of 400 indents were made on each plane, Figure 3.9. The mechanical properties such as the reduced modulus, elastic recovery and hardness of the tooth were mapped.

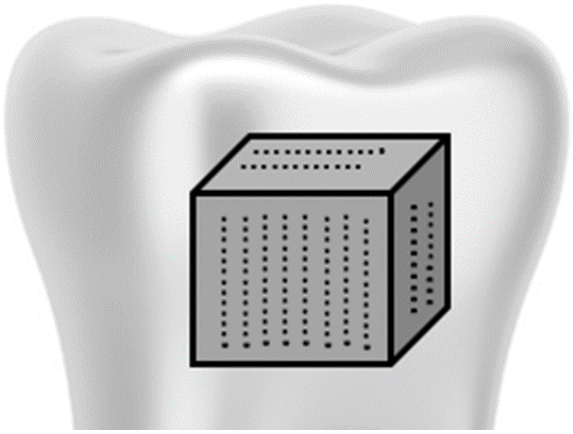

Figure 3.8: Bovine tooth sectioned so that three planes are visible. Nano-indentation carried out across the three planes of the bovine tooth.

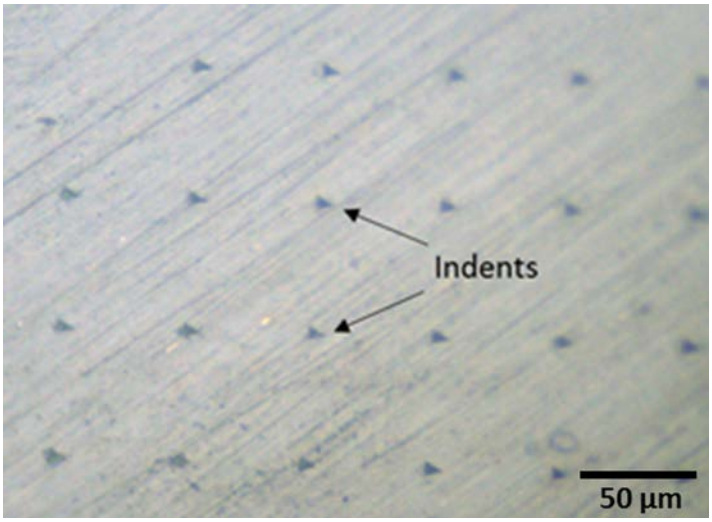

Figure 3.9: Nano- indents on one plane of the bovine tooth.

Scratch testing

To study the mechanistic wear behaviour of enamel, multi-pass scratch tests were performed on hydrated bovine enamel using the nano-indenter. A hydrated bovine disc was nano-scratch tested using a 5µm spherical diamond tip, and loads of 20mN, 50mN, 80mN and 100mN to observe the mechanical response of enamel. Table 3 7 shows the parameters used for the multi-pass wear tests.

Table 3 7: Parameters used for multi-pass wear tests.

Parameters	
Scanning velocity (µm/s)	16.66
Scanning length (µm)	500
Number of passes	3
Number of scratches per topography	1
Scratch load (mN)	20, 50, 80, 100
Loading rate mN/S	4.12
Unloading rate (mN/S)	0.001

Micro-indentation of hydrated and dehydrated teeth

The properties of enamel change with the storage conditions. Dehydration of human teeth can result in brittle behaviour and decreased strain at fracture. Toughness of the tooth is also decreased with dehydration. The need to test fully hydrated teeth is vital as the mechanical properties of the tooth can change and the tooth is liable to crack. In the oral cavity the teeth are hydrated by saliva and oral fluids [220].

One bovine tooth specimen which had been stored in thymol solution at 5 °c for 24 hours was dehydrated by placing it in ethanol solution for 24 hours. The tooth was then removed, wiped free of ethanol and left to dry for 72 hours.

The dehydrated tooth was hardness tested using the Vickers hardness machine. A test load of 300g was used, for a test time for 20 seconds.

The dry tooth was weighed with an electronic balance (Genius, Sartorius ME2355) and immersed in water for 24hours to rehydrate. The progress of rehydration was followed gravimetrically. The bovine tooth was suspended in 20 mL of water and removed at regular intervals. The tooth was wiped free of surface water and weighed using an electronic balance after 30 minutes, 1 hour and then consecutively at hourly intervals up to 8 hours. Immediately after each weighing the bovine tooth was submerged in water again.

The percentage weight change of the hydrated tooth was calculated using Equation 3.1. Where W is the weight of the tooth.

$$\frac{W_{final} - W_{original}}{W_{original}} \; x \; 100 \qquad \text{...Equation 3.1}$$

Filament analysis

In order to count toothbrush filaments the Wild Makroskop M420 was used. It is a zoom microscope designed for low power high resolution work. The M420 has a trinocular head and is connected to a KC 1500 electrical light source. It has a zoom range from 6.2 to 32 times [221]. The tufts of the toothbrush were counted and the number of filaments in a tuft were recorded.

Nano-indentation of filaments

Nano-indentation was carried out in order to determine whether there was a significant difference in mechanical properties between the clear and coloured filaments of the Tek Pro® firm toothbrush. A nano-indenter was used (NanoTest Vantage, Micrometrics) with a diamond Berkovich (3-sided pyramid) indenter tip.

To differentiate between the properties of the coloured and clear filaments, a total of 24 filaments were indented; 12 clear and 12 coloured filaments on the toothbrush. For each filament, 3 indents were made, Figure 3.10. The nano-indentation tests were carried out at a fixed loading rate. The test parameters are shown in Table 3.8.

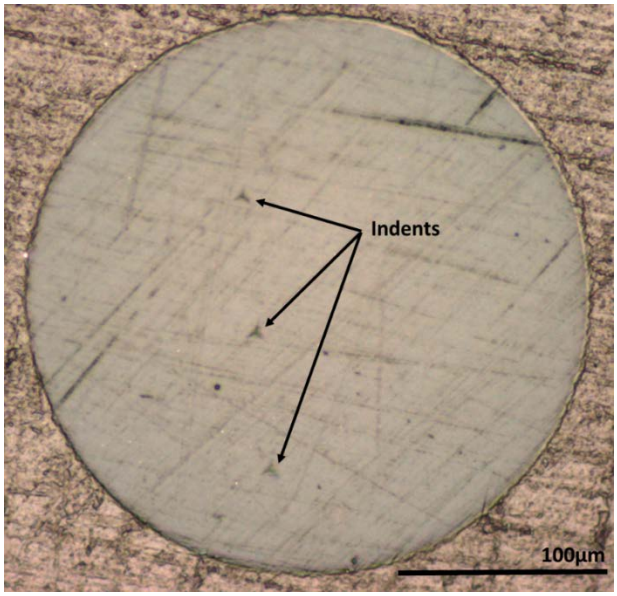

Figure 3.10: Three indents on a Tek Pro® firm clear filament.

Table 3.8: Parameters used for load controlled indentation.

Parameters	
Initial load (mN)	4
Cut off load (mN)	0.10
Loading and unloading rate (mN/s^{-1})	0.2
Dwell time at maximum depth (s)	60
Number of indents	3
Spacing between each indent (µm)	40

3.4 Slurry preparation

3.4.2 Abrasive slurry

The abrasive slurry solution was prepared according to the BS EN ISO 11609:2010 Dentistry-Dentifrice guidelines [83].

The base of the paste consists of 0.5% carboxymethylcellulose (CMC) in 10% glycerine. To prepare 1L of the paste, 50ml of glycerine is added to 5g of CMC. The mixture was allowed to stabilise by continuously agitating using a magnetic stirrer. Once the mixture was homogenous, another 50ml of glycerine was added. Finally, 900ml of distilled water was added. This is the reference diluent.

To prepare the abrasive slurry for the TE77 wear tests, 10 grams of the abrasive powder was diluted with 50ml of the reference diluent [83].

For the TE66 micro-abrasion tests, the slurry was based on a volume fraction approach. Equation 3.1 was used to calculate the mass of abrasives (g/ml) in the slurry solution. Table 3.9 shows the density of abrasives used to calculate the mass of abrasive, Table 3.10.

$$Mass\ of\ abrasives = Density \times Volume \quad \text{.... Equation 3.1}$$

Table 3.9: Density of abrasives.

Density	**g/cm^3**
Alumina	3.95
Silica	2.65
Spherical silica	2.196

Table 3.10: Mass of abrasives used in slurry solution.

			Mass of abrasive / g		
		Volume of slurry base / ml	**Alumina**	**Silica**	**Spherical silica**
Volume fraction of abrasives	0.05	95	0.20	0.13	0.11
	0.10	90	0.40	0.27	0.22
	0.15	85	0.59	0.40	0.33
	0.20	80	0.79	0.53	0.44

3.5 Test sequence

3.5.1 TE66 micro-abrasion tests

Micro abrasion tests were performed using the TE66 micro- scale abrasion rig (Phoenix Tribology, UK).The TE66 rig is a widespread robust tool which is used for many applications including bio-tribology. Tests carried out on the TE66 micro-abrasion rig are repeatable and robust and give good repeatability values which can be compared with other literature values. It has the ability to reproduce two-body and three-body wear.

A schematic of the test apparatus is shown in Figure 3.11. The coaxial shafts hold the ball and this is driven by an electric motor. A pivoted arm holds the specimen in place and loading of the ball to the specimen takes place by a dead weight. A peristaltic pump syringe feeds the abrasive slurry onto the contact interface of the ball [148].

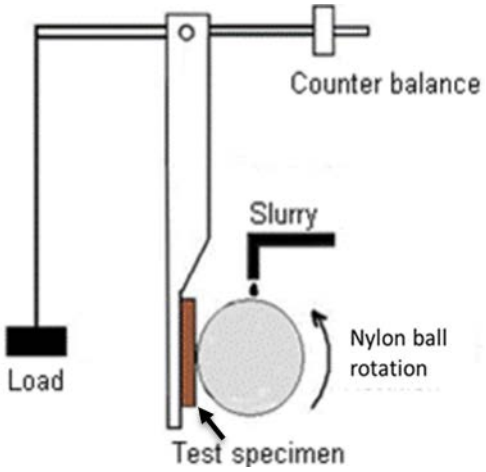

Figure 3.11: Schematic of TE66 micro- abrasion tester.

A rotating ball is loaded against the test specimen by dead weight loading and an abrasive slurry consisting of artificial saliva is fed through the interface of the ball and specimen, Figure 3.12.

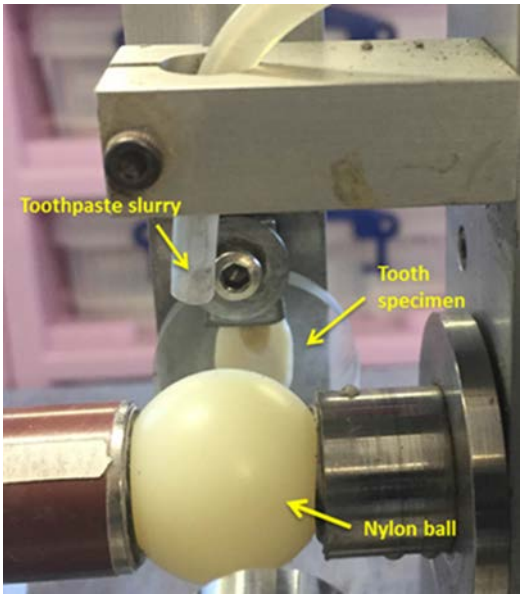

Figure 3.12: TE66 micro- abrasion rig set-up.

The specimens were prepared according to the test sequence in section 3.3.1. Before the tests, the bovine enamel discs were hydrated for 24 hours. A nylon ball (25.4mm diameter, Dejay Distribution Ltd, UK) was chosen for the tests to simulate the tooth brush material and due to the excellent test repeatability with a nylon ball. The nylon ball was conditioned by running multiple abrasion tests against the bovine enamel disc with 1.0 g cm^{-3} of alumina for 126m in distilled water.

A new ball was used for every change in particle type and the same run in procedure was repeated to condition the ball. The purpose of ball conditioning was to roughen the surface of the ball. A rough ball improves the particle entrainment process and gives good test repeatability. If at any point during the test the nylon ball appeared to be worn, it was replaced with a new ball [150].

The tests were performed at 3 loads of 0.1N, 0.2N and 0.5N. Eight repeats were carried out for each abrasive particle, resulting in eight craters being formed on the enamel. This was to determine the reliability of the wear scars. For each particle size and material. slurries were made with concentrations of 5%, 10%, 15% and 20% volume fraction of abrasive. All slurries were manufactured using artificial saliva which adhered to BS EN ISO 11609:2010 guidelines. An additional slurry was manufactured by mixing two mono-sized particles, 5 µm and 9µm alumina, or 5µm and 10µm silica, to produce a slurry with a bimodal particle size range. The test conditions are outlined in Table 3.11.

Table 3.11: Tests conditions for micro- abrasion tests.

Test conditions	Quantities
Load (N)	0.1, 0.2, 0.5
Speed (m/s)	0.035
Temperature (°C)	18
Volume concentration of abrasives (v/v)	0.05, 0.10, 0.15, 0.20
Slurry feed rate (ml/s)	0.125
Sliding distance (m)	2
Ball material	Nylon
Ball diameter	1", 25.4 mm
Abrasive particles	Alumina 1µm, Alumina 5µm, Alumina 9µm, GSK 9µm alumina, silica 5µm, silica 10µm, GSK 8µm silica, 5µm spherical silica, GSK 6.5µm spherial silica
Counterface material	Enamel
Time (minutes)	1

The wear scars were measured using an Alicona optical microscope in accordance with the guidelines set out by Gant and Gee et al. [212]. The wear mechanism was interpreted by scar analysis using the Scanning Electron Microscope (SEM).

Average groove width for the groove analysis was calculated by taking a mean measurement of the wear scar. Multiple groove measurements were taken and an average groove width was reported.

The wear volume was calculated using Equation 3.2 [11].

$$V = \frac{\pi b^4}{64R} \quad (b<<R) \qquad \text{...Equation 3.2}$$

where *V* is the volume of wear, *b* is the diameter of the wear scar and *R* is the radius of the ball. Using the Archard equation the specific wear rate *(K)* was calculated using Equation 3.3. Where *N* is the applied load and *L* is the sliding distance.

$$K = \frac{V}{LN} \qquad \text{...Equation 3.3}$$

To define where 2-body grooving and 3-body rolling abrasion, Adachi and Hutchings [13] mapped wear regimes. The wear mode is a function of two dimensional parameters, severity of contact (Sc) and the hardness ratio between the ball and the specimen.

To determine the wear- mode, the severity of contact, *Sc*, can be calculated Equation 3.4.

$$S_c = \frac{L}{AvH'} \qquad \text{...Equation 3.4}$$

where *L* is the applied load, *A* is the area of the wear scar and *υ* is the volume fraction of abrasives in the slurry.

A is given by Equation 3.5.

$$A = \pi\, a^2 + 2RD \qquad \text{...Equation 3.5}$$

where *a* is the Hertizan contact, *R* is the radius of the ball and *D* is the diameter of the particle.

The hardness ratio between the ball (H_b) and the specimen (H_s) is given by, Equation 3.6.

$$\frac{1}{H'} = \frac{1}{H_b} + \frac{1}{H_s}$$ …Equation 3.6

The average volume loss per particle was calculated using Equations 3.7 – 3.9. Where V is the volume loss.

$$Volume\ per\ particle = \frac{4}{3}\pi r^3$$ …Equation 3.7

$$no.of\ particles = \frac{volume\ per\ particle}{volume\ fraction\ of\ abrasives}$$ …Equation 3.8

$$V_{average}\ per\ particle = \frac{V_{average}}{no.of\ particles}$$ …Equation 3.9

The synergy volume loss was calculated using Equations 3.10 – 3.12. Where *V* is the volume loss.

$$Synergy\ V\ alumina = Bimodal\ 7\mu m\ V - (\frac{9\mu m\ alumina\ V}{2} + \frac{5\mu m\ alumina V}{2})$$ …Equation 3.10

$$Synergy\ V\ silica = Bimodal\ 7.5\mu m\ V - (\frac{10\mu m\ silica\ V}{2} + \frac{5\mu m\ alumina V}{2})$$ …Equation 3.11

The percentage synergy was calculated using Equation 6.4, 6.5 and 6.6.

$$\%\ syngery\ V\ alumina = \frac{Synergy V\ alumina}{Bimodal\ 7\mu m V}\ x\ 100$$ …Equation 3.12

$$\%\ synergy\ V\ silica = \frac{Synergy\ V\ silica}{Bimodal\ 7.5\mu m V}\ x\ 100$$ …Equation 3.13

3.5.2 TE77 reciprocating tribometer

The TE77 high frequency friction tribometer (Phoenix tribology, UK) is a well-established research and development tool for the evaluation of materials and coatings. It consists of a carrier system which mounts the moving specimen. Sliding contact conditions can be achieved with the tribometer. Oscillating movements of the specimen against the fixed lower specimen takes place mechanically. A motor driven cam makes up the mechanical drive which runs inside an oil bath. Adjustment of the cams allow the stroke length to be altered mechanically. A lever mechanism loads the moving specimen against the fixed specimen. The applied load was measured using a strain gauge transducer mounted on the load lever. The friction force was measured using a piezo-electric transducer with sensitivity of 45.7 pC/N. The force on the specimen is transmitted via a cam that is situated on the carrier head [187].

The reciprocating brushing movement is better simulated on the TE77 tribometer making it an ideal choice of equipment for the accelerated wear tests. With frequency values ranging up to 50 Hz and the variable stroke length settings, it is an appropriate tool to obtain wear and friction values for enamel.

Standard metallurgical procedures were used to polish the bovine surface to a 1µm roughness (Ra) finish. Prior to testing, the bovine discs were hydrated by immersion in a static saliva solution for 24 hours at room temperature. This was carried out to better simulate the conditions of hydrated teeth in the mouth.

Bovine discs were mounted on PVC plates using epoxy resin. A novel toothbrush head was manufactured for the wear tests and was secured on the arm of the TE77, Figure 3.13. In order to correctly locate the geometry of the slurry feed, a small amount of slurry was first applied to the test surface. A toothpaste slurry prepared according to the BS EN ISO 11609:2010 guidelines (Section 3.4.2) was drip fed via a feeding hose attached to a beaker. The slurry was continuously stirred on a magnetic stirrer to avoid particle agglomeration. Prior to sliding, the slurry feed was adjusted and allowed to stabilise. Two clamps were secured to the tubing to alter the feed rate of the slurry. The clamps were gently tightened to allow the desired feed rate. The lubricant bath had a drain which consisted of tubing, to feed out the used slurry. Fresh slurry was always fed through the interface of the disc and the toothbrush, Figure 3.14.

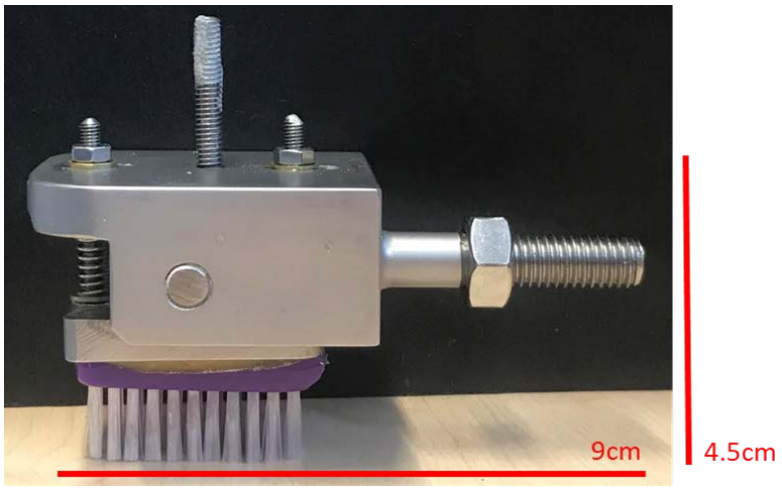

Figure 3.13: TE77 novel head design

Tests were stopped at test intervals of 120 minutes, cleaned with distilled water and profile measurements were taken with the Talysurf profilometer which allowed changes in topography of the bovine surface to be recorded during the test, by measuring small surface variations. This allowed wear depth comparisons to be made and any deformation of the bovine surface to be measured. The samples were placed in the same position and the test sequence run again.

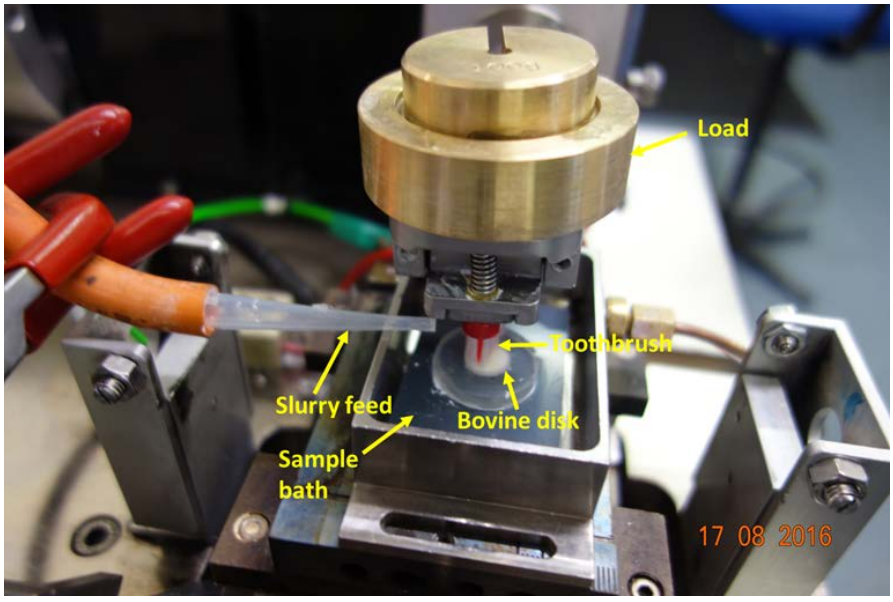

Figure 3.14: Test set-up.

The brushing load was set to 5N to simulate the maximum tooth brushing force applied orally in the mouth [19] and a cycle start- stop velocity programme commenced. Figure 3.15 shows a schematic of the orientation of the toothbrush to the bovine disc. The toothbrush was positioned over the bovine disc, so that the filaments contacted the majority of the enamel centre. The friction was continuously monitored throughout the test by a friction force transducer. The coefficient of friction for the tests was calculated by dividing the measured friction force (r.m.s signal from the piezo-electric transducer) by the normal load which was 5N in the present study. Tests were conducted with slurries containing GSK 9µm alumina + saliva base, GSK 8µm silica + saliva base, GSK 6.5µm spherical silica + saliva base and control saliva base. The total test time was 6 hours per test. The test conditions are outlined in Table 3.12. The oral speed for tooth brushing is between 1.5 - 2 Hz. The frequency was set to 4 Hz in the experiment to allow for an accelerated test. The stroke length was set to 4mm to cover the centre of the bovine disc, relative to the size of the bovine enamel centre.

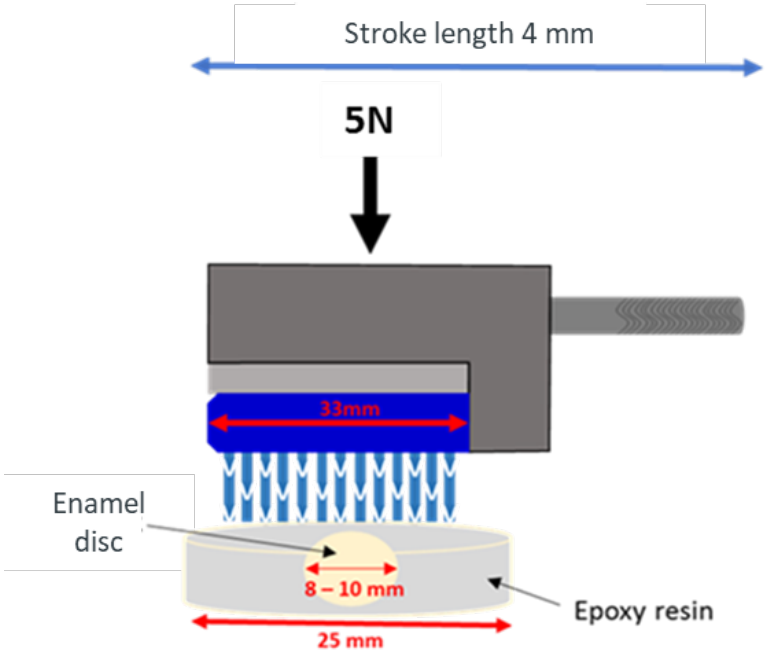

Figure 3.15: Schematic of the test set-up.

The test was repeated three times in order to obtain repeatability of data. Instantaneous high speed friction force data was captured every 10 minutes at 1 kHz, in order to determine the filament position along the stroke. Primary roughness data was collected from a data length of 4.8mm and cut off length according to the ISO standard. Three repeats for each tests were carried out.

A Scanning Electron Microscope (SEM) was used to analyse the wear mechanisms and changes on the bovine surface after the brushing tests.

Table 3.12: Test conditions for the brushing tests.

Test conditions	**Quantities**
Alignment of brush head to bovine disc	Horizontal
Load / N	5
Frequency /Hertz	4
Stroke length /mm	4
Slurry concentration (g/cm^3)	0.5% Carboxymethyl cellulose (CMC) + 10% Glycerine (base) + 20% abrasive (in accordance to BS EN ISO 11609:2010 Dentistry guidelines for abrasive testing slurry solutions) [83]
Counterface material	Enamel disc

The volume loss of enamel was calculated using Equation 3.16. Where *V* is the volume loss. The unworn bovine surface was considered as the datum (reference surface). The wear depth was calculated using the datum and the final measurement of the worn enamel (R_v) after the wear test.

$$V = wear\ depth\ x\ cross\ sectional\ area \quad \text{....Equation 3.16}$$

The specific wear rate of enamel was calculated using Equation 3.17. Where SWR is the specific wear rate, *V* is the volume loss (from Equation 3.2) , *L* is the sliding distance and *N* is the applied load.

$$SWR = \frac{V}{LN} \quad \text{....Equation 3.17}$$

4. Material characterisation results

4.1 Introduction

To understand the behaviour of the test materials, it is vital to connect the material properties that could potentially influence the wear of enamel. This chapter describes the mechanical properties, microstructural and topographical characterisation of the test materials. It brings together the bovine tooth characterisation, toothbrush chemistry and particle size and morphology. A brief discussion on how these parameters affect the wear rate of enamel is presented at the end of the chapter.

4.2 Bovine specimens

Due to the variations in the bovine teeth, bovine discs were used that were consistent and homogeneous. The discs had a circular enamel centre embedded in epoxy resin, Figure 4.1a. The discs measured 25mm in dimeter with a depth of 4mm, Figure 4.1b.

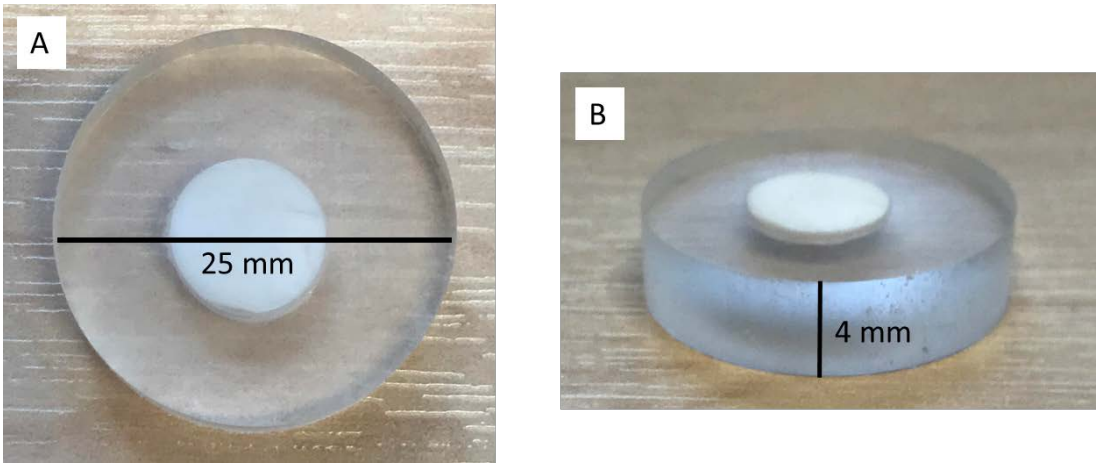

Figure 4.1: Enamel bovine disc (a) diameter; (b) depth.

The unpolished bovine specimen was placed under the Alicona microscope before the polishing procedure. Figure 4.2a shows the unpolished sample. Scratches in the region of 13 µm were present. The bovine surface was very rough with an average Ra value of 3.86µm. After the polishing procedure, the bovine specimen had significantly less surface scratches with an average Ra of 0.14µm. The bovine discs were polished to a 1µm finish. Figure 4.2b shows the polished bovine disc.

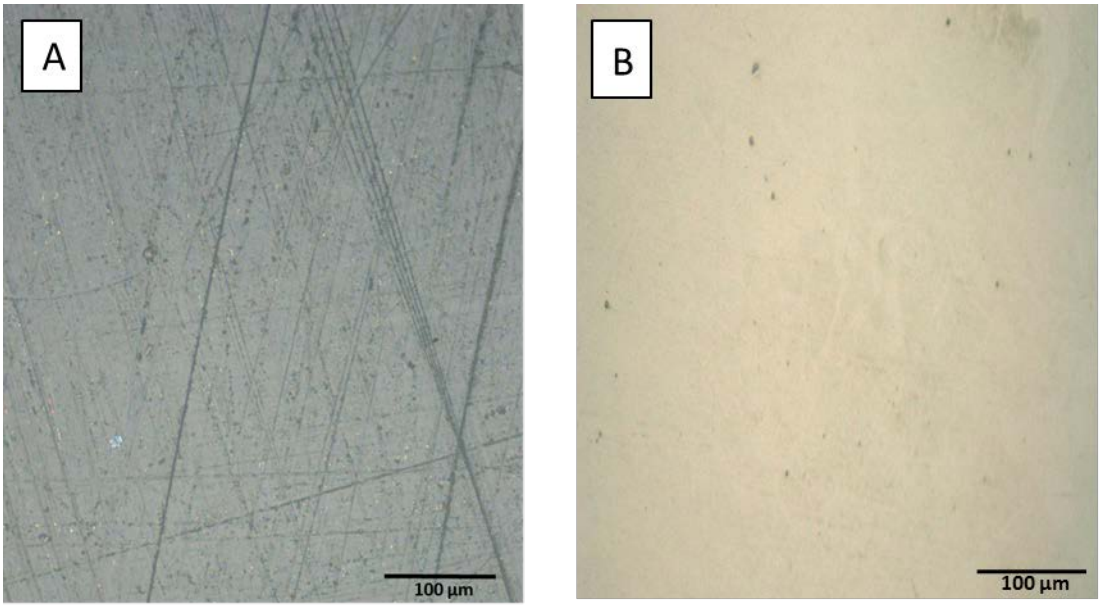

Figure 4.2: Bovine disc surface (a) unpolished; (b) polished.

4.2.1 Enamel thickness

To measure the enamel thickness, a polished bovine disc was sectioned horizontally and placed under the Alicona microscope, Figure 4.3a and Figure 4.3b.

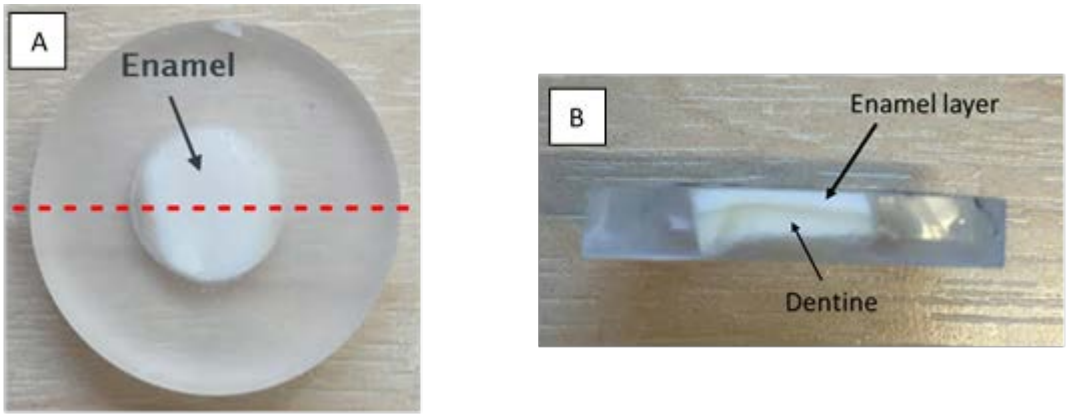

Figure 4.3: Bovine disc (a) bovine disc front view (b) sectioned bovine disc.

The measurement analysis function on the Alicona non- contact microscope was used to measure the thickness of enamel. Figure 4.4a shows the enamel and dentine layer. 15 readings were taken across the enamel surface, Figure 4.4b.

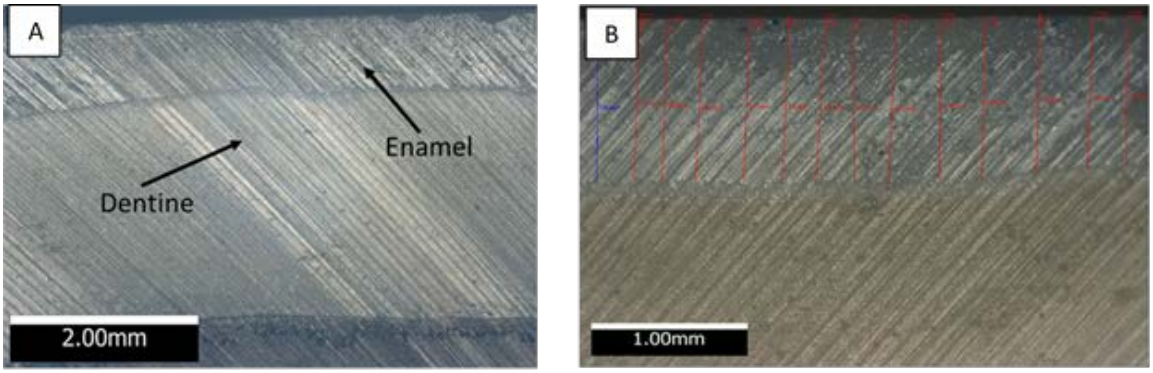

Figure 4.4: Cross section of bovine disc (a) Enamel and dentine; (b) enamel measurements.

The mean thickness of enamel is 839 µm with a standard deviation of 71 (n=15).

4.2.2 Enamel structure

As introduced in chapter 2, enamel has an anisotropic structure and differences in mechanical properties are reported with the location and arrangement of the enamel rods. The bovine enamel discs were etched with 37% phosphoric acid for 45seconds and rinsed with distilled water to observe the direction of the enamel rods. The enamel rods have a key hole structure with a distinctive head and tail. Figure 4.5 shows the enamel prism orientation from the facial side of a central incisor.

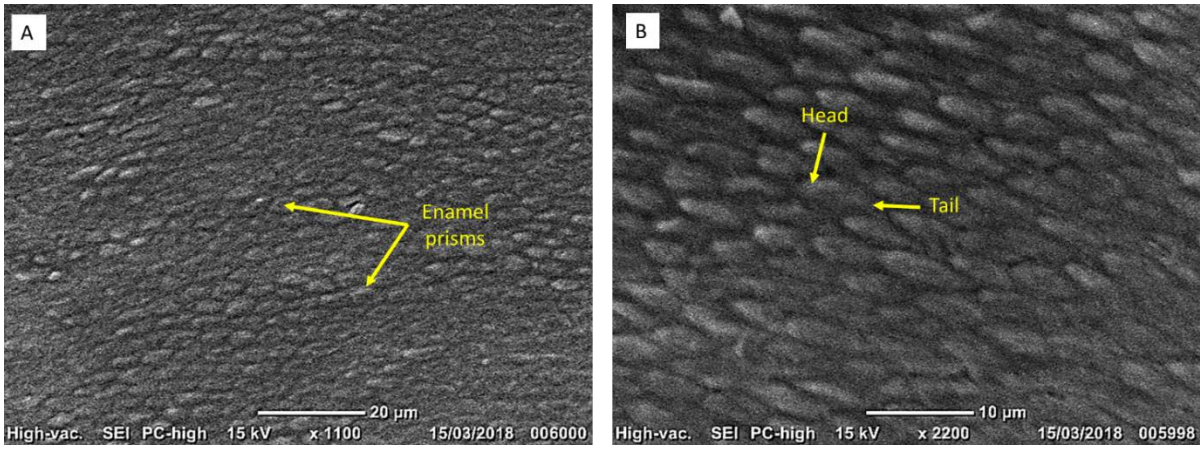

Figure 4.5: Enamel prism orientation at the centre of the bovine disc (a) enamel prisms; (b) enamel prisms at a higher magnification 2200x.

4.2.3 Enamel microstructural properties

Scratch tests were performed on the bovine enamel disc to observe the mechanistic response of enamel and to better understand the wear mechanisms. The hydrated enamel was shown to be chipped and displaced at the sides of the scratch. No visible pile up was observed. Figure 4.6 shows the scratch on the bovine disc.

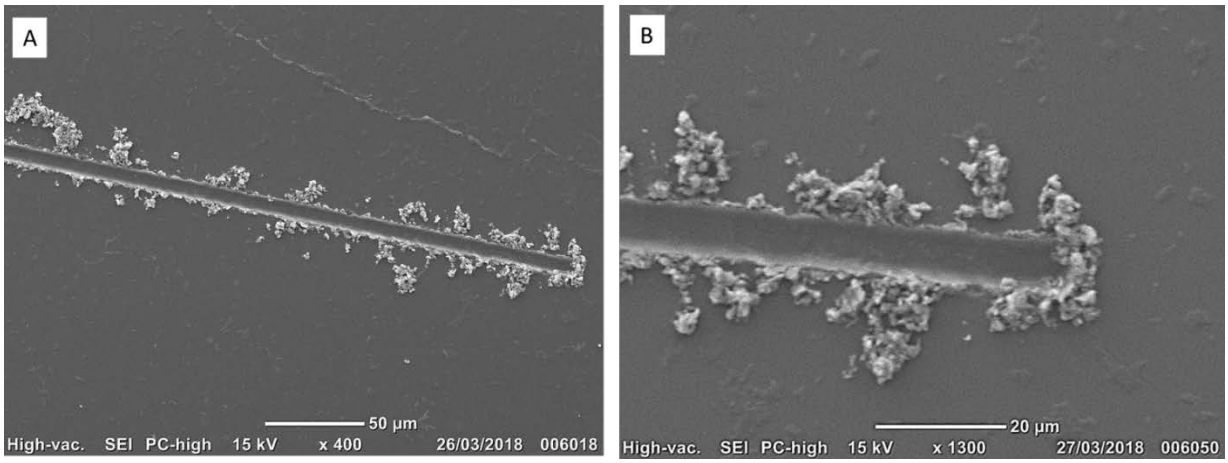

Figure 4.6: SEM of scratch on bovine disc at a load of 80mN (a) enamel displaced at the sides of the scratch; (b) close up of the tip of scratch. No pile up is visible.

4.2.4 Mechanical properties of dehydrated teeth

Nano-indentation was carried out on a sectioned bovine disc to map the mechanical properties of the dehydrated tooth tissues. Five sections of bovine disc were indented 40 times and the measurements were averaged to give one value for each sample. Three distinct layers were present in the bovine disc,

Figure 4.7. A dentino-enamel junction (DEJ) layer exists between the enamel and dentine.

Table 4.1 shows the hardness values for the tooth tissues. The nano-indentation values were found to correspond to the micro hardness values from the literature. Three distinct layers make up the bovine tooth and a drop in hardness was observed from each of the layers. The hardness values of enamel and dentine are reported as; 270 – 360 HV and 50 – 63 HV. When converted to GPa the values for enamel and dentine were; 2.65 – 3.5GPa and 0.48 – 0.62GPa. The results from nano-indentation reported a mean hardness of enamel as 2.90 GPa. The hardness values reported in the literature for enamel are in the region of 283 – 374 HV and for dentine the values reported are in the region of 53 – 63 HV. When the literature values are converted to GPa the values for enamel and dentine were; 2.78 – 3.67 GPa and 0.52 – 0.62 GPa [1, 28]. A dentino-enamel junction (DEJ) area was present in the bovine tooth; dentine had a similar mean value to that of the literature,

0.62GPa respectively. The mean value for dentine from the nano-indentation test was 1.74 GPa. This is the transition layer between the enamel and dentine.

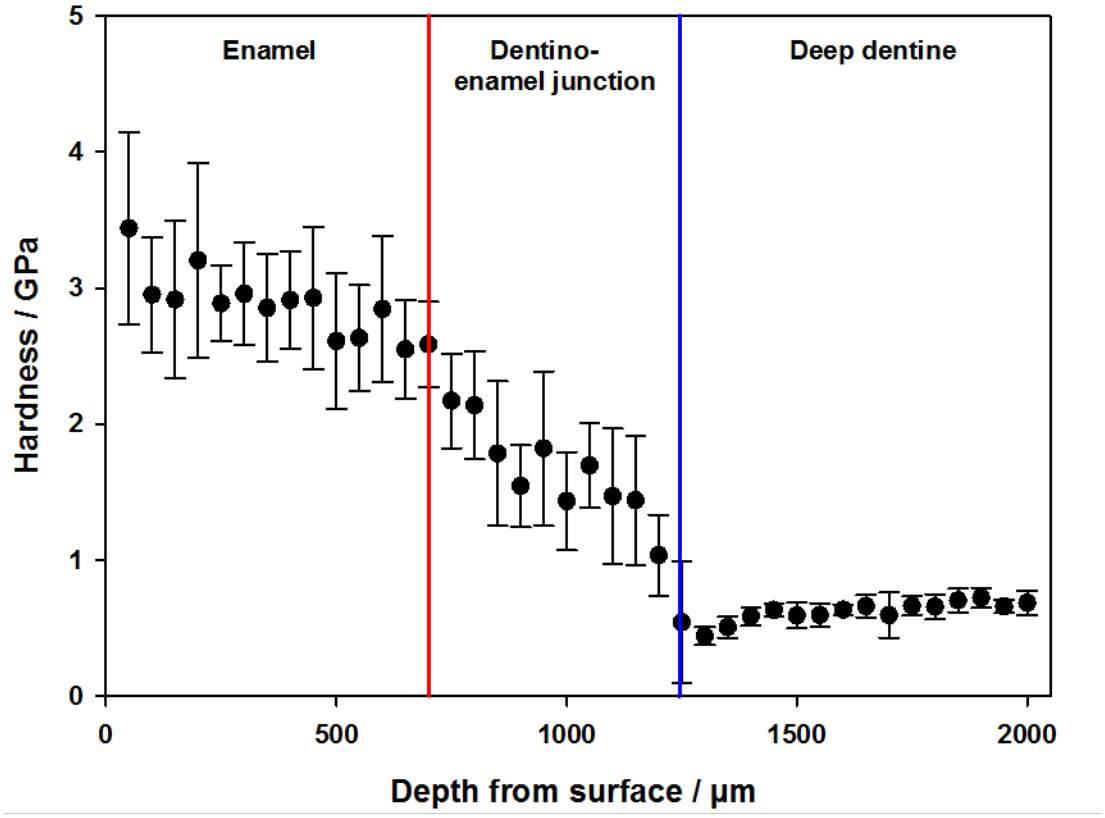

Figure 4.7: Hardness of a dehydrated bovine disc.

Table 4.1: Hardness values for the tooth tissues.

Tooth tissue	Mean Hardness / GPa	Standard deviation (n=15)
Enamel	2.92	0.48
Dentino-enamel junction (DEJ)	1.80	0.39
Dentine	0.62	0.10

The Youngs Modulus (E) of the dehydrated disc showed the disc was made up of three distinct layers, Figure 4.8. A drop in Youngs Modulus was observed across the dentino-enamel junction. The values for Youngs Modulus are stated in Table 4.2.

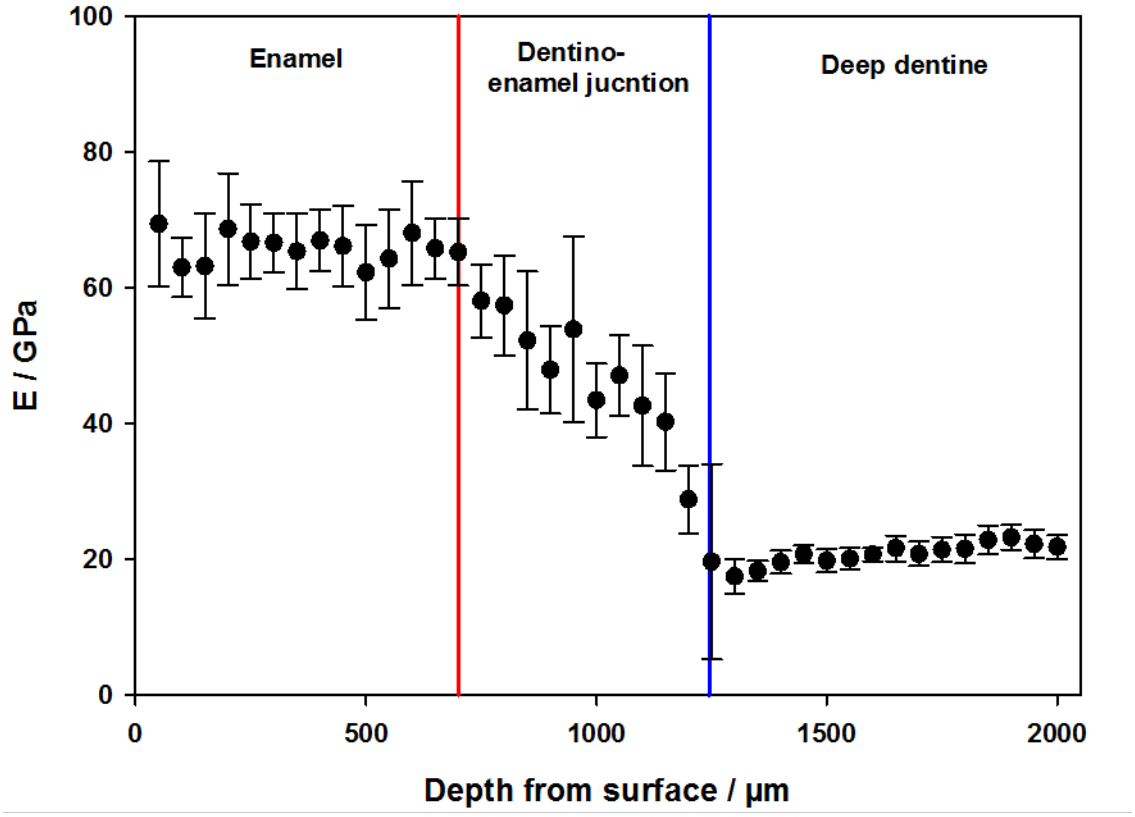

Figure 4.8: Youngs modulus (E) of dehydrated bovine disc

Table 4.2: Youngs modulus (E) values for the tooth tissues.

Tooth tissue	Mean E / GPa	Standard deviation (n=15)
Enamel	65.83	6.30
Dentino-enamel junction (DEJ)	47.16	7.54
Dentine	20.72	2.57

4.2.5 Mechanical responses of hydrated teeth

Hydration of a bovine tooth had a very significant effect on the hardness of the tooth. The teeth were hydrated for 24 hours in artificial saliva solution. A total of 9 readings were taken of the hydrated tooth. Figure 4.9 shows the mass of a hydrated tooth, recorded at time intervals. The three hardness regions for hydrated enamel were not present.

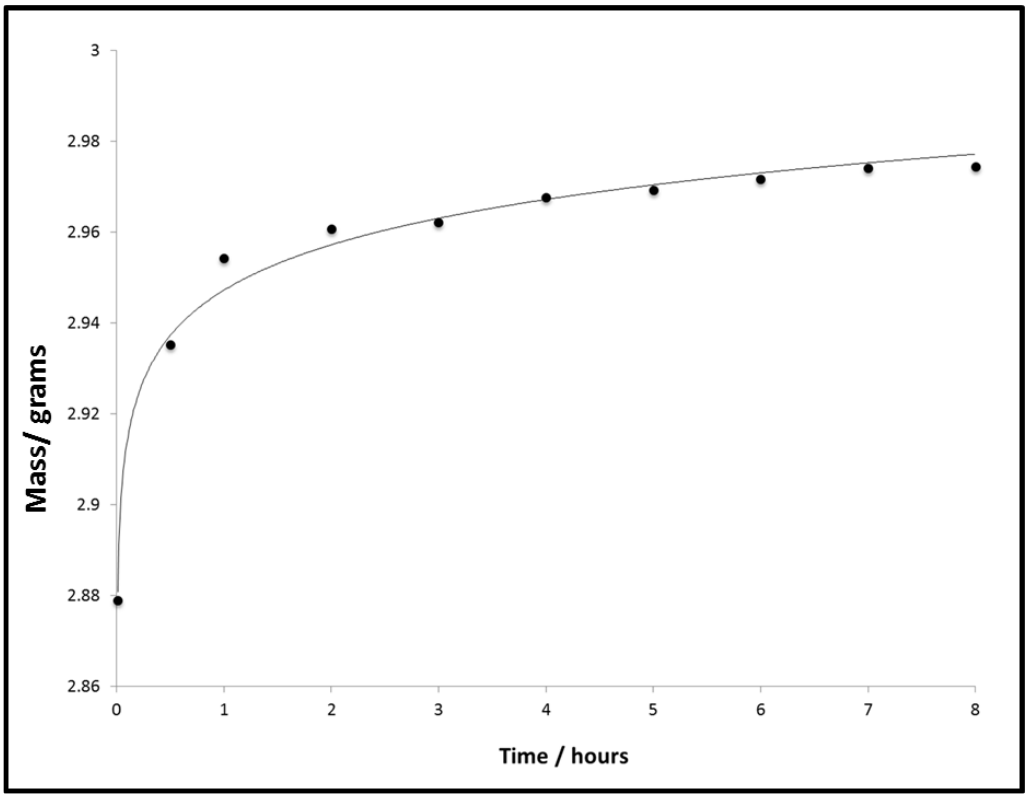

Figure 4.9: The mass of a hydrating tooth recorded at time intervals.

The increase in mass shows asymptotic growth. The final percentage weight increase of the hydrated tooth was 3.3 %.

Three hydrated bovine discs were nano-indented 20 times on the enamel section. The measurements were averaged to give one value for hardness and Youngs Modulus for hydrated enamel, Table 4.3.

Table 4.3: Mechanical properties of hydrated enamel.

Tooth tissue	**Mean Hardness/ GPa**	**Standard deviation of hardness (n=20)**	**Mean E / GPa**	**Standard deviation of E (n=20)**
Enamel	1.69	0.18	57.31	3.04

4.3 Toothbrushes

The toothbrush selected for the wear test was the Tek Pro® firm toothbrush. The toothbrush had the same geometry and standardised flat filaments. Figure 4.10 shows the Tek Pro® firm toothbrush captured using a 8-megapixel iSight camera.

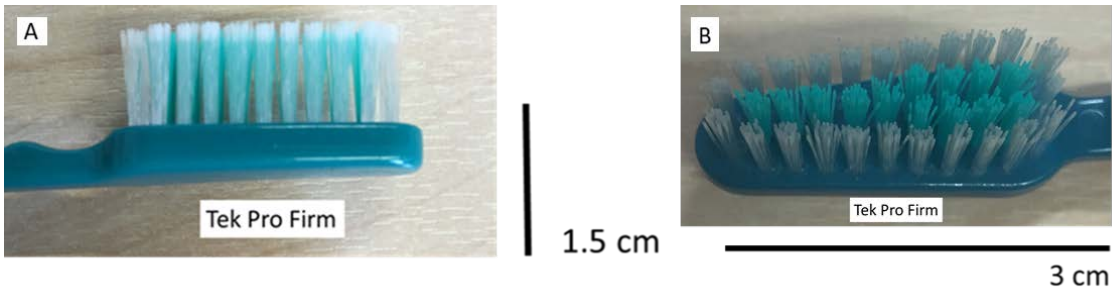

Figure 4.10: Tek Pro® firm toothbrush (a) side view; (b) top view.

Figure 4.11 shows a tuft arrangement and toothbrush filament, which can also be referred to as a filament.

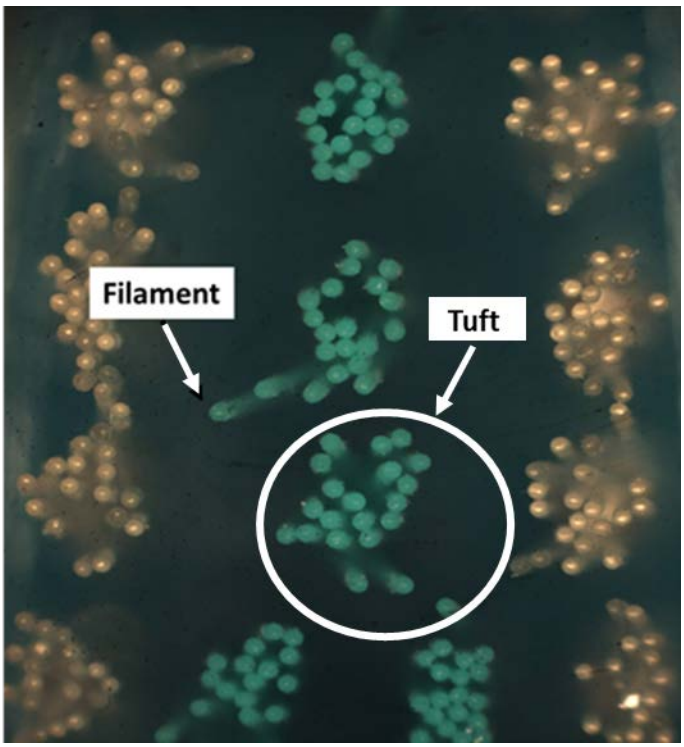

Figure 4.11: Optical images of the filaments of Tek Pro® firm toothbrush.

The Tek Pro® firm inner filaments (Figure 4.12a) and outer filaments (Figure 4.12b) showed a mean filament diameter of 246 µm with a standard deviation of 7.3 µm.

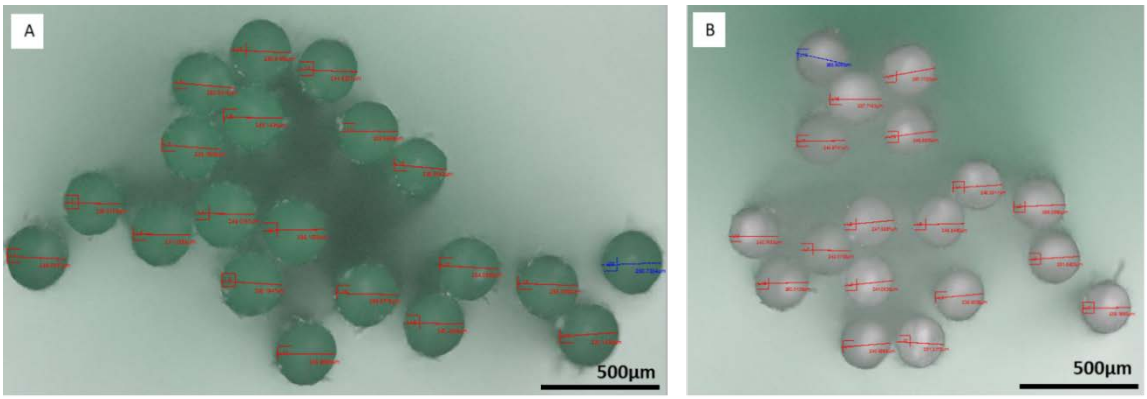

Figure 4.12: Optical images of Tek Pro® firm toothbrush using 2D measurement tools to measure the filament diameter of (a) inner tufts; (b) outer tufts.

In order to compare the filaments of the toothbrush, images were taken using the Makroskop optical microscope and the number of filaments in a tuft were analysed. Three Tek Pro® firm toothbrushes were analysed; filaments were counted from 3 sets of toothbrushes. The number of filaments in every tuft were counted using the Makroskop optical microscope and properties of the brushes were compared, Table 4.4. Table 4.5 shows the statistical data for the Tek Pro® firm toothbrush.

Table 4.4: Filament properties of the Tek Pro® firm toothbrush.

		Tek Pro®
No. of Filaments in a Tuft		**Firm**
Mean	Clear	19
	Coloured	21
Standard deviation	Clear	0.84
	Coloured	0.55

Table 4.5: Statistical data for the filament properties of Tek Pro® firm toothbrush.

Brush Type	**No. of Tufts**		**Length of Filaments (mm)**	**Filament Diameter (μm)**	**Filament Tip Shape**	**Filament Material**
	Clear	**Coloured**				
Firm	23	13	11	246	Elongated pointed	Nylon 6

4.3.1 Tek Pro® Firm Toothbrush

The Alicona microscope was used in order to analyse the filament tips at a higher magnification. Tek Pro® firm filament tips exhibited a sharp elongated pointed filament tip with slight convex edge, Figure 4.13a. Figure 4.13b shows a close up of one filament. The elongated filament tip is very prominent.

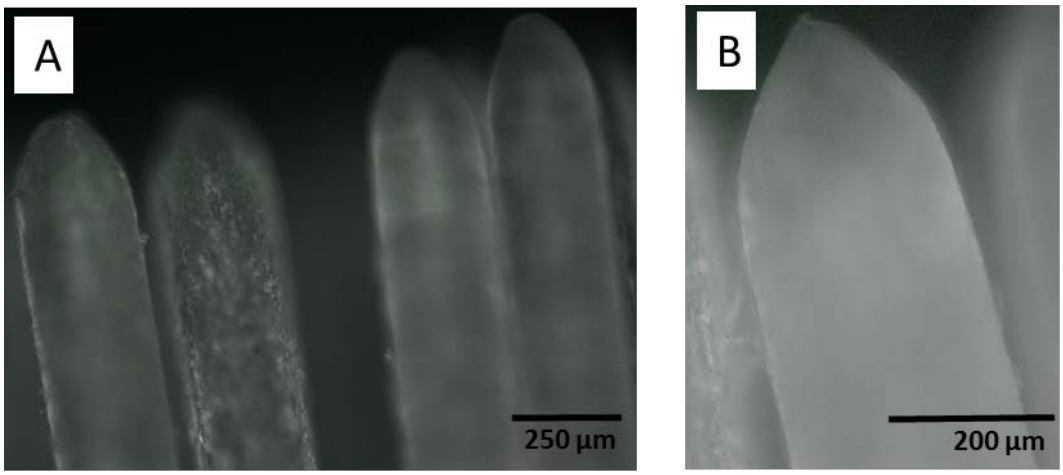

Figure 4.13: Side view of Tek Pro® firm filaments (a) a clump of filaments; (b) close up of one filament.

4.3.2 Filament tip characterisation

The electron micrographs of the filament tips showed the filaments at different magnifications. Tek Pro® firm filaments exhibited an elongated filament tip, Figure 4.14.

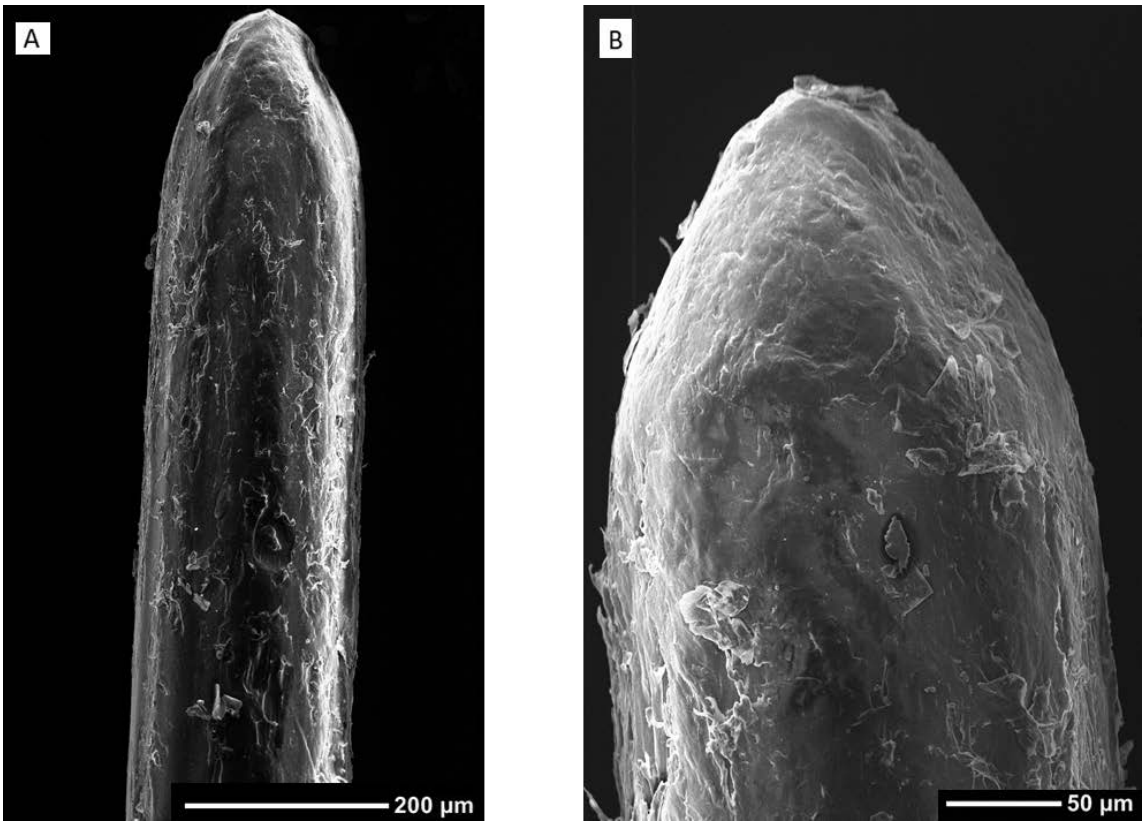

Figure 4.14: SEM of single Tek Pro® firm filament (a) 20x magnification; (b) 100x magnification.

4.3.3 Stiffness of filaments

The stiffness of toothbrush filaments is an important property to consider and can influence the amount of wear of enamel. Using the Euler's column equation, the stiffness of filaments was calculated [222]. This is the maximum permissible load required to bend a filament.

The Euler column equation was employed to calculate the stiffness of the filaments, Equation 4.1.

$$F = \frac{n\pi^2 EI}{L^2} \quad \text{..Equation 4.1}$$

where F is the allowable load (N), n is the factor accounting for the end conditions of the filament, E is the modulus of elasticity (Pa), L is the length of the filament (m) and I is the moment of inertia (m^4).

The moment of inertia can be calculated from the following equation, Equation 4.2 [3].

$$Moment\ of\ inertia = \frac{\pi r^4}{4}$$ …Equation 4.2

where r is the radius of the filament.

With one end of the toothbrush filaments being fixed in the head of the toothbrush and the other end free, the factor accounting for the end conditions is n = 0.25, Figure 4.15.

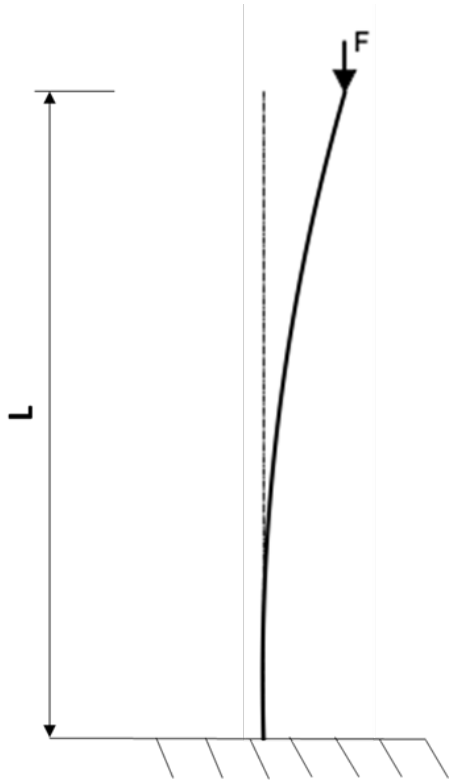

Figure 4.15: The factor accounting for the end conditions of the column (filament). One end fixed, one end free n =0.25 [222].

The force required to bend the filament of the firm toothbrush, Equation 4.3.

$$F = 0.25 \times \pi^2 \times 2.71 \times 10^9 \times \frac{\left(\frac{\pi \times 0.0001234}{4}\right)}{0.011^2}$$ …Equation 4.3

$$\approx 10mN$$

4.3.4 Mechanical properties of filaments

Nano indentation was carried out on the filaments. The mechanical properties of the filaments are summarised in Table 4.6. All results are averages taken of three measurements (t-test, two tailed).

Table 4.6: Statistical data of the filaments.

	Filaments	
	Firm	
	Green	**Clear**
Mean Modulus / GPa	2.30	2.19
Standard deviation (n=12)	0.124	0.061
Mean Hardness / GPa	0.11	0.11
Standard deviation (n=12)	0.009	0.005

There is a significant difference ($p<0.05$) between the modulus of the clear and coloured filaments of the firm toothbrush. However, there is no significant difference between the hardness of the filaments.

The modulus of the coloured filaments is higher than the clear filaments. This could be due to the pigment reinforcing properties of the coloured filaments resulting in a composite effect, which affects the modulus values of the filaments. The Poisson's ratio of nylon 6 is 0.39.

4.4 Abrasive particles

Three abrasive particles were provided by GSK; namely, GSK 9µm alumina, GSK 8µm silica and GSK 6.5µm spherical silica. The other abrasive particles were sourced for the wear tests by taking into consideration the size range of abrasive particles in toothpastes.

4.4.1 Size distribution

Table 4.7 shows the size distribution of the particles used in the wear tests. The mean value for the GSK silica particle, (brand name Silica Zeodent) was 8 µm. This figure is comparable to that given by Huber (2011) [223], who found the typical mean value for a silica zeodent particle to be 10µm. The maximum particle size for the 5µm silica is 4.6x higher than the mean particles size of 5µm and the maximum particle size for 10µm silica is 2.8x higher than the mean particle size of 10µm silica.

Table 4.7: Size distribution of the particles.

	Particle size / µm								
	GSK alumina	**GSK silica**	**GSK spherical silica**	**1µm alumina**	**5µm alumina**	**9µm alumina**	**5µm silica**	**10µm silica**	**5µm spherical silica**
Mean	9	8	6.5	1	5	9	5	10	5
Maximum	10.4	9	8.8	1.79	8.1	10.2	23	28	6.1
Standard deviation	2.69	2.67	1.25	0.46	2.08	2.01	8.26	7.47	1.10

4.4.2 Particle morphology

The morphology of the abrasive particles was shown by SEM observation. Figure 4.16 shows the angular alumina particles. All the abrasive particles were angular in feature with sharp knife-like edges, despite the difference in their size and distribution.

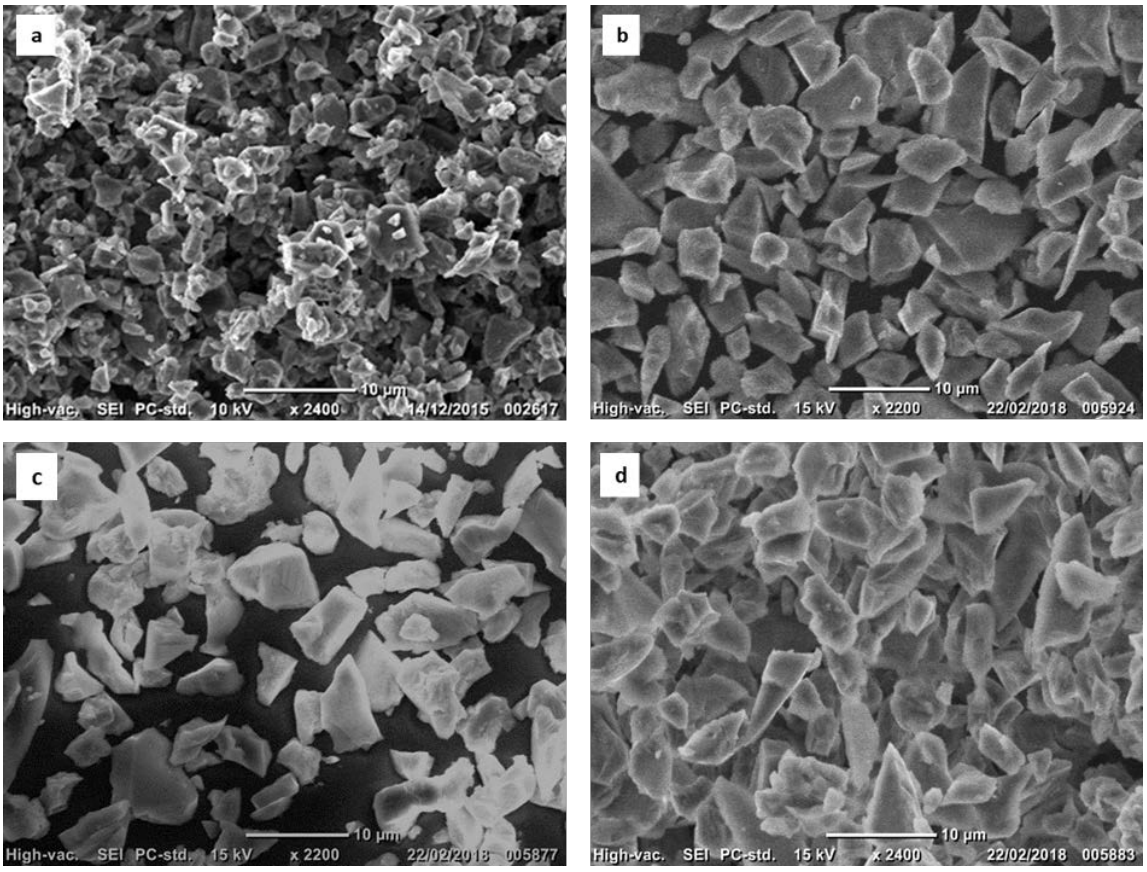

Figure 4.16: Angular alumina (a) 1µm alumina; (b) 5µm alumina; (c) 9µm alumina; (d) GSK 9µm alumina.

Figure 4.17 shows the angular silica particles. Despite the difference in the particle size and distribution, the silica particles were all angular in feature. Figure 4.18a and Figure 4.18b show the 5µm silica and 10µm silica particles. Many large particles >14µm were present and fragments of smaller particles <5µm were present. There was also evidence of sub-micron particle-debris.

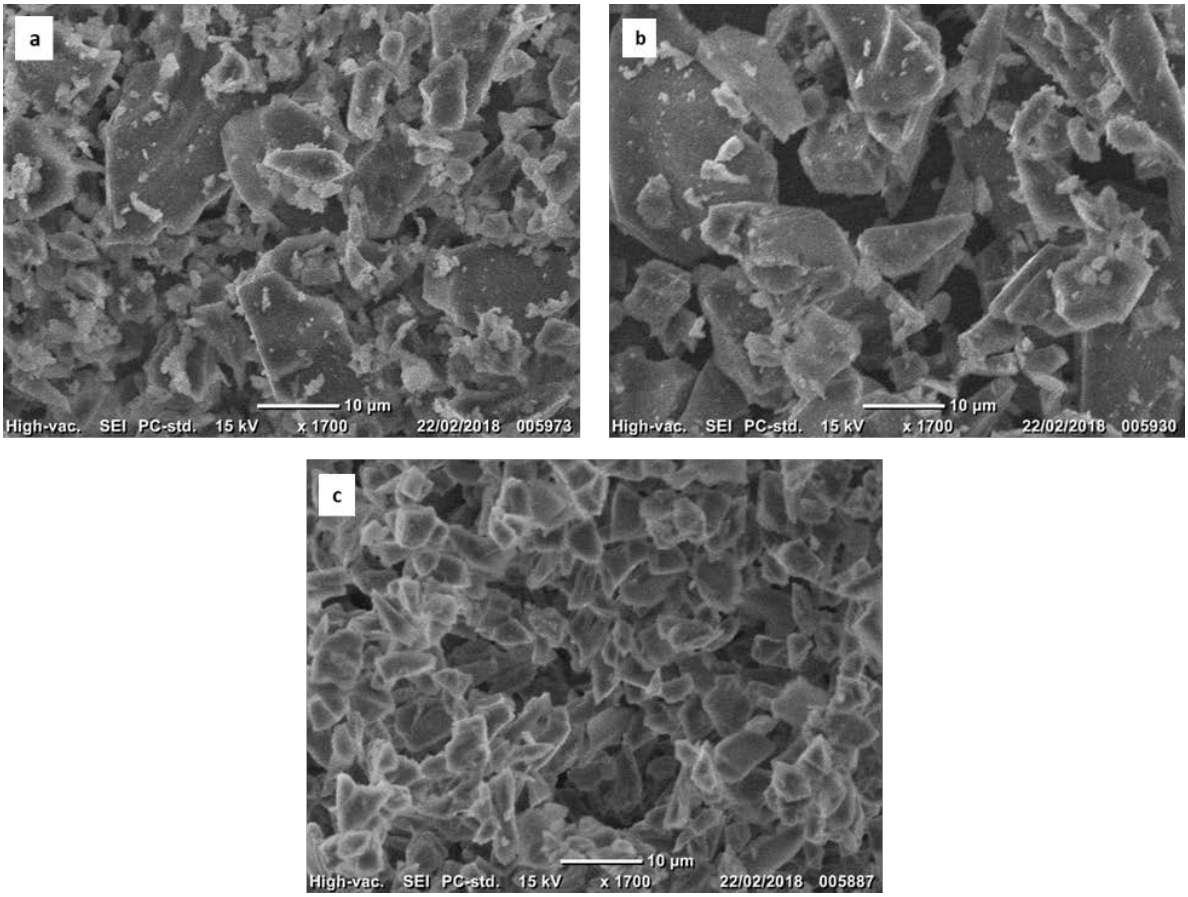

Figure 4.17: Angular silica (a) 5µm silica; (b) 10µm silica; (c) GSK 8µm silica.

Figure 4.18 shows the spherical silica particles. The spherical silica particles were circular with clear well-defined edges.

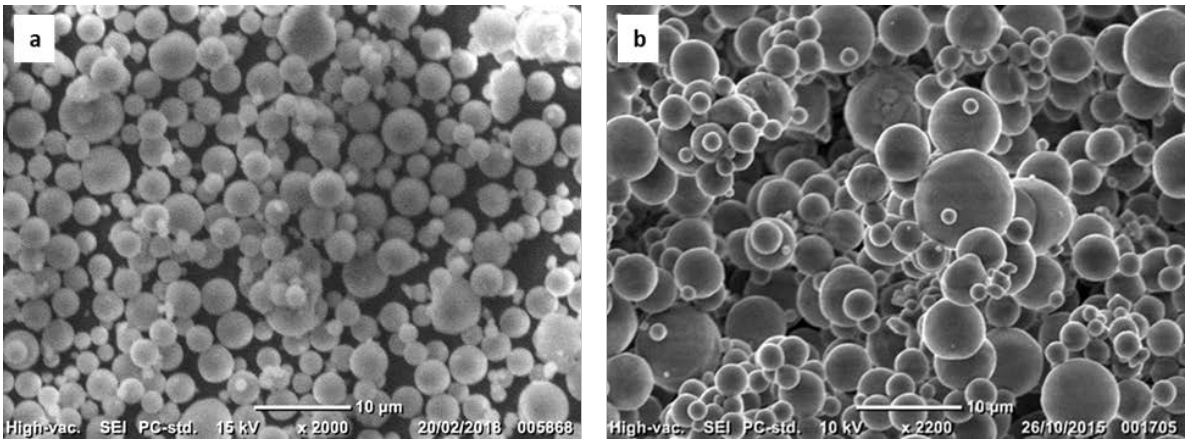

Figure 4.18: Spherical silica (a) 5µm spherical silica ; (b) GSK 6.5µm spherical silica.

4.5 Discussion

The benefit of manual toothbrushes is that they are available in many texture grades, from soft, medium and hard with many varying filament designs such as zig zag and bi-level filaments. The stiffness of filaments is highly influenced by the diameter of the filaments. The Tek Pro® hard toothbrush filaments have a diameter of 0.25 mm which is in contrast to the findings of Sasan et al. [107] who reported a hard toothbrush has a filament diameter of 0.4 mm [107, 123]. Factors such as modulus of elasticity, trim length of filaments, moisture and temperature can affect the stiffness of filaments and should be taken into account when assessing the stiffness [123]. The current study found the Youngs modulus of the bristles to be different for the inner and outer coloured bristles. What is surprising is that the hardness of the inner and outer coloured bristles were the same.

Filament tips can direct how much wear is observed on the enamel surface. The majority of brush filaments function as a family of filaments and not as individual filaments, due to one filament touching another. This can be seen in Figure 4.13 where the tuft of the Tek Pro® firm filaments are tightly packed. This finding was in agreement with Bass [123] and Drisko et al. [224] who concluded that a greater degree of surface abrasion was caused by sharp, pointed filaments. In addition, the flat-ended filaments have been observed to trap fewer particles at the region of the filament tip, compared to rounded filament tips. This implies that a higher and more thorough cleaning efficiency is achieved with filaments with rounded tips [107]. However, it was found by Dyer et al. [76] found softer brushes caused a greater amount of abrasion on tooth surfaces than harder brushes. This can be explained by the ability of softer brushes to carry more paste. The small diameter filaments of soft toothbrushes hold the dentifrice better than hard filaments, since the contact area of the filaments with the tooth surface is increased, due to the greater flexion of soft filaments under a specific load [76]. This allows an increased amount of dentifrice to move across the tooth surface [104].

A study conducted by Bass [123] described the end rounding of filaments as an important characteristic to optimise toothbrush design. This was also confirmed by Breitenmoser et al. [121] who found that rounding filament ends prevented damage to the tooth surfaces [121, 123]. The results of this study show the firm filaments have a pointed filament tip shape.

Stiff filaments that are packed in tight tufts deflect together on loading; they are able to trap particles more effectively, compared to tufts with flexible filaments, which on loading splay out and obstruct the entry and exit of particles from the region of the tip [98]. However, a greater splay of toothbrush filaments allows the brush to enter the crevices and grooves in between teeth. The firm

bristles in the current study have a stiffness of ~10mN. A study carried out by Lewis et al. [127] looked at the effect of stiffness and the tip shape of filaments with the role of particle entrapment. Little deflection was seen on loading with a large tuft and stiff filaments. During particle entrapment, the particles stayed lodged in their original positions at the filament tip. This was due to the stiffness of the toothbrush filaments. However, under the same applied load, more deflection and splay was seen with flexible filaments. When using more flexible filaments, less trapping of particles occurred and the particles were able to pass through the filament tips [6, 98].

The filament stiffness of the toothbrushes dictates how long the particles remain trapped as well as the splay of the filaments on loading. When comparing the effectiveness at trapping partides with stiff and flexible filaments it was found that stiff filaments were more effective at trapping particles than flexible filaments. Tightly packed tufts of stiff filaments do not splay on loading compared to flexible filaments. Flexible filaments that splay are more prone to the exit and entry of particles from the tip [140].

Dentifrice abrasiveness depends on three factors; particle hardness, particle size, and particle shape [81]. The two most common abrasive particles found in dentifrices are silica and alumina. These particles have a hardness that is higher than enamel, which is 270 HV – 360 HV [2]. Alumina has a hardness of 2500 HV. It is widely used in dentifrices due to its polishing qualities [225]. The hardness of silica is 1000 HV - 1200 HV [4]. If the abrasive agent is highly concentrated in toothpaste, there is more chance of abrasion of the tooth surface [81].

Controlling particle size is important in many applications. The size and shape of abrasive partides in dentifrices can influence properties such as flow and rheology, as well as have an effect on the other active ingredients in the dentifrice [133]. The typical size distribution of abrasive particles in a dentifrice is commonly in the range of 4µm – 12µm [210]. Table 4.7 shows the particle size distribution. Particles in the size range of 5µm – 8µm are the optimum size and will result in a significant amount of abrasion on the tooth surface. In the current study, the 5µm and 10µm silica particles had a wide particle size range, which could indicate the milling process was not controlled. This was surprising and could be The filament tip contact will retain these particles resulting in good contact with the tooth surface [2]. The largest particle size recorded for the 10µm silica particle in the current study was 28µm. These large particles would remain between the filament tips and stay lodged causing little or no abrasion [110]. However, if the large particles remain entrained in the contact, an increased amount of wear could be observed [110].

The shape of the particle can also influence the amount of wear. Angular particles are found to be more damaging than spherical particles, due to the irregular sharp edges [11]. The spherical silica particles showed well defined circular edges, Figure 4.18.

A large spread of particle sizes will result in varying differences of wear on the bovine surface. Separation and dilution of particles during the dispersion process could have caused the particles to collide at fast speeds, causing parts of the particles to break off into smaller fragments [13, 226]. This implies higher variability in size distribution of the particles. This could be due to a high degree of fragmentation, which distorts the mean value and results in a high standard deviation. Small fragmented particle debris was observed with all the angular silica particles, Figure 4.17. Small particles in the size range of 2µm – 3µm size will pass through the filament contact region resulting in a limited amount of abrasion due to their smaller size [140]. It is encouraging to compare this finding with the particle size of the 1µm alumina in the current study, which could suggest most of the particles would pass through the filament tips, due to the small size range of the particles.

A study conducted by Pace Technologies [227] found agglomeration to be a big issue with alumina particles. Electrostatic attraction between small, dry, powder particles causes attraction between the particles resulting in the formation of larger particles [227].

It is questionable whether the large particles are due to agglomeration. The Saturn Digisizer uses a dispersion technique which prevents particle agglomeration. During the stirring process, the particles are dispersed in a liquid containing sodium hexametaphosphate, which is a dispersing agent. This liquid aids the prevention of particles agglomerating. An ultrasonic probe can also be used to maintain particle dispersion, as well as assist in re-dispersion of particles. This prevents agglomeration of particles and allows for accurate size distributions to be obtained [14]. It can therefore be suggested that the large particle sizes are primary particles that failed to be crushed during the manufacturing process of the abrasive. However, a study carried out by Huber [223] found that processes used to improve the dispersion of agglomerates caused changes to the size distribution of particles, as well as affecting the state of the particles [223]. The implications of this finding would have little effect on the present study, as particle dispersion was carried out with a magnetic mixing device.

5. Influence of particle shape, size and composition on the volume loss of enamel

5.1 Introduction

This chapter investigates the effect of the shape, size and composition of particles on the volume loss of enamel. Comparisons between the volume loss, volume loss per particle, groove sizes and wear mechanisms are reported. Synergy is introduced, but later discussed in detail in chapter 8. The aim of this chapter was to obtain a better understanding of the relationship between the size and shape of particles in toothpastes on the volume loss of enamel.

The most commonly used abrasive particles in toothpastes are alumina and silica particles with a typical size between 4µm – 12µm. The standard volume concentrations of abrasive in toothpaste is 0.15 v/v [1]. The objective of this study was to investigate the effect of size, composition and morphology of abrasive particles on the volume loss of enamel using a micro-abrasion rig and develop an understanding of the magnitude of wear caused by two-body, three-body and mixed-mode abrasion (Chapter 2).

5.1.1 Experimental details

A large and systematic experimental programme was undertaken to investigate the influence of particle shape, size and composition; microabrasion testing was performed using a nylon ball against an enamel surface. The sliding velocity was kept constant at 0.035ms^{-1} for a test duration of 1 minute at room temperature, with eight repeats performed for each test setup. 7 different angular particles with controlled size distributions of two different materials were used (1µm alumina, 5µm alumina, 9µm alumina, GSK 9µm alumina, 5µm silica, 10µm silica and GSK 8µm silica). To investigate the effect of wider particle size ranges and to investigate if the combination of two particle sizes provide a synergistic effect of the level of wear, the single sized particles were mixed to provide a bimodal 7 µm alumina and a bimodal 7.5 µm silica. To determine the effect of particle shape, tests were also performed with a 5 µm spherical silica and compared with angular 5µm silica and GSK 8µm silica. Each particle was used in slurry form, with 4 volume fractions of abrasive (0.05, 0.10, 0.15 and 0.20 v/v) used to identify any changes in the wear mechanism and rate. The test conditions are summarised in Table 5.1.

Table 5.1: Test conditions for microabrasion tests.

Test conditions		
Ball sliding velocity (ms^{-1})	0.035	
Volume fraction of abrasives	0.05, 0.10, 0.15, 0.20	
Ball material	Nylon	
Temperature/ ^{o}c	18	
Counterface material	Enamel	
Time/ minute	1	
	Mean particle size / µm	**Maximum particle size / µm**
Abrasive particles	**Angular**	
	1µm alumina	1.79
	5µm alumina	8.1
	9µm alumina	10.2
	Bimodal 5µm + 9µm alumina	
	GSK 9µm alumina	10.4
	5µm silica	23
	10µm silica	28
	Bimodal 5µm + 10µm silica	
	GSK 8µm silica	9
	Spherical	
	5µm spherical silica	6.1
	GSK 6.5µm spherical silica	8.8
No. of repeats per test (craters formed)	8	

5.1.2 Wear profiles

Figure 5.1 shows the typical wear scars produced for grooving, mixed-mode and rolling abrasion. From the craters, it is clear that the test conditions produced a spherical scar geometry. This validates the use of measuring the diagonals of the wear scar to determine the SWR. The wear scars were measured using an Alicona optical microscope in accordance with the guidelines set out by Gant and Gee et al. [178].

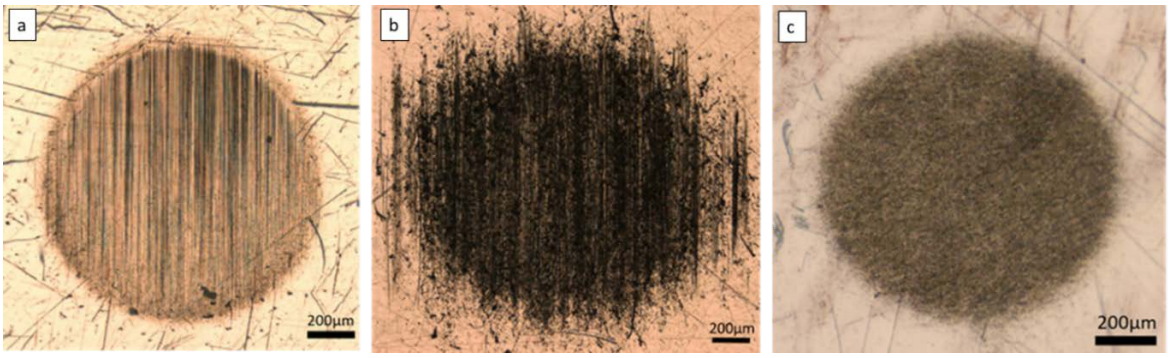

Figure 5.1: Typical wear scars for (a) grooving; (b) mixed mode; and (c) rolling.

5.2 Effect of particle shape on volume loss of enamel

In this section, the effect of particle shape on the volume loss of enamel will be investigated. Angular silica particles will be compared with spherical silica particles. The maximum particle size for angular 5µm silica is 23µm, whereas the 8µm GSK silica particle has a much more controlled particle size with a maximum size of 9µm. In this case, both versions of angular silica will be compared with 5µm spherical silica.

5.2.1 Particle shape: angular vs spherical

In order to compare the volume loss of enamel, micro-abrasion tests were conducted using angular 5µm silica, angular 8µm GSK silica and spherical 5µm silica varying volume fractions between 0.05 – 0.20 v/v. The tests were independent of load and the sliding distance, as these were held constant at 0.1N, 0.2N or 0.5N and 2m.

Figure 5.2a-c shows the average volume loss for 5µm angular silica, 5µm spherical silica and 8µm GSK silica. 5µm angular silica shows the highest volume loss compared to the 5µm spherical silica and 8µm GSK silica. There was a significant difference in the volume loss of 5µm angular silica compared to the 5µm spherical silica ($p<0.05$). Between 0.05 v/v and 0.10 v/v, there was a change from grooving to mixed-mode abrasion, which caused an increase in volume loss for the angular 5µm silica, GSK 8µm silica and spherical 5µm silica. A change in wear mechanism from grooving to mixed-mode for the angular 5µm tests results in 2.5x more wear and a 0.0025mm^3 increase. Groove analysis was conducted for all the tests using measurement analysis on the Alicona microscope and SEM in volume loss from 0.0010mm^3 at volume fraction 0.05 – 0.10 v/v, Figure 5.2a – c. A change in wear mechanism from grooving to mixed-mode for the 5µm spherical silica tests results in 5x more wear and an 0.0023mm^3 volume loss increase from 0.0005mm^3 of enamel for volume fractions 0.05 – 0.10 v/v, Figure 5.2a-c. A decrease in volume loss of enamel was observed for the 5µm spherical silica above 0.10 volume fraction for

Figure 5.2a-c. A decrease in volume loss above 0.10v/v is due to increased rolling action and less grooving which reduces the damage on the enamel surface and results in a decrease in volume loss of enamel. The statistics demonstrated there was a significant difference between the volume loss of GSK 8µm silica and 5µm spherical silica ($p<0.05$).

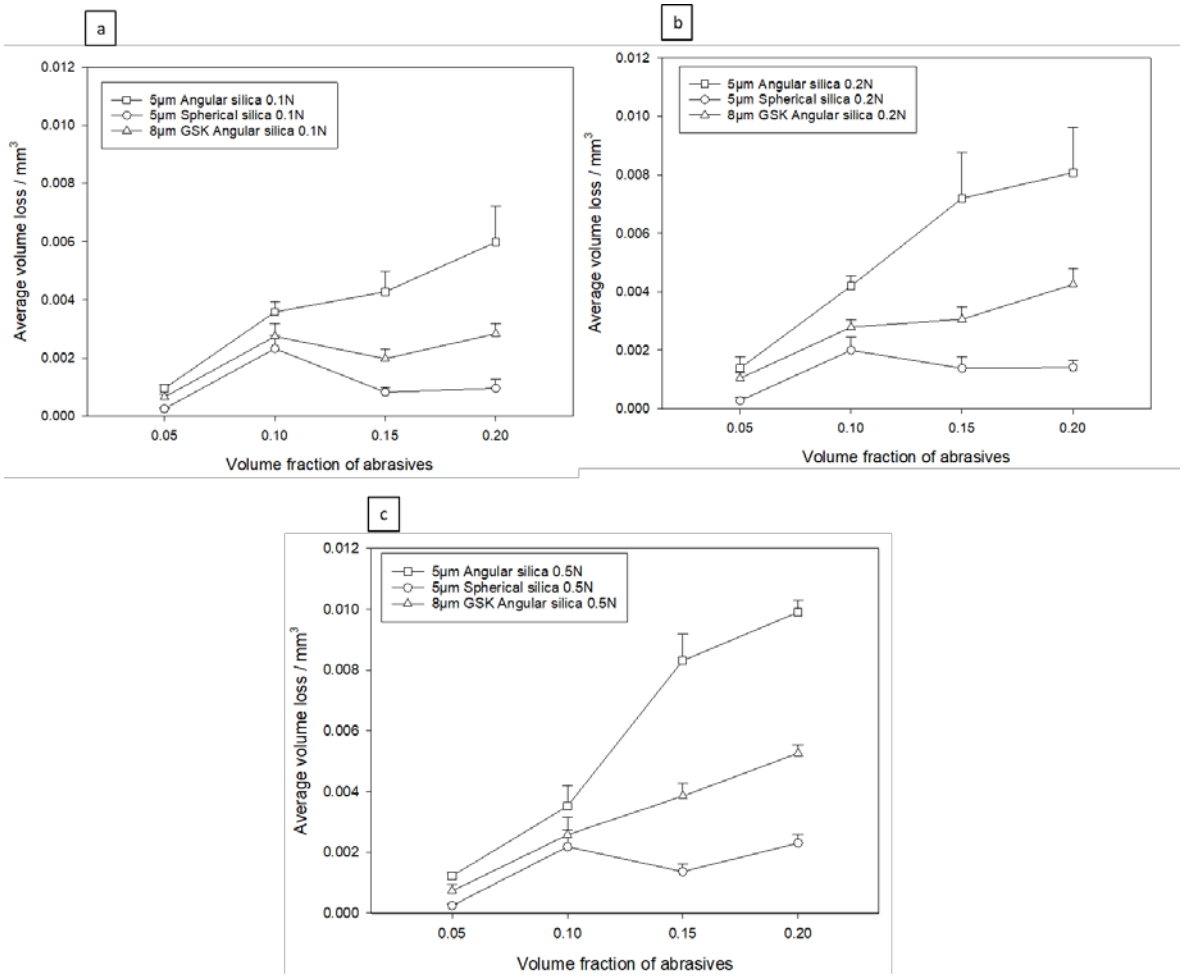

Figure 5.2: Average volume loss for 5µm angular silica, 8µm GSK silica and 5µm spherical silica (a) 0.1N; (b) 0.2N; (c) 0.5N.

5.2.2 Influence of particle shape on the wear scar profile

In order to investigate the influence of particle shape on the wear mechanisms of enamel, SEM images were obtained at the centre of wear scars for the different test conditions.

Figure 5.3 shows SEM images of the typical wear scars produced with 5µm angular silica. These wear scars are representative of the typical wear scars that are produced for grooving and mixed-mode abrasion for all the angular 5µm silica tests. The sliding direction (S.D) is indicated on the images. All the grooving wear scars appear similar and consist of multiple parallel grooves aligned with the sliding direction across the enamel surface, indicating two-body grooving was the dominant mechanism, Figure 5.3a. There was a change in wear mechanism from grooving to mixed-mode at volume fractions higher than 0.05 v/v. The wear scars produced for the 5µm angular silica for mixed-mode show a different wear scar morphology. The wear scars consist of some grooves and multiple indented surfaces with chipping of enamel, Figure 5.3b. The indents are a result of densification of the enamel tissue, which causes enamel structural damage.

Figure 5.3c and Figure 5.3d shows SEM images of the typical wear scars produced with 5µm spherical silica. These wear scars are typical representations of all the wear scars produced with 5µm spherical silica. The grooving observed on the 5µm spherical silica consisted of multiple grooves, whereas the mixed-mode transition at 0.15v/v shows a surface with indents and grooves, however the wear morphology is different to that of 5µm angular silica with more spherical indents and removal of material. This is reflected in Figure 5.2 where above 0.10 v/v there is a decrease in volume loss for volume fractions 0.15 v/v and 0.20 v/v with the 5µm spherical silica compared to the 5µm angular silica and GSK 8µm silica. The 5µm spherical silica mixed-mode surfaces were less damaged than the angular 5µm silica. This could be due to the morphology of the spherical particles and resulting contact stresses.

Figure 5.3e and Figure 5.3f shows the typical wear scars produced with angular GSK 8µm silica. These wear scars typically represent all the GSK 8µm silica scars. The grooving mechanism showed directionality, whereas the mixed-mode surface showed signs of fracture and chipping of enamel. Less grooving is observed in the mixed-mode state with GSK 8µm silica (Figure 5.3f) compared to the mixed-mode 5µm angular silica, Figure 5.3b.

With a change in particle shape from spherical to angular, the wear damage for the mixed-mode region appeared to be worse. When comparing the wear damage for the mixed mode region for 5µm spherical silica (Figure 5.3d) to GSK 8µm angular silica (Figure 5.3f), the wear scar appeared to

consist of more fracture, chipping and indents. Less grooves were visible however, the surface showed more signs of chipping and fracture of the enamel surface. Surface damage of enamel was observed as an uneven, textured surface, where there was evidence of fracture and chipping of enamel rods.

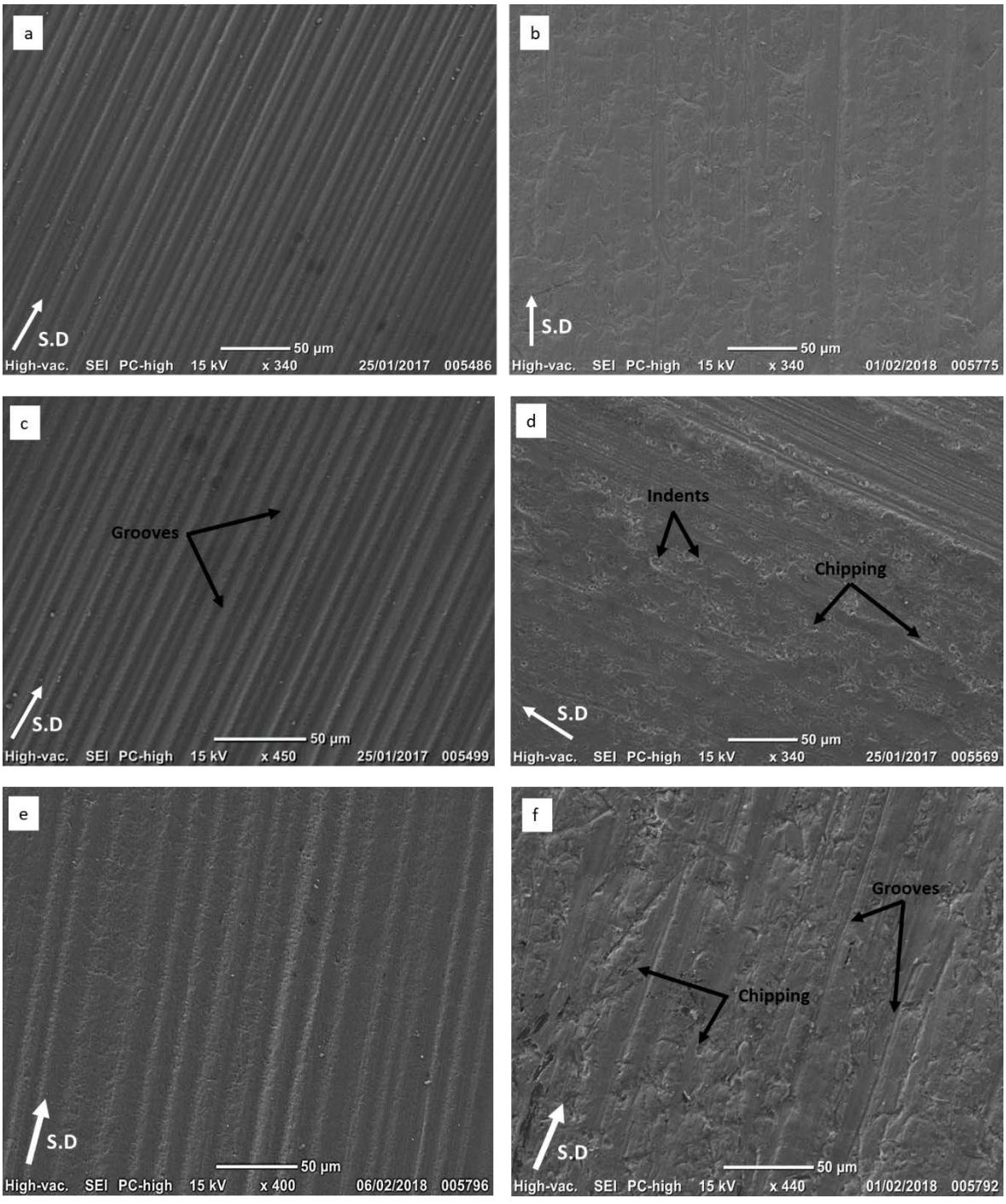

Figure 5.3: SEM images of wear scars at a load of 0.2N (a) 5µm angular silica grooving; (b) 5µm angular silica mixed-mode; (c) 5µm spherical silica grooving; (d) 5µm spherical silica mixed-mode; (e) GSK 8µm angular silica grooving; (f) GSK 8µm angular silica mixed mode. Figures a,c and e are all 0.05 v/v and Figures b, d and f are all 0.10 v/v.

5.2.3 Influence of particle shape on groove width

This section details groove analysis conducted on wear scars by using measurement analysis. The groove widths were measured, by taking multiple measurements of the grooves and the average groove width was calculated for each mechanism. The maximum and mean particle sizes are also shown.

Table 5.2 shows the groove width data for 5µm angular silica, GSK 8µm angular silica and 5µm spherical silica.

There was a change in groove width, with a change in shape of the particles. The 5µm spherical silica particles generated narrower grooves than the 5µm angular silica and the GSK 8µm angular silica for the grooving mechanism. For the mixed-mode mechanism there was no significant difference ($p>0.05$) in average groove width between the angular 5µm silica and spherical 5µm silica, however there was a significant difference between the groove widths for GSK 8µm angular silica and 5µm spherical silica ($p<0.05$).

Table 5.2: Average groove width data for 5µm angular silica, GSK 8µm silica and 5µm spherical silica.

	Grooving		**Mixed- mode**	
	Average groove width / µm	**Standard deviation**	**Average groove width / µm**	**Standard deviation**
Spherical silica 5µm Maximum – 6.1µm Mean – 5µm	5.28	0.63	6.96	1.23
Angular Silica 5µm Maximum – 23µm Mean – 5µm	6.48	0.58	7.36	1.71
GSK 8µm silica Maximum size–9µm Mean size – 8µm	8.39	0.37	10.08	1.07

5.3 Changes in abrasive size on volume loss of enamel

In order to see if a change in abrasive size affected the volume loss of enamel, mono-sized angular particle sizes were investigated. In this section, comparisons are made with mono-sized angular particles of alumina and silica slurries. The bimodal slurries (bimodal alumina and bimodal silica) were made by mixing 50% of the two monosized particles to produce a slurry with a bimodal particle size range. The bimodal alumina slurry contained 50% of 5µm alumina particles and 50% of 9µm alumina particles and the bimodal silica slurry contained 50% of 5µm silica particles and 50% of 10µm silica particles. The average volume loss per particle was calculated for the tests. This was calculated using the Equation 3.9 in Chapter 3. The percentage synergy will be plotted against the volume fraction of abrasives for the bimodal alumina and bimodal silica to investigate whether the mono-sized particles cause more or less damage than the bimodal particles.

5.3.1 Angular alumina

Figure 5.4 shows the average volume loss for angular alumina, 1µm, 5µm, 9µm, bimodal alumina and GSK 9µm alumina. At volume fraction 0.05 v/v for the 1µm, 5µm, 9µm and GSK 9µm alumina grooving abrasion dominated the wear mechanism. There was a change in wear mechanism at volume fractions above 0.05 v/v for the 1µm, 5µm, 9µm and GSK 9µm alumina from grooving to mixed-mode abrasion. Mixed-mode abrasion dominated all the bimodal alumina tests at all the volume fractions. For the GSK alumina, grooving dominated 0.05 v/v - 0.10 v/v and then there was a change in wear mechanism to mixed-mode. This is shown in Figure 5.4a.

Figure 5.4b shows for the GSK 9µm alumina, grooving dominated for 0.05 v/v and then there was a change to mixed-mode above 0.05 v/v, whereas for

Figure 5.4c there was a change above 0.15 v/v to mixed mode for the GSK alumina. Rolling abrasion was observed for 9µm alumina at 0.20v/v, Figure 5.4a. There was a significant difference between the 1µm alumina and bimodal alumina tests, ($p<0.05$).

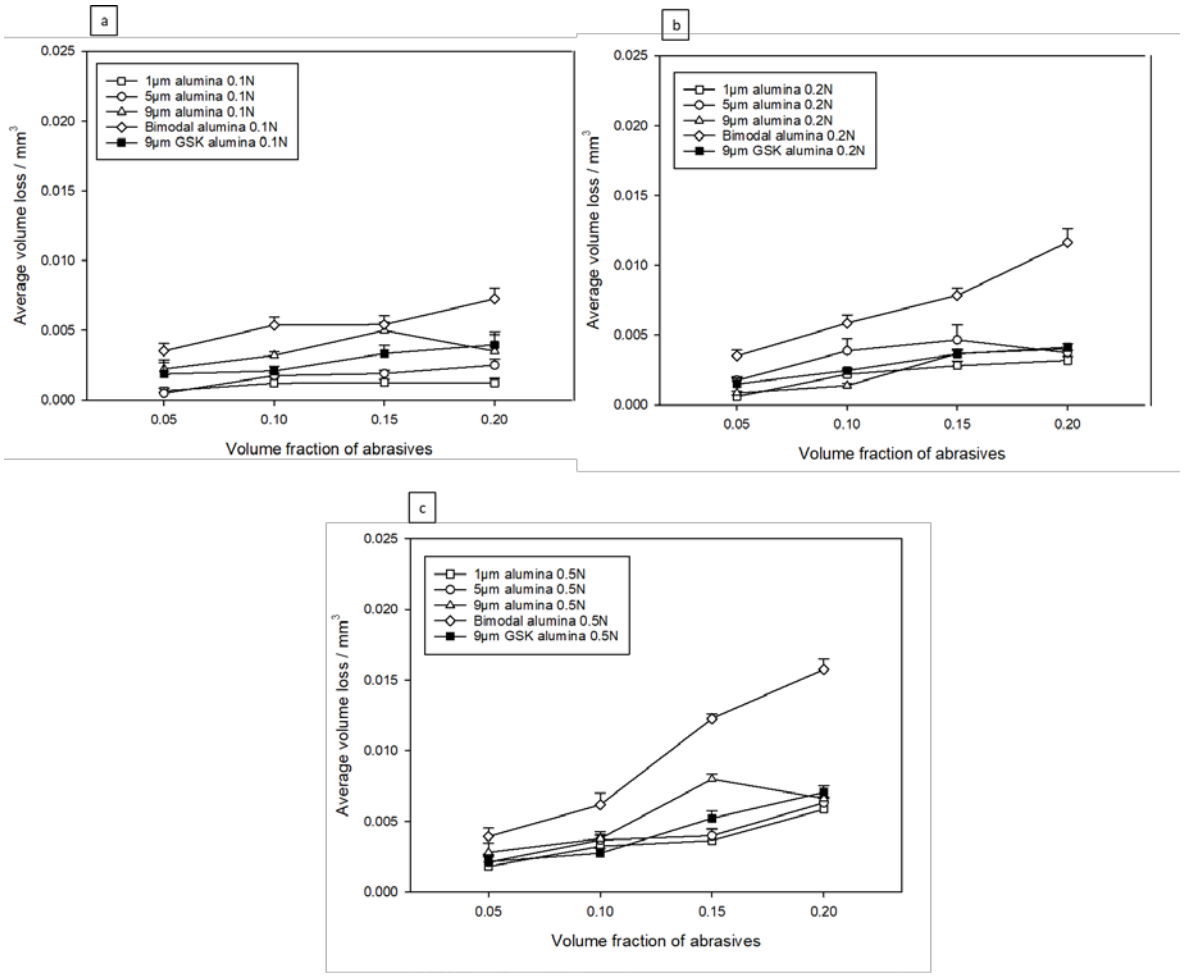

Figure 5.4: Average volume loss for 1µm alumina, 5µm alumina, 9µm alumina, bimodal alumina and 9µm GSK alumina (a) 0.1N; (b) 0.2N; (c) 0.5N.

The average volume loss per particle was calculated to observe the damage of the individual sized particles. As the size of the particle changes, so does the number of particles for a constant concentration. This approach was used for the silica tests and the spherical silica tests.

Figure 5.5 shows the average volume loss per particle for the alumina tests. This is the number of particles in the slurry solution for the required volume of abrasive. The average volume loss per particle was calculated using Equation 3.9.

The following assumption was made:

- When calculating the number of particles, the angular particles are assumed to be spheres.

The GSK alumina test generated the highest volume loss per particle for

Figure 5.5a at a fixed load of 0.1N. For a fixed load of 0.2N, GSK alumina dominated the average volume loss per particle for volume fractions 0.05 v/v – 0.15 v/v. This is shown in Figure 5.5c. For volume fraction 0.20 v/v , bimodal alumina dominated the volume loss per particle. At a fixed load of 0.5N, the 9µm alumina dominated the average loss per particle for volume fractions 0.05 v/v – 0.15 v/v and at 0.20 v/v, bimodal alumina dominated the average loss per particle, Figure 5.5c.

A direct comparison can be made with the GSK 9µm alumina and 9µm alumina. Both particles have a particle size of 9µm. Figure 5.5a shows the 9µm GSK alumina produced a higher volume loss of enamel. A possible reason for this is the morphology of the GSK 9µm alumina, with sharp angular particles, Figure 4.16d. A difference is observed in volume loss for Figure 5.5c, which shows the 9µm alumina dominating the GSK 9µm alumina at volume fractions 0.05 v/v – 0.15 v/v. This could be due to the angular GSK 9µm particles exerting a higher load per particle and hence doing more damage whereas the clustered 9µm GSK particles distribute the load over the cluster, which results in a lower load per particle and less damage. Another possibility could be due to the alumina powders being from different dental batches.

There is 5.8x more particles in 5µm alumina compared to 9µm alumina. There is 1.9x more partides in the 5µm alumina slurry compared to the bimodal alumina tests. The differences in the volume of particles between the 5µm alumina and 9µm alumina show to be significantly different ($p<0.05$).

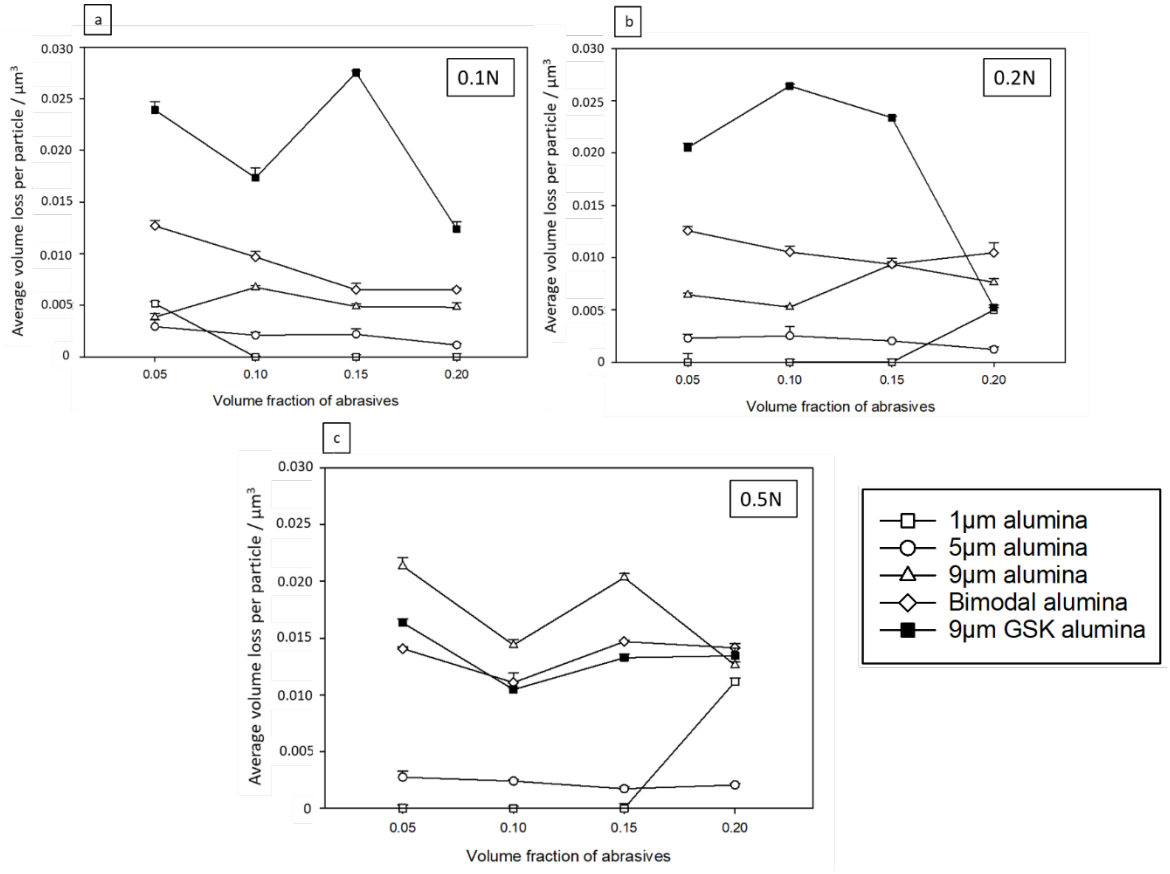

Figure 5.5: Average volume loss per particle for 1µm alumina, 5µm alumina, 9µm alumina, bimodal alumina and 9µm GSK alumina (a) 0.1N; (b) 0.2N; (c) 0.5N.

5.3.2 Angular silica

Figure 5.6 shows the average volume loss for the silica tests. At 0.05v/v the 5µm silica and GSK 8µm silica produced grooving abrasion on the enamel surface. There was a change in wear mechanism for the 5µm angular silica above 0.05v/v where it changed from grooving to mixed-mode abrasion. The 10µm silica and bimodal silica (5µm + 10µm) tests all generated mixed-mode abrasion, Figure 5.6. The bimodal silica tests always dominate the mono-sized silica tests.

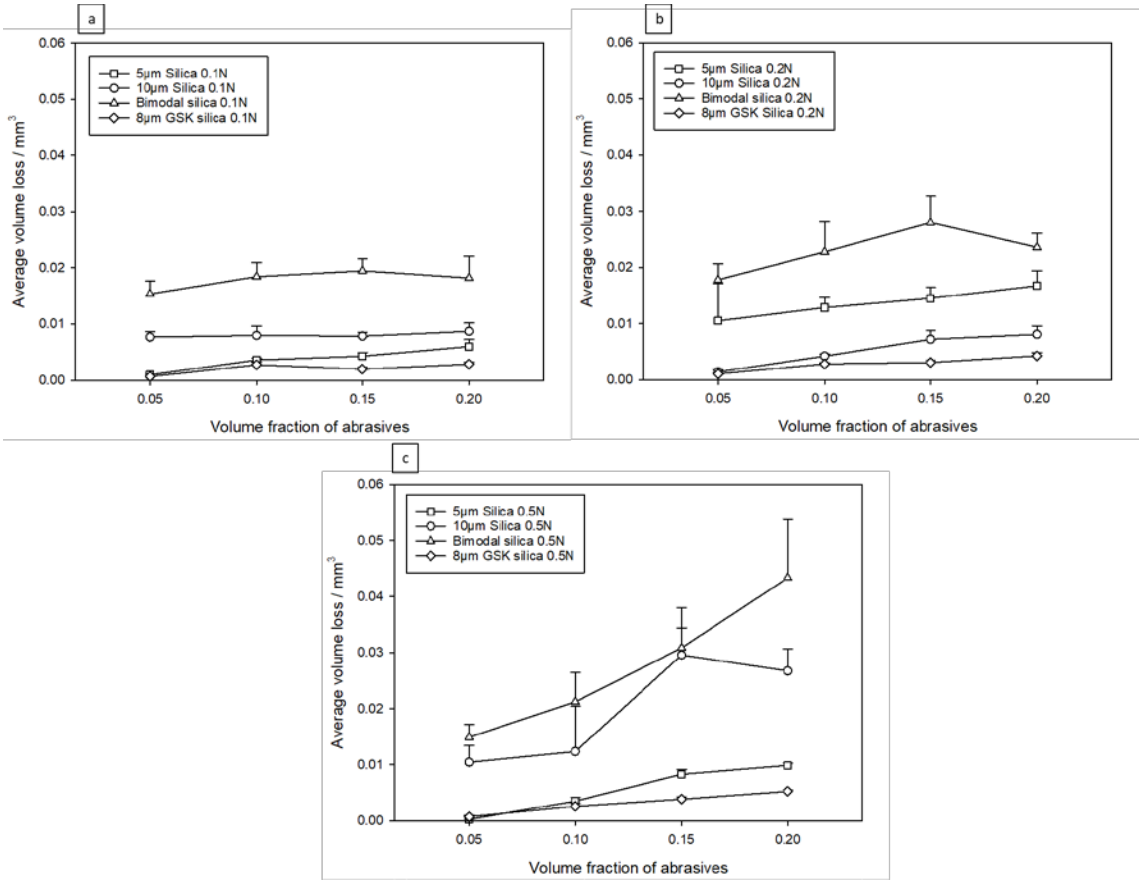

Figure 5.6: Average volume loss for 5µm silica, 10µm silica, bimodal silica and 8µm GSK silica (a) 0.1N; (b) 0.2N; (c) 0.5N.

The average volume loss per particle for the silica tests is dominated by the mono-sized 10µm silica, resulting in more enamel removal and damage caused by the 10µm silica, Figure 5.7. However, at a fixed load of 0.1N at volume fraction 0.15v/v, bimodal silica dominates the average volume loss per particle, by a slight fraction, Figure 5.7a.

There is 8x more particles in 5µm silica compared to 10µm silica. There is a significant difference in the volume of 5µm silica particles compared to 10µm silica ($p<0.05$).

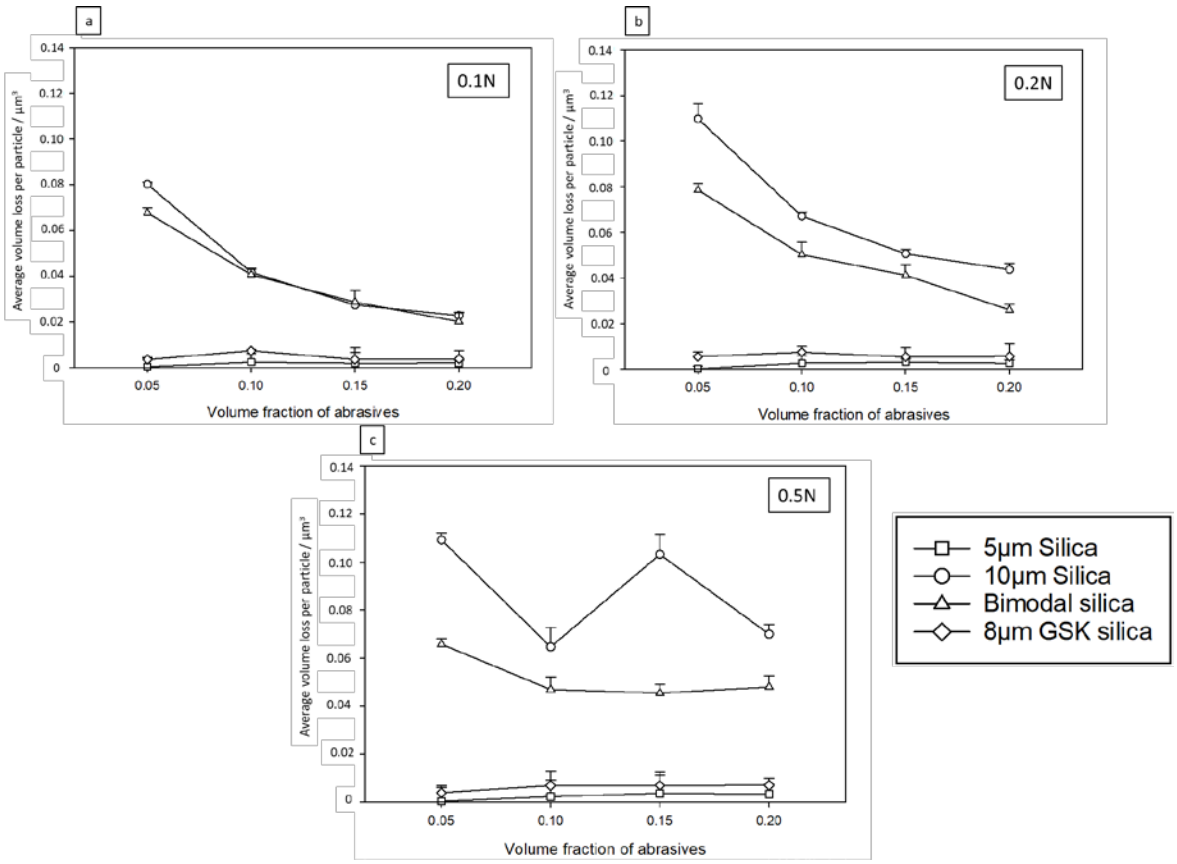

Figure 5.7: Average volume loss per particle for 5µm silica, 10µm silica, bimodal silica and 8µm GSK silica (a) 0.1N; (b) 0.2N; (c) 0.5N.

5.3.3 Spherical silica

Figure 5.8 shows the average volume loss for the spherical silica tests. At 0.05v/v, grooving abrasion dominated both the 5µm spherical silica and GSK 6.5µm spherical silica. The GSK 6.5µm spherical silica generated a higher volume loss than the 5µm spherical silica for all the tests, a-c.

Figure 5.8a-c. There was a significant difference in the average volume loss between both the particles, ($p<0.05$). There was a drop in volume loss of enamel observed for the 5µm spherical silica above 0.10 v/v. This is due to an increased rolling action and less grooving taking place above 0.10v/v, resulting in a decrease in volume loss of enamel, Figure 5.2 a-c.

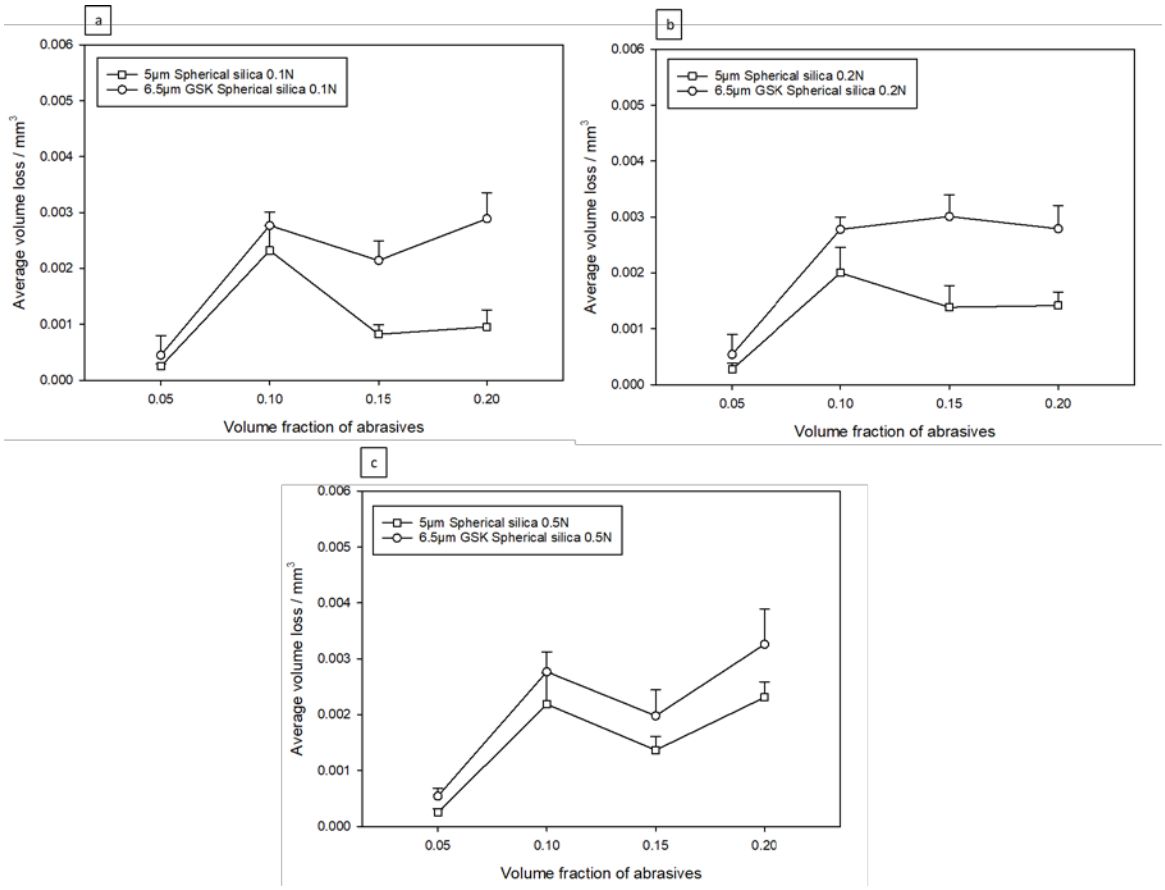

Figure 5.8: Average volume loss for 5µm spherical silica and 6.5µm spherical silica (a) 0.1N; (b) 0.2N; (c) 0.5N.

Figure 5.9 shows the average volume loss per particle for the 5µm spherical silica and the GSK 6.5µm spherical silica tests. The GSK 6.5µm spherical silica dominated the volume loss per particle.

There is 2.2x more volume of particles in the GSK 6.5µm spherical silica compared to the 5µm spherical silica. There is a significant difference in the volume per particle ($p<0.05$).

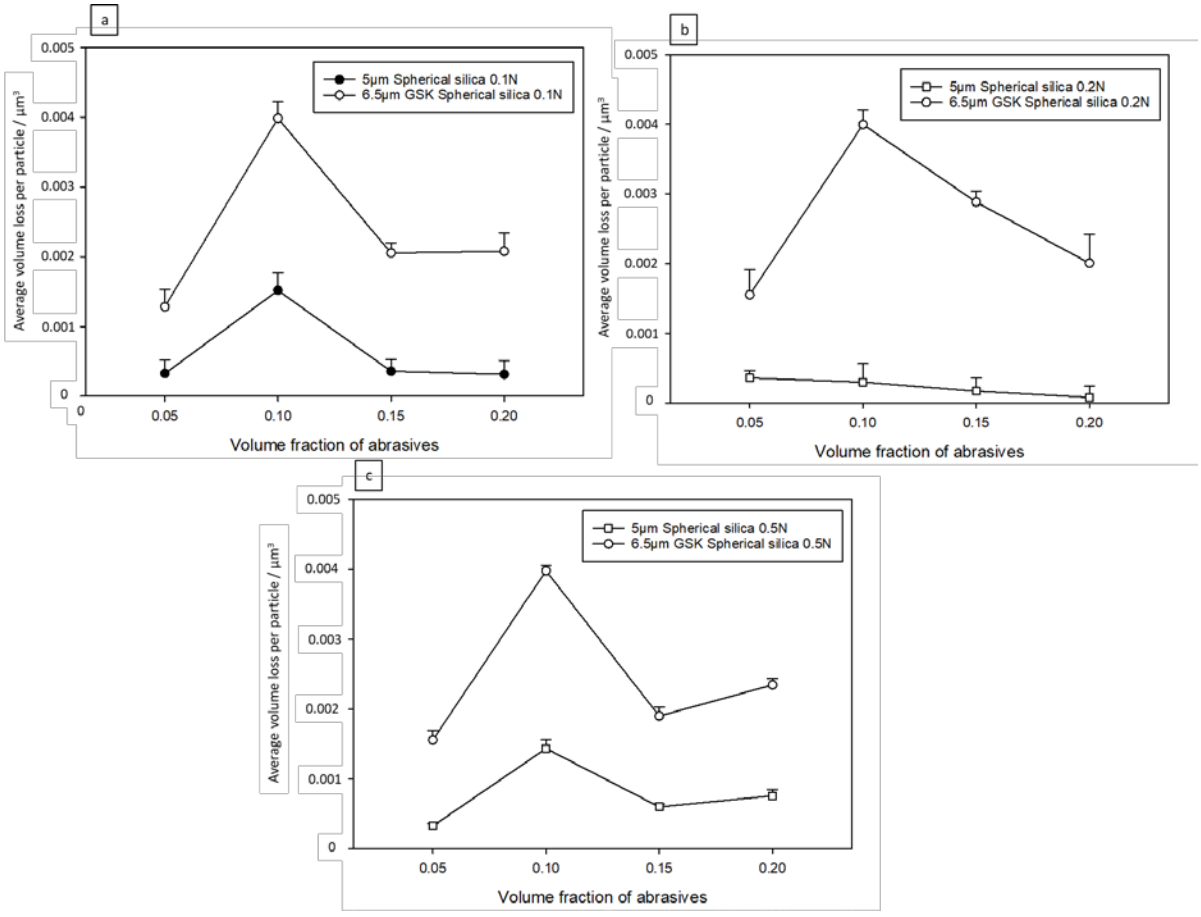

Figure 5.9: Average loss per particle for 5µm spherical silica and 6.5µm GSK spherical silica (a) 0.1N; (b) 0.2N; (c) 0.5N.

5.3.4 Synergy evaluation

Chapter 3.5 details the equations that were used to calculate the percentage synergy for the bimodal alumina and bimodal silica tests. Synergy was evaluated to observe the interaction between the different sizes of particles. For there to be synergy the below equations need to exist, Equation 5.1 and Equation 5.2. Where V is volume loss.

$$\frac{1}{2}V\ 5\mu m + \frac{1}{2}V\ 9\mu m\ or\ 10\mu m\ < V_{Bimodal} \quad \text{...Equation 5.1}$$

If Equation 5.1 is true, there is synergy.

$$\frac{1}{2}V\ 5\mu m + \frac{1}{2}V\ 9\mu m\ or\ 10\mu m\ > V_{Bimodal} \quad \text{...Equation 5.2}$$

If Equation 5.2 is true, antagonism is present.

Figure 5.10 shows the percentage synergy for bimodal alumina. There is a 35% – 65% positive synergy, which indicates the bimodal particles are affecting the volume loss of enamel and causing more wear, compared to the mono-sized particles.

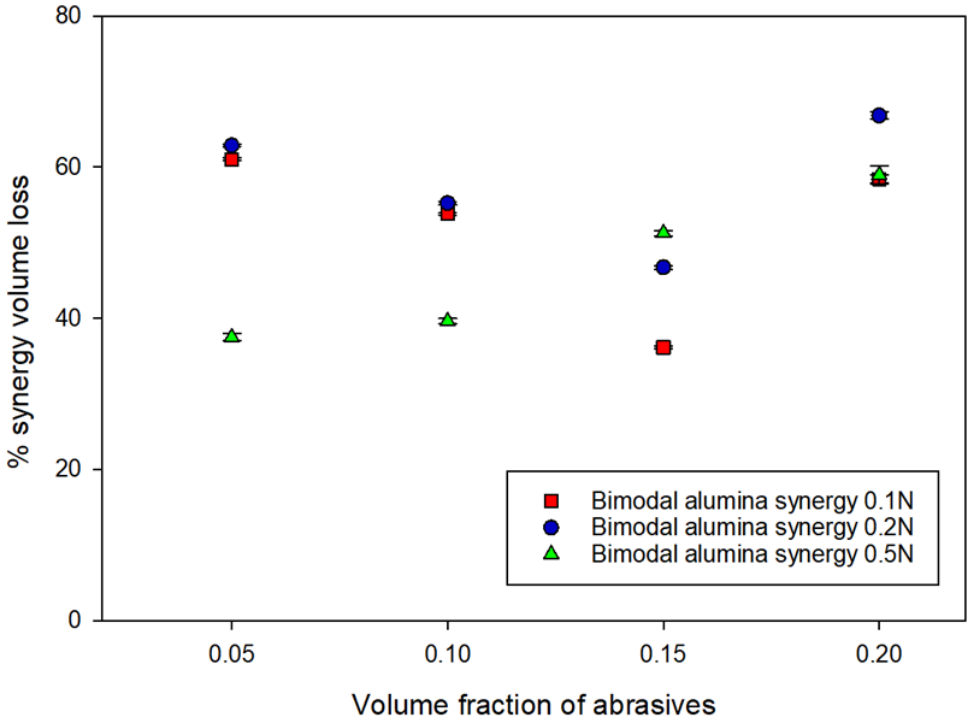

Figure 5.10: Percentage synergy for bimodal alumina.

Figure 5.11 shows the percentage synergy for bimodal silica. There is a 25% - 58% positive synergy, which indicates the combination of the bimodal particles effect the volume loss of enamel and this results in a higher volume loss of enamel, hence the positive synergy.

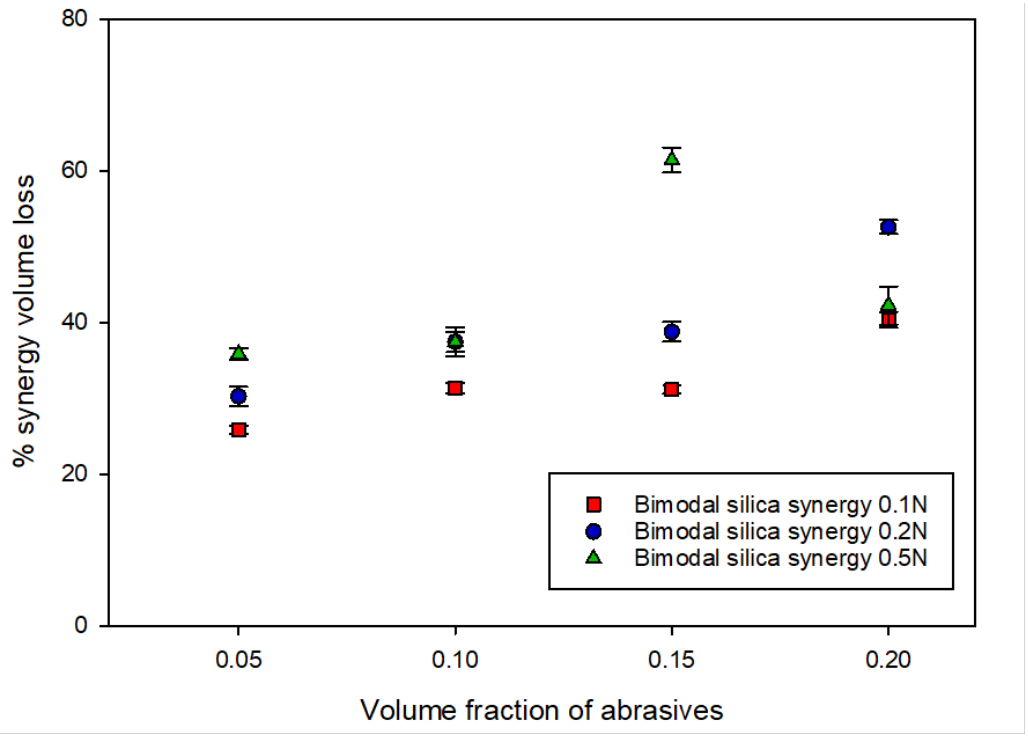

Figure 5.11: Percentage synergy for bimodal silica.

5.3.5 Influence of abrasive size on the wear scar profile

Figure 5.12 shows the wear scars produced with angular 1µm, 5µm, 9µm, and GSK 8µm alumina. These wear scars are also a typical representation for the wear scars produced with angular, 5µm silica, 10µm silica and GSK 8µm silica. Figure 5.12 a, c, e and g all show the grooving mechanism. The grooving abrasion wear scar consisted of multiple grooves.

Figure 5.12 b, d,f and h show the mixed-mode mechanism. The mixed-mode wear scar consisted of grooves, fracture, chipping and an indented surface with shallow pits.

The typical representation of the grooving mechanism observed for all the tests is grooves, indicating 2-body grooving. For the mixed- mode wear scar it consists of multiple grooving, fracture of enamel, indents and chipping. Brittle mechanisms such as chipping are observed, which results in an uneven, textured surface, (Figure 5.14).

With an increase in particle size, the grooves appeared to get larger. There was subtle differences with the mixed-mode wear mechanism, Figure 5.12.

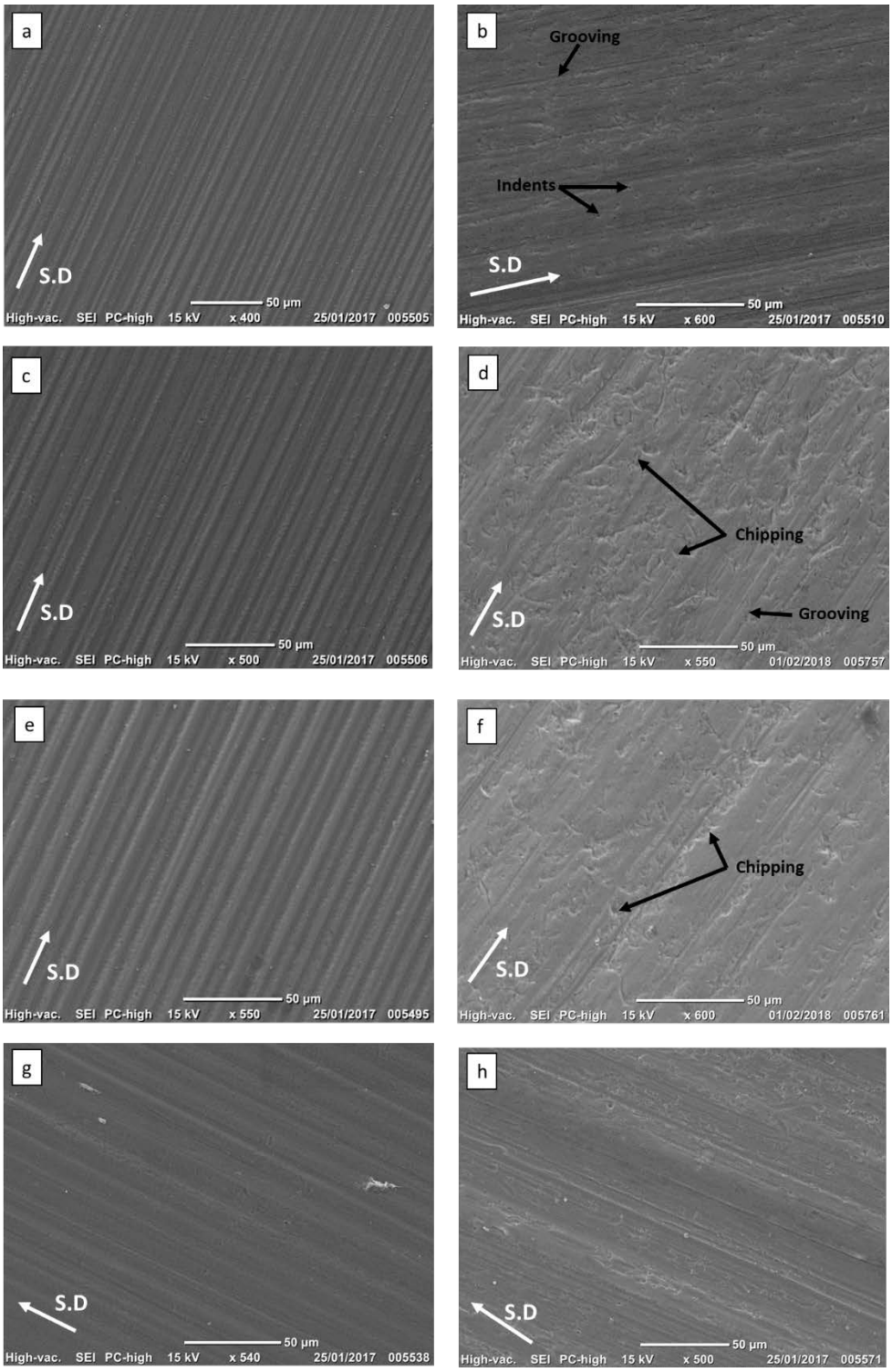

Figure 5.12: SEM images of angular alumina wear scars, at 0.2N (a) 1µm, grooving; (b) 1µm, mixed-mode; (c) 5µm, grooving; (d) 5µm, mixed-mode; (e) 9µm, grooving; (f) 9µm, mixed-mode; (g) GSK 9µm alumina, grooving; (h) GSK 9µm alumina, mixed-mode. Figures a,c,e and g are all 0.05 v/v and Figures d,b,f and h are all 0.10 v/v.

Figure 5.13 shows the wear scar produced for 9µm angular alumina at a load of 0.1N and a volume fraction of 0.20v/v. The wear scar appears to have an indented surface throughout, indicating rolling abrasion. The mechanism for rolling abrasion is a combination of chipping and indenting, with multiple indents removing/ damaging material from the enamel surface.

Figure 5.14 shows typical wear scars produced with bimodal silica (5µm + 10µm). The mixed-mode mechanism shows signs of chipping, fracture of enamel rods and grooving. The wear scar for mixed-mode is a typical representation of all the wear scars produced with bimodal silica (5µm + 10µm) and bimodal alumina (5µm + 9µm).

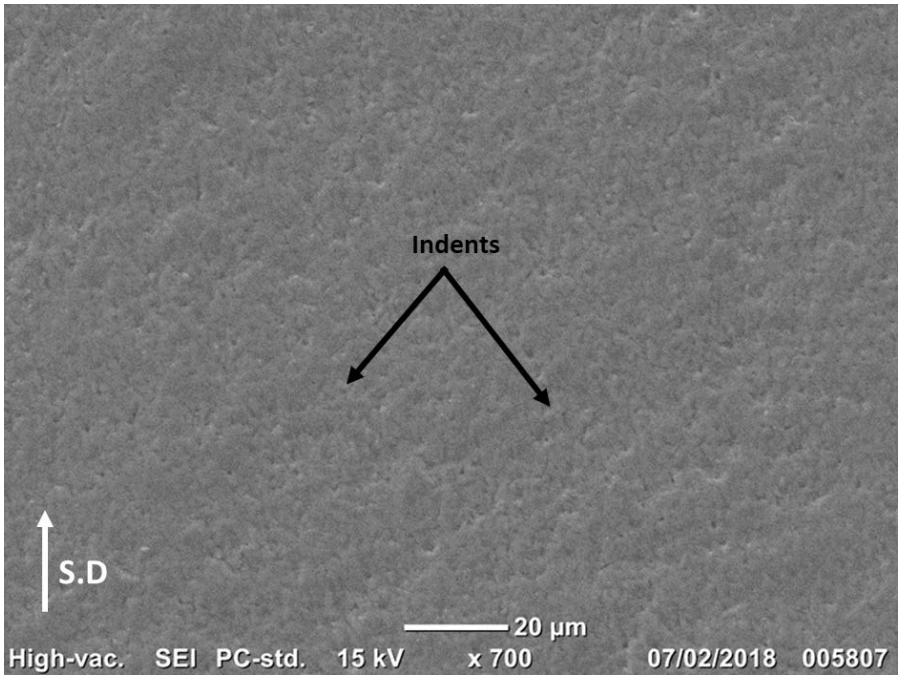

Figure 5.13: SEM images of wear scar produced with 9µm angular alumina, 0.1N at 0.20 v/v showing 3-body rolling.

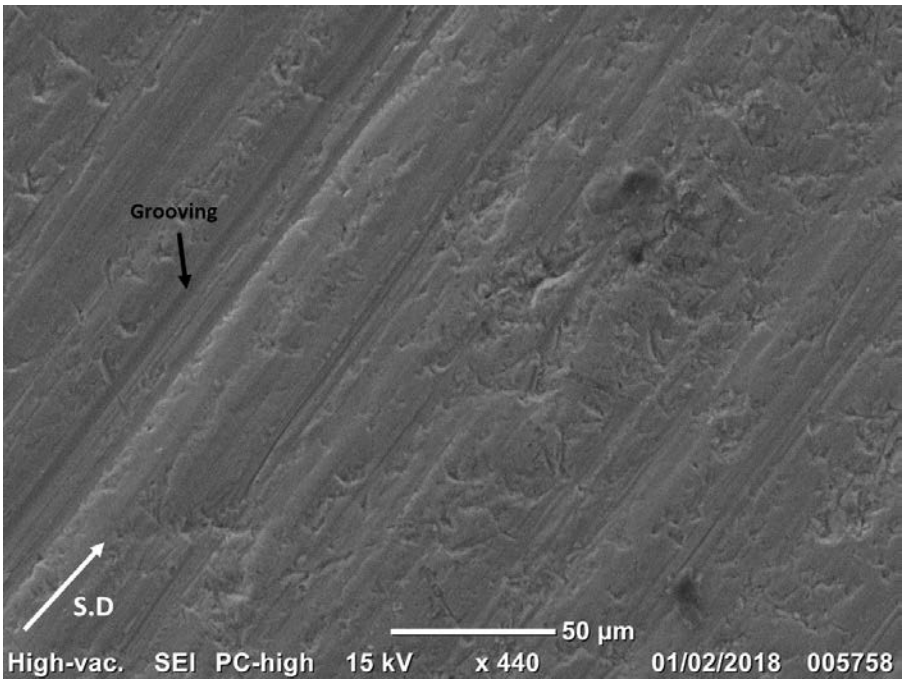

Figure 5.14: SEM images of wear scar with bimodal silica (5µm + 10µm), load 0.2N, 0.10v/v.

Figure 5.15 shows the typical wear scars produced with 5µm spherical silica (Figure 5.15a and Figure 5.15b) and GSK 6.5µm spherical silica (Figure 5.15c and Figure 5.15d). These wear scars are a typical representation of the wear scars produced with the 5µm spherical silica and GSK 6.5µm spherical silica tests. The grooving wear scar shows grooves and the mixed-mode wear scar shows signs of grooving, fracture and chipping. An increase in the groove width for the grooving mode is evident, from 5µm spherical silica to GSK 6.5µm spherical silica, Figure 5.15a and Figure 5.15c. There were subtle differences in the wear scars produced with 5µm spherical silica and GSK 6.5µm spherical silica.

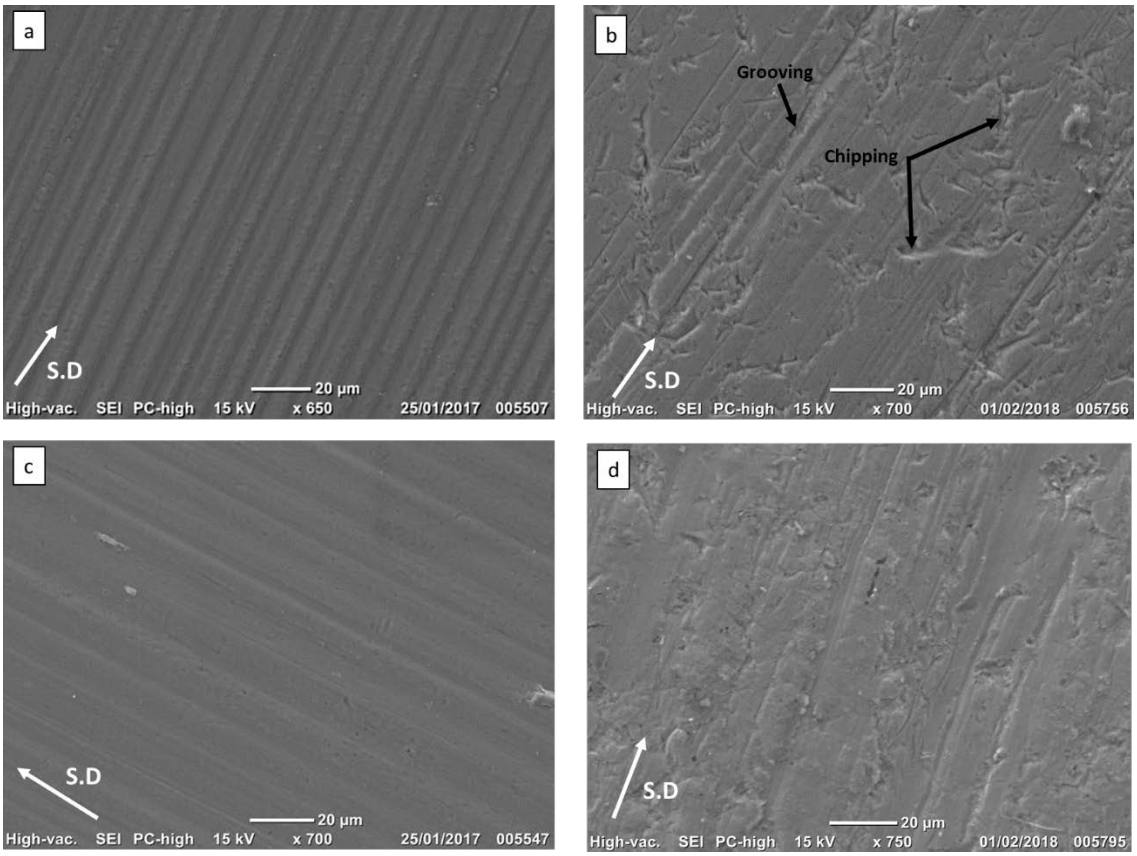

Figure 5.15: SEM images of wear scar of spherical silica at a load of 0.2N (a) 5µm spherical silica grooving; (b) 5µm spherical silica mixed-mode; (c) GSK 6.5µm spherical silica grooving; (d) GSK 6.5µm spherical silica mixed-mode. Figures a and c are 0.05 v/v and Figures b and d are 0.10 v/v.

5.4 Influence of particle size on groove width

The change in particle size can play a significant role in the size of the groove width. This section details groove analysis conducted on wear scars by using measurement analysis. The groove widths were measured by taking multiple measurements of the grooves and the average groove width was calculated for each mechanism. The maximum and mean particle sizes are also shown.

Table 5.3 shows the groove widths for angular alumina, 1µm, 5µm, 9µm, bimodal alumina and GSK 9µm alumina for grooving and mixed-mode wear mechanisms.

There was an increase in groove width from 1µm alumina to 5µm alumina, and an increase in groove width from 5µm alumina to 9µm alumina and GSK 9µm alumina, for both grooving and mixed-mode wear mechanisms.

For bimodal alumina, which contained an equal distribution (50% of each) of 5µm and 9µm alumina particles, there was an increase in groove width for both the wear mechanisms. There was no significant difference between the grooving and mixed mode wear regimes for 9µm alumina and the GSK 9µm alumina ($p>0.05$).

The groove width for the bimodal alumina (5µm + 9µm) was reported as 11.01µm. The maximum size of particles in the alumina 5µm and alumina 9µm slurry are doing the most damage to create this large groove width, Figure 5.16.

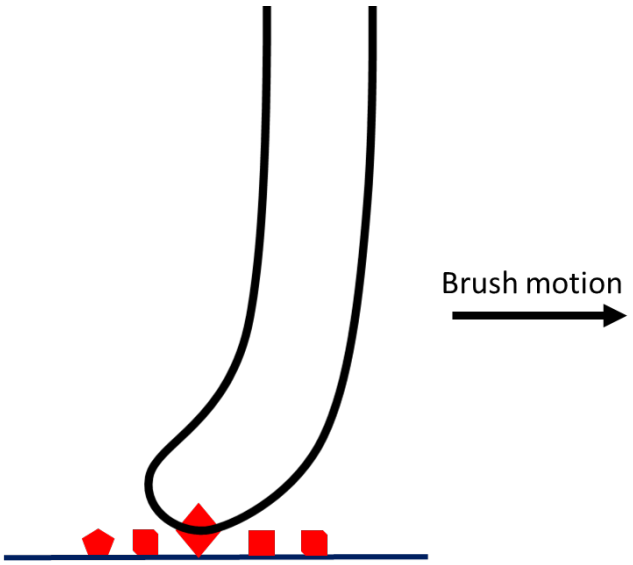

Figure 5.16: Particle size interaction

Table 5.3: Average groove width data for angular alumina 1µm, 5µm, 9µm, bimodal and GSK alumina.

	Grooving		Mixed- mode	
	Average groove width / µm	**Standard deviation**	**Average groove width / µm**	**Standard deviation**
Alumina 1µm Maximum– 1.79µm Mean – 1µm	3.31	0.73	3.73	0.65
Alumina 5µm Maximum – 8.1µm Mean – 5µm	6.94	1.72	7.67	1.36
Alumina 9µm Maximum– 10.2µm Mean – 9µm	9.01	1.64	11.63	1.72
Bimodal alumina 5µm + 9µm Mean - 7µm	11.01	1.16	14.91	1.54
GSK 9µm alumina Maximum – 10.4µm Mean – 9µm	9.22	0.77	11.97	0.93

Table 5.4 shows the groove width for angular silica, 5µm, 10µm silica, GSK 8µm silica and bimodal silica tests. There is an increase in groove width from 5µm silica to 10µm silica for both the grooving and mixed-mode mechanism. The bimodal silica showed no signs of grooving and the wear mechanism was dominated by mixed-mode. The largest groove widths were observed with the bimodal silica. This is due to the large 10µm particles in the bimodal silica test, resulting in a higher load per particle, whereas in the 10µm silica tests there are more 10µm silica particles, which results in a lower load per particle, hence the smaller groove. The large groove width for the bimodal silica (5µm + 10µm) mixed mode is a result of the maximum particle size of the silica 5µm and silica 10µm tests.

Table 5.5 shows the groove width data for 5µm spherical silica and GSK 6.5µm spherical silica. There is an increase in groove width from 5µm spherical silica to GSK 6.5µm spherical silica for the grooving and mixed-mode mechanism.

Table 5.4: Average groove width data for silica 5µm, silica 10µm, bimodal silica and GSK 8µm silica.

	Grooving		Mixed- mode	
	Average groove width / µm	**Standard deviation**	**Average groove width / µm**	**Standard deviation**
Silica 5µm Maximum – 23µm Mean – 5µm	6.48	0.58	7.36	1.71
Silica 10µm Maximum – 28µm Mean – 10µm	10.28	1.09	11.83	2.72
Bimodal silica 5µm + 10µm Mean – 7.5µm	-	-	16.17	1.96
GSK 8µm silica Maximum size– 9µm Mean size – 8µm	8.39	0.37	10.08	1.07

Table 5.5: Average groove width data for 5µm spherical silica and GSK spherical silica.

	Grooving		Mixed- mode	
	Average groove width / µm	**Standard deviation**	**Average groove width / µm**	**Standard deviation**
5 µm Spherical silica Maximum size – 6.1µm Mean size – 5µm	5.28	0.65	6.96	1.23
GSK 6.5µm spherical silica Maximum size – 8.8µm Mean size – 6.5µm	5.87	0.87	8.08	0.95

5.5 Discussion

In this chapter, the influence of particle shape, size and composition on the volume loss of enamel has been examined. This section will discuss the main findings of the shape and size effects of abrasive particles, on the volume loss of enamel.

5.5.1 Limitations

The 5µm and 10µm angular silica particles have a wide distribution with maximum particle sizes of 23µm and 28µm respectively. In section 5.2.1, the volume loss of enamel would be influenced by the maximum particle size of the 5µm silica particle, which is 23µm. The comparison of particle shape on the volume loss of enamel would not represent the morphology changes; the maximum particle size of the angular 5µm silica particle would be dominating the comparison. This matter has been addressed and for this reason in Section 5.2.1, the addition of angular GSK 8µm silica has been included for comparison purposes, as this particle has a more controlled mono-sized particle distribution compared to the 5µm silica.

5.5.2 Nature of abrasives

The hardness of the abrasives could affect the amount of enamel loss, with the hardness of enamel being in the region of 1.47 GPa - 1.60GPa [228]. The silica tests resulted in a higher volume loss of enamel (

Figure 5.6), compared to the alumina tests, Figure 5.5. This is unexpected, as alumina is a harder abrasive than silica. Alumina has a hardness of 24.5GPa, whereas silica has a hardness of 11.7GPa [229, 230]. An explanation for this could be the wide particle distribution for the 5µm and 10µm silica. The maximum particle size for the 5µm silica was reported to be 23µm and the maximum particle size for the 10µm silica was 28µm respectively. The groove analysis showed, larger grooves for the angular silica tests.

5.5.3 Influence of particle shape

The particle shape can influence the behaviour of the particles and thus the volume loss of enamel. In the current study it was found that the angular particles have sharp edges, which can chip the enamel, whereas the spherical particles have round edges. A study carried out by Speerschneider et al. [231] on the wear damage of stainless steel by alumina filled PTFE material. found a reduction in abrasive damage by the spherical particles compared to the angular alumina particles. The particle size of both particles was 7µm. It has been noted that using a geometrically shaped particle such as a spherical particle, reduces the abrasive damage and thus differences in wear and friction are observed with specific geometrically shaped particles. This was observed in the present tests, where 5µm spherical silica generated a lower volume loss of enamel compared to the 5µm angular silica and angular GSK 8µm silica,

Figure 5.2. The volume loss of enamel was higher with angular silica particles compared to spherical silica particles. This can be explained by the angular particles removing more material than the spherical particles, due to the geometry of the angular particles. The grooving wear scar was similar in appearance for the angular 5µm silica, spherical 5µm silica and angular GSK 8µm silica (Figure 5.3a, c, e). However, there were more indents observed with the 5µm spherical silica with a decrease in volume loss of enamel above 0.10 v/v (Figure 5.17). This was due to more rolling abrasion and less grooving. The indenting osberved on the enamel surface is likely to be a result of densification of the enamel tissue. After a number of loading cycles, this results in removal of enamel and break up of the enamel prism surface.

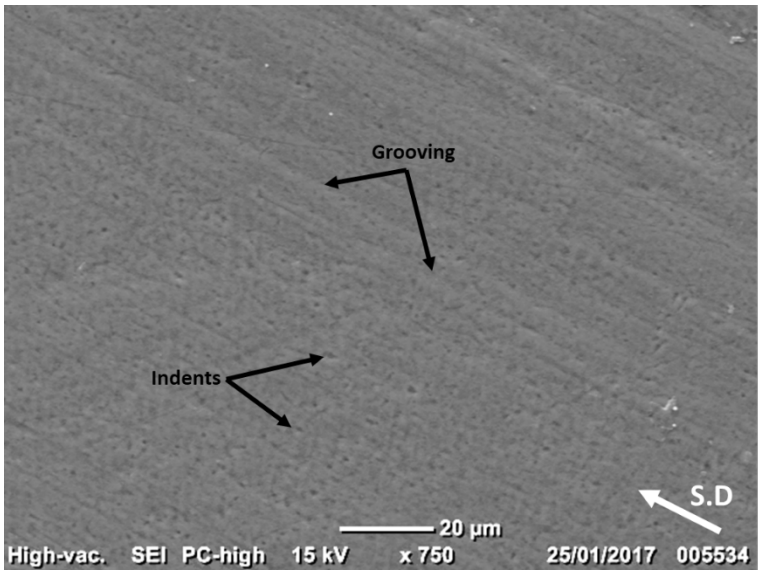

Figure 5.17: SEM image of mixed-mode wear scar for 5µm spherical silica at 0.5N and volume fraction 0.20 v/v.

The spherical silica particles produced indents indicating rolling abrasion in the mixed-mode wear regime. The 5µm spherical silica particles roll when they are in the contact between the nylon ball and the enamel disc, Figure 5.18. This is proved by the rolling indentation scar, Figure 5.3d. The spherical particle penetrates the enamel surface resulting in indents [232].

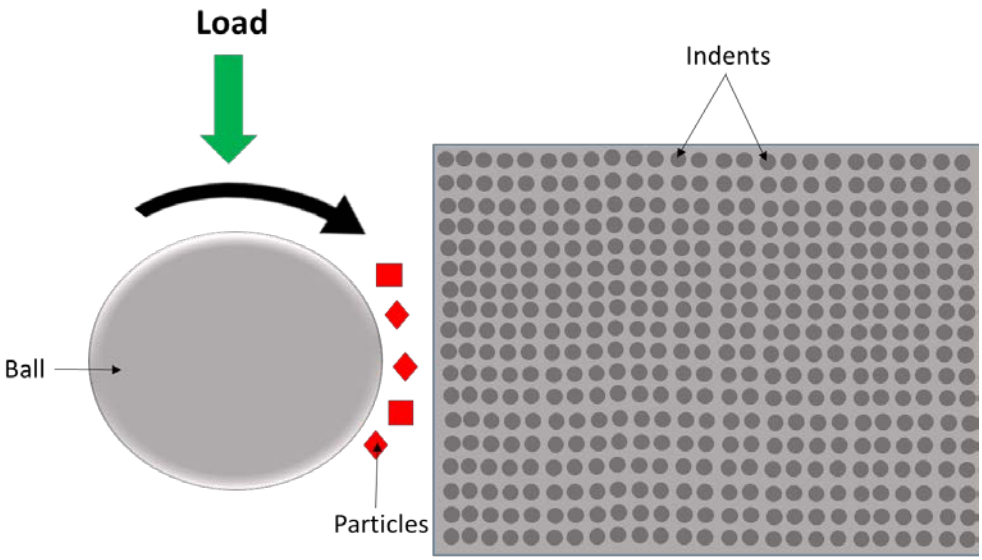

Figure 5.18: Schematic of rolling particle interaction.

A study carried out by Pena et al. [147] found that the angular particles in the slurry caused wear damage at random directions. This is evident in the current study, in which the mixed-mode regime shows signs of an irregular surface, where the indents and fracture of enamel occur at random directions. This is consistent with results in previous studies [147, 233].

A study conducted by Silva, et al. [234] used a hard martensitic steel ball on a steel substrate and used alumina and silica abrasive particles in a slurry solution consisting of water at a concentration of 75gcm^3. The silica particles were spherical in shape whereas the alumina particles were angular. Silva et al. [234] confirmed that angular sharp particles such as alumina give higher SWR and cause more wear than spherical particles. This is confirmed by the current study with angular particles generating higher wear rates than the spherical particles [234].

The influence of particle shape indicates the presence of a mixed-mode region that can highly increase the removal of enamel. Bai et al. [232] carried out tests on a diamond-like carbon film using sand particles. The study found the shape of the particle to influence the movement modes

of particles which in turn effects the volume loss of material [232]. For the present study, a higher volume loss of enamel was observed in the mixed-mode region. The increase of volume loss of enamel in mixed- mode can be due to a number of reasons, such as the angular shape of the particles, the contact stresses exerted by the angular particles on the enamel surface and the entrainment of particle in the contact.

5.5.4 Influence of particle size

The effect of particle size is considered by changing the radius of the particle size. Bimodal tests were also conducted that had a mean particle size of the small and large particle. Figure 5.15 shows the typical wear scar for mixed-mode abrasion for all the tests. The indents on the SEM show damaged enamel and removal of material.

Figure 5.6 shows the average volume loss of enamel for the silica tests. The GSK 8µm silica particles produced the lowest volume loss. These particles had a tighter particle distribution to the angular 5µm silica particles. Smaller sized particles can reduce volume loss by reducing the contact stress and penetrating the surface [232]. This is due to an increase in friction force with smaller particles and the ability of the small particles to form a flat layer and thus reduce the contact stress. More particles in the slurry result in a lower force per particle.

Figure 5.13 shows the typical wear scar for rolling abrasion. The rolling abrasion causes a rough surface topography with clear indent features at the scale of the abrasive particles. The removal of material is due to fracture and crushing of enamel rods and subsequent surface damage or removal of enamel rods by other particles. Pena et al. [147] reported plastic deformation and brittle delamination on the enamel surface when wear tests were conducted. What is surprising is that in the current study no signs of plastic deformation were observed.

Mixed mode (2-body grooving with 3-body rolling) abrasion provided higher wear rates than solely 2-body grooving in all the tests. The bimodal tests produced higher wear rates than the single component sized particle tests. This can be explained by the bigger particles receiving a higher load per particle as they go through the contact, causing more damage on the enamel surface. Bimodal silica particle tests caused more wear than bimodal alumina particle tests, due to the 10µm silica dominating the bimodal silica.

The highest wear rates were produced by the bimodal particle size distributions due to a shift to mixed-mode abrasion. Mixed mode gave higher wear rates compared to 2-body grooving in all the tests. This was caused by the increase in size of the silica particles.

Bai et al. [232], mentions that three body abrasion is a complicated process and many factors can influence the 3-body wear process such as the size, shape, number and density of abrasive particles. Three body rolling wear was observed with the 9µm alumina at 0.20v/v volume fraction and a load of 0.1N. Rolling abrasion is often observed with a high volume fraction and low loads. The present study confirms this finding. This could be due to the entrainment of particles in the contact, resulting in rolling abrasion. It was found that a higher volume loss of material was observed by the grooving mechanism than three-body rolling. This occurrence is not observed in the current study, as grooving abrasion resulted in a lower volume loss of enamel than the rolling mechanism, Figure 5.5a.

A study conducted by Katra et al. [235] highlighted the difficulty in quantifying a bimodal distribution for a test. It suggested, the combination of two sizes of particles changes the distribution of particles and for this reason, a mean particle size cannot be correctly assumed for bimodal tests. Gava et al. [236] suggests using the maximum particle size to quantify the bimodal tests, due to the largest particles in the bimodal slurry being dominant, or alternatively by taking an average of the two particle sizes [2]. The latter method of taking the average particle size has been used for these tests. The bimodal aspect of the test is novel and has not been carried out before, nor do bimodal sized particles exist in toothpastes currently [3].

The abrasive size also has an effect on the severity of wear. An increase in force per abrasive particle is seen with an increase in mean size of abrasive. Increasing the mean abrasive size reduces the number of particles at the interface of the ball and sample, which then results in an increase in force per particle. The bigger the size of the abrasive particle, the greater the wear rate. This was observed in the current study with the 9µm alumina and 10µm silica producing higher wear rates than the smaller sized particles. These findings further support the idea of the size of the abrasive is the one of the most important factors in controlling the wear rate and mechanism, alongside load per abrasive particle. This is also confirmed in the current study, with the bimodal tests generating the highest wear rates [234].

As expected, an increase in the particle size within the slurry, contributed to an increase in the volume of material loss and the specific wear rate. The origin of this effect lies in the load per particle as it travels through the contact. In the current study, the slurries were manufactured on the basing of volume fraction and therefore the smaller sized particle slurries contained a higher

number of particles. The load was therefore distributed between more particles in the small- size particle slurries, producing less damage than the larger-size and more highly loaded particles. In the bimodal slurries, the larger particles are fewer in number however, when they are drawn through the contact they are subject to the highest load per particle causing the increased level of damage seen.

The increased levels of volume loss and SWR of the silica tests compared to the alumina tests is due to the difference in the size distribution. An explanation for this result could be due to the alumina mono-sized particles, which have a tightly controlled size range within 3µm, whereas the silica contain particles as large as 28µm. The larger particles within the silica tests have elevated the volume losses and SWR for the reasons outlined above.

5.6 Conclusions

The effects of changing the particle shape and size on the volume loss of enamel were investigated using the micro-abrasion tester. The following conclusions can be made:

- Particle size and the magnitude of the distribution of the particle sizes is a key variable in determining the volume loss of enamel, with smaller particles and narrow distributions of the particle size reducing the enamel loss.

- Mono-sized particles distribute the load across lots of particles. A wider particle distribution, as in the silica tests results in the larger particles taking the higher load and this results in more damage on the enamel surface.
- The few large particles in the bimodal slurry take a higher load and cause more damage.

- A change in shape of particles for the silica particles from angular to spherical caused a decrease in volume loss of enamel, due to lower contact stresses of the spherical partides when contacting the enamel surface.

- The wider grooves are caused by the large particles, which generate a higher load per particles and cause larger grooves.

- A positive synergy is produced for the bimodal alumina and bimodal silica tests, highlighting the fact the bimodal particles cause more enamel removal than the mono-sized particles.

- The wear volume was affected by the wear mechanism, with 2 body-grooving generating less damage than the mixed mode wear regime.

- The grooving mechanism is a result of the abrasive particles being trapped by the nylon ball under loading. The abrasive particles micro-chip the enamel surface and enamel removal takes place, which results in 2-body grooving.

- The mixed-mode mechanism is observed as a combination of grooving, fracture and indents on the enamel surface. Brittle mechanisms such as chipping, crushing and fracture of enamel rods are observed on the enamel surface. Indenting is a result of densification of the enamel tissue, which causes enamel structural damage.

- 5µm alumina particles generate more volume loss of enamel compared to the GSK 9µm alumina. The distribution of particles with the 5µm alumina is ±3.1µm. The GSK 9µm alumina have a tighter size distribution (±2.69µm).

6. The effect of load on the wear rate and severity of contact of enamel

6.1 Introduction

Following the previous chapter which describes the influence of shape and size on the volume loss of enamel, this chapter aims to investigate the effect of varying the load on the wear rate of enamel. This chapter presents the results of micro-abrasion tests varying the load and volume concentration of abrasives. The specific wear rates (SWR) were compared between the different tests and possible wear mechanisms are discussed. The severity of contact, which includes load per particle results are presented. The wear scar profiles were characterised for microstructural and topographical changes, with detailed investigation into groove analysis. Synergy was calculated for each load for the bimodal alumina and bimodal silica tests, which will be discussed in detail in chapter 8.

6.1.1 Experimental details

The experimental method is laid out in full in chapter 3. To investigate the effect of load on the wear rate of enamel, microabrasion testing was performed using a nylon ball against an enamel surface. The sliding velocity was kept constant at 0.035ms^{-1} for a test duration of 1 minute at room temperature, with 8 repeats performed for each test set up. 7 different angular particles with controlled size distributions of two different materials were used (1µm alumina, 5µm alumina, 9µm alumina, GSK 9µm alumina, 5µm silica, 10µm silica, GSK 8µm silica). Tests were also performed with a 5µm spherical silica and 6.5µm GSK spherical silica. The single sized particles of 5µm and 9µm angular alumina and 5µm and 10µm angular silica were mixed to provide a bimodal distribution of bimodal 7µm alumina and bimodal 7.5 µm silica, to investigate the synergistic effect of load. Each particle was used in slurry form, with 4 volume fractions of abrasive (0.05, 0.10, 0.15 and 0.20 v/v) used to identify any changes in the wear mechanism, wear rate and severity of contact. The test conditions are outlined in Table 6.1.

Table 6.1: Tests conditions for the micro-abrasion tests.

Test conditions		
Ball sliding velocity (ms^{-1})	0.035	
Volume fraction of abrasives	0.05, 0.10, 0.15, 0.20	
Ball material	Nylon	
Temperature/ $^{\circ c}$	18	
Counterface material	Enamel	
Time/ minute	1	
	Mean particle size / µm	**Maximum particle size / µm**
Abrasive particles	**Angular**	
	1µm alumina	1.79
	5µm alumina	8.1
	9µm alumina	10.2
	Bimodal (5µm + 9µm) alumina Mean- 7µm	
	GSK 9µm alumina	10.4
	5µm silica	23
	10µm silica	28
	Bimodal (5µm + 10µm) Silica Mean – 7.5µm	
	GSK 8µm silica	9
	Spherical	
	5µm spherical silica	6.1
	GSK 6.5µm spherical silica	8.8
No. of repeats per test (craters formed)	8	

6.2 Specific wear rate comparisons

Mono sized angular particles were tested, namely, angular 1µm alumina, 5µm alumina, 9µm alumina, GSK 9µm alumina, silica 5µm, silica 10µm and GSK 8µm silica. Bimodal slurries were made either containing 50% angular alumina particles of sizes 5µm and 9µm, or 50% angular silica containing, 5µm and 10µm silica particles.

6.2.1 Angular Alumina

Figure 6.1 shows the distribution of wear modes observed for 1µm angular alumina. For the 1 µm alumina there was a change in wear mechanism from grooving to mixed mode above 0.05 v/v for all three loads, Table 6.8. An increase in load resulted in a decrease in SWR for 1µm alumina. There was a significant difference in decreasing SWR with an increase in load ($p < 0.05$).

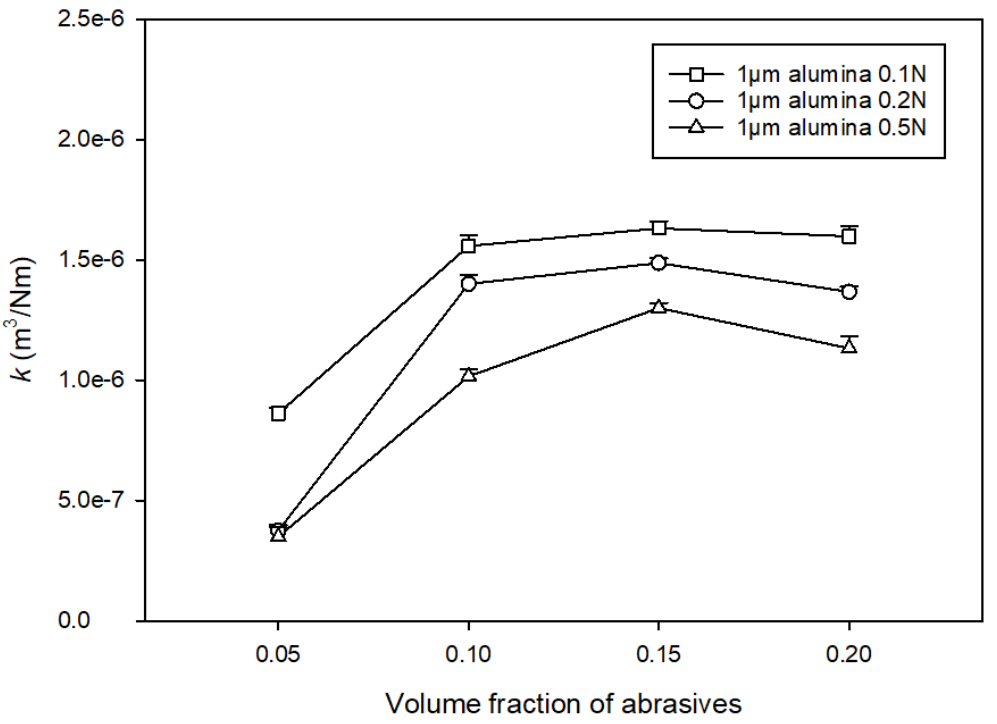

Figure 6.1: Specific wear rate (k) for 1µm angular alumina.

Table 6.2: Wear mechanisms of 1µm alumina.

	1µm Alumina			
	Volume fraction of abrasives			
Load	**0.05**	**0.1**	**0.15**	**0.20**
0.1N	Grooving	Mixed	Mixed	Mixed
0.2N	Grooving	Mixed	Mixed	Mixed
0.5N	Grooving	Mixed	Mixed	Mixed

Figure 6.2 shows the specific wear rates observed for angular 5µm alumina, 9µm alumina and bimodal alumina as a function of volume fraction of abrasives in the slurry. The wear mode changed from grooving to mixed mode for the 5µm alumina above 0.05 v/v for all three loads. At each volume fraction (0.05 – 0.20v/v) there was a decrease in SWR with an increase in load. The wear transitions of 5µm alumina are shown in Table 6.3.

For 9µm alumina there was a change in wear mechanism from grooving to mixed-mode above 0.05 v/v for loads of 0.1N and 0.2N. This change is shown in Table 6.4. At 0.5N there was a later change in wear mechanism above 0.10v/v for grooving to mixed-mode.

For the bimodal alumina tests a change of wear mechanism was observed above 0.05v/v for a load of 0.5N from grooving to mixed mode abrasion. Decreasing the load resulted in a mixed-mode response for 0.05 – 0.20v/v for loads of 0.1N and 0.2N, Table 6.5.

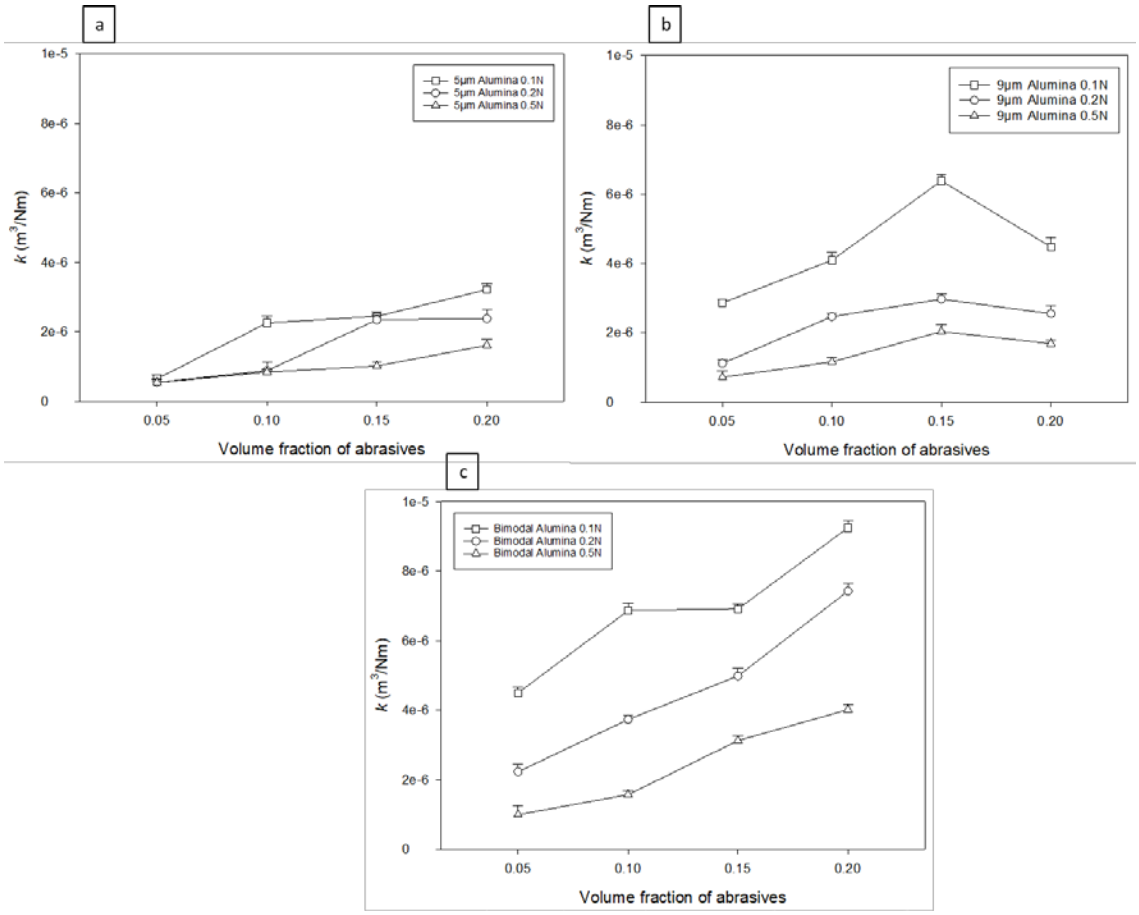

Figure 6.2: Specific wear rate (k) for angular alumina (a) 5µm alumina; (b) 9µm alumina; (c) bimodal alumina.

Table 6.3: Wear transitions of 5µm alumina.

	5µm Alumina			
	Volume fraction of abrasives			
Load	**0.05**	**0.1**	**0.15**	**0.20**
0.1N	Grooving	Mixed	Mixed	Mixed
0.2N	Grooving	Mixed	Mixed	Mixed
0.5N	Grooving	Mixed	Mixed	Mixed

Table 6.4: Wear transitions of 9µm alumina.

	9µm Alumina			
	Volume fraction of abrasives			
Load	**0.05**	**0.1**	**0.15**	**0.20**
0.1N	Grooving	Mixed	Mixed	Rolling
0.2N	Grooving	Mixed	Mixed	Mixed
0.5N	Grooving	Grooving	Mixed	Mixed

Table 6.5: Wear mechanisms of bimodal alumina 7µm.

	Bimodal alumina 5µm + 9µm			
	Volume fraction of abrasives			
Load	**0.05**	**0.1**	**0.15**	**0.20**
0.1N	Mixed	Mixed	Mixed	Mixed
0.2N	Mixed	Mixed	Mixed	Mixed
0.5N	Grooving	Mixed	Mixed	Mixed

Figure 6.3 shows the specific wear rates for GSK 9µm alumina. The GSK 9µm alumina showed a change in wear mechanism from grooving to mixed mode above 0.15 v/v for loads of 0.1N and 0.5N. At a load of 0.2N the change in wear mechanism was observed above 0.05 v/v. The wear transitions are shown in Table 6.6. An increase in load generated a significant decrease in SWR for all the volume fractions ($p<0.05$).

For all the angular alumina tests, an increase in load from 0.1N – 0.5N, resulted in a significant decrease in SWR for all the volume fractions ($p<0.05$).

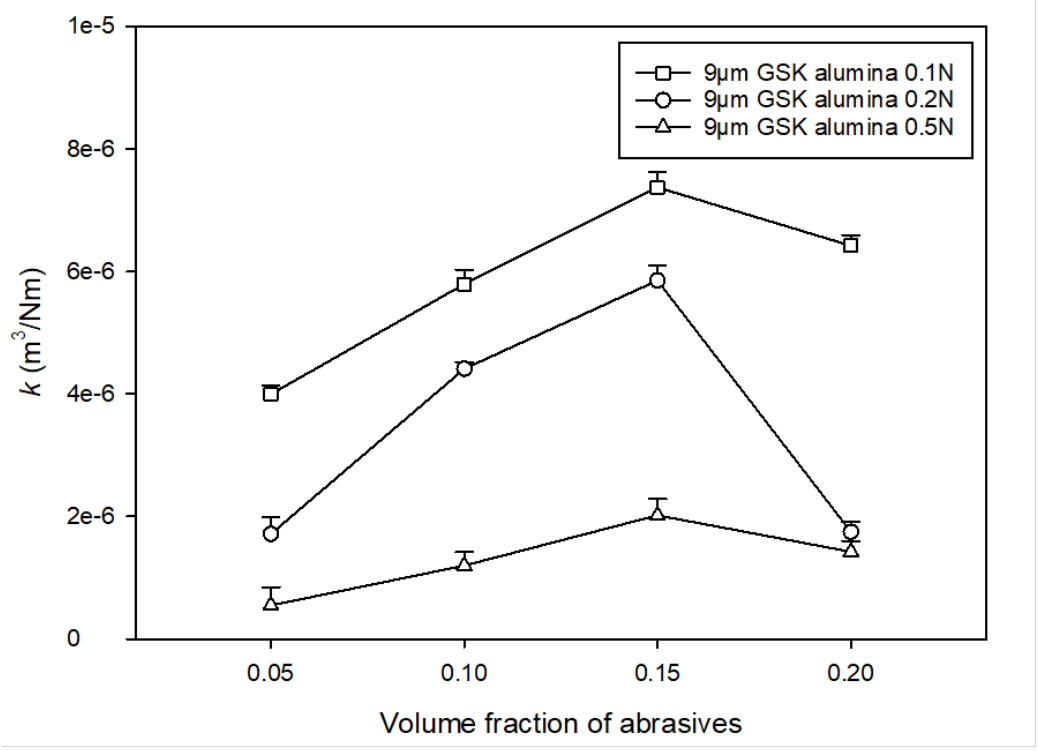

Figure 6.3: Specific wear rate (k) for GSK 9µm alumina tests.

Table 6.6: Wear mechanisms of GSK 9µm alumina.

	GSK 9µm alumina			
	Volume fraction of abrasives			
Load	**0.05**	**0.1**	**0.15**	**0.20**
0.1N	Grooving	Grooving	Mixed	Mixed
0.2N	Grooving	Mixed	Mixed	Mixed
0.5N	Grooving	Grooving	Mixed	Mixed

6.2.2 Angular silica

Figure 6.4 shows the specific wear rates observed for angular 5µm silica, 10µm silica and bimodal silica.

For the 5µm silica tests, there was a change in wear mechanism from grooving to mixed-mode above 0.05v/v for all the loads, Table 6.7. The 10µm silica wear transitions are shown in Table 6.8. For a fixed load of 0.2N and 0.5N, there was a change in wear mechanism from grooving to mixed-mode above 0.05v/v. The mixed mode wear mechanism dominated all the bimodal wear tests, Table 6.9. As the load increased, the specific wear rate decreased for the 5µm, 10µm and bimodal silica tests. There was a significant difference in SWR with an increase in load for all the tests ($p < 0.05$).

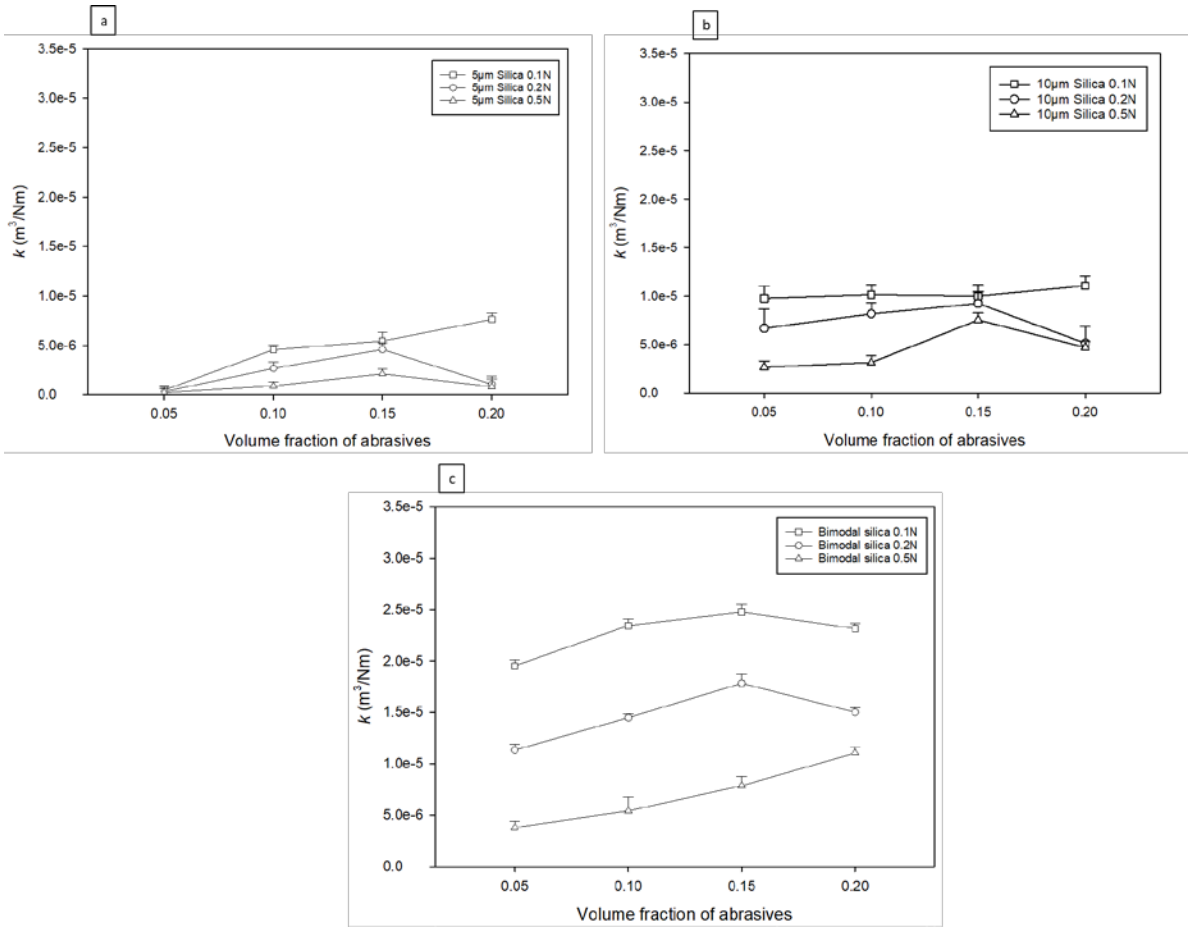

Figure 6.4: Specific wear rate (k) for angular silica (a) 5µm silica; (b) 10µm silica; (c) bimodal silica.

Table 6.7: Wear mechanisms for 5µm silica.

	5µm Silica			
	Volume fraction of abrasives			
Load	**0.05**	**0.1**	**0.15**	**0.20**
0.1N	Grooving	Mixed	Mixed	Mixed
0.2N	Grooving	Mixed	Mixed	Mixed
0.5N	Grooving	Mixed	Mixed	Mixed

Table 6.8: Wear mechanisms for 10µm silica.

	10µm Silica			
	Volume fraction of abrasives			
Load	**0.05**	**0.1**	**0.15**	**0.20**
0.1N	Mixed	Mixed	Mixed	Mixed
0.2N	Grooving	Mixed	Mixed	Mixed
0.5N	Grooving	Mixed	Mixed	Mixed

Table 6.9: Wear mechanisms for bimodal silica.

	Bimodal silica 5µm + 10µm			
	Volume fraction of abrasives			
Load	**0.05**	**0.1**	**0.15**	**0.20**
0.1N	Mixed	Mixed	Mixed	Mixed
0.2N	Mixed	Mixed	Mixed	Mixed
0.5N	Mixed	Mixed	Mixed	Mixed

Figure 6.5 shows the specific wear rates for GSK 8µm silica. There is a change in wear mechanism observed above 0.05v/v for loads of 0.1N, 0.2N and 0.5N, Table 6.10. A significant trend that is clearly visible from the graph is a decrease in SWR with an increase in load, ($p<0.05$).

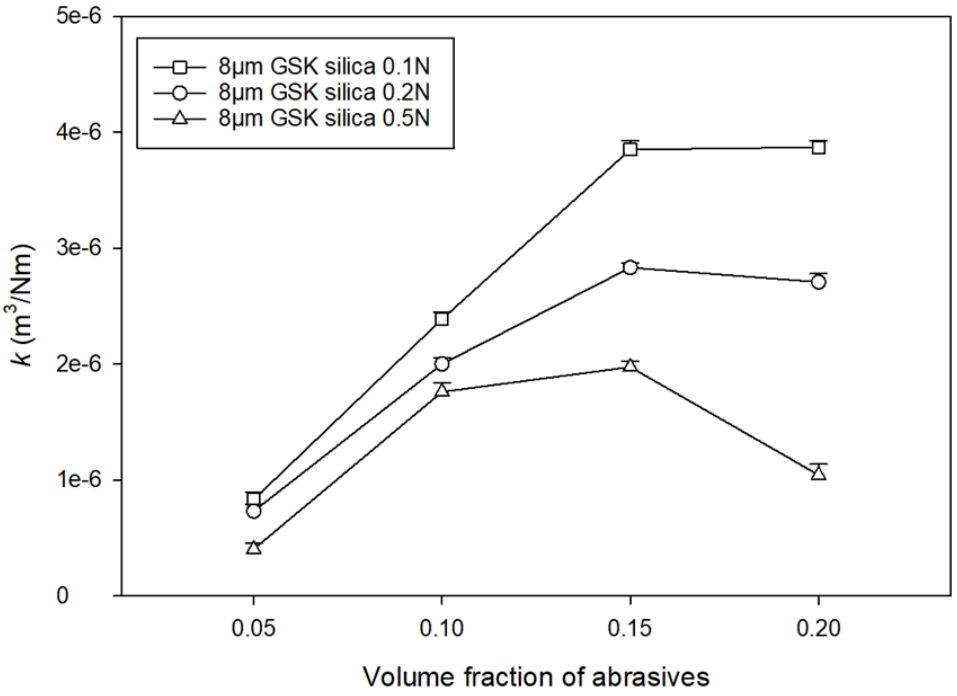

Figure 6.5: Specific wear rate (k) for 8µm GSK silica.

Table 6.10: Wear mechanisms for 8µm GSK silica.

	8µm GSK silica			
	Volume fraction of abrasives			
Load	**0.05**	**0.1**	**0.15**	**0.20**
0.1N	Grooving	Mixed	Mixed	Mixed
0.2N	Grooving	Mixed	Mixed	Mixed
0.5N	Grooving	Mixed	Mixed	Mixed

6.2.3 Spherical silica

Comparisons have been made between the wear rates of 5µm spherical silica and GSK 6.5µm spherical silica.

Figure 6.6 shows the specific wear rates for 5µm spherical silica. There was a significant decrease in SWR with increasing load from 0.1N to 0.5N, ($p<0.05$). Table 6.11 shows the wear mechanisms for 5µm spherical silica. There was a change in wear mechanism from grooving to mixed- mode above 0.05 v/v for all the loads.

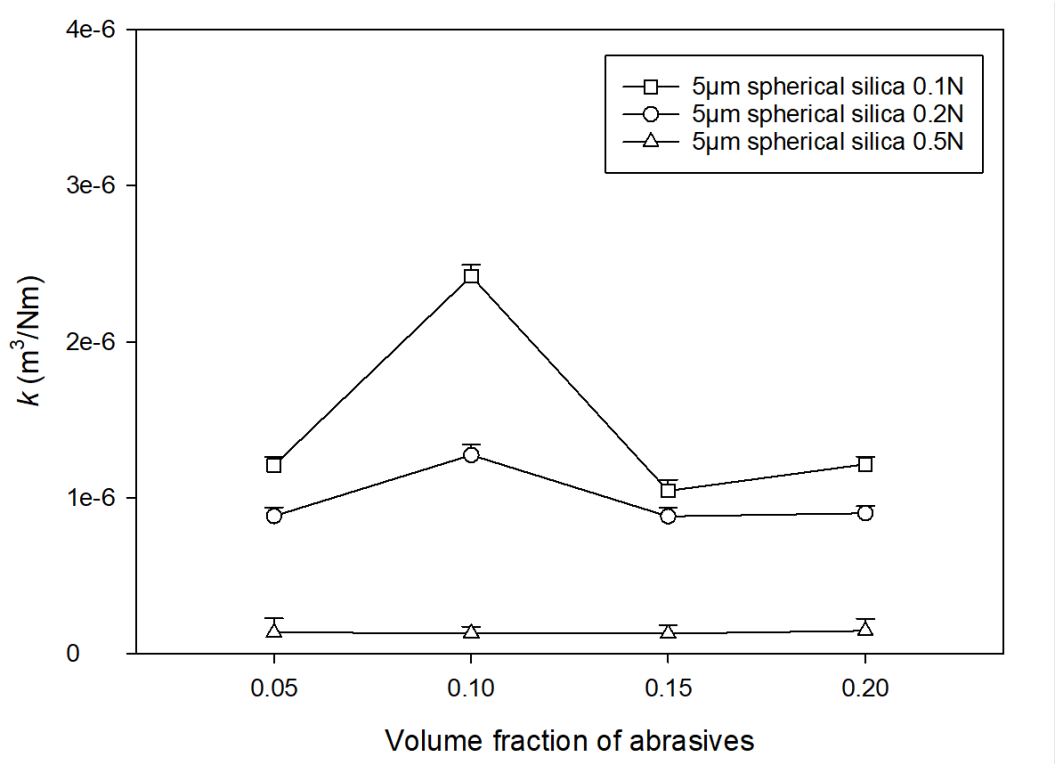

Figure 6.6: Specific wear rate (k) for 5µm spherical silica tests.

Table 6.11: Wear mechanisms of 5µm particle size spherical silica.

	5µm Spherical silica			
	Volume fraction of abrasives			
Load	**0.05**	**0.1**	**0.15**	**0.20**
0.1N	Grooving	Mixed	Mixed	Mixed
0.2N	Grooving	Mixed	Mixed	Mixed
0.5N	Grooving	Mixed	Mixed	Mixed

Figure 6.7 shows the specific wear rates for GSK 6.5µm spherical silica. There was a change in wear mechanism observed above 0.05 v/v for all the loads, Table 6.12.

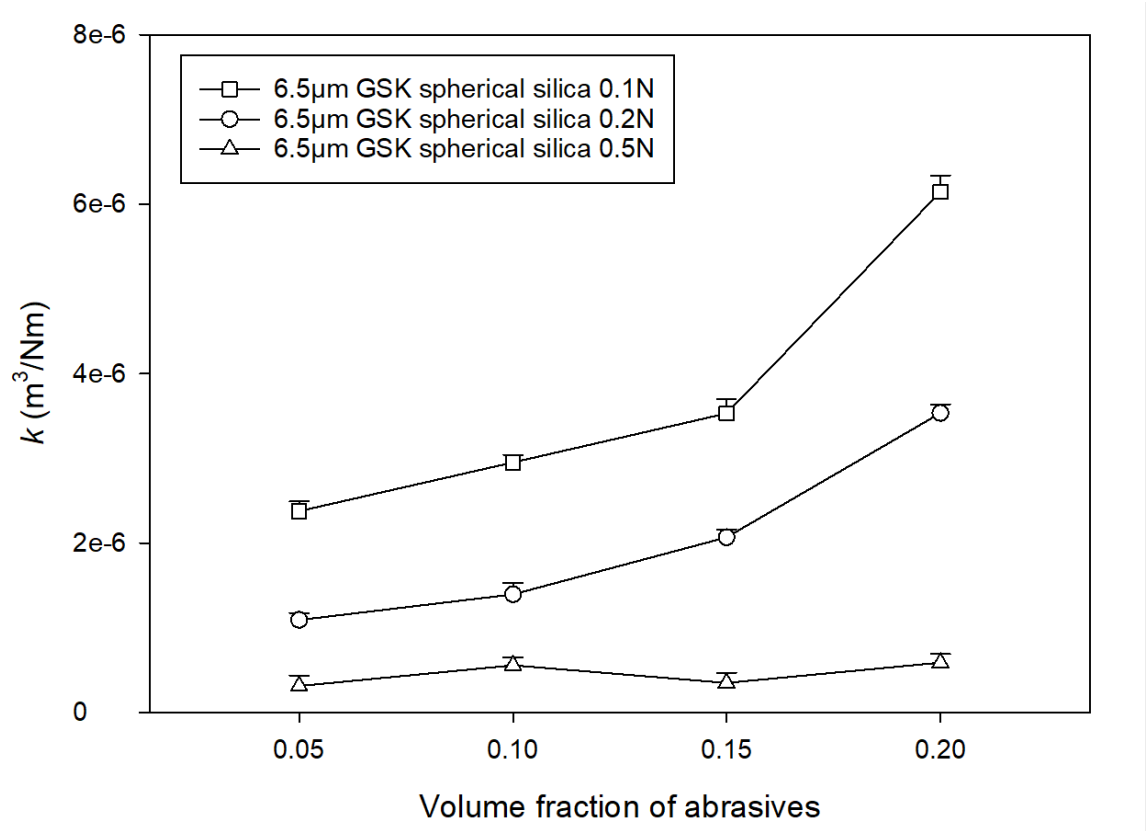

Figure 6.7: Specific wear rate (k) for 6.5µm GSK spherical silica tests.

Table 6.12: Wear mechanisms of 6.5µm GSK spherical silica.

	6.5µm GSK spherical silica			
	Volume fraction of abrasives			
Load	**0.05**	**0.1**	**0.15**	**0.20**
0.1N	Grooving	Mixed	Mixed	Mixed
0.2N	Grooving	Mixed	Mixed	Mixed
0.5N	Grooving	Mixed	Mixed	Mixed

6.3 Groove analysis

Groove analysis was conducted for all the tests using measurement analysis on the Alicona microscope and SEM. The groove width was measured for each wear scar at each volume fraction and the average groove width and standard deviation (σ) was calculated for each wear mechanism. The groove width was reported independent of volume fraction. The statistics demonstrated that there was no significant changes in groove width between the volume fractions 0.05 - 0.20v/v, ($p>0.05$). Groove width analysis has not been reported previously in the literature and this is the first time the wear scars have been analysed for groove width comparisons.

6.3.1 Angular alumina

Table 6.13 shows the groove width data for angular 1µm alumina, 5µm alumina, 9µm alumina, bimodal alumina and GSK 9µm alumina. There was an increase in groove width for all the loads with an increase in particle size. The groove widths reported for the mixed-mode mechanism for alumina 1µm, 5µm, 9µm and GSK 9µm alumina were higher than the grooving mechanism. A significant difference was reported between the groove widths for the grooving and mixed mode regime between 1µm alumina and 5µm alumina ($p<0.05$). No statistical difference was observed in groove widths between the grooving and mixed mode mechanism for the 9µm alumina and GSK 9µm alumina ($p>0.05$). There was no grooving observed for loads of 0.1N and 0.2N for the bimodal alumina. For all the loads (0.1N, 0.2N and 0.5N) the overall trend in groove widths was observed to be similar. There was no significant difference in the groove widths for all the tests across the three

loads (p>0.05). The highest groove widths were observed for the bimodal alumina mixed-mode regime.

Table 6.13: Groove width data for angular 5µm alumina, 9µm alumina, bimodal alumina and GSK 9µm alumina, average of volume fraction 0.05-0.20 v/v.

	Groove width / µm									
	Alumina 1µm		Alumina 5µm		Alumina 9µm		Bimodal alumina 5µm + 9µm		GSK 9µm alumina	
Load	Grooving	Mixed	Grooving	Mixed	Grooving	Mixed	Grooving	Mixed	Grooving	Mixed
0.1N	3.24 σ = 0.69	4.18 σ = 0.17	7.69 σ = 0.64	7.90 σ = 1.38	8.28 σ = 1.26	12.23 σ = 2.44	-	15.41 σ = 1.41	8.28 σ = 0.70	11.92 σ = 1.07
0.2N	2.91 σ = 0.44	3.43 σ = 0.91	6.62 σ = 0.22	7.11 σ = 1.63	9.18 σ = 1.00	11.07 σ = 1.67	-	15.22 σ = 1.97	9.77 σ = 0.68	12.45 σ = 0.97
0.5N	3.77 σ = 1.06	3.57 σ = 0.88	6.5 σ = 0.84	8.01 σ = 1.06	8.96 σ = 2.67	11.58 σ = 1.05	11.01 σ = 1.16	14.09 σ = 1.23	9.61 σ = 0.93	11.53 σ = 0.74

6.3.2 Angular silica

Table 6.14 shows the groove width for angular 5µm silica, 10µm silica, bimodal silica and GSK 8µm silica. There was an increase in groove width from grooving to mixed-mode for all the silica tests, with the mixed-mode mechanism generating the highest groove widths. No 2-body grooving was observed for bimodal silica, with all scars showing a mixed wear regime. There was no significant differences observed in the groove widths across the three loads for all the tests and there was no significant difference between the grooving and mixed-mode regime for the 5µm silica (p>0.05), however there was a significant difference in the groove widths between the grooving and mixed regime for the 10µm silica (p<0.05).

Table 6.14: Groove width data for angular 5µm silica, 10µm silica, bimodal silica and GSK 8µm silica, average of volume fraction 0.5-0.20 v/v.

	Groove width / µm							
	Silica 5µm		Silica 10µm		Bimodal silica 5µm + 10µm		GSK 8µm silica	
Load	Grooving	Mixed	Grooving	Mixed	Grooving	Mixed	Grooving	Mixed
0.1N	6.65 σ = 0.60	7.10 σ = 2.33	10.58 σ = 0.93	12.66 σ = 2.78	-	16.87 σ = 1.56	8.58 σ = 0.33	9.86 σ = 1.18
0.2N	6.26 σ = 0 .81	7.79 σ = 1.07	10.20 σ = 1.47	11.29 σ = 3.05	-	16.40 σ = 1.88	7.94 σ = 0.31	10.91 σ = 0.96
0.5N	6.54 σ = 0.34	7.18 σ = 1.73	10.07 σ = 0.86	11.54 σ = 2.32	-	15.25 σ = 2.43	8.65 σ = 0.48	9.46 σ = 1.07

6.3.3 Spherical silica

Table 6.15 shows the groove widths for GSK 6.5µm spherical silica and 5µm spherical silica. There was an increase in groove width from grooving to mixed mode, for both the GSK 6.5µm spherical silica and 5µm spherical silica. The overall trend across the loads generated similar groove widths. The GSK 6.5µm spherical silica generated the highest groove widths for grooving and mixed-mode, in comparison to the 5µm spherical silica. No significant difference was observed between the groove widths for the three loads ($p>0.05$), however there was a significant difference between the groove widths between the grooving and mixed-mode mechanism for the GSK 6.5µm spherical silica and 5µm spherical silica ($p<0.05$).

Table 6.15: Groove width data for GSK 6.5µm spherical silica particle size spherical silica and 5µm spherical silica, average of volume fraction 0.05-0.20 v/v.

	Groove width / µm			
	GSK 6.5µm spherical silica		Spherical silica 5µm	
Load	Grooving	Mixed	Grooving	Mixed
0.1N	6.02 σ = 0.92	8.69 σ = 1.04	4.89 σ = 0.79	7.21 σ = 1.01
0.2N	5.37 σ = 0.78	7.55 σ = 1.15	5.01 σ = 0.51	7.04 σ = 1.48
0.5N	6.22 σ = 0.90	8.01 σ = 0.65	5.94 σ = 0.66	6.63 σ = 1.19

6.4 Wear mechanisms

The wear scars for the tests were analysed using optical microscopy and the SEM. This allowed the wear mechanisms to be analysed.

6.4.1 Angular alumina

Figure 6.8 shows optical images of the wear scars produced for 5µm angular alumina at loads of 0.1N (Figure 6.8 a and b), 0.2N (Figure 6.8c and d) and 0.5N (Figure 6.8e and f). The images were taken from the centre of the wear scar. Figure 6.8a, c and e show grooving abrasion. Figure 6.8b, d and f shows mixed- mode abrasion, which consist of grooves and indents. At a load of 0.1N (Figure 6.8b) the mixed-mode wear scar was observed to be more severe than the mixed-mode wear scar at 0.5N (Figure 6.8f) These optical images are typical images for the wear scars observed for angular alumina 1µm, 9µm, and GSK 9µm alumina.

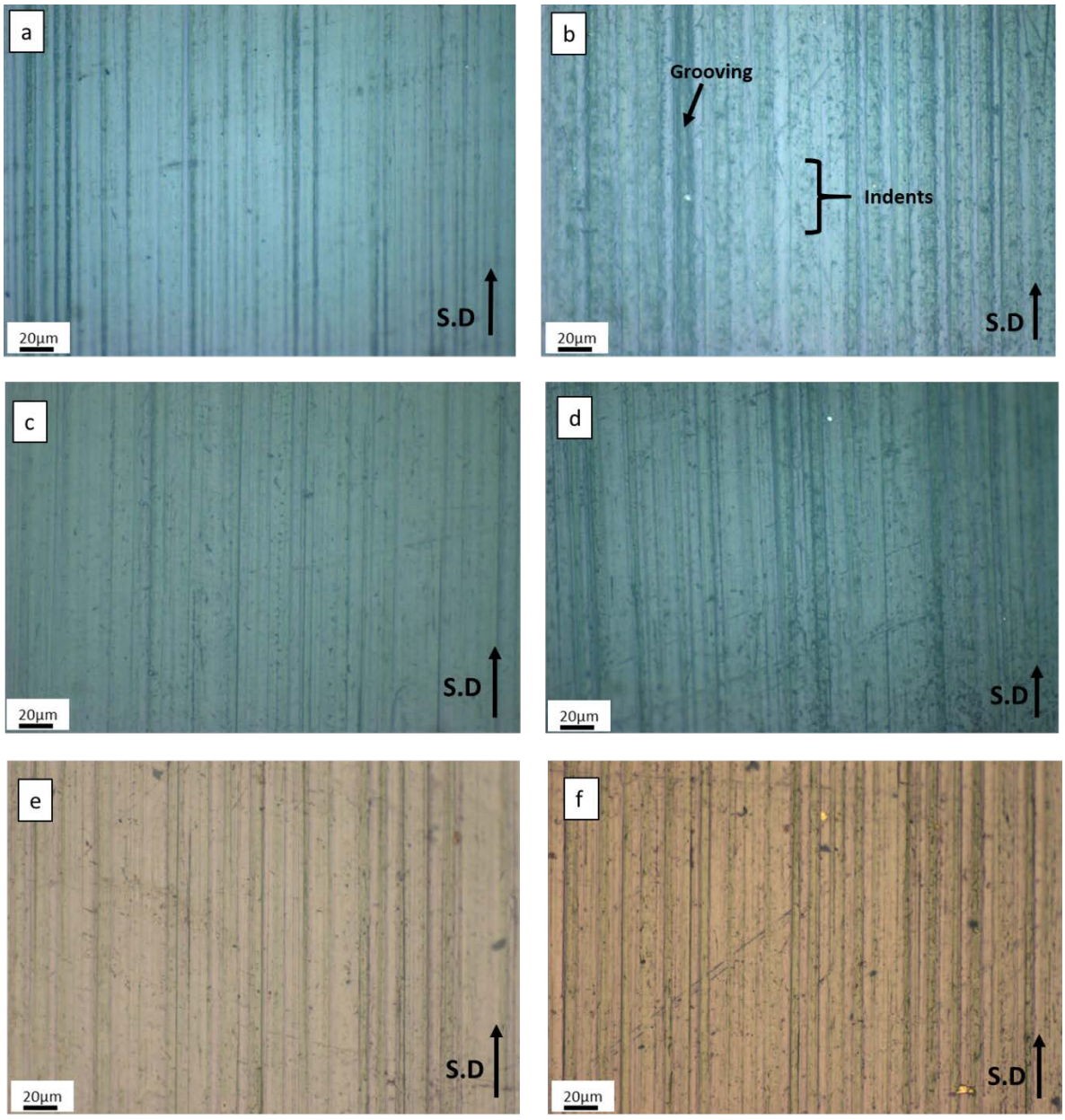

Figure 6.8: Optical image of wear scars for 5µm alumina (a) 0.1N grooving; (b) 0.1N mixed-mode; (c) 0.2N grooving; (d) 0.2N mixed-mode; (e) 0.5N grooving; (f) 0.5N mixed-mode. Figures a,c and e are all 0.05 v/v and Figures b, d and f are all 0.10 v/v.

Figure 6.9 shows SEM images of the wear scars observed for grooving and mixed-mode for 5µm alumina. Figure 6.9a, c and e shows grooving. At a load of 0.1N (Figure 6.9b) there is progressively more severe mixed-mode wear compared to the lower load of 0.5N (Figure 6.9f). These SEM images are typical images observed for angular alumina 1µm, 9µm and GSK 9µm alumina. The mixed-mode wear mode shows signs of chipping, fracture of the enamel rods and grooving. Less signs of grooving is observed at a load of 0.1N (Figure 6.9b). Indenting is also evident which causes removal and damage of the enamel surface, as a result of densification of the enamel tissue.

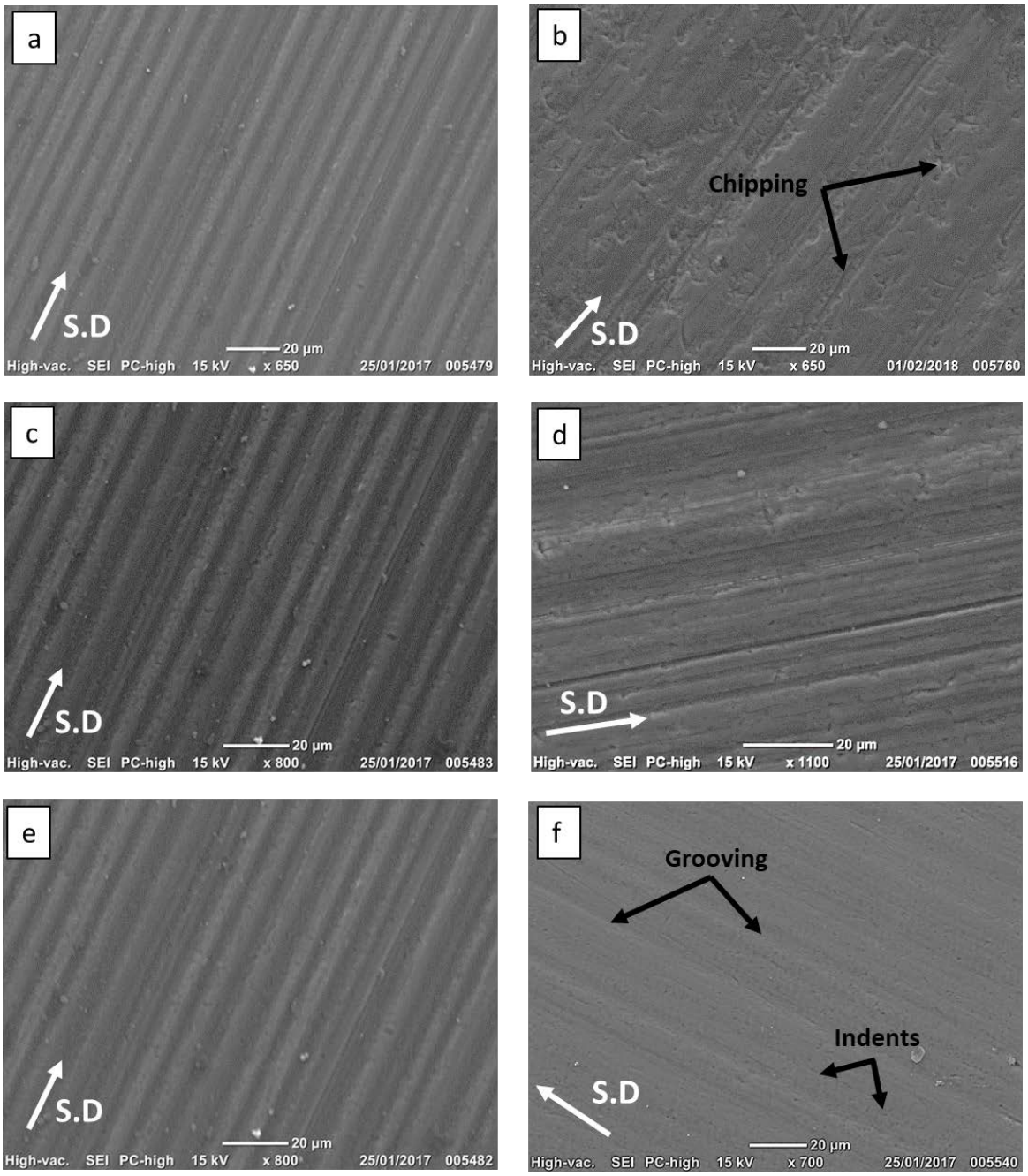

Figure 6.10: SEM images of wear scars for angular 5µm alumina (a) 0.1N grooving; (b) 0.1N mixed-mode; (c) 0.2N grooving; (d) 0.2N mixed-mode; (e) 0.5N grooving; (f) 0.5N mixed-mode. Figures a, c and e are all 0.05 v/v and Figures b, d and f are all 0.10 v/v.

Figure 6.9 shows the wear scars for the rolling abrasion which was observed for angular 9µm alumina at 0.1N and volume fraction 0.20 v/v. The images show rolling abrasion which consist of an indented surface. No grooves are visible.

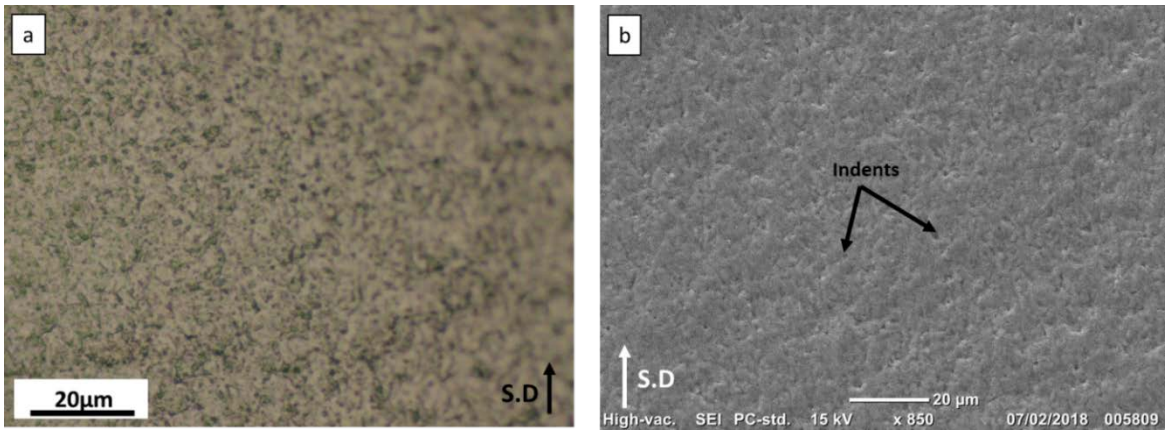

Figure 6.9: Wear scar for 9µm alumina, 0.1N, 0.20 v/v (a) optical image; (b) SEM.

Figure 6.10 shows the wear scars produced by bimodal alumina (5µm + 9µm). The optical wear scars of the mixed-mode region consist of grooving and indenting. The mixed- mode wear scar has clusters of indents surrounding the grooves. The grooves are less distinctive, due to the clusters of indents. No signs of chipping or fracture are visible on the optical images, however the SEMs show signs of fracture of enamel rods, chipping and grooving on the enamel surface. Figure 6.10b shows a textured surface with evident grooves and a damaged enamel surface.

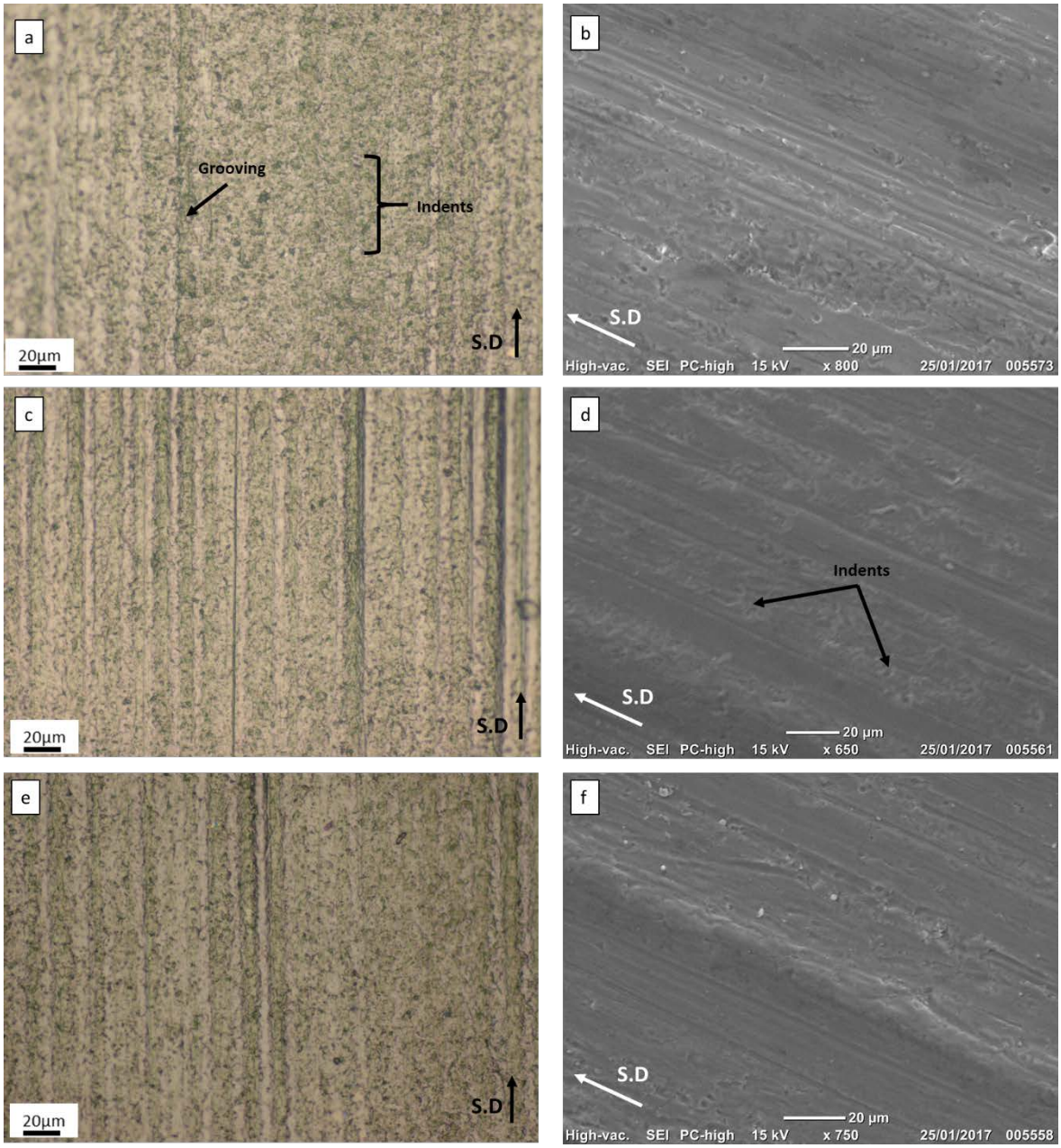

Figure 6.10: Wear scars for bimodal alumina (5µm + 9µm) at 0.15v/v showing all mixed-mode wear scars (a) 0.1N, optical image; (b) 0.1N, SEM; (c) 0.2N optical image; (d) 0.2N SEM; (e) 0.5N optical image; (f) 0.5N SEM.

6.4.2 Angular Silica

Figure 6.11 shows the optical images of the wear scars produced with 5µm silica at loads of 0.1N (Figure 6.11a and Figure 6.11b), 0.2N (Figure 6.11c and Figure 6.11d) and 0.5N (Figure 6.11e and Figure 6.11f). The grooving wear mode shows signs of parallel grooves. The mixed mode mechanism shows signs of grooving with indents. A load of 0.1N for the mixed mode wear scar (Figure 6.11b), shows a highly damaged surface with grooves and many indents, compared to a load of 0.5N (Figure 6.11f).

These wear scars are typical representations of wear scars produced for 10µm silica and GSK 8µm silica tests.

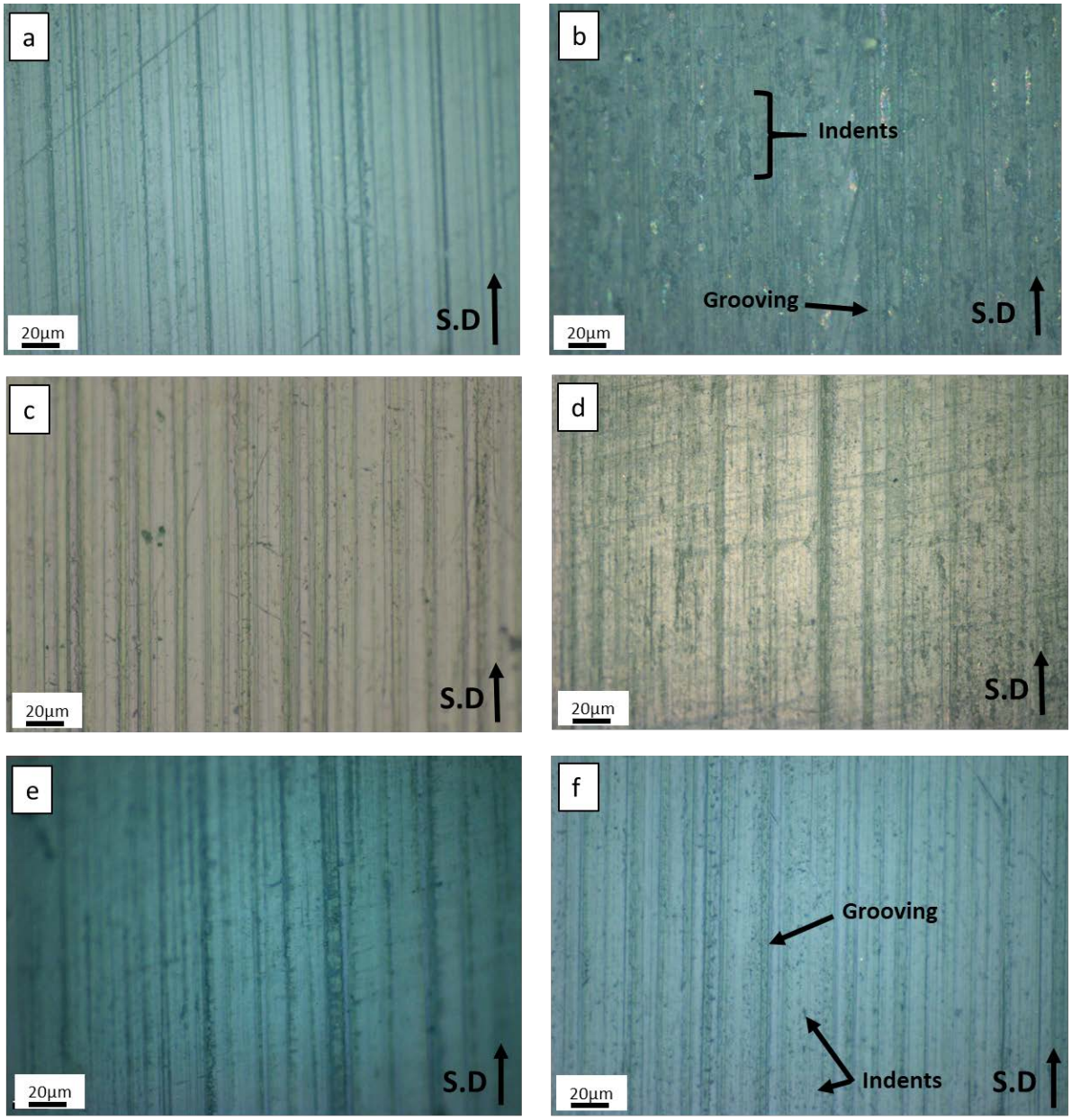

Figure 6.11: Optical image of wear scars for 5µm silica (a) 0.1N grooving; (b) 0.1N mixed-mode; (c) 0.2N grooving; (d) 0.2N mixed-mode; (e) 0.5N grooving; (f) 0.5N mixed-mode. Figures a, c and e are all 0.05 v/v and Figures b, d and f are all 0.10 v/v.

Figure 6.12 shows the SEM wear scars for angular 5µm silica at loads of 0.1N (Figure 6.12a and Figure 6.12b), 0.2N (Figure 6.12c Figure 6.12d) and 0.5N (Figure 6.12e and Figure 6.12f). The grooving consisted of parallel grooves which were similar in appearance. However, the mixed-mode wear scars progressively showed more damage with a lower load. Regions of chipping and fracture of enamel rods were visible. Chipping is observed as missing fragments and small sections of enamel. A fractured enamel surface is observed as damaged fragments and breakage/disintegration of enamel. An indented enamel surface is observed as circular recesses or notches in the enamel.

Figure 6.12b shows the mixed mode wear scar for angular 5µm silica at a load of 0.1N. The wear scar shows a surface with indents, fractures and grooving, compared to a load of 0.5N (Figure 6.12f).

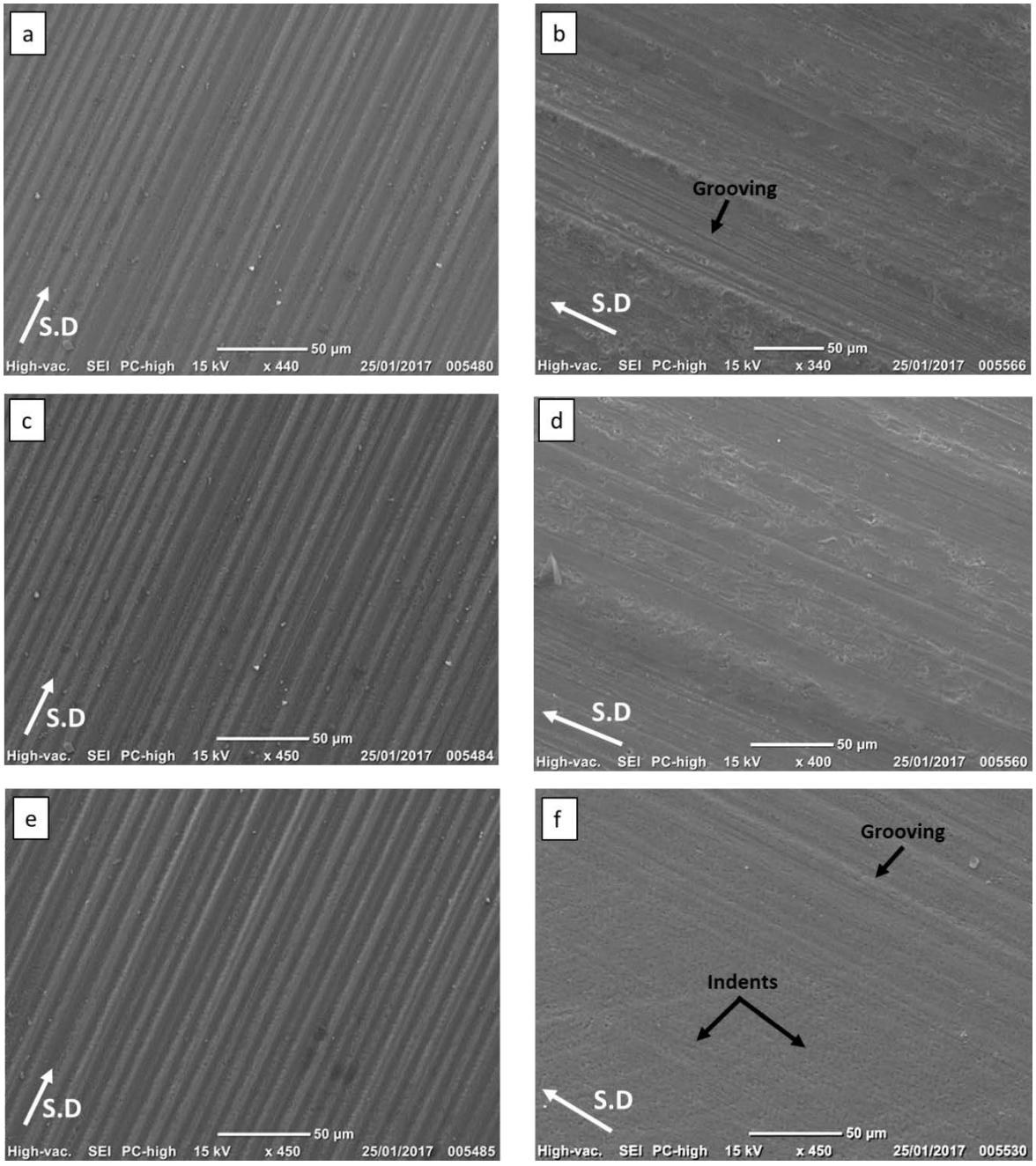

Figure 6.12: SEM images of wear scars for angular 5µm silica (a) 0.1N grooving; (b) 0.1N mixed-mode; (c) 0.2N grooving; (d) 0.2N mixed-mode; (e) 0.5N grooving; (f) 0.5N mixed-mode. Figures a, c and e are all 0.05 v/v and Figures b, d and f are all 0.10 v/v.

Figure 6.13 shows the typical wear scars for bimodal silica (5µm + 10µm). The optical images show the mixed-mode wear scar with many indents clustered with grooving (Figure 6.13a, Figure 6.13c and Figure 6.13e). The SEM shows a more detailed examination of the wear scars. From the SEM images, grooves, fractures and chipping is evident for the mixed-mode region (Figure 6.13b, Figure 6.13d and Figure 6.13f) . There are subtle differences with the SEM images. At a load of 0.1N the optical image shows severe mixed-mode damage, (Figure 6.13a), compared to a load of 0.5N (Figure 6.13e).

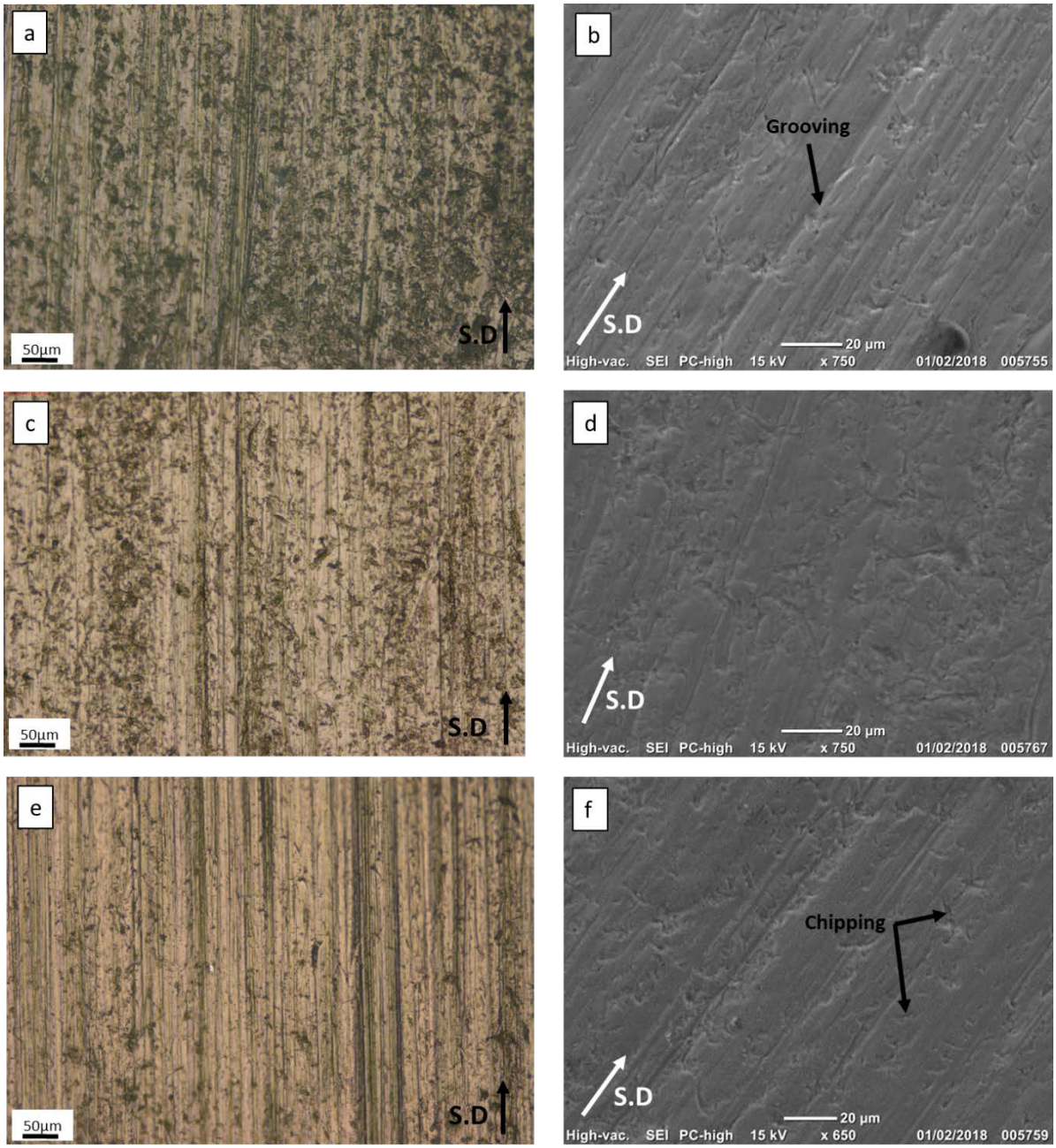

Figure 6.13: Wear scars for bimodal silica (5µm + 10µm) at 0.15v/v showing all mixed-mode wear scars (a) 0.1N, optical image; (b) 0.1N, SEM; (c) 0.2N optical image; (d) 0.2N SEM; (e) 0.5N optical image; (f) 0.5N SEM.

6.4.3 Spherical silica

Figure 6.14 shows the optical images of the wear scars observed for 5µm spherical silica. For the grooving mechanism, there is evidence of grooves, however the grooves do not appear to be deeply formed (Figure 6.14a, Figure 6.14b and Figure 6.14e). The mixed mode wear scar shows grooves with scattered areas of indents (Figure 6.14b, Figure 6.14d and Figure 6.14f). These wear scars are a typical representation of the wear scars produced with GSK 6.5µm spherical silica. At a load of 0.1N for the mixed- mode regime, there is more wear evident (Figure 6.14b) compared to the 0.5N mixed-mode wear scar (Figure 6.14f).

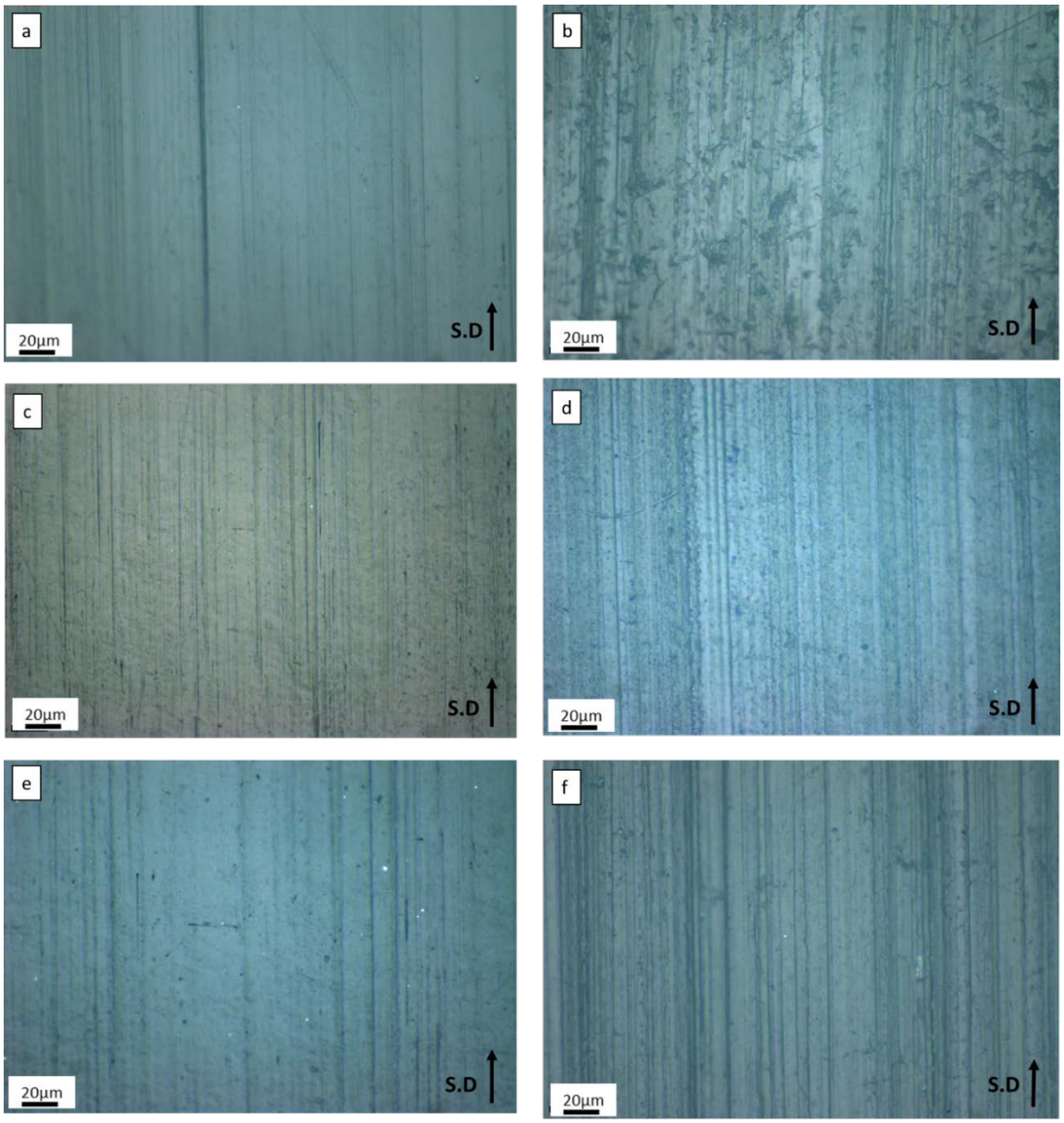

Figure 6.14: Optical image of wear scars for 5µm spherical silica (a) 0.1N grooving; (b) 0.1N mixed-mode; (c) 0.2N grooving; (d) 0.2N mixed-mode; (e) 0.5N grooving; (f) 0.5N mixed-mode. Figures a, c and e are all 0.05 v/v and Figures b, d and f are all 0.10 v/v.

Figure 6.15 shows the SEM images of the wear scars produced by 5µm spherical silica. Many narrow grooves are visible, Figure 6.15a. The wear scars for the grooving mechanism consisted of parallel grooves, which were all similar in appearance (Figure 6.15a, Figure 6.15c and Figure 6.15e). The mixed mode wear scars showed signs of material removal and damage on enamel which is observed by indents and fracture of the enamel rods (Figure 6.15b, Figure 6.15d and Figure 6.15f). These wear scars are a typical representation of the wear scars produced with GSK 6.5µm spherical silica.

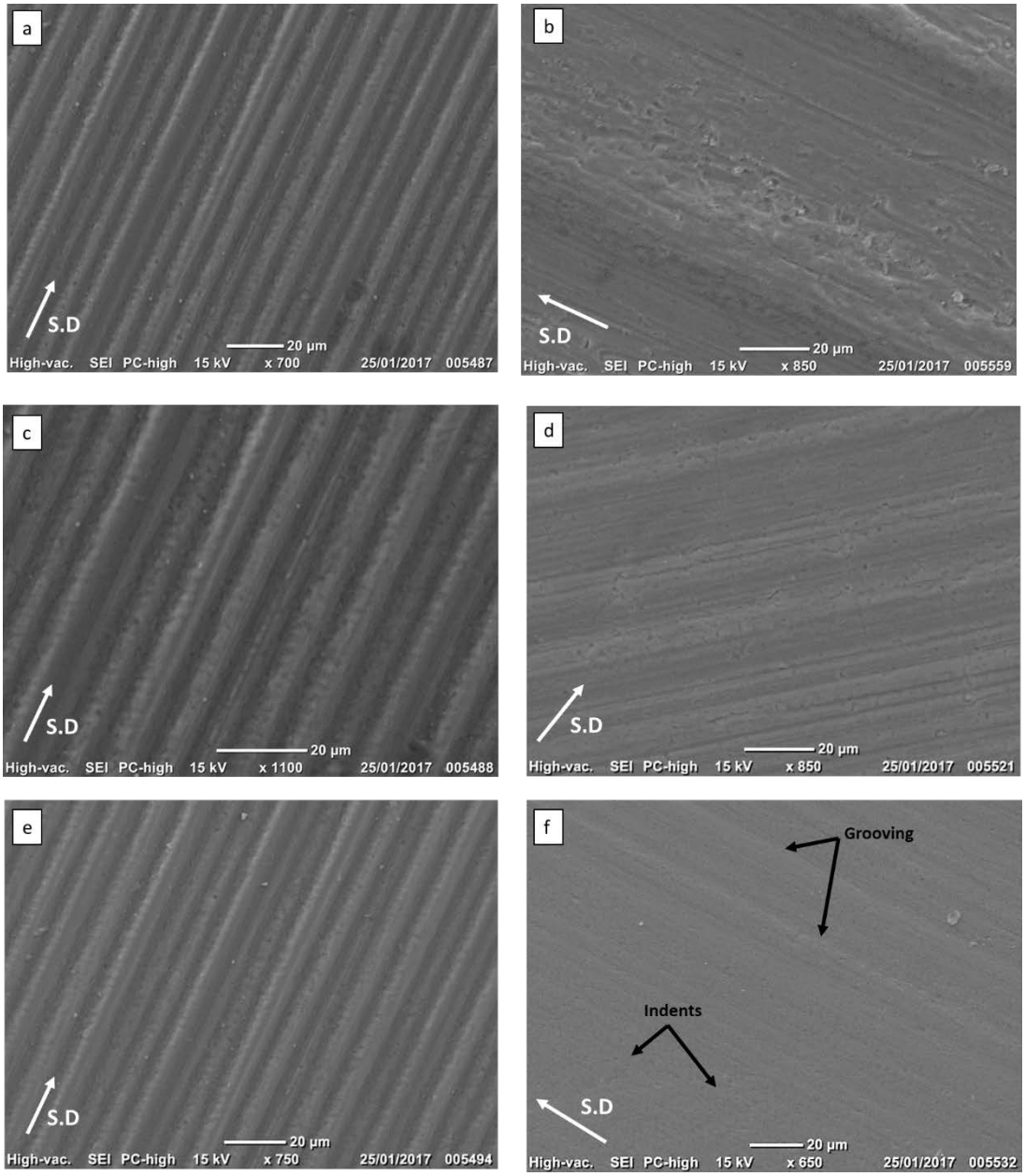

Figure 6.15: SEM images of wear scars for 5µm spherical silica (a) 0.1N grooving; (b) 0.1N mixed-mode; (c) 0.2N grooving; (d) 0.2N mixed-mode; (e) 0.5N grooving; (f) 0.5N mixed-mode. Figures a, c and e are all 0.05 v/v and Figures b, d and f are all 0.10 v/v.

6.5 Synergy evaluation

Synergy is when the combined effect of two variables is greater than the individual variables.

Figure 6.16 shows the percentage synergy volume loss for alumina. At 0.1N, 0.2N and 0.5N a positive synergy exists. A positive synergy indicates the bimodal alumina generates more wear than the mono-sized alumina. A complex trend was observed with an increase in load for volume fractions (0.05 -0.20v/v). This trend will be further discussed in detail in chapter 8.

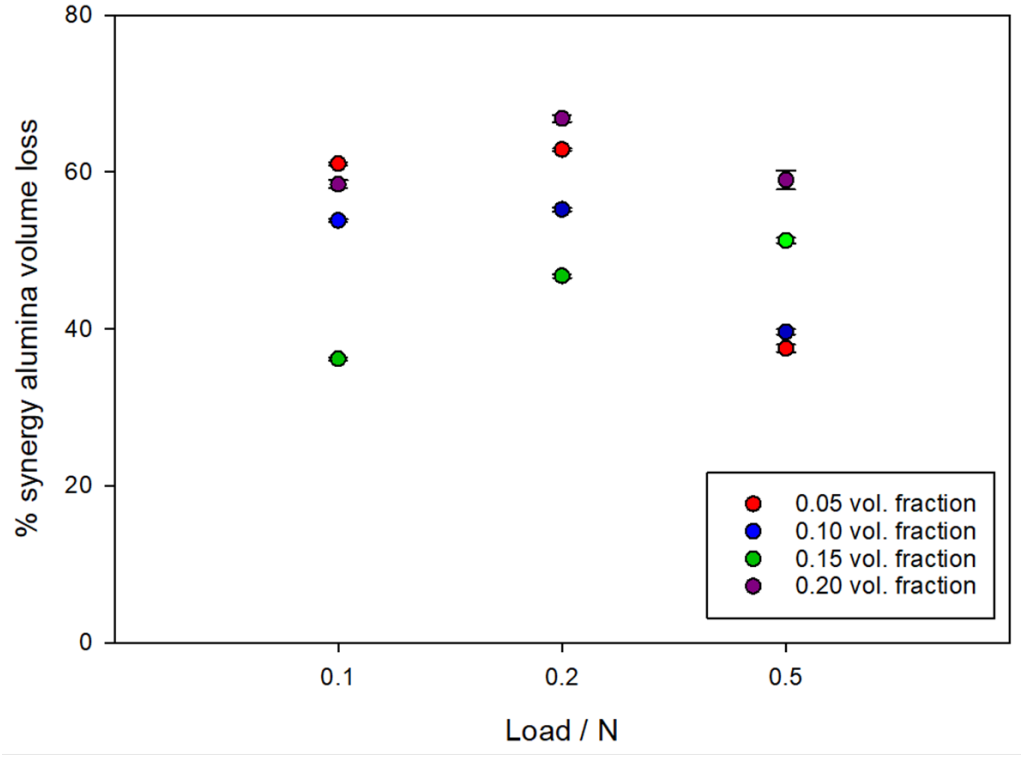

Figure 6.16: Percentage synergy for alumina.

Figure 6.17 shows the percentage synergy loss for silica. At loads of 0.1N, 0.2N and 0.5N a positive synergy exists, which indicates the bimodal silica is generating more wear than the mono sized silica. An increase in load for the silica synergy results in an increase in synergy.

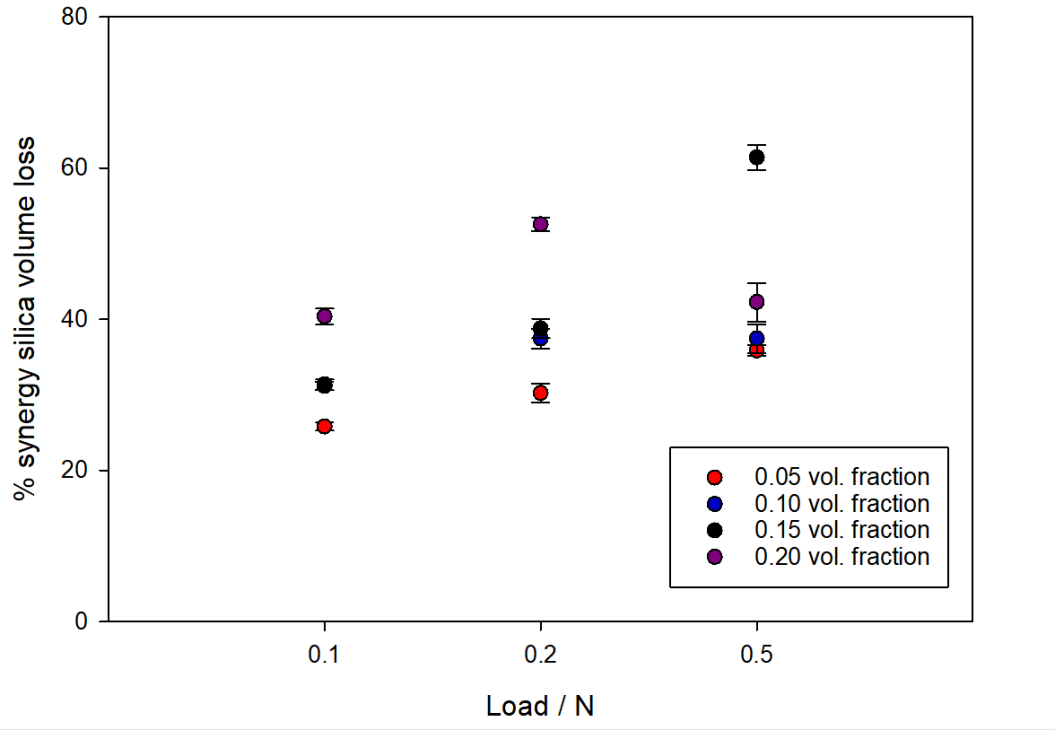

Figure 6.17: Percentage synergy for silica.

6.6 Severity of contact

Adachi and Hutchings proposed a model for severity of contact (Sc), using the three possible wear mechanisms of grooving, mixed-mode and rolling abrasion, to display micro-abrasion results [148]. The severity of contact is a recently introduced parameter and it defines the transitions between the regimes of grooving, mixed-mode and rolling abrasion. The severity of contact (Sc) was calculated using Equation 6.7.

Sc = W / AvH' ....Equation 6.7

where *W* is defined as the applied load between the ball and the specimen, *A* is the wear scar area, *v* is the volume fraction of abrasive in the slurry and *H'* is the hardness of the specimen and the ball.

H' can be calculated using Equation 6.8.

$$\frac{1}{H'} = \frac{1}{H_b} + \frac{1}{H_s} \quad \text{....Equation 6.8}$$

where H_b is the hardness of the ball and H_s is the hardness of the specimen.

A is given by Equation 6.9.

$$A = \pi a'^2 = \pi(a^2 + 2RD) \quad \text{... Equation 6.9}$$

A is the interaction area between the abrasives particles and the surfaces of the specimen and ball, a is the radius of the Hertizan contact area, *R* is the radius of the ball and *D* is the diameter of the abrasive particle.

The bimodal results will not be included in the severity of contact evaluation. A study carried out by Gava et al. [236] used the average particle size for bimodal particles to calculate the Sc [236]. This is not a true representation of the particle size as there are large particles in the bimodal slurry, which the average particle size does not account for. There is a large difference between the average particle size and maximum particle size, due to this reason, the bimodal tests will be omitted from the Sc graphs.

6.6.1 Alumina

Figure 6.18 shows the specific wear rates as a function of severity of contact (Sc) for angular 1µm alumina, 5µm alumina, 9µm alumina and GSK 9µm alumina. The highest severity of contact was generated from the grooving mechanism for all the alumina tests. The mixed-mode generated a lower severity of contact than grooving, with the rolling mechanism generating the lowest severity of contact.

A decrease in particle size gives an increase in Sc. This is observed for the 1µm alumina tests,

Figure 6.18a. An increase Sc gives lower wear rates. The GSK 9µm alumina presented scatter for the mixed-mode state,

Figure 6.18d.

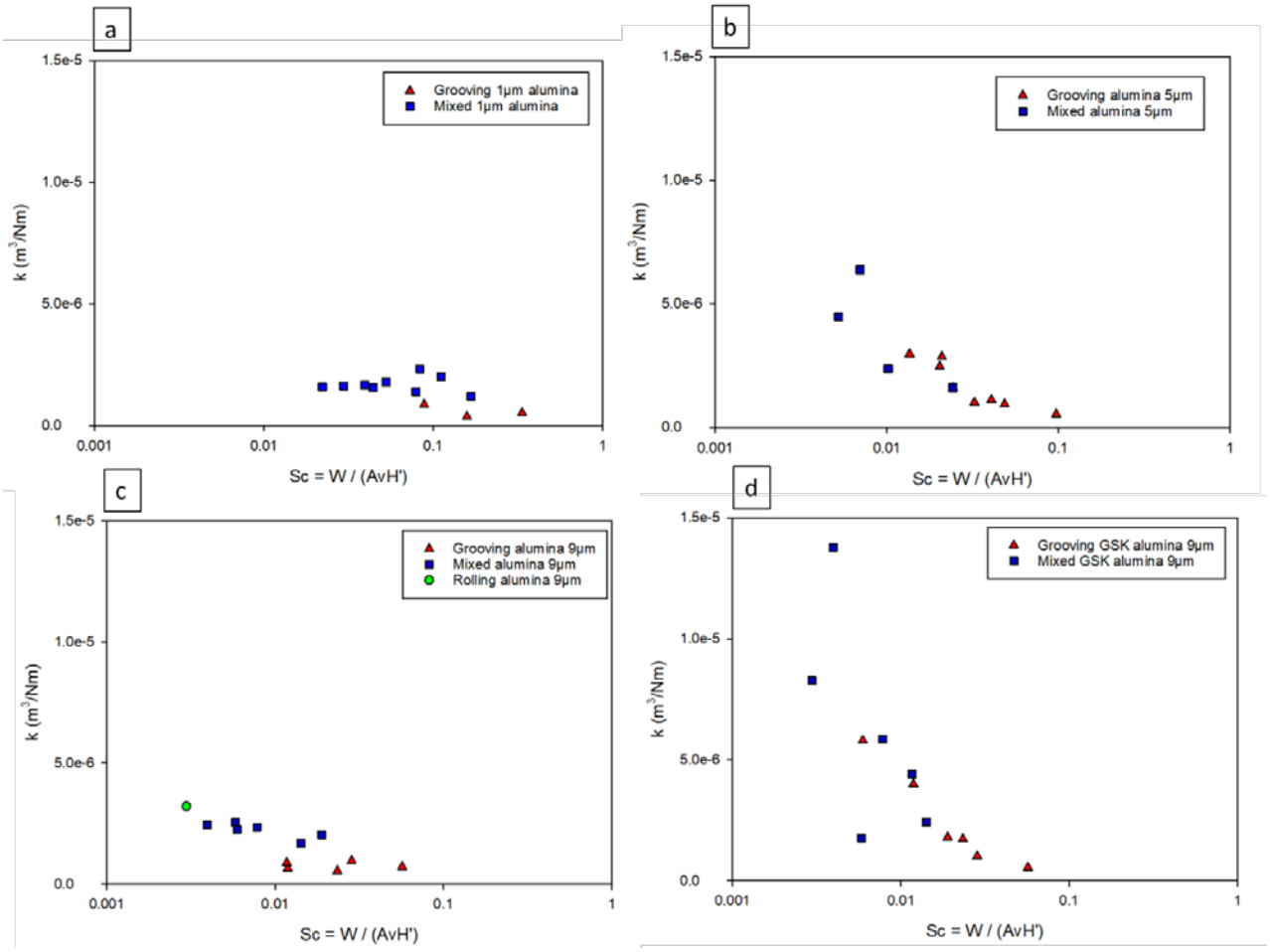

Figure 6.18: Specific wear rate (k) plotted against Severity of Contact (Sc) for angular alumina (a) 1µm alumina; (b) 5µm alumina; (c) 9µm alumina; (d) 9µm GSK alumina.

6.6.2 Silica

Figure 6.19 shows the specific wear rates as a function of severity of contact (Sc) for silica 5µm, silica 10µm and GSK 8µm silica. The highest Sc is observed for the 5µm silica, Figure 6.19a. The smaller particle sizes generate higher Sc, Figure 6.19a. The grooving mechanism generates high values for Sc, whereas the mixed-mode mechanism generates low Sc values.

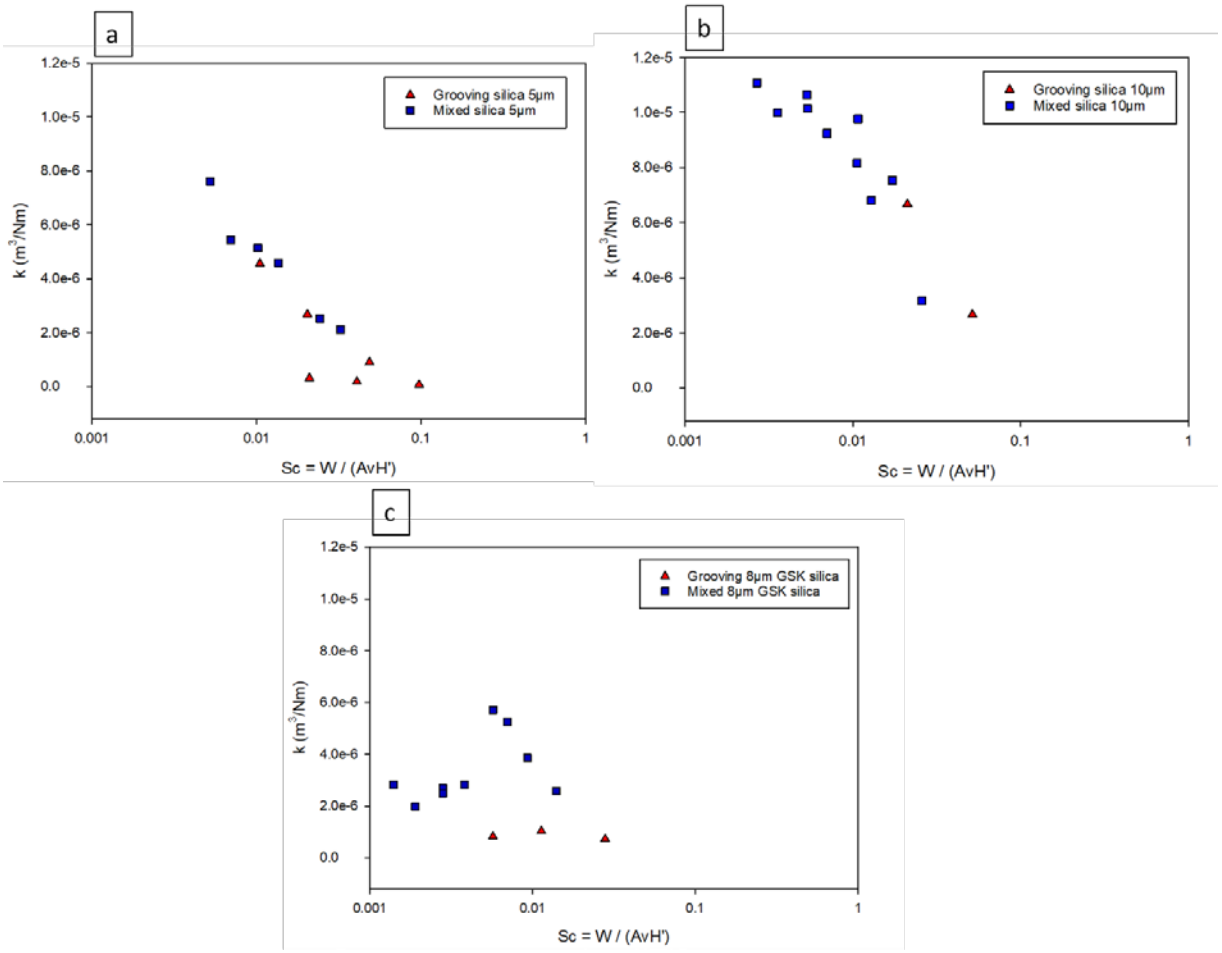

Figure 6.19: Specific wear rate (k) plotted against Severity of Contact (Sc) for angular silica (a) 5µm silica; (b) 10µm silica; (c) GSK 8µm silica.

6.6.3 Spherical silica

Figure 6.20 shows the specific wear rates as a function of severity of contact (Sc) for spherical silica 5µm and GSK 6.5µm spherical silica. The 5µm spherical silica generates the highest Sc in the grooving state, whereas the GSK 6.5µm spherical silica in the mixed-mode state gives the lowest Sc.

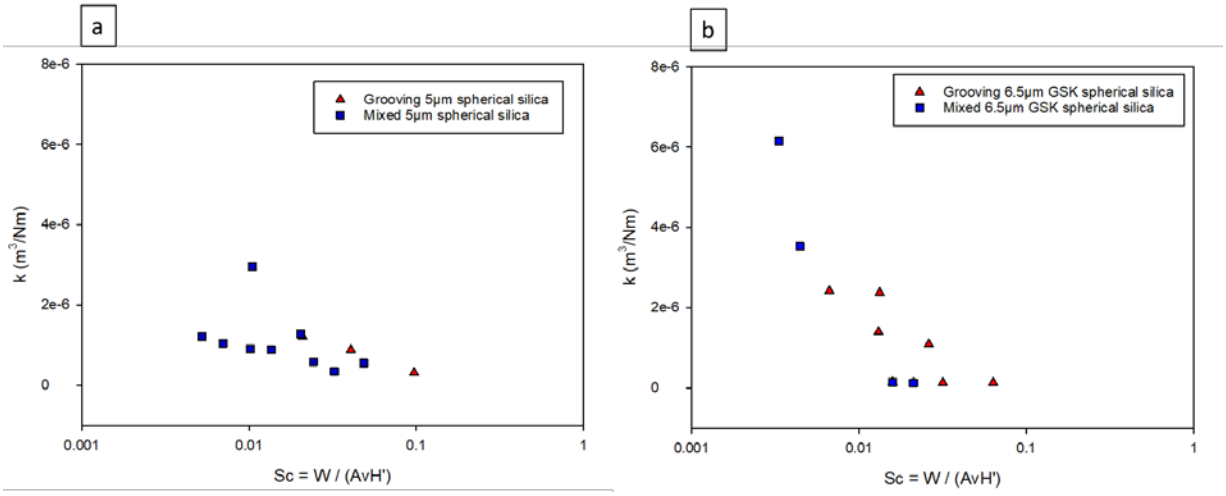

Figure 6.20: Specific wear rate (k) plotted against Severity of Contact (Sc) for spherical silica (a) 5µm spherical silica; (b) 6.5µm GSK 6.5µm spherical silica.

6.7 Discussion

This section will discuss load related results obtained from the micro-abrasion tests.

6.7.1 Effect of load on the wear rate of enamel

From the results obtained, the highest SWR was observed for bimodal alumina at 0.1N. As the load increased the SWR decreased. The decrease in SWR for all the particle tests with load, was attributed to the reduction in entrainment of the larger particles in the contact, resulting in a reduction in SWR. This effect was also observed for the silica tests, with bimodal silica at a load of 0.1N generating the highest SWR. As the load increased to 0.5N, there was a decrease in SWR. A possible explanation for this could be due to the larger particles not entraining in the contact, and smaller particles entraining efficiently.

The largest groove widths were observed for the bimodal alumina and bimodal silica tests at the mixed-mode phase. There was a 1.95x increase in groove width from the mixed-mode phase of alumina 5µm to the mixed- mode phase of bimodal alumina, Table 6.16. There is a correlation between particle size and groove width. An increase in particle size causes an increase in groove width. There was a 2.4x increase in groove width with 5µm silica at the bimodal mixed-mode phase, compared to the mixed-mode 5µm alumina phase, Table 6.17. This result may be explained by the particle sizes in the bimodal tests, which generate the higher wear rates and groove sizes.

Table 6.16: Ratio of groove widths for angular alumina. Data used from section 6.3.

	Groove width/ µm	$\boldsymbol{Ratio} = \frac{Groove\ width\ bimodal\ alumina}{Groove\ width\ 5\mu m\ alumina}$
Alumina 5µm Load-0.1N, mixed-mode	7.90	1.95x
Bimodal alumina Load- 0.1N, mixed-mode	15.41	

Table 6.17: Ratio of groove widths for angular silica. Data used from section 6.3.

	Groove width/ µm	$\boldsymbol{Ratio} = \frac{Groove\ width\ bimdoal\ silica}{Groove\ width\ 5\mu m\ silica}$
Silica 5µm Load- 0.1N, mixed-mode	7.10	2.4x
Bimodal silica Load- 0.1N, mixed-mode	16.87	

Mixed-mode wear was observed to be more damaging than grooving. It is observed as a combination of chipping and rolling (indents) on the enamel surface which break up the enamel rods. Mixed-mode wear causes an increased amount of damage to the surface integrity of enamel. All the grooving was similar in appearance, with parallel grooves running across the centre of the wear scar, however for mixed-mode there were indent features present within the grooves. For mixed-mode abrasion there was evidence of grooving and indenting, which resulted in the higher wear rates. Adachi and Hutchings suggests mixed mode abrasion is defined and observed as grooving and indenting [148].

An unexpected result was observed for the wear rate of 9µm alumina at a load of 0.1N and volume fraction of 0.20v/v. A rolling mechanism was evident. It could be due to the 9µm alumina particles entraining the contact differently and more of the maximum sized particles of the 9µm alumina being entrained.

For the spherical silica particles, the highest SWR was observed with GSK 6.5µm spherical silica at a load of 0.1N. The groove widths for the mixed-mode mechanism were higher than the grooving mechanism widths for both the GSK 6.5µm spherical silica and 5µm spherical silica. The mixed mode GSK 6.5µm spherical silica generated the highest groove widths.

A three-body wear mechanism was dominant for the alumina tests in da Silva et al. [234] study. A damaged surface was observed by the abrasive particles rolling between the ball and the sample surface resulting in a multiple indented wear surface. The 3-body wear surface observed by da Silva et al. [234] had no directionality [234]. This findings seems to be consistent with the present finding which observed rolling with no directionality for the 9µm alumina test at a load of 0.1N and a volume fraction of 0.20v/v.

The grooving mechanism observed in the current study resulted in a series of parallel grooves on the enamel surface, Figure 6.21. The abrasive particles slide at the interface of the specimen and the ball without any rolling taking place. It is encouraging to compare this findings with that found by Trezona et al. [155] who suggested that the abrasive particles embed into the softer material of the ball and act as indenters. What is surprising is that no signs of abrasive particle embedment in the nylon ball were observed for the present study [149].

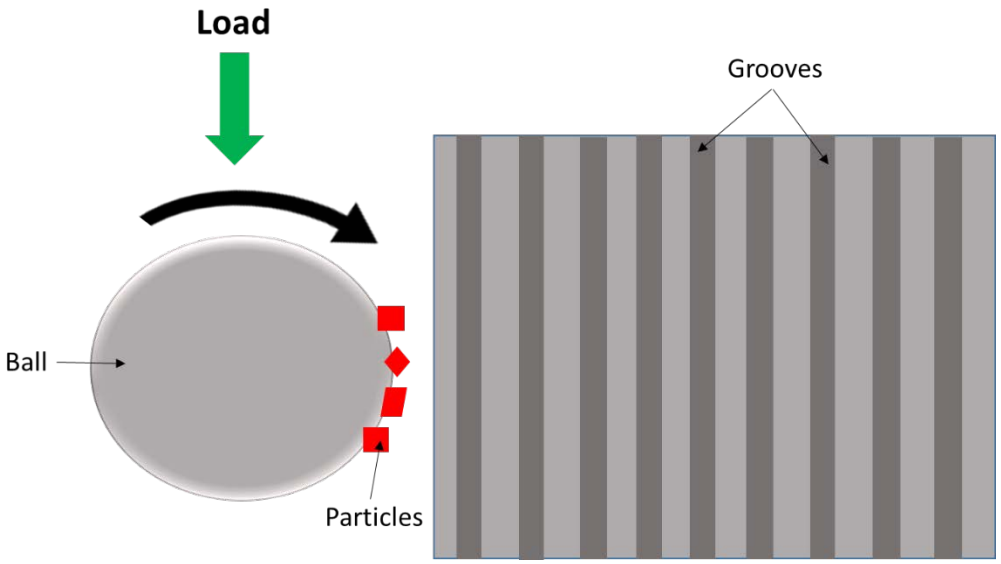

Figure 6.21: Schematic of grooving particle interaction.

It was reported that a critical condition for the change in transition from two-body grooving to 3-body rolling abrasion was due to a change of particle motion, from rolling to sliding in the contact region (Equation 3.6) [148].

A study conducted by Bello et al. [151] on polyamide coatings using silicon carbide as the abrasive and steel as the ball, found the specific wear rate (SWR) to decrease with increasing load. This was due to a rolling mechanism. An increase in load to 0.5N resulted in a decrease in wear rate for all the tests in the present study [151] . This is also confirmed by a study carried out by Bose et al. [152] who found the wear rate decreased with an increase in load [152]. This finding of a decrease in SWR with increasing load for soft materials has also been confirmed by other authors [151, 177, 237]. A possible explanation for a decrease in SWR with an increase in load is due to the formation of ridges from grooving abrasion. The ridging is observed where the contact pressure is the highest, in the centre of the wear scar. These ridges then suppress further wear. The ridges are sites for abrasive particle entrapment, therefore a decrease in wear rate with higher loads is observed. In contrast to

the findings, no evidence of ridging or embedment of abrasive particles was detected in the present study, therefore it cannot explain the results. The sensitivity of the SWR to the applied load is dependent on the test material properties and the abrasive action of the abradant [177].

The increased levels of volume loss and SWR of the silica tests compared to the alumina tests is due to the difference in the size distribution of the abrasive particles. The reduction in SWR with load is associated with the reduction in entrainment of the larger particles through the contact. This is supported by the reduction in the groove width seen within the wear scars.

The grooves are wider than the average particle size due to the entrainment of large sized partides in the contact and the smaller sized particles being pushed to the sides. This is evident from Table 6.13, Table 6.14 and Table 6.15 showing the groove widths for the alumina, silica and spherical silica tests.

Figure 6.22 shows a typical wear scar for mixed-mode mechanism. The wear scar shows a combination of chipping and fracture of rods on the enamel surface, Figure 6.23. For the mixed-mode phase, the lower volume fraction of 0.10v/v shows a fractured enamel surface with indents surrounding grooves, Figure 6.22a. At a higher volume fraction of 0.20v/v the mixed-mode wear phase shows a severely damaged enamel surface with chipping and grooving.

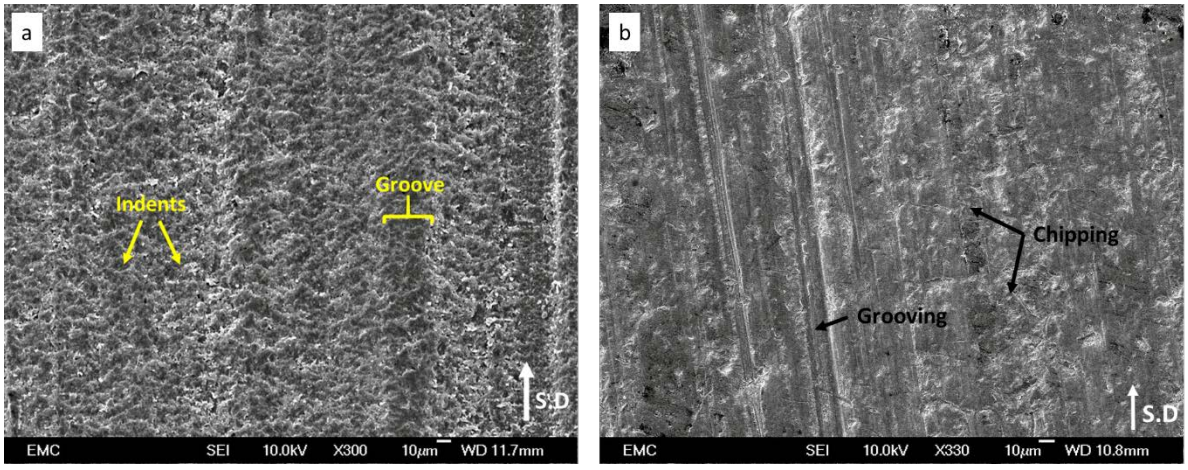

Figure 6.22: SEM wear scar for angular 9µm alumina at 0.5N (a) 0.10 v/v; (b) 0.20 v/v.

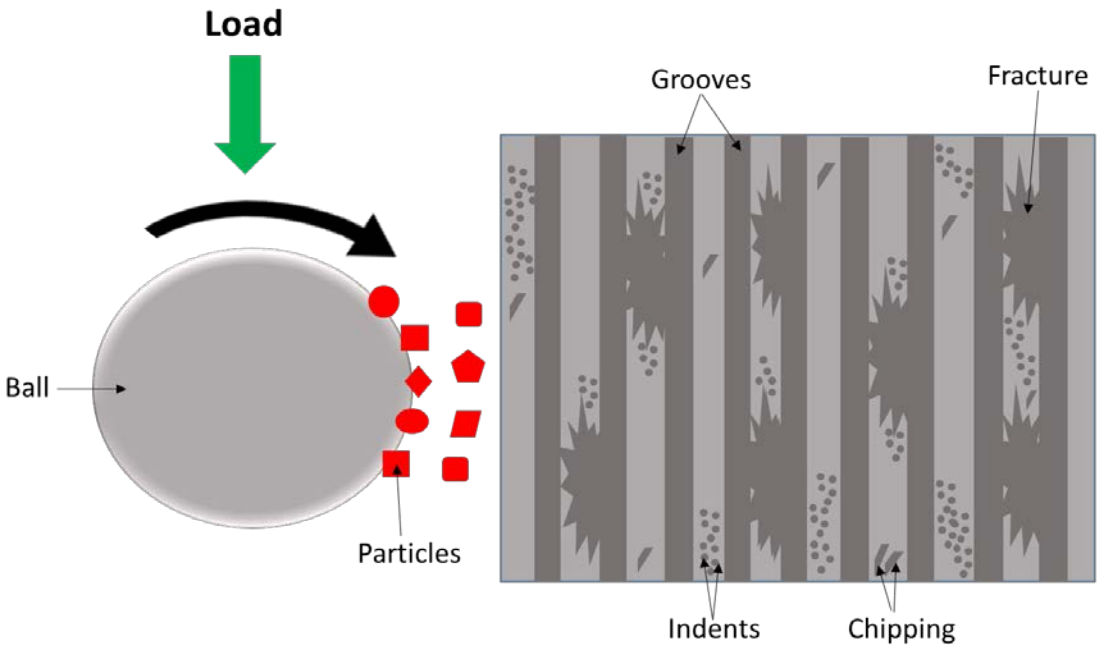

Figure 6.23: Schematic of mixed-mode particle interaction.

The abrasive particles microchip the enamel surface to cause grooves. The nylon ball entrains the particles under loading. The particles are not completely entrained in the nylon ball and are released once the load is removed. The enamel surface is damaged and material removal takes place to form grooves, Figure 6.12a. The rolling and indents on the enamel surface are a result of densification of the enamel prisms. After a number of loading cycles, this results in removal of enamel and crushing/breakup of the enamel prisms, Figure 6.24. Plastic deformation was reported on the enamel surface by Pena et al. [147] who found evidence of ploughing, indentation and micro-cracking on the enamel surface [147]. The present study found no signs of plastic deformation on the mixed-mode wear scar.

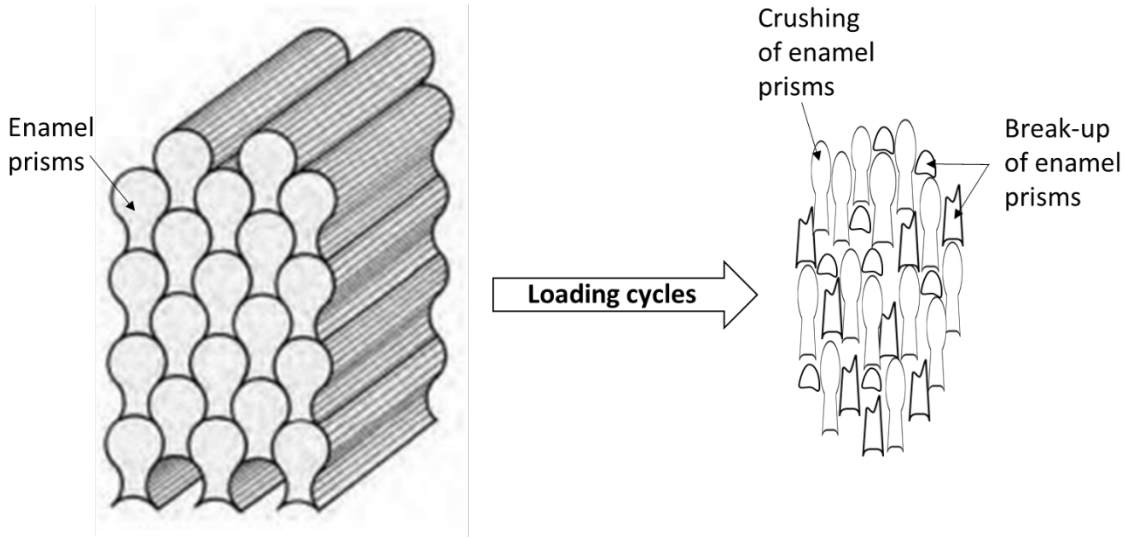

Figure 6.24: Structural changes of enamel prisms after loading cycles.

6.7.2 Severity of contact evaluation

The specific wear rate as a function of severity of contact was plotted. The bimodal tests were not included as a function of severity of contact, due to the ambiguity of the mean particle size in recording and plotting the results.

The highest severity of contact was observed for the smaller particle sizes, with angular 1µm alumina generating the highest severity of contact in the grooving phase. This occurrence was also observed for the silica tests with 5µm silica generating the highest severity of contact [148].

The lowest severity of contact for all the tests was observed by the biggest particle size. For the silica tests, 10µm silica generated the lowest severity of contact in the mixed-mode phase. The lowest severity of contact was observed with 9µm alumina in the rolling phase.

A study carried out by Adachi and Hutchings on PMMA and steel using silicon carbide as the abrasive found sharp transitional changes in the Sc between 2-body grooving and 3-body rolling motion [148]. These transitional changes are not observed in the present study.

A study carried out by Bose et al. [152], reported the wear rate to decrease with an increase in severity of contact. This was due to uniform wear scars being produced with an increase in sliding distance. The severity of contact was found to decrease with an increase in scar area. This was

observed in the present tests. Typically the wear rate should increase with Sc. One thing to note is, the study carried out by Bose et al. [152] compared the severity of contact with the hardness of the ball and specimen [152]. In the present study, the hardness of the ball was not varied. These results therefore need to be interpreted with caution.

6.7.3 Synergy comparison with load

An increase in synergy was observed with an increase in load for volume factions 0.05 – 0.20 v/v. There are many possibilities for this occurrence such as the low load per particle with increased volume fraction of abrasive. Another possibility could be the entrainment of particles in the contact.

There was no general trend with synergy for the alumina tests. This could be due to entrainment effects of the particles in the contact. An increased trend in synergy was observed for the silica tests. An explanation for this increase could be due to the effect of rolling of abrasive particles in the contact; which results in breakup of the enamel prisms. This rolling action with the combined action of grooving, results in an increase in synergy with load for the silica tests.

6.8 Conclusions

- Reliable abrasion wear rates of enamel can be made using the TE66 micro- abrasion rig, with the wear rates and wear mechanisms sensitive to the test conditions.

- The mixed mode mechanism caused more damage and a higher SWR than two body grooving.

- The grooving mechanism is due to abrasive particles adhered to the soft nylon ball, which result in grooves on the enamel surface by a micro-chipping action. Mixed- mode abrasion results in severe structural damage to the enamel rods. Crushing and fracture of the enamel rods is observed, which results in a damaged enamel surface and loss of material. For rolling abrasion, indents are observed as a result of densification of the enamel tissue. After a number of loading cycles, this results in removal of enamel and breakup of the enamel prism surface.

- Load is an important variable affecting the load per particle, with higher loads per particle expected to result in greater wear, however in this test the increase in load affected the entrainment of the larger particles resulting in a reduction in SWR.

- The highest severity of contact is observed with the smallest particle size, due to a better entrainment with the smallest particle sizes in the slurry.

- Bimodal alumina (5µm + 9µm) and bimodal silica (5µm + 10µm) tests at 0.1N give the highest specific wear rate of enamel for all the tests. An increase in groove width is observed for bimodal tests with a decrease in load.

- There is no significant change in groove widths across the three loads with all the mono-sized particle tests.

7. Brushing test results

7.1 Introduction

In this chapter, the results detailing the effects of abrasive slurries on the wear of enamel are reported. The aim of the study is to compare the abrasivity of alumina, silica and spherical silica particles in a brushing simulation test, using a TE77 reciprocating tribometer. Topography changes of enamel are reported with detailed roughness analysis. This is then followed by wear and friction comparisons. The chapter concludes with a summary on the friction and wear characteristics of enamel.

7.1.1 Experimental details

Bovine enamel discs were provided by GSK. The discs were hydrated for 12 hours before testing. Prior to the reciprocating sliding tests, reference areas were marked on the bovine disc. The registration technique used which consisted of drilling reference markers in the side of the epoxy resin was to allow site specific monitoring of roughening. The experimental details are outlined in Table 7.1. A Tek Pro® firm toothbrush was used for the test. Talysurf profiles were taken at the start of the test and then at two hour intervals. Tests were stopped at test intervals of 2 hours, cleaned with distilled water and profile measurements were taken using the Talysurf profilometer. The samples were placed in the same position and the test sequence run again. Tests were conducted with slurries containing 0.2 v/v volume fraction, GSK 9µm alumina + saliva base, GSK 8µm silica + saliva base, GSK 6.5µm spherical silica + saliva base and control saliva base. The tests were independent of concentration. Chapter 3.7 gives more details on the experimental procedure.

Table 7.1: Test conditions for the brushing tests.

Test conditions	Quantities
Alignment of brush head to bovine disc	Horizontal
Load / N	5
Frequency /Hertz	4
Stroke length /mm	4
Slurry concentration (g/cm^3)	0.5% Carboxymethyl cellulose (CMC) + 10% Glycerine (base) + 20% abrasive (in accordance to BS EN ISO 11609:2010 Dentistry guidelines for abrasive testing slurry solutions) [83]
Counterface material	Enamel disc

7.2 Surface analysis and wear depth

In this section, the results detailing the surface topographical changes of enamel will be presented. In order to calculate the mean and standard deviation values of roughness (Ra), skewness (Rsk), valley depth (Rv) and total height of profile (Rt), five profile measurements were taken in a perpendicular direction to the brushing direction. The average wear depth was calculated by subtracting the wear after the test to the original start data. To characterize roughness of a surface profile the following parameters were used: Ra -average roughness, Rsk – skewness, Rv – valley depth and Rt – total height of profile [238].

7.2.1 Roughness profiles and wear

There was an overall increase in roughness (Ra) and negative skewness (Rsk) with the alumina, silica and spherical silica group, Figure 7.1a and Figure 7.1b. The alumina particle test group showed the highest increase in Rsk after the six hours of testing with a Rsk of -7.41 µm, Figure 8a. An increase in negative skewness is a result of groove formation. As the test duration increased, more grooves were visible on the bovine surface.

No wear was observed on the bovine disc with the saliva slurry tests, hence there was no change in the skewness with the saliva control test. An increase in Rv and Rt was observed during the wear test for the particle groups, Figure 7.1c and Figure 7.1d. The depths of the grooves increased during the wear test for the particle groups, which is reflected in the increase of Rv and Rt. There was no quantifiable increase or change in the saliva control test group.

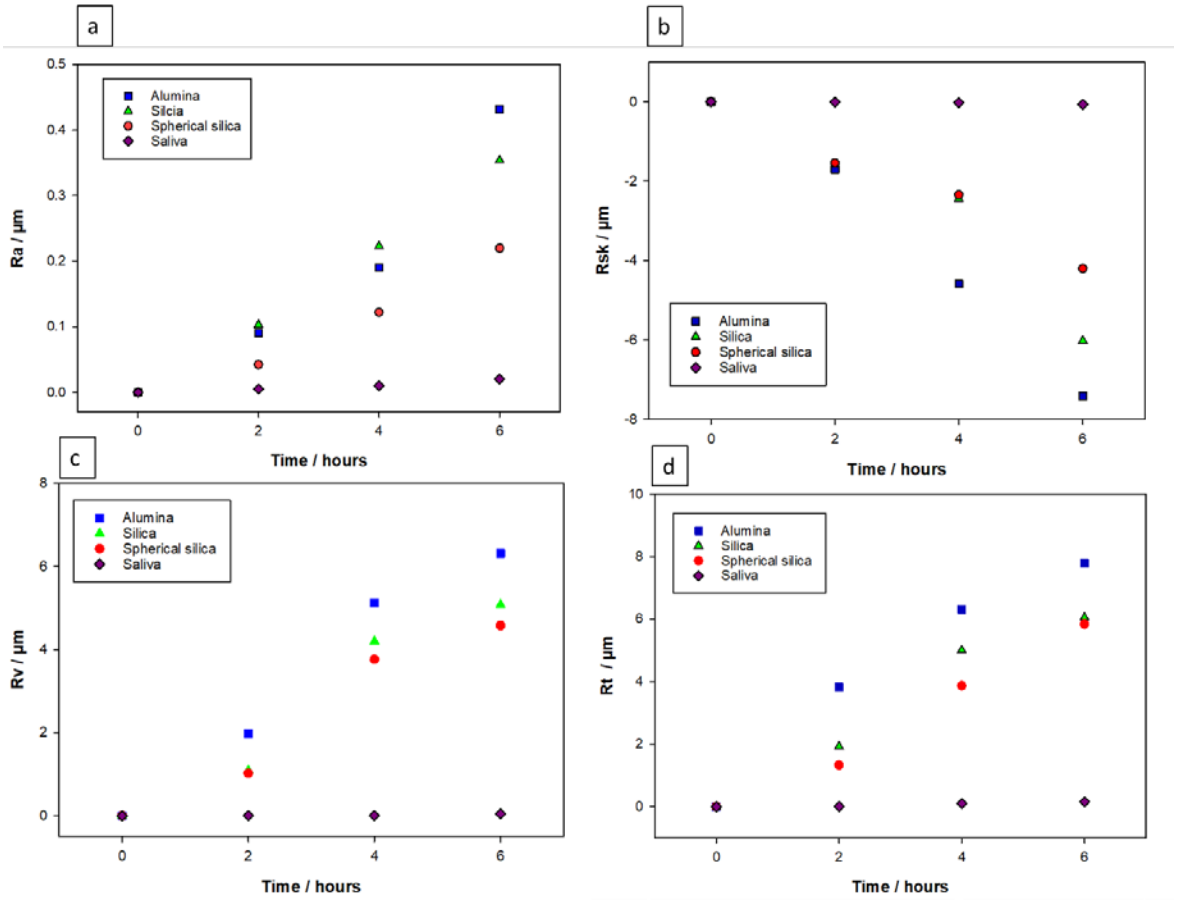

Figure 7.1: Surface profile data plotted against time, relative to pre-test values (a) roughness, R_a; (b) skewness, R_{sk}; (c) valley depth, R_v; (d) total height of profile, R_t.

Figure 7.2 shows the average wear depth after six hours for the particle and control saliva group. The average wear depth was calculated from direct pre-test and post-test measurements. The average wear depth for alumina was 7.8 µm, silica 5.4 µm and spherical silica 3.5µm respectively. Table 7.4 shows the wear depth. A higher wear rate for alumina corresponded to a higher Rv value, due to the increased groove formation. A minimal amount of material removal (0.034µm) was observed for the saliva control group. The average wear depth for all the tests is less than 10% of the thickness of enamel (~70µm). Table 7.3 shows the Ra, Rsk, Rv, Rt and data for the tests.

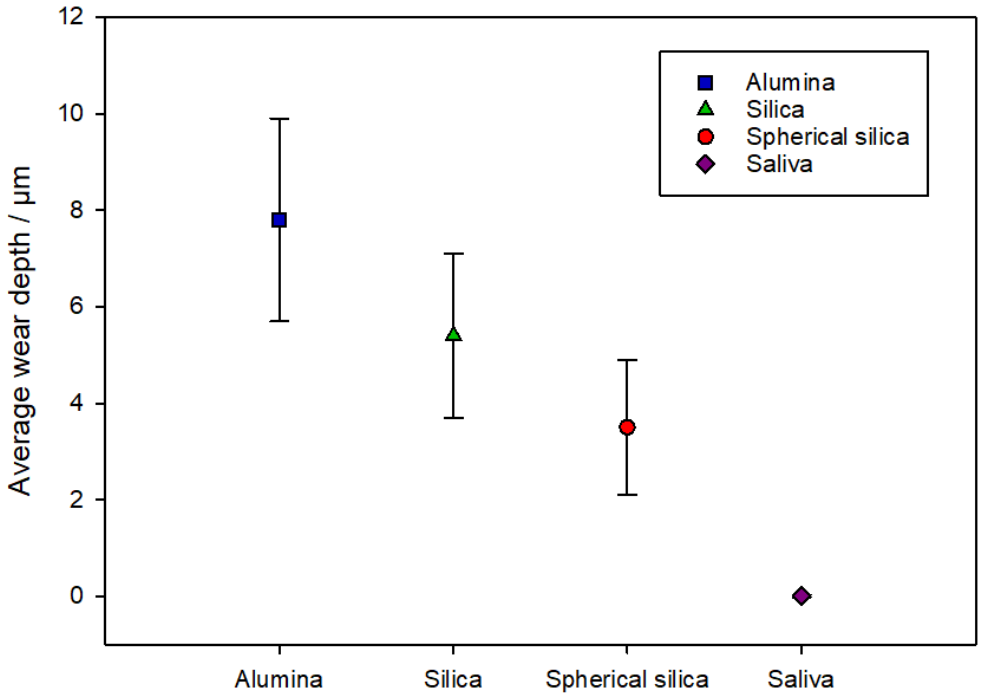

Figure 7.2: Average wear depth for the particle and control tests after the six hour test.

Table 7.2: Average wear depth, volume loss and specific wear rate (SWR) data.

	Average wear depth / µm	Volume loss / μm^3	Specific wear rate / mm^3/Nm^{-1}
Alumina	7.8 σ ± 2.1	34.97 σ ± 6.4	8.74×10^{-10} σ ± 0.00023
Silica	5.4 σ ± 1.7	21.66 σ ± 4.8	5.42×10^{-10} σ ± 0.00019
Spherical silica	3.5 σ ± 1.4	18.17 σ ± 3.7	4.68×10^{-10} σ ± 0.00022
Saliva (control)	0.007 σ ± 0.024	-	-

Table 7.3: Ra, Rsk, Rv and Rt data for the bovine disc.

	Roughness (R_a) / µm				Skewness (R_{sk}) / µm			
	0 hours	**2 hours**	**4 hours**	**6 hours**	**0 hours**	**2 hours**	**4 hours**	**6 hours**
Alumina	0	0.09 σ ± 0.14	0.19 σ ± 0.25	0.43 σ ± 0.12	0	-1.70 σ ± 0.45	-4.59 σ± 2.43	-7.41 σ± 2.91
Silica	0	0.10 σ± 0.15	0.22 σ ± 0.23	0.35 σ ± 0.14	0	-1.58 σ ± 0.29	-2.44 σ± 0.47	-6.02 σ± 2.62
Spherical silica	0	0.04 σ ± 0.23	0.12 σ ± 0.21	0.22 σ ± 0.09	0	-1.54 σ ± 0.14	-2.34 σ ± 0.22	-4.2 σ ± 1.97
Saliva	0	0.005 σ±0.023	0.012 σ±0.021	0.02 σ±0.028	0	0.0032 σ ± 0.024	-0.028 σ±0.013	-0.068 σ±0.009
	Valley depth (R_v) / µm				**Total height of profile (R_t) / µm**			
	0 hours	**2 hours**	**4 hours**	**6 hours**	**0 hours**	**2 hours**	**4 hours**	**6 hours**
Alumina	0	1.98 σ ± 2.91	5.12 σ ± 2.08	6.31 σ ±2.74	0	3.83 σ ± 1.71	6.31 σ± 2.20	7.79 σ± 2.96
Silica	0	1.10 σ± 0.38	4.20 σ ± 0.87	5.09 σ ±1.05	0	1.93 σ ± 0.92	5.00 σ± 0.83	6.06 σ± 1.06
Spherical silica	0	1.02 σ± 0.42	3.76 σ± 0.31	4.58 σ± 0.94	0	1.33 σ± 0.65	3.87 σ± 0.44	5.94 σ± 0.88
Saliva	0	0.003 σ± 0.01	0.003 σ± 0.07	0.042 σ±0.004	0	0.005 σ ± 0.04	0.10 σ± 0.06	0.12 σ± 0.04

7.3 Friction measurements

Friction was measured over a period of 6 hours and the test was stopped at intervals of 2 hours to record profile measurements.

There was a noticeable drop in coefficient of friction after 10 minutes for the alumina, silica and spherical silica tests. This is referred to as the run in period; where the asperity peaks on the surface of the bovine disc are worn away by the abrasive particles or the time it takes for the partides to build up on the filaments. There is no run-in period with the saliva test, Figure 7.3d. The cut off for the run in period for static friction was taken from when the values levelled off and showed stability. From this, the mean coefficient of friction was calculated which is shown by the red line in Figure 7.3. The red line indicated the average friction, excluding the start-up data. At the start of every test, the run in period caused the coefficient to rapidly increase and then steadily drop down. For the run in period, the tests were conditioned with the particles. Once conditioned, there was no run-in period. It took a longer period of time for the run-in period to level off for alumina at 3600 seconds, whereas the run in time for silica levelled off at 2700 seconds and for spherical silica at 1700 seconds., Figure 7.3a-c.

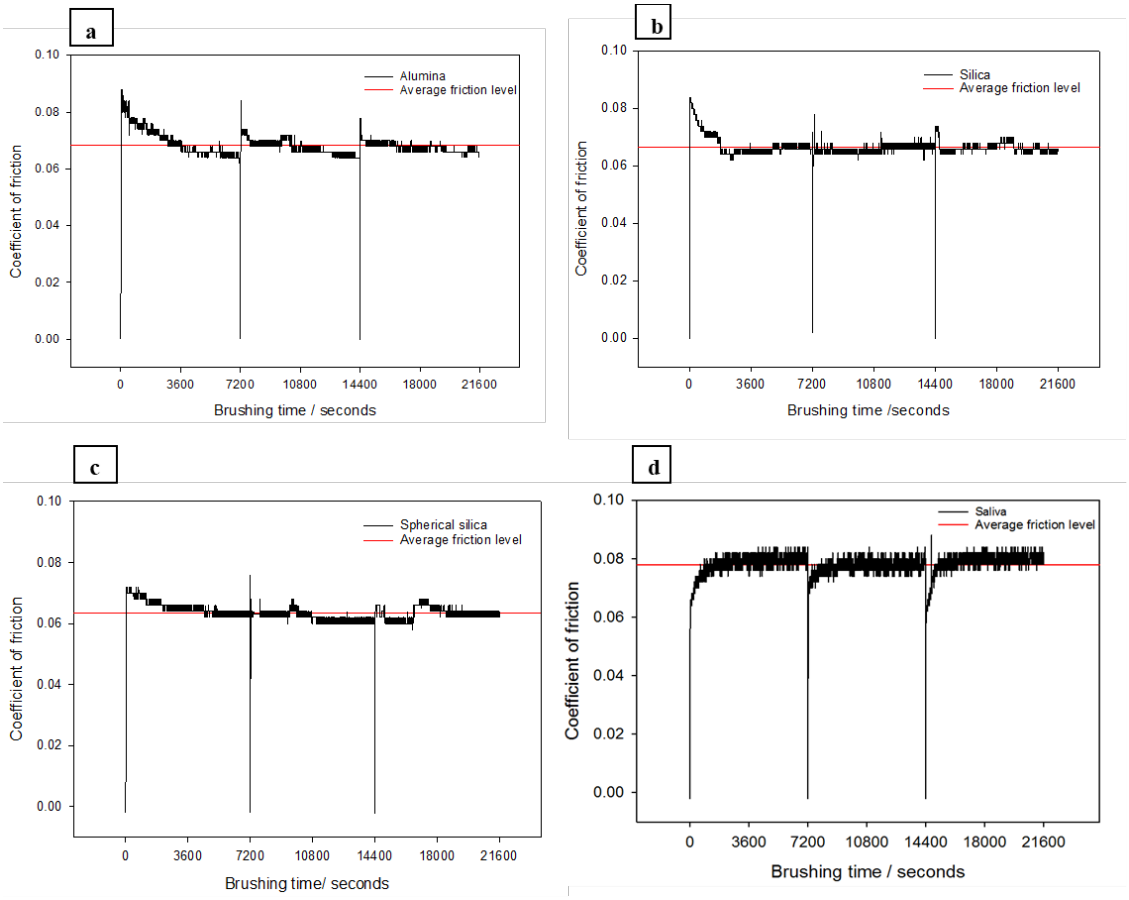

Figure 7.3: Coefficient of friction plotted against brushing time (a) alumina; (b) silica; (c) spherical silica; (d) saliva.

The friction for the alumina, silica and spherical silica tests was lower than the saliva control group. The saliva control exhibited a slightly larger friction value possibly due to the adhesion forces between the nylon and enamel resulting in nylon transfer to enamel or surface film formation. The mean coefficient of friction values for the tests are recorded in, Table 7.4. The coefficient of friction reported for the GSK alumina, GSK silica and GSK spherical silica was lower than the saliva control tests. There was a significant difference in the coefficient of friction between the particle tests and the saliva tests ($p<0.005$).

Table 7.4: Coefficient of friction values and the standard deviation (σ) for the wear tests.

Mean coefficient of friction			
GSK 9µm alumina	**GSK 8µm silica**	**GSK 6.5µm spherical silica**	**Saliva**
0.071 σ ± 0.001	0.066 σ ± 0.001	0.063 σ ± 0.003	0.078 σ ± 0.004

Friction tests were carried out at a frequency of 4 Hz and the data acquisition rate was set to 1 kHz a second. A low pass filter was used which filtered anything above 300Hz. The Nyquist limit applies to the Fast Fourier Transform (FFT) plots which is equal to half the sampling rate. The friction force and time graphs show the effect of filament buckling which can also be referred to as splaying or deflection of filaments, shown in Figure 7.4. Figure 7.4 shows one cycle taken from the high speed data for 250 milliseconds (ms) and the consistency in the data. The 3 plots on Figure 7.4 are three separate time frames of data taken from the same test. One cycle is equivalent to two brushing strokes. The friction force and time plots showed a change in direction of force at 125 milliseconds for the alumina, silica and spherical silica. The red line on Figure 7.4a, d, g, j indicated a change of direction of the brush at 125ms, hence the change in friction force. There was no visible pattern of buckling of filaments with the saliva control test at 125 seconds. The high speed friction plots are a visual aid to show the change of filament direction at 125ms.

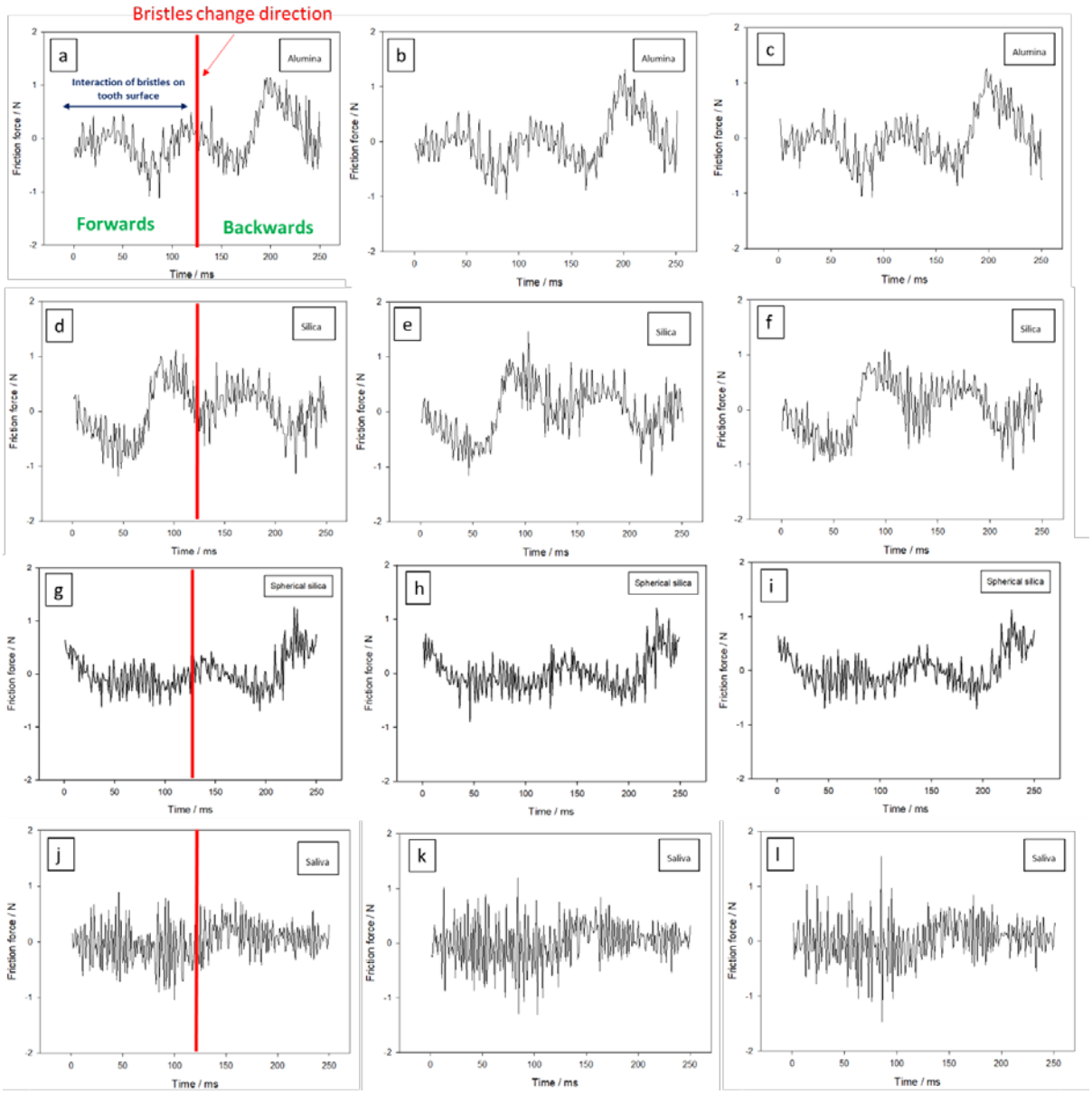

Figure 7.4: High speed friction data for 250 ms. 3 separate times of data for the same test (a)- (c) alumina test group.; (d) – (f) silica test group; (g) – (i) spherical silica; (j) – (l) saliva control.

High speed friction data can also be plotted against stroke displacement, which is shown in

Figure 7.5. The displacement is the movement of the toothbrush; the red line indicates the forward movement of the filaments and the blue line shows the backwards movement. The asymmetric friction loop on

Figure 7.5a-c show the influence of the slurry feed at one end. The overall shape of the friction loop is caused by the head position of the toothbrush and the change of direction of the filaments (buckling). The buckling of filaments is independent of the brush head movement. The direction of the filaments and buckling of the filaments is out of sync with the head position of the toothbrush. The shape of the friction loop for the particle groups show a distinctive loop compared to the saliva control which shows no distinctive feature. A change of sliding direction causes the force on the filaments to fold over, resulting in time for the particles to agglomerate on the filaments.

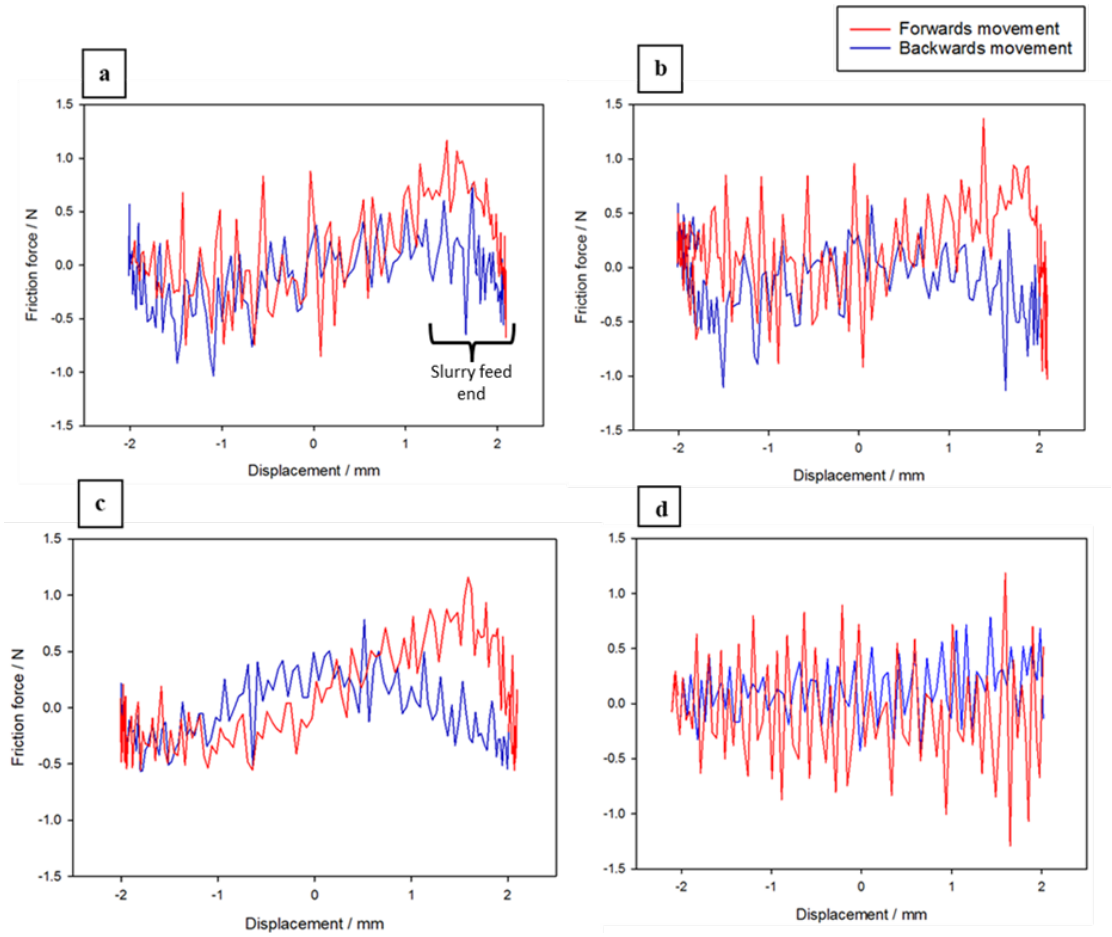

Figure 7.5: Friction force and stroke displacement data (a) alumina; (b) silica; (c) spherical silica; (d) saliva.

The friction force/ time graphs were converted to FFT graphs, Figure 7.6. The reciprocating peaks on the graphs are due to the reciprocating harmonic motion during the test. All the graphs have similar peaks at 100Hz and 200Hz. This is multiple filament interactions on the tooth surface. There are ~25 tufts in contact with the enamel centre, which have 20 filaments each; this results in the peaks at 100Hz and 200Hz. The peaks are due to the interaction of the filaments with the bovine centre. Figure 7.6d shows the control saliva test FFT which has a lower magnitude of peaks at these frequencies. This could be due to no particles in the slurry and no run-in period.

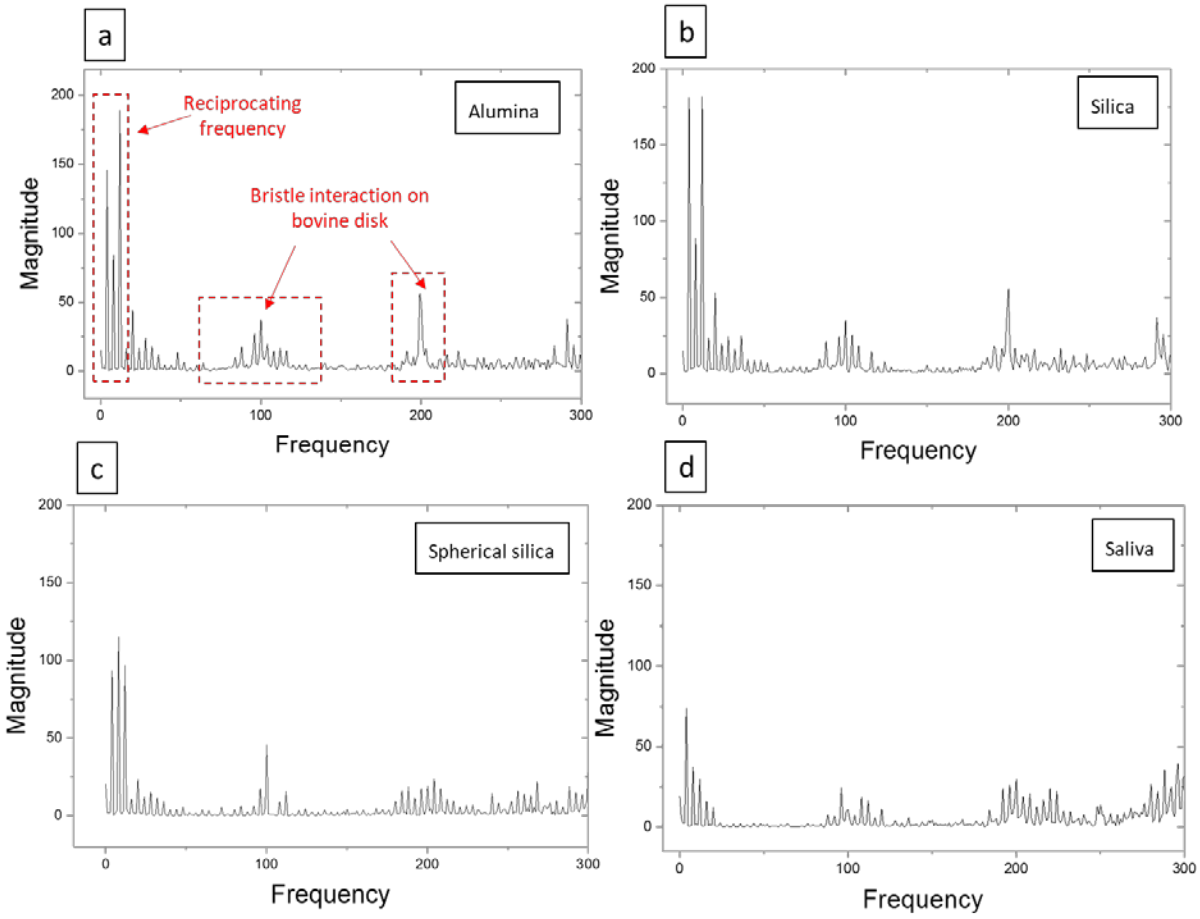

Figure 7.6: FFT graphs (a) alumina; (b) silica; (c) spherical silica; (d) saliva.

7.4 Surface analysis

An SEM of the bovine disc after brushing shows the surface consisted of various sizes of 2-body grooves in the shape and width of both the filaments and particles, Figure 7.7a-c. The control test group showed no signs of wear or grooving, Figure 7.7d. No rolling or three body wear was evident on the bovine discs for all the tests.

Small grooves in the region of 12µm were visible in-between the larger grooves (130µm) for the particle tests. Grooving on the bovine disc would appear to be caused by high contact stresses between the filament/enamel and entrainment/ agglomeration of particles onto the filament. The filaments with the agglomerated particles groove the enamel and result in the enamel being micro-chipped. Smaller particle grooves are present in the bigger grooves which explains that the partides are agglomerating on the filament tips.

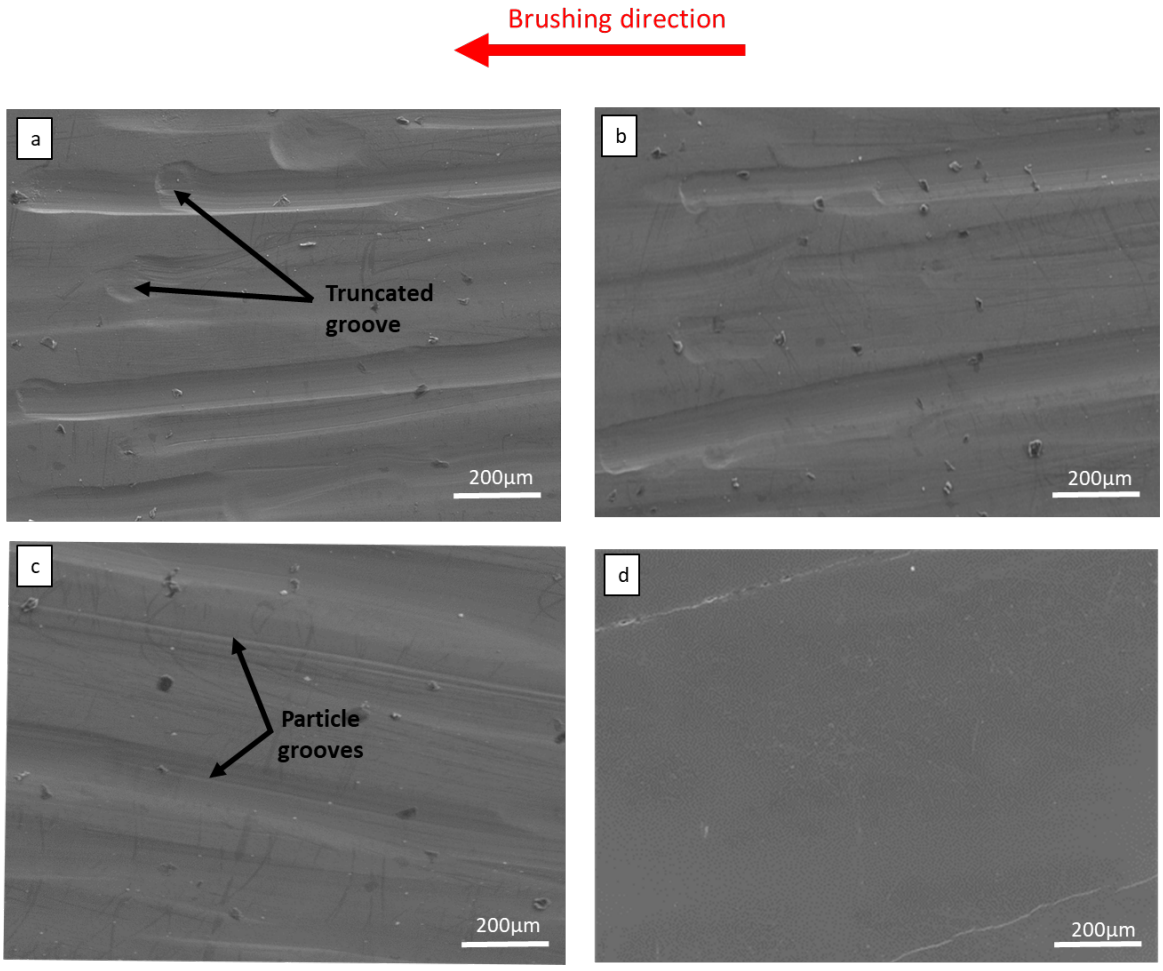

Figure 7.7: Bovine disc wear scar (a) alumina; (b) silica; (c) spherical silica; (d) saliva.

Truncated grooves, which is recognized as a short groove on the bovine surface were observed on the bovine discs. There were two types of truncated grooves. The first type was formed where the tuft of the filaments stopped during the stroke and the brush turned back to a reversal stroke. The ratio of truncated grooves to normal full length grooves was 6:1. The ratio of per particle grooves to filament grooves was 7:5. Figure 7.7 a-b shows the truncated grooves in the same end-position, highlighting where the tuft of the filaments stopped during the stroke. The second type of truncated groove was formed when the abrasive particle was released from the filament mid-stroke, Figure 7.8 and Figure 7.9. From the bovine discs, there was evidence of particle grooves and filament grooves.

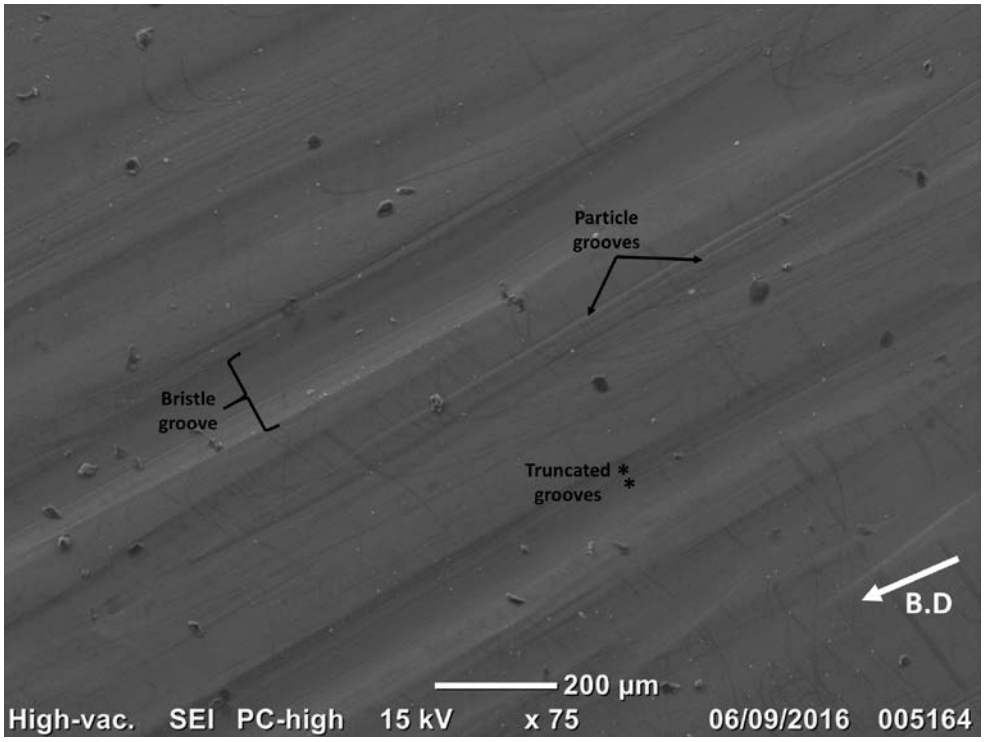

Figure 7.8: Bovine disc wear scar with GSK alumina particles showing grooves and truncated grooves indicated by the black asterisks.

Figure 7.9: Bovine disc wear scar with GSK silica particles showing truncated groove indicated by the red asterisks.

7.5 Discussion

This section identifies and discusses the main factors contributing to abrasive tooth cleaning.

7.5.1 Friction

The coefficient of friction was measured over the duration of the tests. The saliva control tests generated the highest friction coefficient value which was unexpected. This is thought to be due to the high friction between hydrated enamel and nylon, compared to the particle tests where there is a particle/ hydrated enamel contact.

A study conducted by Zheng et al. [159] reported the coefficient of friction values of enamel to be in the region of 0.026 – 0.87. The study used loads in the region of 20N, whereas the present study conducted used a load of 5N. From the SEM images, the wear scar observed by Zheng et al. [159] was two body grooving which is also confirmed in the present study. It was concluded that the removal of enamel was by a micro-cracking process [159, 239]. What is surprising is that no micro-cracking was visible in the present study.

An explanation for the difference in run-in time for the particle groups could be due to the agglomeration time of particles on the filaments or the level of polishing on the bovine surface, which resulted in an increased time for the asperity peaks to wear away by the abrasive particles in the slurry. There was a small appreciable amount of time for the saliva run-in period. This was due to no abrasive particles present in the slurry, resulting in no abrasion of the bovine surface, hence a very small run in period.

The presence of no particles in the slurry increases the coefficient of friction value. A possible reason for this could be due to the inherent higher friction between wet nylon and hydrated enamel, compared to the friction between the particles and the enamel, Table 7.4. Another possibility of the high coefficient of friction for saliva could be due to adhesive processes such as material transfer of nylon onto enamel. Brushes that are loaded heavily have a tendency to trap the particles between the filaments or at the shoulder of the deflected filament. In the absence of particles, the high load on the toothbrush filaments could result in transfer of nylon from the filaments to the enamel surface resulting in high adhesion between the nylon and enamel [102]. Another reason for the high coefficient of friction value with the saliva control group could potentially be due to a formation of a transfer film of nylon. Friction can be affected by the formation of transfer films or a lubrication film [240]. One of the most common features of adhesive wear is the transfer of material from one surface to another. The transfer takes place by bonding

of the solid surfaces that contact. it is encouraging to compare this with a study conducted by Bely et al. [241] who found that the most important characteristic of adhesive wear in polymers is the transfer of material/ polymer. Friction transfer is a common occurrence [242].

Friction between similar materials can occur if a transfer film is held in place. Many literature studies [35-38], have cited the formation of a transfer film however, there is no sign of a transfer film in the current study. There is a higher friction exhibited with the control slurry tests. A possible reason could be the transfer of nylon from the filaments to the tooth enamel, resulting in a nylon-nylon contact, however, there is no direct evidence of transfer of nylon in the current study [242].

At the start and end of the brushing stroke the filament/enamel contact is likely to be in boundary lubrication. During the boundary lubrication phase, the coefficient of friction is the highest. As the sliding speed increases, the particle entrainment between the bovine disc and filaments increases which relieves the asperity contact; the coefficient of friction drops to a steady value. This is known as mixed lubrication and takes place in the middle of the brushing cycle. A mixed lubrication phase is desirable to avoid any wear [243]. Another factor to consider is the static and dynamic friction. The brushing test stops moving at each end of the brushing cycle which results in a steady value for the coefficient of friction.

With a high brushing load of 5N being used for the present study, very low co-efficient of friction values were obtained. We can see this in other examples of sliding engine wear. A study carried out by Tung et al. [244] looked at the surface interaction between piston ring coatings and engine oils using an energy- conserving lubrication regime. Piston coatings running in oils of molybdenum friction modifier for 10 hours exhibited low coefficient of friction values in the region of 0.04 – 0.075 [244]. These low friction values reported for oil lubricated systems are similar to those found in the current study and demonstrate that brushing contacts dissipate low frictional energy.

It is possible that stick-slip may be present in the current study. Stick- slip is due to filament-filament interactions. Filament interactions on the bovine disc could potentially create peaks at 100Hz and 200Hz on the FFT graphs, Figure 7.6. The number of tufts in contact with the bovine disc are ~25 at any given time, with the reciprocating frequency of 4Hz; this explains the peaks at 100Hz and 200Hz. The peaks observed at frequencies of 4Hz, 8 Hz, 12Hz, 16Hz are natural harmonic peaks.

The stiffness of the outer filaments to the inner coloured filaments could affect the friction. The coloured filaments have a higher Youngs Modulus compared to the clear inner filaments, hence the higher stiffness with the coloured filaments. The stiffer filaments generate higher friction forces, due to the nature of the stiff surface and more likely being in boundary lubrication [245].

During reciprocating movement the brush stroke changes direction from a backwards to forwards motion. The buckling of filaments can be seen in Figure 7.4 at 125 seconds where a change in direction of the filaments takes place, indicated by the red line on Figure 7.4a. The trend of the friction loop shows the splaying of filaments and the change of direction of the brush. It was found by Lewis et al. [6] that particles were re-entrained in the filaments during a change in brush stroke direction. This is confirmed by the present tests.

The complexity of the interface leads to a complex friction motion. When two surfaces contact, bonds are formed, which leads to junction development. The adhesion component of friction is controlled by the rupture and formation of the junctions. Bowden and Tabor [246] proposed a model which highlighted the junction model. Typically, Van der Waals forces and hydrogen bonds exist for polymers. The frictional force is formed by the shearing of junctions under the tangential force. Transfer of polymer and material fracture can take place if stronger bonds exist with interfacial bonding, than cohesive forces of the weaker material. If this takes place, fracture of the material is observed, assuming no lubricant film [246].

7.5.2 Groove analysis

Agglomeration of particles can occur during the wear test. The particles that have entered the contact, have the ability to agglomerate to neighbouring particles in the slurry. When the partides are trapped between the filaments they make contact with the bovine disc. This process takes place by the deflection of filaments. The loaded particles act by grooving the surface of the bovine disc. This is two-body abrasion. The results from the tests show that 2-body grooving was observed on the bovine discs. Two-body grooving was also reported by Lewis et al. [6] who reported partides being spread evenly around the filament tips. The abrasives particles agglomerated to the filaments groove the enamel by a micro-chipping process [147]. The control saliva test showed no signs of wear highlighting the fact the filament alone is unable to damage the surface.

Figure 7.7a and Figure 7.7b show the particles agglomerated on a single filament tip. As the toothbrush filaments change direction mid stroke, the particles remain accumulated on the insides of the filament tips. As the brushing motion takes place the particle is pressed against the enamel surface by the deflected filaments. The head position of the toothbrush does not relate to the filament direction. Increasing the load on the filament results in a higher cleaning efficiency. A possible explanation of this could be due to the increase in load on the particles that are trapped in the filament tips [102].

When the toothbrush filament deflects on the start of the stroke, the filament tip has no signs of particle accumulation, resulting in no abrasion at the onset of the wear test. This is confirmed by analysis of the high speed friction data at the start of the test, which shows the friction plots are similar to the saliva control test,

Figure 7.5, indicating that particle accumulation on the filaments results in wear. Particle agglomeration is evident at the sides of the filaments where the filaments bend. The loops on

Figure 7.5a-c are due to the abrasive particle slurry feed, giving evidence for particle accumulation.

Figure 7.10, shows the truncated groove process. Truncated grooves were visible on the SEM images, Figure 7.8. A possibility for the formation of a truncated groove could be due to particle release from the filament; the particle could have been dislodged by many reasons such as an increased load on the filament or the change of direction of the brush. Another possible explanation for the truncated grooves could be the position of the middle filaments on the toothbrush. The middle filaments only reciprocate half way across the stroke length of the bovine disc and do not achieve the full stroke length.

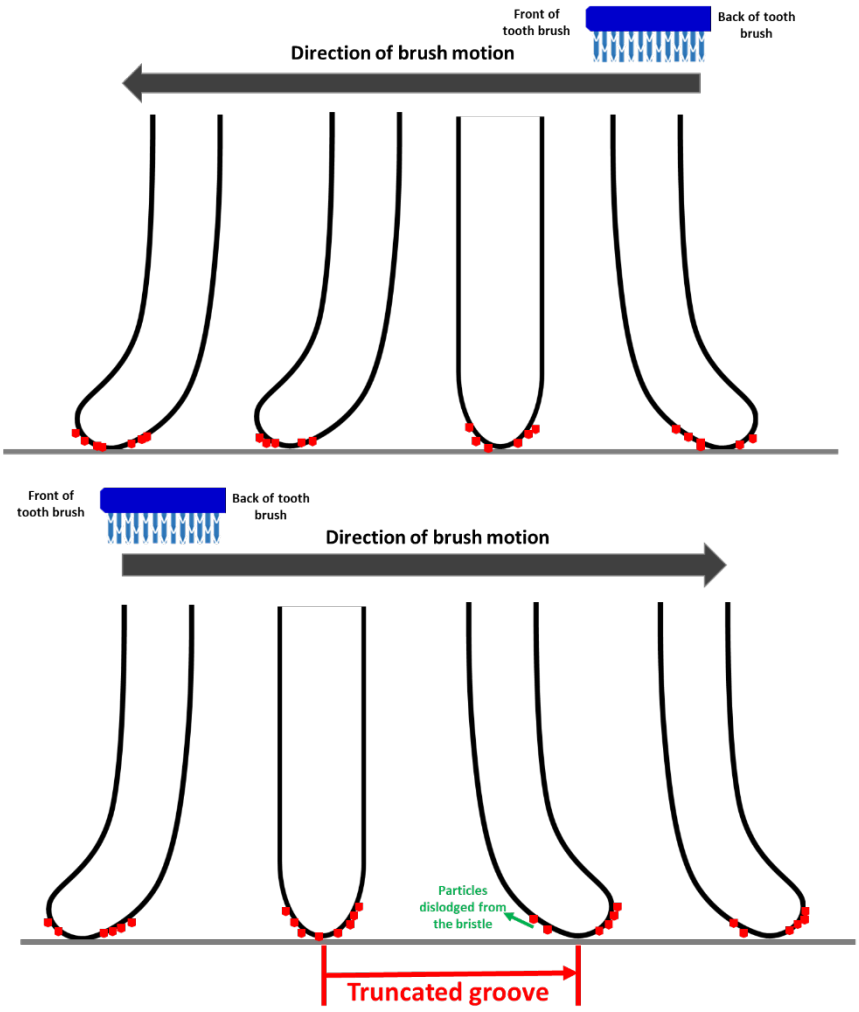

Figure 7.10: Schematic after several brushing strokes, after particle agglomeration.

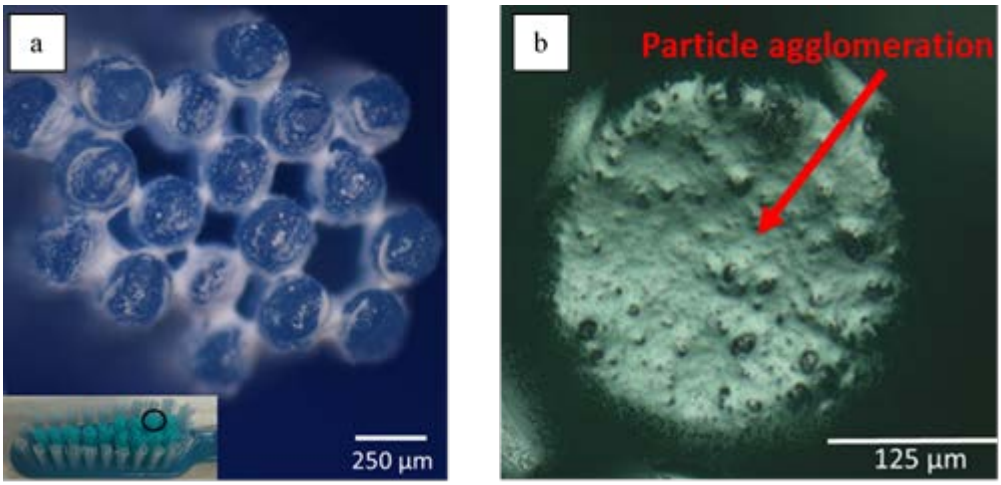

Figure 7.11: Particle agglomeration (a) alumina particles agglomerated in and around the filaments; (b) alumina particle agglomeration on a single filament tip.

From the SEM not all the scratches were continuous in length on the bovine disc, Figure 7.7. Highly loaded filaments rest on neighbouring filaments, delivering the load on the neighbouring filaments and this results in scratches that are not continuous [7]. The presence of grooves on the enamel surface can act as reservoirs for particles to be lodged into and cause smaller grooves. This was evident from the SEM images, where there was evidence of two-body grooves due to particles agglomerated to the filaments and smaller particle grooves in the larger grooves, Figure 7.7.

From the SEM images of the wear scar, Figure 7.7, it can be seen that the length of the wear scar does not equal the length of the brush stroke. A complex splaying motion of filaments exists. The head position of the toothbrush and direction of brush, changes at the end of the stroke, which may lead to a phase lag in filament motion. During the wear test, many reciprocating motions are needed before the particles are trapped in the filaments. Particles have to be trapped in a specific orientation in the filaments for the scratches to form.

The width of the grooves on the bovine discs are in the size range of the diameter of the deflected filament tip and particles, Table 7.5. Many conditions such as the load, brushing action and deflection of filaments dictate if and how the abrasive particles are trapped in the filaments. Agglomerated particles are trapped in the filament tips and stay wedged in the filament tips during reciprocating movements [6]. Figure 7.11, shows a single filament with particle agglomeration after the wear test.

Table 7.5: Properties of the particles, filaments and width of wear scar grooves.

Mean particle diameter / µm			Filament tip diameter / µm	Deflected filament tip diameter / µm	Width of grooves / µm
GSK alumina	GSK silica	GSK spherical silica			
9	8	6.5	70	110	12 -130

7.5.3 Wear mechanisms

The SEM micrographs in Figure 7.7 show grooving in the wear scar for the particle tests. After the brushing duration of 6 hours, the Rv for alumina was 6.31µm, silica 5.09µm and spherical silica 4.58µm, confirming groove formation on the bovine surface. There was an increase in negative skewness after 6 hours of brushing, for alumina an Rsk of -7.41µm, -6.02µm for silica and -4.2 for spherical silica respectively. The increase in Rv and Rsk confirms the finding of groove formation. The average wear depth of alumina to be 7.8µm, 5.4µm for silica and 3.5µm for spherical silica respectively.

This increased material removal for alumina can be due to factors such as the hardness, size and particle geometry of the abrasive particles. A study conducted by Pace Technologies, 2006 [227] found alumina to be a harder abrasive than silica and have a higher strength.

Factors not related to particle size, such and the particle angularity and hardness could result in the higher material loss for the alumina tests. This is inferred by Coronado, 2012 [247] who found large sized alumina particles to have rounded edges, whereas a greater angularity in shape was observed with smaller sized particles [247]. The relative hardness of the particle to enamel influences the wear rate/mechanism. The hardness of bovine enamel is 150 HV and the relative hardness of alumina and silica are 2500HV and 1200HV respectively [40]. The hardness of the abrasive partides compared to enamel are high, which could contribute to increased wear.

It can be concluded that under loading, the front edge of the particle is chipping away the enamel surface. The contact pressure is highest at the front loaded edge of the particle, which results in an increase in wear. A study carried out by Zhou et al. [158] found increasing the load on enamel, resulted in an increase in wear. This was due to the mechanical properties of enamel under load. At lower loads the favourable properties of enamel such as the high hardness and high mineral content result in resistance to wear [158].

During the test there was an increase in negative skewness for the alumina and silica tests, Table 7.3. After two hours there was not much of an increase in negative skewness for alumina, silica and spherical silica. The wear grooves were not as prominent after 2 hours but after 4 hours the wear was more pronounced, with more valleys formed on the bovine disc. This can be explained by the time it takes for a scratch to form. Many filament strokes take place, before a scratch is formed [6]. The formation of the grooves resulted in an increase in Rv and Rt over the duration of the wear test, Table 7.3.

Upon inspection of the toothbrushes after the present study, there were no signs of frayed filaments. A possible explanation for this is that, a 3-body mode takes over and the particle is swept away in a 3-body motion. Another possibility is the neighbouring filaments allow the loaded filament to rest on them, relieving the load on the filament during the motion [205].

The specific wear rate (SWR) of enamel was found to be in the region of $4.68 – 8.74 \times 10^{-4}$ mm^3/Nm^{-1} with alumina and silica abrasive particles in the slurry, Table 7.2. The specific wear rate was found to increase with alumina grain size, with the geometry of the abrasive contact greatly affecting the wear behaviour [248].

A micro-abrasion study conducted by Pena et al. [147] on human enamel and dental restorative materials found the SWR of enamel to be 9.35×10^{-12} mm^3/Nm^{-1} with an artificial saliva- SiC slurry. The wear mechanism was reported as plastic deformation and brittle delamination. It was suggested that due to the brittle nature and organic structure of enamel, the wear rates were higher compared to the wear rates of dental composites, which were in the region of $2.92 – 4.12 \times 10^{-2}$ mm^3/Nm^{-1} [7]. This value for SWR was lower than the value in the present study (Table 7.2) and could be due to the different test conditions employed and the dissimilar interface between the contacting surfaces [147]. A steel ball and a load of 0.25N was used in the tests carried out by Pena et al. [147], whereas the present study used nylon filaments and a load of 0.5N.

7.6 Conclusions

Based on the present study of using the TE77 reciprocating tribometer to evaluate wear and friction performance of abrasive slurries on hydrated enamel, the following conclusions can be made:

- The coefficient of friction was higher for the saliva control test. A possibility of this is due to a high friction between wet nylon and hydrated enamel.

- Spherical silica tests generated the lowest wear rates compared to the alumina and silica tests and produced a smoother surface, with a Ra of 0.22μm.

- An important factor to consider is the agglomeration of particles on filaments. The use of dispersants should be considered to control agglomeration, or the use of super-hydrophobic surfaces/ coating on filaments, to stop particle agglomeration.

- A complex filament movement in the stroke leads to an asymmetric friction/ wear evolution. The middle coloured filaments have a different stiffness to the inner filaments influencing the wear rate.

.

- Increased groove formation during the duration of the test resulted in an increase in negative skewness (R_{sk}), valley depth (R_v) and total height of profile (R_t).

- The wear scratches formed on the bovine disc indicate a 2-body grooving mechanism. The wear on enamel appeared to be caused by the particles and filaments, showing that enamel removal is dominated by a micro-chipping action, where particles are embedded in the filament tips.

- The results show an increase in wear is produced on the bovine disc with alumina. Care should be taken when brushing with an alumina paste, to avoid an increased amount of enamel removal.

8. General discussion

8.1 Introduction

This chapter aims to integrate the various experiments from chapters 5, 6 and 7 and expand the understanding on which factors and mechanisms directly affect enamel wear. The gaps in the literature will be addressed such as the synergistic effects of bimodal particles in toothpastes vs. mono sized particles. Comparisons will be made between the groove widths observed during micro-abrasion and brushing tests. No direct comparison of the mixed-mode mechanism will be made, as no signs of mixed mode or rolling abrasion was observed with the TE77 brushing tests. The volume loss of enamel and specific wear rates (SWR) will be compared for both sets of experiments. As introduced in chapters 5 and 6, synergy will be discussed in detail. This chapter will bring together the interplay between the applied test conditions/ particle entrainment with a soft ball in the TE66 tests, or a toothbrush in the TE77 tests. The variables in the TE66 micro-abrasion test and the TE77 brushing test are presented in Table 8.1.

Table 8.1: Variables of the TE66 and TE77 tests.

	Variables	**Constant**
TE66 micro-abrasion	• Particles - Size - Shape - Composition • Load • Volume fraction of abrasives • Total test time – 60 seconds	• Sliding distance
TE77 brushing tests	• Particles - Size distribution • Total test time – 6 hours	• Load • Sliding distance • Concentration of slurry

8.2 Evaluation of the micro-abrasion and brushing tests

This section aims to bring together and compare the data and wear mechanisms from the TE66 micro-abrasion tests and the TE77 brushing tests.

8.2.1 Groove width comparison

Figure 8.1 shows the groove widths for the TE66 micro-abrasion tests and the TE77 brushing tests for the filaments and particle. The average groove width in the TE77 tests for the particles was 13µm and for the filaments it was 113µm respectively. These figures are represented in Table 8.2. There was a significant difference ($p<0.05$) in groove widths generated by the particles for the TE66 test and both the TE77 tests. The average groove widths generated by the particles were lower in the TE66 micro-abrasion tests than the TE77 brushing tests. A reason for this could be due to the different delivery of particles in both sets of tests, with particles agglomerated on the filament in the TE77 tests, compared to particles embedded in the nylon ball in the TE66 tests.

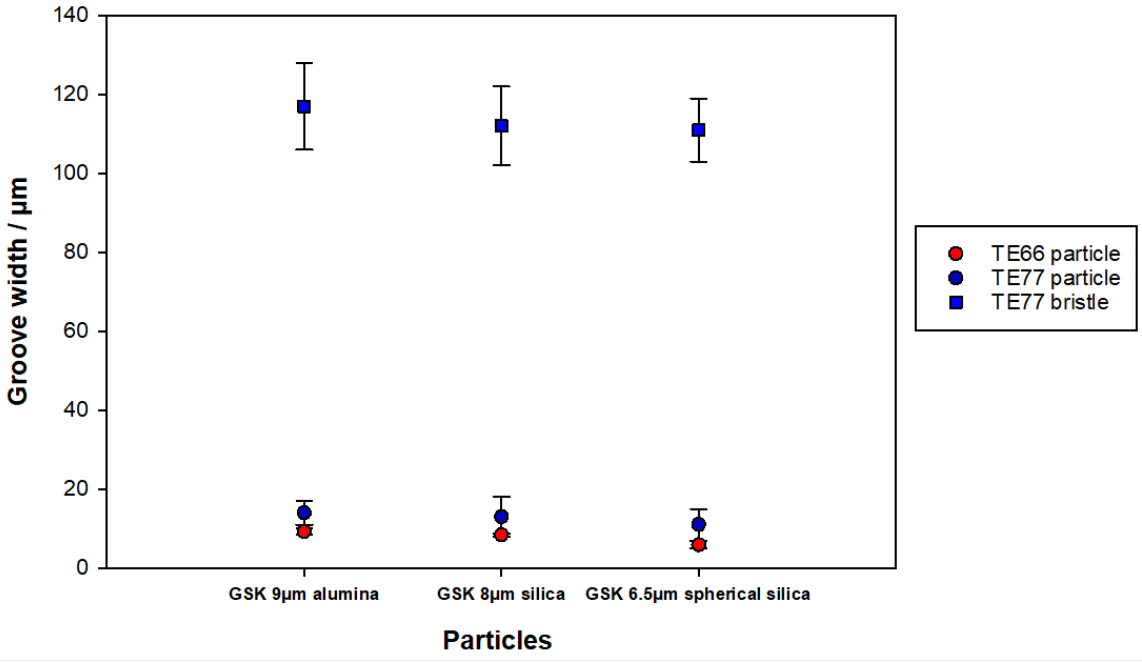

Figure 8.1: Groove widths for the particles and filaments in the TE77 tests.

Table 8.2: Groove width data for the particles and filaments in the TE77 tests.

	TE77 brushing tests		TE66 micro-abrasion test
	Average particle groove width / µm	Average filament groove width / µm	Average groove width / µm
GSK 9µm Alumina Maximum size – 10.4µm Mean size – 9µm	14 σ ± 3	117 σ ± 11	9.22 σ ± 0.77
GSK 8µm Silica Maximum size – 9µm Mean size – 8µm	13 σ ± 5	112 σ ± 10	8.39 σ ± 0.37
GSK 6.5µm Spherical silica Maximum size – 6.1µm Mean size - 5µm	11 σ ± 4	111 σ ± 8	5.87 σ ± 0.87

8.2.2 Volume loss and SWR comparison

Table 8.3 shows the comparison of the SWR and volume loss for the TE66 micro-abrasion tests and TE77 brushing tests. There was no direct comparison for the mixed-mode and 3 body rolling regimes for the TE77 brushing tests and for this reason only the grooving data is evaluated.

The wear rates and volume loss of enamel were higher for the TE66 tests with the highest wear rate reported with alumina at 0.1N. For the TE66 micro-abrasion tests, the average volume loss and SWR measurement was taken from volume fraction 0.05 v/v for the grooving mechanism.

Table 8.3: TE77 and TE66 volume loss, SWR and wear mechanism comparisons.

	TE77 brushing tests		TE66 micro-abrasion tests					
	Volume loss / μm^3	Specific wear rate (SWR) / mm^3/Nm^{-1}	Average volume loss / μm^3			Average specific wear rate (SWR) / mm^3/Nm^{-1}		
			0.1N	0.2N	0.5N	0.1N	0.2N	0.5N
GSK Alumina	34.97 $\sigma \pm 6.4$	8.74×10^{-10} $\sigma \pm 2.3 \times 10^{-10}$	3.13×10^{6} $\sigma \pm 8.11 \times 10^{5}$	2.69×10^{6} $\sigma \pm 4.31 \times 10^{5}$	2.14×10^{6} $\sigma \pm 3.13 \times 10^{5}$	1.56×10^{-3} $\sigma \pm 8.11 \times 10^{-4}$	6.72×10^{-3} $\sigma \pm 4.31 \times 10^{-4}$	2.14×10^{-3} $\sigma \pm 3.13 \times 10^{-4}$
GSK Silica	21.66 $\sigma \pm 4.8$	5.42×10^{-10} $\sigma \pm 2.5 \times 10^{-10}$	8.31×10^{6} $\sigma \pm 1.02 \times 10^{5}$	1.08×10^{6} $\sigma \pm 2.04 \times 10^{5}$	7.30×10^{6} $\sigma \pm 2.11 \times 10^{5}$	4.16×10^{-3} $\sigma \pm 1.02 \times 10^{-4}$	2.68×10^{-3} $\sigma \pm 2.04 \times 10^{-4}$	7.30×10^{-3} $\sigma \pm 2.11 \times 10^{-4}$
GSK Spherical silica	15.69 $\sigma \pm 1.3$	4.68×10^{-10} $\sigma \pm 2.0 \times 10^{-10}$	5.41×10^{6} $\sigma \pm 1.02 \times 10^{5}$	5.40×10^{6} $\sigma \pm 3.12 \times 10^{5}$	4.46×10^{6} $\sigma \pm 2.11 \times 10^{5}$	2.71×10^{-3} $\sigma \pm 1.02 \times 10^{-4}$	1.35×10^{-3} $\sigma \pm 3.12 \times 10^{-4}$	4.46×10^{-3} $\sigma \pm 2.11 \times 10^{-4}$
Wear mechanisms	2-body grooving		2-body grooving *Mixed-mode *3-body rolling *No direct comparison of the wear mechanism with TE77 tests.					

8.2.3 Wear mechanism comparison

Figure 8.2 shows the 2-body grooving wear scar from the TE66 micro-abrasion tests and the TE77 brushing tests. The grooves generated from the micro-abrasion tests (Figure 8.2a) were narrower than the grooves generated from the brushing tests, Figure 8.2b. The appearance of the grooves from the brushing tests were much wider.

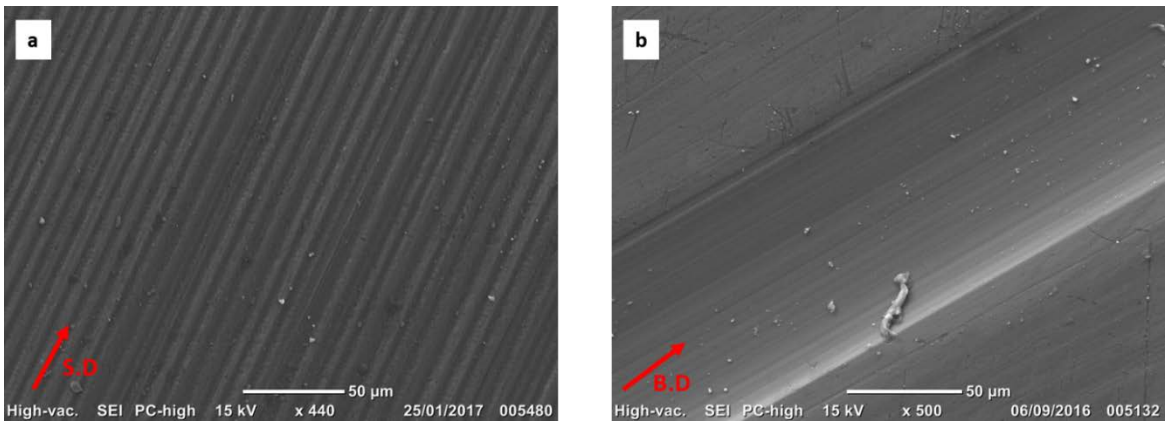

Figure 8.2: Typical 2-body grooving (a) TE66 micro-abrasion tests; (b) TE77 brushing tests. Where S.D is the sliding direction and B.D is the brushing direction.

8.3 Discussion

Previous chapters have discussed individually how the wear processes and wear rate of enamel are influenced by the shape, size, size distribution and morphology of abrasive particles. This chapter aims to combine the individual discussions from the previous chapters to understand how the wear factors all interconnect.

The particles used in toothpastes have the potential to harm the tooth tissues. Therefore, understanding the wear process of enamel subjected to abrasive slurries is a key point to improve the overall future toothpaste formulation. It is difficult to correlate the different oral tribology tests as many tests have used various simulating devices with different test conditions. This, then, results in a lack of comparisons of the data to be made and only broad trends can be drawn. In addition, another thing to consider is translating the in-vitro results to in-vivo tooth wear. This is due to the complexity of the oral environment.

A higher volume loss and SWR was observed with the TE66 microabrasion tests. The volume loss and SWR for the TE66 tests was much higher than the TE77 brushing tests, due to the increased contact area over many filaments for the brushing tests. These high values for the TE66 test were expected due to the consistent and efficient entrainment of particles and the harsh nature of the test. The brushing test was more representable of the conditions in the mouth, whereas the TE66 was a robust and reproducible test. The wear mechanism observed for the TE77 test was 2-body grooving only, which is the same of that observed in the oral environment.

Human enamel in a real life situation in the mouth undergoes a two-body abrasion process under abrasive wear [250]. The present findings in the TE77 test showed the enamel to undergo a two-body wear process.

Under normal conditions it was reported that the wear of enamel is 20- 40µm a year [251]. The TE77 tests were carried out to simulate 3 months of brushing and the average wear depth found was 24.10µm. A possible explanation for this high wear rate could be due to the harsh nature of the TE77 test.

8.3.1 Wear behaviour

The lack of standardisation of enamel wear related literature has its disadvantages. The experimental methods vary and to generate measurable wear thousands of brushing strokes are often used. There is an importance in using a test technique which in an accurate way reproduces the oral cavity function, the movements, forces and the physical environment of the mouth [255]. Many oral tribology studies focus on wear of enamel when in contact with dental restorative materials, such as gold, amalgam, zirconia, ceramic and glass. No published study has examined the wear and friction behaviour of bovine enamel when subjected to toothpaste abrasive particles [240, 255-258].

The main wear mechanism can be classified into three types, two-body grooving, mixed-mode and three body rolling. Chapter 2 explains these terms in detail.

A study concluded by Mondelli et al. [259] concluded that the rate of abrasion observed on dental hard tissues depends on many factors such as the speed of toothbrusing, the pressure/ force applied, the type of toothbrush, the type of toothpaste and the water/ toothpaste ratio. It was found that toothbrusing with an abrasive toothpaste resulted in significant wear, which was supported by the present research which concluded that the wear of enamel is increased when toothbrusing with an abrasive slurry.

In the present TE77 study, to simulate the everyday situation of toothbrusing as closely as possible, abrasive slurries were wear tested on bovine enamel. It has been concluded that during polishing to achieve a flat surface of enamel, the top layer of enamel is removed which can influence the severity of the abrasive process. Flattening and polishing the bovine teeth removes the outer-most surface prism layer [261]. In addition, flattening impacts the abrasion resistance. Attin et al. [40] reported that bovine enamel specimens could vary in hardness from one specimen to another and this could affect the wear behaviour of enamel. Therefore, in the present study, which used a load of 5N, the results could be overestimated due to the standard metallurgical procedure used to polish the bovine samples [262]. The bovine enamel was polished before the wear test, and Sharifi et al. [172] reported an improvement in wear performance with polished and smooth surface of materials [172, 175].

The wear mechanisms observed on the enamel surface were a combination of micro-chipping, fracture, and crushing of enamel rods, Figure 5.14 and 6.14. The surface features on the mixed-mode wear scar were in the scale range of the size of the enamel rods, confirming crushing and fracture of clusters of rods, Figure 8.3.

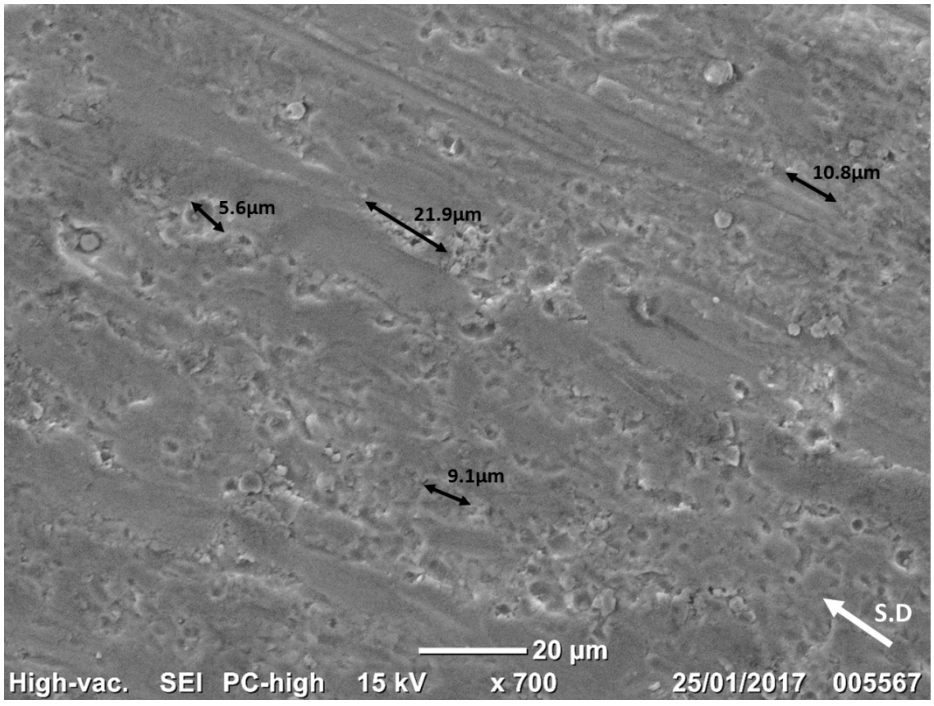

Figure 8.3: SEM of mixed mode wear scar on bovine enamel. The arrows show the size of the surface features.

A study carried out by Sharifi et al. [172] on Y-TZp dental restorative implant material using a polyethylene ball and coffee as the slurry, found embedment of alumina particles into the ball surface and reported the dominant mechanism to be 2-body grooving. What is surprising is that In the present study, there was no signs of wear on the nylon ball. A possible explanation for the observation of no wear on the nylon ball could be due to the abrasive particles being held in a two-body position under load and once the load is released, the particles have the ability to move.

Figure 6.18 – Figure 6.20 shows wear maps for enamel with the abrasive particles. These provide a good visual tool to compare the results in a qualitative manner [32]. The wear mechanism maps are a useful way to predict wear. One of the advantages of the wear maps is that there are no set guidelines for the factors that can affect the mechanistic wear changes [32].

The wear maps show the severity of contact decreases with increasing the wear rate. This can be due to transitions in wear regimes from two-body grooving to mixed mode. A reason for this occurrence has been described by Holmes et al. [32] who states the formation of tribofilms can result in a change of conditions at the interface. At the surface of the test specimen, the presence of abrasive particles can influence the interface. At higher loads, the concentration of the abrasive slurry reduces at the interface of the ball and the specimen and the presence of a tribofilm interface can act to protect the specimen surface [32]. In the present study, no signs of a tribofilm was evident.

A study carried out by Zhou et al. [159] on the friction and wear behaviour of enamel found that enamel showed better wear resistance and a lower coefficient of friction compared to dentine. The worn enamel appeared to have micorcracks in the worn region; there was also evidence of particle attachment to the enamel surface, which was reported to be a result of micro-cracking. Removal of the enamel, by crushing and chipping of the enamel rods was observed from the micro abrasion tests, Figure 6.8b and Figure 6.9. However, there were no visible cracks present in the present study. Indentation scratch tests carried out on bovine enamel saw the enamel displace at the edges of the wear scar by a brittle process. An interesting finding was that there was no signs of enamel pile up, Figure 4.11.

Zhou et al. [20] concluded that a micro fracture process produced wear on enamel. Wear resistance was also influenced by the position of the enamel rods and the different test locations. The friction and wear behaviour of enamel was reported by Zhou et al. [159] who found ploughing and delamination wear mechanisms for enamel wear. There was no signs of ploughing and wear delamination in the present tests.

A study carried out by Lucas et al. [263] used dust particles and enamel chip pieces on a nanoindenter to test the abrasivity resistance of enamel. The mechanical properties of enamel and the particle geometry of the enamel chips was crucial in dictating how much wear was achievable. Particles of a known morphology, hardness and composition were mounted on a nanoindenter tip. It was found that two actions could damage the enamel, that of rubbing and abrasion. It was found that elastic/ plastic chipping of enamel could also take place. No plastic deformation, plastic flow or slip lines were visible at the microscale level on enamel in the present study. The term prowing was used to describe a ridge formation after an indentation on enamel, with no material removal but rearrangement of the enamel surface. The prow mechanism was recognised as the rubbing action and no loss of material was observed with this action. In the enamel, surface depressions are formed both by abrasion and the rubbing mechanism. This is observed in Figure 4.11 where there is no material removal of enamel after nano-indentation scratch tests; however, the enamel has been displaced at the edges. There is evidence of chipping and fracture of the enamel rods from the SEM images Figure 5.2b and Figure 6.12b. Abrasive particles, which possess a high attack angle and have a high hardness can make strong contacts with enamel and result in material removal. Enamel is abrasion resistant due to its high hardness and its roughness, which protects it from particles which are softer [263].

Not all abrasive particles inflict wear on enamel; some particles lack the attack geometry and contact of enamel with these particles becomes a rubbing action, which just rearranges the enamel surface, however no material removal takes place. Eventually this rubbing action can lead to wear, however several contacts are required before the enamel cracks and tissue detaches and leads to wear. In the present study there was no evidence of enamel cracks, a reason for this could be the enamel surface has suppressed the cracks and the larger scale indenting could have taken over. After many loading cycles and indents, there is removal of enamel and breakup/ crushing of the enamel prism. The enamel prisms provides a source of toughness to the enamel. In wear papers, the structure of enamel is often not reported and this could be due to the material properties of enamel, such as the prism boundaries and the shape of the crystallites [263].

A study conducted by Holmes et al. [32] observed the two-body mechanism was the most dominant wear mechanism, which resulted in a higher degree of volume loss. This was not the case for the present tests, as it was shown that mixed-mode was the dominant wear mechanism and produced the most wear of enamel [32].

8.3.2 Friction

Chapter 7 discusses the coefficient of friction values obtained for the brushing tests on bovine enamel using four different slurries, namely containing, alumina particles, silica particles, spherical silica particles and a control saliva test. The morphology of the abrasive surface, geometric and load parameters, the area of the contact surfaces and the shape of the contact surfaces influence the coefficient of friction values. An increase in coefficient of friction which results in increased wear can be attributed to factors such as the roughness of two surfaces, the high sliding speeds and high loads. Microscopic irregularities are observed in all surfaces, even the enamel surface, regardless of a meticulous polishing procedure. The friction between two opposing surfaces is due to the interaction between the asperities of the two surfaces. A higher coefficient of friction is observed when there is a close contact between two surfaces with an aqueous slurry in-between. What is a surprising result is that the saliva control test generates the highest coefficient of friction. This could be due to a high friction between wet nylon and hydrated enamel, as compared to the friction between wet nylon and the particles.

An interesting aspect of a study conducted by Hiyasat et al. [257] found after the wear test on the enamel, there was some gold and grey patches visible. This finding was also noticed by a study conducted by Hacker et al. [240]. This finding can be linked to the present study and adhesive transfer of the nylon filaments to the enamel, resulting in a nylon- nylon contact for the control slurry group, hence this could be another explanation for the higher coefficient of friction, Table 7.4. Hacker et al. [240] found an adhesive wear mechanism was resulting in the gold adhering to the enamel [240, 257].

There was no measurable wear observed by the saliva tests, Figure 7.2. A reason for this could be that the saliva is resulting in abrasion resistance. A study conducted by Vieira et al. [264] reported that enamel left in artificial saliva had shown signs of reminselaistion and this improves the resistance of abrasion. Artificial saliva remineralisation of enamel can reduce the amount of enamel loss by 33% before any wear tests.

It has been reported that saliva reduced boundary friction. This was linked to the effect of the tooth's pellicle, which provided a lubrication effect and reduced the abrasion on the tooth surfaces. The tooth enamel absorbs the pellicle which results in enamel having an increased resilience and thus makes it difficult for toothpaste ingredients to remove the absorbed pellicle. The pellide provides the enamel with protective properties and protects it from damage from a highly abrasive toothpaste. However, one thing to note is if there is an increased force used during tooth brushing

or if there is an increase in brushing time, this can have an effect of complete removal of the pellide layer, removing its ability to provide protection to the enamel surface [265].

The coefficient of friction for enamel on enamel was found to be in the region of 0.4 ±0.3 [159]. In the present study the coefficient of enamel when subjected to abrasive slurries was in the region of 0.063 – 0.078. This coefficient was much lower than the coefficient reported with an enamel on enamel contact.

The high speed friction data showed the buckling effect of the filaments in one cycle. A change in friction force was observed with a change in filament direction, Figure 7.4.

To better represent the movement of the toothbrush the stroke data was used to interpret the high speed data, Figure 7.5. For the particle tests there was a visible loop at the end of the tests indicating the slurry feed end, whereas for the saliva control test there was no distinct loop. This could be due to the presence of no particles in the saliva control test. Another reason for the shape of the friction loops could be due to the movement of the toothbrush and the buckling of the filaments.

In the present study, the FFT graphs showed peaks at 100Hz and 200Hz, for all the tests, Figure 7.6. There were 25 tufts in contact with the enamel section at any given time with a reciprocating frequency of 4Hz. The higher magnitude of peaks for the particles tests is due to the filament and tuft interactions on the bovine surface with addition of particles. The saliva control test shows peaks at a noticeably lower magnitude, which could be due to the presence of no particles in the saliva slurry, Figure 7.6d.

8.3.3 Load

The Archard equation suggests a linear relationship between the wear rate and applied loads. However, this is not always the case as observed in chapter 6. From the results in chapter 6, Figure 6.5, it is seen that the wear rate decreases with an increase in load. This could be due to entrainment issues at higher loads with the abrasive particles. It also could be due to earlier wear mechanism transitions to the mixed-body state. A reduction in frequency in particle entrainment is observed when the high loads produce a pressure increase in the contact area. The enamel has a high hardness, and the particles could take potentially longer to entrain the enamel. The ball used was a nylon ball and Stack et al. [174] highlights the difficult in using a nylon ball; it does not always facilitate the entrainment of particles [150, 172, 174, 175]. All the factors which influence wear rate are not taken into account with the Archard equation.

As from chapter 6, it is observed that there was no direct increase with wear rate and applied load; this is linked to the entrainment of particles at higher loads [172, 175]. It has also been reported that after the ball rotates, once the sample is fully perforated, the wear rate increases rapidly and there is more material loss. Increased particle entrainment leads to full perforation, and the wear scars become more circular, smoother, deeper and uniform [172, 175].

Tribological factors can also influence tooth wear. It has been reported by Morozova et al. [4] that using high load and pressure whilst toothbrusing horizontally can cause wear of enamel. [4]. During toothbrusing, the force can vary from 1N to 11N. The amount of wear with manual toothbrushes is higher than electric toothbrushes, due to variability in the force applied [129]. Increasing the load on the filament results in a higher cleaning efficiency, due to an increase in load on the particles that are trapped in the filament tips [15].

It has been reported by Trezona et al. [149, 155] that when high concentration of abrasives are present in the slurry, the wear rate is independent of load. This trend is observed in the present study.

Many of the studies relating to enamel wear investigate the abrasion of enamel after erosive attack from dietary acids [40, 225, 264, 266, 267]. A study conducted by Hooper at al. 2003 [59] concluded that the wear of enamel by toothpaste over a lifetime of brushing is negligible. It was reported that the wear of enamel by toothpaste abrasion is enhanced when there is erosion by soft drinks. Acidic drinks before toothbrusing can result in softening of enamel [59].

A load of 5N was used for the brushing tests in the present study to achieve measurable wear, however it is recommended that a load of 1N – 2N load is sufficient and does not damage the tooth tissues, [264]. To achieve measurable wear and use a load near the normal brushing force, it may have been beneficial to undergo an erosive challenge on the enamel. This would have resulted in measurable wear [168].

On intact and sound enamel, there is no effect of toothbrush abrasion alone. This is observed in the current study; Figure 7.7d where there was no reported signs of wear with the toothbrush and saliva control slurry [268].

A study carried out by Hiyasat et al. [257] compared the wear of enamel when subjected to dental restorative materials. It was reported that during the initial stage of the wear test, the load is distributed over a small contact area, between the enamel and the opposing surface (nylon filaments) and results in a high coefficient of friction and wear rate. Over time, the contact region increases in area and the load is distributed over a large area, hence the steady wear rate of enamel

[256, 257]. As seen in Figure 7.3, the initial coefficient of friction is high and then plateaus off to a steady value.

8.3.4 Abrasive conditions

Controlling particle size is important in many applications. The size and shape of abrasive particles in dentifrices can influence properties such as flow and rheology, as well as have an effect on the other active ingredients in a dentifrice [133].

Dentifrice abrasiveness depends on three factors; particle hardness, particle size, and particle shape [81]. The loss of material has previously been strongly link to the hardness of the abrasive, however scientific studies also have reported the roughness of the contacting surfaces, the microstructure and environmental influences can also influence loss of material [269].

A study carried out by Wojda et al. [270] on human enamel exposed to composite filler materials, one containing spherical particles and the other containing angular particles found the spherical filler particles showed a reduced amount of enamel wear. It was assumed that the shape of the spherical particles was having this effect on the enamel surface. This is observed throughout the current study, where the spherical particle tests produce lower wear rates on enamel than the angular particle tests, Figure 5.1 [270].

A study conducted by Hilgenberg et al. [271] evaluated the effect of whitening toothpastes on the roughness of bovine enamel. It was found that toothpaste containing silica as the abrasive resulted in an increase in enamel roughness. This was related to the abrasive properties of silica. This is similar for the results in chapter 7, where the angular abrasives caused an increase in roughness for bovine enamel during the wear test, Table 7.3 [271].

One thing the abrasion studies on dental tissues fail to consider is the shape of the abrasive particles. The results from chapter 5 show that the shape, size and size distribution are important factors that need to be considered when selecting abrasive particles for toothpastes.

8.3.5 Filament conditions

Many conditions such as the load, brushing action and deflection of filaments dictate if and how the abrasive particles are trapped in the filaments. It was reported that a reciprocating motion produced more particle entrapment than a sliding brushing motion [102]. An explanation of this could be during reciprocating movements, particles are trapped in the filament tips and stay wedged in the filament tips. The only way to dislodge the particles is by increasing the frequency.

During a reciprocating movement of the brush, the stroke direction changes, from going forward to moving backwards. It was found by Lewis et al. [102] that particles were re-entrained in the filaments during a change in brush stroke direction [102]. This finding was confirmed in the present study.

When the particles are trapped between the filaments, they make contact with the bovine disc. This process takes place by the deflection of the filament. The particles that are loaded act by grooving and scratching the surface of the bovine disc. This is two-body abrasion. The results from the TE77 brushing tests show that 2-body grooving abrasion was observed on the bovine discs, Figure 7.7. Lewis et al. [6] found that not all the scratches produced on the counterface material were consistent. Some scratches varied in size; consisting of a few microns in length. An explanation for this is that a three body mode takes over and the particle is swept away in the three-body motion, or the neighbouring filaments allow the loaded filament to rest on them, relieving the load on the filament during the motion [213]. An interesting observation in the present study was that of truncated grooves, Figure 7.7a which indicate a particle has been released from the filaments mid-stroke.

The scratches observed during the TE77 tests were similar in width to the size of the particles and filament tip diameter, Table 7.5. It can be concluded that under loading, the front edge of the particle is chipping away the enamel surface. This can be explained by the connection in size and width of the grooves. A study carried out by Zhou et al. [158] found increasing the load on enamel, resulted in an increase in wear. This was due to the mechanical properties of enamel under load. At lower loads the favourable properties of enamel such as the high hardness and high mineral content result in a resistance to wear.

8.3.6 Stain removal

The first layer which is formed on the tooth is the pellicle layer which is 1 – 10µm in thickness. This layer is free from bacteria and is formed by proteins. The addition of biofilms and stain layers on the enamel surface could have an effect on the behaviour of the abrasive particles and the amount of enamel damage observed. The hardness of biofilm is in the region of 0.20 – 0.40 GPa [272]. It is much softer than enamel and does not require hard abrasive particles to be removed. However, if the stain is left to develop it may require a harder abrasive such as alumina and silica for removal [2].

A study carried out by Lewis and Dwyer-Joyce [7] developed a model to study stain removal. This model could be applied for different shaped particles; as in the present study. The particle design must not be overlooked and is an important factor to consider in material removal. This is an important factor to note in the present study, with two different morphologies of particles being used, spherical and angular, Figure 8.4 [7].

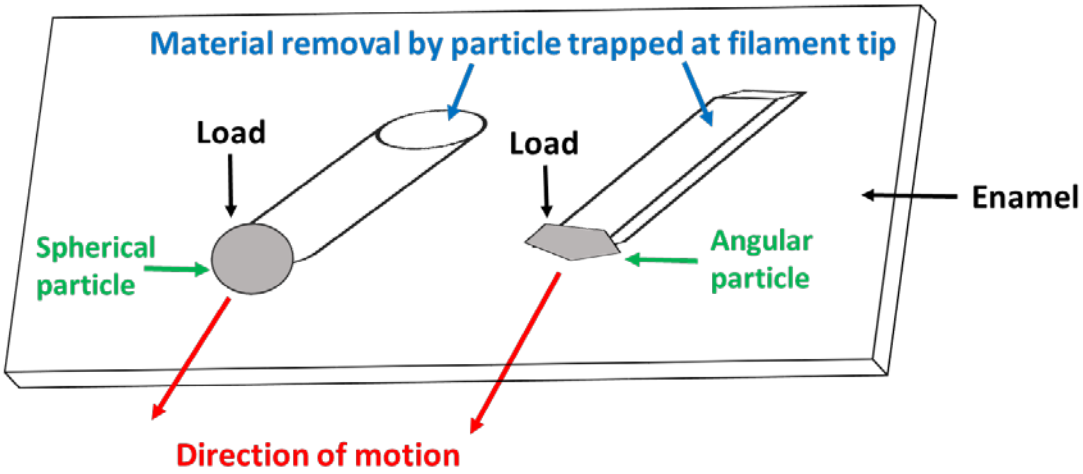

Figure 8.4: Material removal comparison by a spherical and angular particle.

A study carried out by Lewis and Dwyer-Joyce [7] developed a model to study stain removal. Two types of particles were used; silica and perlite. The silica particles differed in shape to the perlite particles, with the silica particles being granular in shape, whereas the perlite particles had a flat nature, with a thickness of ~2µm and widths ranging up to ~100µm. Tests were carried out with perlite particles, to observe how the shape of the particles and the wear results differed from the silica tests. The flat nature of the perlite particles resulted in the particles passing through the filament tip in a flat orientation, as compared to the silica particles which were seen to build up on the filament tips. No accumulation around the filaments was observed with the perlite particles and it was observed that the particles re-orientated before coming into contact with the filament. At low loads some silica particles were observed to pass through the contact. When comparing the ability for the largest particles to pass through the filament, the perlite particles were able to pass through the filament, whereas the silica particles deflected away from the top of the filament and were unable to pass through the filament tip. An increase in load resulted in the perlite particles not being able to enter the contacts and this was also observed for the silica tests. A possible reason for this could be due to the shape of the deflected filaments. Whereas at

lower loads the silica particles accumulated at the edge of the filament tip and contact area. It can be speculated in the current study, the angular particles are able to pass through the filament tip, whereas the spherical particles are deflected and are unable to pass through the contact efficiently resulting in less wear [7].

The behaviour of different shaped particles can be modelled to obtain stain removal values. In the case of the perlite particles, the flat nature of them can be modelled as flat discs or squares. Cutting can be assumed on one edge or corner of the shape. In the present study, the angular alumina and silica particles could be modelled as cubes and the spherical particles as spheres, thus making it easier to predict stain removal rates [7].

An interesting finding by Lewis and Dwyer-Joyce [7] reported that stain removal is possible at low loads. This is due to the trapping ability of particles at the filament tip contacts and the low deflection of the filaments which results in stain removal. When the load is increased, stain removal decreases due to the ability of less particles being trapped in the filament tips, due to the higher deflection of filaments under load. When the filaments are not under load, the particles accumulate around the filament tip. A greater amount of stain removal takes place when the load on the filament tip continues to increase. This results in more particles being able to accumulate around the filament tip, which results in more stain removal. This is due to a greater force on the stain layer by the particles accumulated around the tips. In the present study, the inclusion of stain could result in less damage on the enamel surface and less signs of grooving, chipping and fracture to the hydroxyapatite crystals due to the protection of enamel by the stain layer. However, continued brushing strokes and the continued increase of load on the filament tip could result in enamel removal and signs of enamel fracture and chipping, once the stain has been fully removed, Figure 8.5 [7].

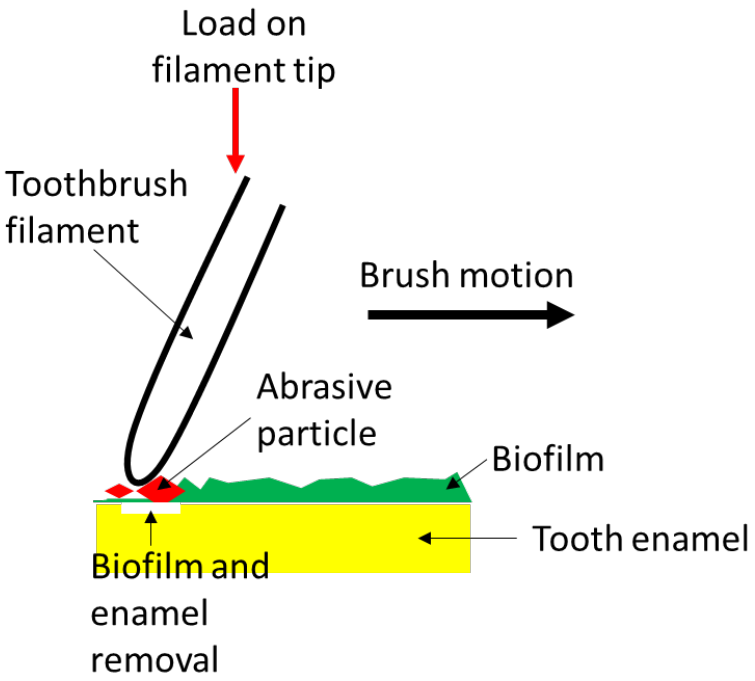

Figure 8.5: Biofilm and enamel removal during abrasive tooth cleaning.

8.3.7 Synergy evaluation

There have been no previous attempts in understanding synergy in oral tribology and many synergy studies are performed with cavitation erosion of engineering alloys. Synergy between toothbrusing and the use of abrasive slurries has not been reported in previous literature. Synergy can be described as the effect of two factors combined together will be greater than the sum of the separate individual factors [273].

From chapters 5 and 6, there was a 35-65% positive synergy with the alumina tests (Figure 6.17) as compared to as 25% - 60% synergy with the bimodal silica (Figure 6.18) tests. This explains there were other factors besides the size of the particles, which have an effect on the synergy. This could be factors such as the entrainment of particles, load per particle and the wear mechanisms such as the micro-chipping of enamel.

The positive synergy indicates that the bimodal particles give more wear than the mono-sized particles and an increased wear rate (Figure 6.17 and Figure 6.18). The consequence of using bimodal sized particles is that the two different sized particles have a higher particle diameter and thus damage the enamel surface more, due to the bigger average size of the particles. The effect of

grooving, chipping and fracture takes place, from crushed or densified enamel rods. This contributes to the positive synergy.

One possible explanation for the increase in synergy with load for silica (Figure 5.10) could be due to the change in particle entrainment with load. Another factor could be due to the mechanistic component of synergy. Rolling abrasion breaks up the enamel rods and results in indents. This results in sub-surface damage and densification of enamel rods. After a number of cycles, the enamel rods are crushed and after further loading cycles this leads to enamel loss enhanced by the micro-chipping and grooving processes.

A complex trend was observed for the alumina synergy, Figure 5.9. A reason for this could be the narrow size distribution of the alumina particles (Table 3.2).

9. Conclusions and future work

9.1 Introduction

This chapter overviews the main findings in relation to the aim of the PhD study and summarises the novelties and experimental/clinical conclusions from this study. At the end of the chapter, potential future work has been recommended.

This PhD was aimed at investigating and understanding the tribology behind the interface of the tooth and toothbrush lubricated by the toothpaste slurry. To understand the tribology, an extensive systematic and robust testing program was carried out on the TE66 micro-abrasion rig and the TE77 high frequency reciprocating tribometer. Comparing the TE66 micro-abrasion tests with the TE77 brushing tests enabled extensive analysis between the wear mechanisms and groove widths to be made, along with comparative analysis of the wear rates, volume loss and the surface properties of the enamel surface. This was also linked to microstructure/ micromechanical properties of enamel and compared with the appropriate two-body wear mechanism which is observed in the mouth. The aim of the research as mentioned in the introduction chapter was to understand the micro-structural changes and abrasivity resistance of enamel when subjected to abrasive slurries.

The first set of experiments carried out on the TE66 micro-abrasion rig aimed at understanding the effect of shape and size of particles on the volume loss of enamel. The second set of experiments on the TE66 micro-abrasion rig investigated the effect of load on the wear arte of enamel. The severity of contact was also used to quantify the damage on the bovine disc. For both sets of experiments, the groove width was investigated and related to the wear mechanisms observed on the enamel surface.

In addition to these experiments, to better simulate the toothbrusing conditions, experiments were conducted on the TE77 high frequency reciprocating tribometer using a novel toothbrush head design. Toothpaste particles provided by GSK, which consisted of alumina, silica and spherical silica were used for the tests. These tests enabled the exploration of the relationship between toothbrusing using abrasive particles and investigated the influence of friction, roughness, and wear of bovine enamel.

The main novelties of this study are:

1. This study has investigated the effect of bimodal sized slurry distributions with mono-sized slurry distributions.
2. This study has detailed synergistic effects of bimodal slurries vs. mono-size slurry distributions.
3. This study has evaluated in depth groove width analysis and understood the wear mechanisms occurring on enamel with extensive topography analysis.
4. This study has compared the difference in wear rate and cleaning ability of spherical silica particles, which GSK provided for extensive research.
5. This study has conducted detailed surface analysis, high speed friction analysis and FFT analysis on the abrasive particles in a tooth cleaning contact.
6. This study has investigated the shape, size and load effects of abrasive particles on the wear rate and volume loss of enamel.
7. This study has aimed to translate the similarities between the experimental results to clinical recommendations and acknowledge the conditions in the oral environment.

These findings have important implications for the development of a less abrasive dentifrice. Careful consideration should be taken when selecting an abrasive to ensure it causes minimal wear to teeth.

The main conclusions drawn from this study are summarised in the following section below.

9.2 Conclusions

The conclusions of this study are sectioned into three parts relating to the TE66 micro-abrasion tests, TE77 brushing tests and the clinical conclusions and their influence on the real life situation of tooth wear respectively. A critical review of the literature focusing on enamel wear showed that very few studies had looked at the wear of enamel when subjected to toothpaste abrasives. Different methods of quantifying wear of enamel included, using staining techniques, gravimetric analyses and material characterisation techniques such as using the SEM and optical microscope to analyse the enamel microstructurally [2, 163, 264] .

9.2.1 Micro-abrasion tests

- In the current research, it was concluded that mixed-mode wear was more severe than grooving. Mixed-mode wear generated a higher volume loss of enamel. It can therefore be concluded that, three-body rolling and mixed mode wear must be avoided in the brush/enamel contact due to the high wear rates generated.

- The particle size and distribution is a key factor in determining the volume loss of enamel. Smaller particles with narrow distributions reduce the volume loss of enamel.

- The grooving mechanism on the enamel surface is due to the abrasive particles embedded into the soft nylon ball, which result in grooves by a micro-chipping action.

- For rolling abrasion, indents are observed as a result of densification of the enamel tissue. After a number of loading cycles, this results in removal of enamel and crushing/breakup of the enamel prism surface. This is observed as indents on the enamel surface.

- The mixed- mode wear scar resulted in a damaged enamel surface with signs of crushing, fracture and chipping of the enamel rods, by a brittle mechanism. No signs of plastic deformation was observed.

- Load is an important variable affecting the load per particle, with higher loads per particle expected to result in greater wear, however in this test, increasing the load affected the entrainment of the larger particles resulting in a reduction in SWR.

- An increase in load resulted in a reduction of large particles being entrained in the contact and more smaller particles, with a high load per particle of the smaller particles, which resulted in a decrease in SWR with an increase in load.

- For the bimodal tests, mixed-mode wear was dominant. Bimodal tests generate high volume loss values of enamel confirming that it is ill-advised to use bimodal sized abrasive particles in toothpaste slurries. The combined effect of two sizes of particles produced a higher wear rate.

- There was a positive synergy for the alumina and silica tests, which indicates increased interaction between the bimodal sized particles compared to the mono-sized particles.

- The severity of contact is affected by the smallest particle size, which generates the highest severity of contact. Rolling abrasion generates the highest severity of contact, whereas grooving abrasion generates the lowest severity of contact.

- The most influential factor is the size and shape of the abrasive particles and these factors should be controlled when creating toothpaste slurries to control enamel wear.

9.2.2 Brushing tests

The results from the micro-abrasion tests helped reinforce and explain the results obtained from the TE77 brushing tests.

- Wear on enamel is caused by agglomerated particles on filaments and individual particles. Enamel removal is dominated by a micro-chipping action, where particles are embedded in the filament tips and groove the enamel.

- Coloured filaments at the sides of the toothbrush have different stiffness properties to the inner filaments, causing increased asymmetrical wear. Truncated grooves are formed by the contact zone of the stiff middle filaments and by particle release mid-stroke during the brushing cycle.

- A higher coefficient of friction for the saliva control test was observed due to a high friction between wet nylon and hydrated enamel. The FFT shows stick-slip of the tufts in contact with enamel.

- A complex filament movement in the stroke leads to asymmetric friction and wear evolution. Asymmetric friction loops show complex filament/ enamel interactions.

- GSK 6.5µm spherical silica is less damaging than GSK 8µm angular silica and produces a smoother surface (Ra- 0.28µm).

9.2.3 Recommendations

To translate the experimental findings into practical implications is a very important aspect. The following conclusions can be made:

- Use light forces, below 5N when tooth brushing.
- Avoid mixed-mode or 3-body abrasion.
- Avoid using particles >9µm in toothpaste.
- Avoid bimodal size distribution of abrasive particles in toothpastes.
- Controlled spherical silica in the size range of 5µm produces less abrasion than angular 5µm silica.
- Higher concentrations of abrasives in toothpaste result in more wear. Stay in the region of 0.1 v/v – 0.15 v/v volume fraction to avoid increased wear.
- Avoid using coloured filaments in toothbrushes as they change the properties such as the modulus of the filaments, which can influence wear. Consider applying a thin layer of a super hydrophobic coating on the toothbrush filaments to stop particle agglomeration.
- Coat filaments with a high surface energy coating to self-clean and stop partide agglomeration.
- Consider the use of dispersants in toothpaste to reduce wear, by inhibiting agglomeration of particles on the filaments.

9.3 Future work

The investigation into enamel wear is an ongoing challenge, both experimentally and at real scale in the mouth. As the demand for a pearly white smile increases and the amount of harsh abrasives used in toothpastes is at an all-time high, there exists a need for continual development of toothpastes that protect against enamel wear. Progress has been made in other oral fields investigating factors such as acid attack on enamel [169] and the discolouration and staining of enamel [2] however, the simplification of techniques and parameters used when studying the abrasivity of enamel currently limit the extent of knowledge.

9.3.1 Low load tests

A significant portion of this research was dedicated to understanding the effects of abrasive slurries on the wear of enamel. Due to the hard nature of enamel and the difficulty in achieving measurable wear, a load of 5N was used in the current study. This load is the maximum brushing load. Going forward, it would be interesting to study the effect of lower loads that are representative of the normal brushing load (1.5N – 2N). Lower loads will give a realistic result on the wear rate of enamel, as they are more representative of the normal brushing load used to brush teeth.

9.3.2 Brushing machine

A new eight-station brushing machine, developed by GSK and manufactured by Plint Tribology has been designed specifically for tooth brushing, Figure 10.1. Currently there has been research undertaken at the University of Southampton on the brushing machine to compare the effect of electric toothbrushes vs manual toothbrushes; however, these attempts have proven an ongoing challenge.

Further tests could be carried out on the brushing machine to better represent and provide a realistic model of the motion of tooth brushing in the mouth. This brushing machine could potentially allow a deeper understanding of the mechanisms occurring in the contact zone between the tooth, toothbrush and slurry.

These experiments can also be extended to look at the different brushing motions that are employed during toothbrusing. In the current study, the reciprocating motion was investigated. The machine has a range of different cams, which allow different motions from reciprocating, elliptical. orbital and circular motions. This could provide a realistic insight into tooth brushing habits and better simulate the tooth bushing actions and techniques.

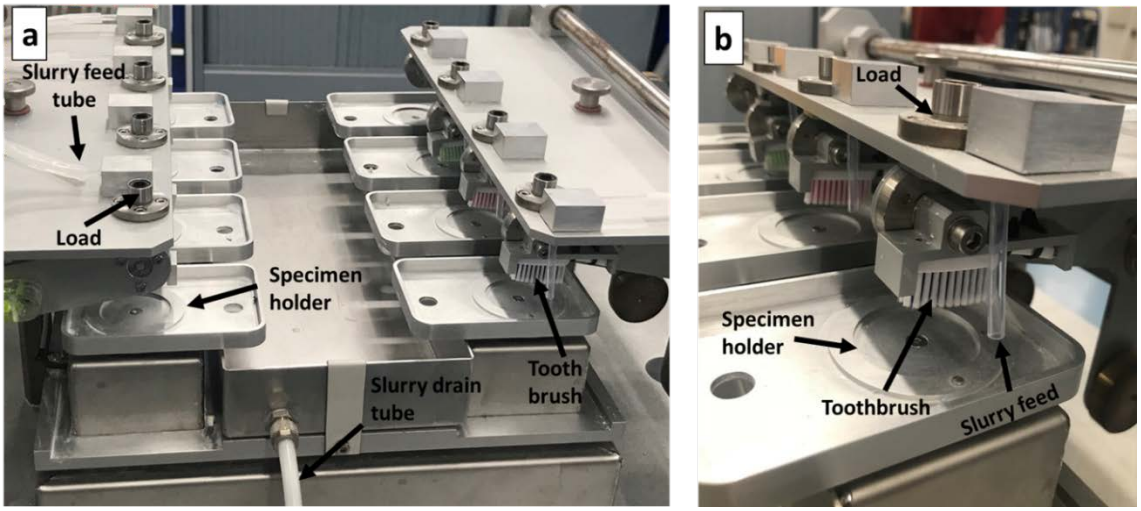

Figure 10.1: Eight-station brushing rig (a) eight-stations; (b) close up of stations.

9.3.3 Brush head design variation

There are many types of toothbrushes available on the market with different filament shapes and sizes. A range of commercially available toothbrushes with different filament designs (rippled, bi-level and zigzag) exist. To improve the wear results and thus improve brush selection, it would be beneficial to test a soft toothbrush type and a range of different brush heads; to observe if partides are delivered to a tooth surface differently with different head designs. Damage analysis such as fraying and wear of the filaments after the wear test would be interesting to see.

9.3.4 Filament deflection

To image filament deflection, high-speed camera videography and confocal imaging, to characterise the deflection and splay of filaments under a given load may be employed. Loads of 0.8N, 1.5N, 2.5N and 4.5N could be employed to the toothbrush head to examine the filament motions. This could have important implications for particle entrapment with consideration given to load.

9.3.5 Toothpaste formulation

More extensive experimental work may be carried out on toothpastes. Over the years, toothpastes have become more complex with a range and array of different ingredients used in the formulation. In order to thoroughly investigate the wear produced by toothpaste particles, a fully formulated toothpaste could be used in the tests. A fluorescent agent could be added to the abrasive toothpaste particles to make them more visible. Such information of toothpaste formulation may provide important indications to the performance of the paste, which can then be used to predict the amount of enamel wear.

9.3.6 Enamel microstructure

To complete this study further and analyse the microscopic changes to the enamel structure; analysis using a Transmission Electron Microscope (TEM) to examine the effect of abrasion on the structure of the hydroxyapatite crystals in enamel would be interesting. Scanning electron microscopy/Energy dispersive X-ray spectroscopy (SEM-EDS) to assess the damage caused to the surfaces of enamel and dentine during the abrasion process would be an insightful addition, as well as using a focused ion beam (FIB) to assess the cross section of enamel and observe surface degradation. The correlation between test parameters such as load employed during toothbrusing and the extent of sub-surface microstructural damage to enamel is yet to be established. This could provide a more in-depth understanding of the changes to the enamel surface under the abrasive wear regime.

As a final note, the next step for the subject as a continuation of the presented work will be to address these factors in the future work section.

References

1. Lewis, R. and R.S. Dwyer- Joyce, *Wear of Human Teeth: A Tribological Perspective.* Journal of Engineering Tribology, 2005. **219**(Part J): p. 1 - 18.
2. Joiner, A., *Review of the extrinsic stain removal and enamel/dentine abrasion by a calcium carbonate and perlite containing whitening toothpaste. .* International Dental Journal, 2006. **56**: p. 175- 180.
3. Maragliano-Muniz, P., *Protected by a safe RDA: Setting the record straight about toothpaste abrasivity*, in *The National Magazine for Dental Hygiene Professionals*. 2016, PennWell: USA.
4. Morozova, S.Y., et al., *Tooth wear-fundamental mechanisms and diagnosis.* Journal of Dental and Medical Sciences, 2016. **15**(5).
5. GSK, *Sensitivity and Acid Erosion - Spherical silica* GSK, Editor. 2016, GlaxoSmithKline: Weybridge, U.K.
6. Lewis, R. and R.S. Dwyer- Joyce, *Interactions Between Toothbrush and Toothpaste Particles During Simulated Abrasive Cleaning.* Journal of Engineering Tribology, 2006. **220**(8): p. 755 - 765.
7. Lewis, R., S.C. Barber, and R.S. Dwyer-Joyce, *Particle Motion and Stain Removal During Simulated Abrasive Tooth Cleaning.* Wear, 2007. **263**: p. 188 - 197.
8. Fonseca, R.B., et al., *Radiodensity and hardness of enamel and dentine of human and bovine teeth, varying bovine teeth age. .* Archives of Oral Biology, 2008. **53**(11): p. 1023-9.
9. Addy, M., *Oral hygiene products: potential for harm to oral and systemic health?* Periodontology 2000, 2008. **48**.
10. Zhou, Z.R. and J. Zheng, *Oral Tribology.* Oral Tribology, 2006.
11. Brand, R.W. and D.E. Isslehard, *Anatomy of orofacial structures*, Mosby, Editor. 2003, Mosby: U.S.A.
12. Longisland. *Basic tooth anatomy* 2015 [cited 2015 17th March]; Available from: http://www.longislandfamilydental.com/dental-health/basic-tooth-anatomy/
13. Spears, I.R., et al., *The effects of enamel anisotropy on the distribution of stress in a tooth.* Journal of Dental Research, 1993. **72**(11): p. 1526-31.
14. Boushell, L.W. and J.R. Sturdevant, *Clinical significance of dental anatomy, histology, physiology and occlusion*, ed. P. Dentistry. 2015.
15. Cuy, J.L., et al., *Nanoindentation Mapping of the Mechanical Properties of Human Molar Tooth Enamel.* Archives of Oral Biology, 2002. **47**: p. 281 - 291.
16. Roy, S. and B. Basu, *Mechanical and tribological characterisation of human tooth.* Materials Characterisation, 2008. **59**: p. 747 - 756.
17. Jeng, Y.R., et al., *Human enamel rod presents anisotropic nanotribological properties.* Journal of the Mechanical Behavior of Biomedical Materials, 2011. **4**(4): p. 515 -522.
18. Braly, A., et al., *The effect of prism orientation on the indentation testing of human molar enamel.* Archives of Oral Biology, 2007. **52**: p. 856- 60.
19. Habelitz, S., S.J. Marshall, and M. Balooch, *Mechanical properties of human dental enamel on the nanometre scale.* Archives of Oral Biology, 2001: p. 173 - 83.
20. Zhou, Z.R., et al., *Dental Biotribology*, ed. Springer. 2013, U.S.A: Springer.
21. Park, S., et al., *Mechancial properites of human enamel as a fucntion of age and location in the tooth.* Journal of Material Science: Materials in medicine, 2008. **19**(6): p. 2317 - 24
22. Murad, A., *Structures of enamel*
23. Hand, A.R. *Enamel structure, compostion and properties*. Pocket Dentistry 2015; Available from: http://pocketdentistry.com/contact/.
24. Weidmann, S.M., J.A. Weatherell, and S.M. Hamm, *Variations of enamel density in sections of human teeth.* Archives of Oral Biology, 1967. **12**(1): p. 85-97.

25. Braden, M., *Biophysics of the tooth.* Frontiers of oral physiology, 1976. **2**: p. 1 - 37.
26. Komabayashi, T., et al., *Dentin Tubule Numerical Density Variations Below The CEJ.* Journal of Dentistry, 2008. **36**(11): p. 953-958.
27. Fong, H., M. Sarikaya, and S.N. White, *Nano-mechanical properties profiles across dentin-enamel junction of human incisor teeth.* Material Science Engineering, 2000. **7**: p. 119-128.
28. Chun, K., H.H. Choi, and J.Y. Lee, *Comparison of mechanical property and role between enamel and dentin in the human teeth.* Journal of Dental Biomechanics, 2014. **5**.
29. Hannig, M. and C. Hannug, *Nanomaterials in Preventive Dentistry.* Nature Nanotechnology, 2010. **5**: p. 565 - 569.
30. Dreamstime. *Tooth isolated over white background.* 2000 [cited 2015 30th June]; Available from: http://www.dreamstime.com/royalty-free-stock-image-tooth-isolated-over-white-background-image29507356
31. Leung, V.W.-H. and B.W. Darvell, *Artifical Salivas For in vitro Studies of Dental Materials.* Journal of Dentistry, 1997. **25**(6): p. 475 - 484.
32. Holmes, D., S. Sharifi, and M.M. Stack, *Tribo-Corrosion of Steel in Artifical Saliva.* Tribology International, 2014. **75**: p. 80 - 86.
33. Lin, J., et al., *Influence of Fluoride-Containing Acidic Artficial Saliva on the Mechanical Properties of Nickel-Titanium Orthodontics Wire.* Indian Journal of Dental Research, 2012. **23**(5): p. 591 - 595.
34. Li, H. and Z.R. Zhou, *Wear Behaviour of Human Teeth in Dry and Artifical Saliva Conditions.* Wear, 2002. **249**: p. 980 - 984.
35. Vieira, A.C., et al., *Tribocorrosion Behaviour of Titanium in Artificial Saliva Solutions.* Metallurgy and Materials Engineering, 2004: p. 1 - 9.
36. Roberts, M.W. and T. Wright, *The Dynamic Process of Demineralization and Remineralization.* Dimensions of Dental Hygiene, 2009. **7**(7): p. 20 - 21.
37. Goldstep, F. *Dental Remineralisation: Simplified*. 2012 [cited 2015 18th March]; Available from: http://www.oralhealthgroup.com/news/dental-remineralization-simplified/1001903148/?&er=NA.
38. Ganss, C., *Definition of Erosion and Links to Tooth Wear.* Monographs in Oral Science, 2006. **20**: p. 9 - 16.
39. Finke, M., et al., *Mechanical properties of in situ demineralised human enamel measured by AFM nanoindentation.* Surface science, 2001. **491**(3): p. 546-467.
40. Attin, T., *Correlation of microhardness and wear in differently erorded bovine dental enamel.* Archives of Oral Biology, 1997. **42**(3).
41. Wongkhantee, S., et al., *Effect of Acidic Food and Drinks on Surface Hardness of Enamel, Dentine, and Tooth-Coloured Filling Materials.* Jounral of Dentistry, 2006. **34**: p. 214 - 220.
42. Foundation, D.H. *Tooth wear* 2016 [cited 2016 18?06/2016]; Available from: http://www.dentalhealth.ie/dentalhealth/causes/toothwear.html.
43. Huot, R.A. *Biofilms and Oral Health*. Threaths to dental health 2016 [cited 2016 18/06/2016]; Available from: http://www.colgate.com/en/us/oc/oral-health/basics/threats-to-dental-health/article/biofilms-and-oral-health-0516.
44. Pandula, V. *Abrasion of teeth*. 2008 [cited 2016 18/06/2016]; Available from: http://www.juniordentist.com/abrasion-of-teeth.html.
45. Rmaile, A., *Mechanical Properties and Disruption of Dental Biofilms*, in *Engineering and The Environment*. 2013, Southampton: Southampton.
46. Aspiras, M., et al., *Clinical Implications of Power Toothbrushing on Fluoride Delivery: Effects on Biofilm Plaque Metabolism and Physiology.* International Journal of Dentistry, 2010: p. 1 - 7.

47. Grippo, J.O., M. Simring, and T.A. Coleman, *Abfraction, Abrasion, Biocorrosion, and the Enigma of Noncarious Cervical Lesions: A 20 Year Perspective.* Journal of Esthetic and Restorative Dentistry, 2012. **24**(1): p. 10 - 23.
48. Balan, I.N., M. Shivakuman, and P.D. Madan Kumar, *Qualitative Assessment of Toothbrush Bristle End Morphology - A Light Microscopic Analysis.* International Journal of Pharmaceutical and Biological Research, 2012. **3**(2): p. 22 - 24.
49. Mead, A. *Plaque vs. "biofilm" and the research that could change dentistry as we know it*. 2011 [cited 2015 10th December]; Available from: http://meadfamilydental.com/2011/11/plaque-vs-biofilm-and-the-research-that-could-change-dentistry-as-we-know-it/
50. Hauser, D.B. *Wildomar Teeth Cleaning and Dental Cleaning*. 2013 [cited 2015 16 March]; Available from: http://lakefrontfamilydentistry.com/teeth-cleaning/dental-cleaning-wildomar-ca.
51. Rmaile, A., et al., *Microbial Tribology and Disruption of Dental Plaque Bacterial Biofilms.* Wear, 2013. **306**: p. 276 - 284.
52. White, D.J., *Processes contributing to the formation of dental calculus.* Biofouling, 1991. **4**(1-3): p. 209-218.
53. Katz, H. *Dental plaque* 1994 [cited 2015 16th March]; Available from: www.therabreath.com/dental-plaque.html.
54. Dimatteo, A. *Dental Plaque*. 2006 [cited 2015 16th March]; Available from: www.yourdentistryguide.com/plaque/.
55. Freidman, M. *What is tartar? 6 tips to control buildup*. 2014 [cited 2015 16th March]; Available from: http://www.webmd.com/oral-health/guide/tartar-dental-calculus-overview?page=2.
56. Allen, K.P. *Is there a home remedy for swollen gums?* 2015 [cited 2015 11th September]; Available from: https://health.howstuffworks.com/wellness/oral-care/products/home-remedy-for-swollen-gums.htm.
57. Jorgensen, G., *Do orthodontic braces cause white spots on teeth?* 2013: N.M.
58. Glazer. *Treating White Spots: New Caries Infiltration Technique*. 2009 [cited 2016 18th June]; Available from: http://www.dentistrytoday.com/restorative/minimally-invasive-dentistry/1492.
59. Hooper, S., et al., *Investigation of Erosion and Abrasion on Enamel and Dentine: A Model In Situ Using Toothpastes of Different Abrasivity.* Journal of Clinical Periodontology, 2003. **30**: p. 802 - 808.
60. Oliveira, M.S., et al., *Evaluation of Different Methods for Removing Oral Biofilm in Patients Admitted to the Intensive Care Unit.* Journal of International Oral Health, 2014. **6**(3): p. 61-64.
61. Jahn, C., *Biofilm removal* ed. PennWell:Oklahoma. 2009.
62. Bainbridge, J. *Sector Insight: Oral healthcare*. 2011 [cited 2015 28th June]; Available from: http://www.marketingmagazine.co.uk/article/1068895/sector-insight-oral-healthcare.
63. Stack, M.M., *Tribology Matters.* UK Power and Process Engineering, 2009(1): p. 33.
64. Williamson, M. *Toothpaste Abrasiveness Ranked by RDA (Relative Dentin Abrasion) Value*. 2015 [cited 2015 21st April]; Available from: https://www.williamsonperio.com/wp-content/uploads/2014/07/Toothpaste-Abrasiveness-Ranked-by-RDA.pdf.
65. Dawson, P.L., et al., *Dental Stain Prevention by Abrasive Toothpastes: A New in vitro Test and its Correlation With Clinical Observations.* Journal of Cosmetic Science, 1998. **49**: p. 275 - 283.
66. Axelsson, P. and J. Lindhe, *Effect of controlled oral hygiene procedures on caries and periodontal disease in adults.* Journal of Clinical Periodontology, 1978. **5**(2): p. 133 - 151

67. Boyd, S. *Receding Gums Causes, Symptoms, Treatment and Prevention*. 2011 [cited 2015 17th March]; Available from: http://ultrablubrush.com/receding-gums-causes-symptoms-treatment.
68. Drescher, S. *Gum Problem Basics: Sore, Swollen, and Bleeding Gums. Oral Health 2013* 2013; Available from: http://www.webmd.com/oral-health/guide/gum-problem-basics-sore-swollen-and-bleeding-gums.
69. Colgate, P. *History of toothbrushes and toothpastes*. 2006 [cited 2015 20th March]; Available from: http://www.colgate.com/app/CP/US/EN/OC/Information/Articles/Oral-and-Dental-Health-Basics/Oral-Hygiene/Brushing-and-Flossing/article/History-of-Toothbrushes-and-Toothpastes.cvsp.
70. Darby, M.L. and M.M. Walsh, *Dental Hygiene Theory and Practice*. Fourth ed, ed. D.M. Bowen. 2014: Elsevier Saunders. 1192.
71. McCauley, H.B., *Toothbrushes, Toothbrush Materials and Design.* The Journal of American Dental Association, 1946. **33**(5): p. 283 - 293.
72. Dupont, *Filament Performance in Brushes*. 1802: USA.
73. Oral, B. *Choosing a good toothrbush*. 2016 [cited 2016 18th June].
74. Lucio, R. *What are toothbrush bristles made of?* 1999 [cited 2015 2nd March]; Available from: http://www.ehow.com/facts_4914951_what-toothbrush-bristles-made.html.
75. Phaneuf, E.A., et al., *Automatic Toothbrush: A New Reciprocating Action.* The Journal of the American Dental Association, 1962. **65**: p. 12 - 25.
76. Dyer, D., M. Addy, and R.G. Newcombe, *Studies in vitro of Abrasion by Different Manual Toothbrush Heads and a Standard Toothpaste.* Journal of Clinical Periodontology, 2000. **27**: p. 99 - 103.
77. Absi, E.G., M. Addy, and D. Adams, *Dentine Hypersensitivity: Uptake of Toothpastes Onto Dentine and Effects of Brushing, Washing and Dietary Acids.* Journal of Oral Rehabilitation, 1995. **22**: p. 175 - 82.
78. Meyers, I.A., et al., *The Surface Effect of Dentifrices.* Australian Dental Journal, 2000. **45**(2): p. 118 - 124.
79. Standardisation, I.O.f., *Dentistry - Dentifrices - Requirements, Test Methods and Marking*. 2010. p. 1 - 19.
80. Johannsen, G., et al., *The Importance of Measuring Toothpaste Abrasivity in Both Quantitative and Qualitative Way.* Acta Odontologica Scandinavica, 2013. **71**: p. 508 - 517.
81. Ashcroft, A.T. and A. Joiner, *Tooth Cleaning and Tooth Wear: A Review.* Journal of Engineering Tribology, 2010. **224**(Part J): p. 539 - 549.
82. Board, N., *Modern Technology of Cosmetics*, ed. A.P.B. Press. 2004, India.
83. Laboratory, N.P., *Dentistry — Dentifrices —Requirements, test methods and marking (ISO 11609:2010)*, in *11609: 2010*. 2010, NPLA: UK.
84. Liljeborg, A., G. Tellefsen, and G. Johannsen, *The Use of A Profilometer For Both Quantitative and Qualitative Measuements For Toothpaste Abrasivity.* International Journal of Dental Hygiene, 2010. **8**: p. 237 - 243.
85. Dorfer, C.E., et al., *Methods to Determine Dentifrice Abrasiveness.* The Journal of Clinical Dentistry, 2010. **21**: p. 1 - 16.
86. Marya, C.M., *A Textbook of Public Health Dentistry*. First Edition ed. 2011, India: Jaypee Brothers Medical Publishers.
87. SCCS, *Opinion on triclosan: Antimicrobial Resistance*. 2010, Directorate- General for Health and Consumers: Brussels.
88. Pader, M., *Rheological Properties of Cosmetics and Toiletries*. Cosmetic Science and Technology, ed. D. Laba. Vol. 13. 1993, New Jersey.
89. Barel, A.O., M. Paye, and H.I. Maibach, *Handbook of cosmetic science and technology*, ed. C. press. 2009.
90. Barron, A.R., *Viscosity. Science and Technology* 2014.

91. Brookfield. *Toothpaste*. 1993 [cited 2015 13th February]; Available from: www.brookfieldengineering.com/education/applications/texture-toothpaste-firmness.asp.
92. Hunter, M.L., et al., *The Role of Toothpastes and Toothbrushes in the Aetiology of Tooth Wear.* International Dental Journal, 2002. **52**: p. 399 - 405.
93. Voronets, J., et al., *Controlled toothbrush abrasion of softened human enamel.* Caries Research, 2008. **42**(4).
94. Turssi, C.P., et al., *An in situ Investigation into the Abrasion of Eroded Dental HARD tissues by a Whitening Dentifrice.* Caries Research, 2004. **38**: p. 473 - 477.
95. Kitchin, P.C. and H.B.G. Robinson, *How Abrasive Need a Toothpaste Be?* Journal of Dental Research, 1948. **27**: p. 501 - 506.
96. Stookey, G.K., T.A. Burkhard, and B.R. Schemehorn, *In Vitro Removal of Stain With Dentifrices.* Journal of Dental Research, 1982. **61**: p. 1236 - 1239.
97. Lamb, D.J., R.A. Howell, and G. Constable, *Removal of Plaque and Stain from Natural Teeth by a Low Abrasivity Toothpaste.* British Dental Journal, 1984. **157**: p. 125 - 127.
98. Bjorn, H. and J. Lindhe, *Abrasion of Dentine by Toothbrush and Dentifrice.* Odontologisk Revy, 1966. **17**(1): p. 17 - 27.
99. Darvell, B.W., *Materials Science for Dentistry*. Ninth ed. 2009, Cambridge: Woodhead Publishing in Materials.
100. Engineering, I. *Bonded Abrasives Information*. 1999 [cited 2015 30th June].
101. Anusavice, K.J., C. Shen, and R.H. Rawls, *Phillips Science of Dental Materials*, K.J. Anusavice, Editor. 2013, Elsevier Saunders.
102. Lewis, R., R.S. Dwyer-Joyce, and M.J. Pickles, *Interaction Between Toothbrushes and Toothpaste Abrasive Particles in Simulated Tooth Cleaning.* Wear, 2004. **257**: p. 368 - 376.
103. Harte, D.B. and R.S. Manly, *Four Variables Affecting Magnitude of Dentifrice Abrasiveness.* Journal of Dental Research, 1976. **55**: p. 323 - 327.
104. Koenigs, P.M. and R.V. Faller, *Fundamentals of Dentifrice: Oral Health Benefits in a Tube*, in *Continuing Dental Education*. 2013, Dentalcare: US.
105. Lussi, A. and C. Ganss, *Erosive Tooth Wear. From Diagnosis to Therapy*. Vol. 25. 2014, Germany: Karger.
106. Ferreira, M.C., et al., *Effect of Toothpastes with Different Abrasives on Eroded Human Enamel: An in situ/ex vivo Study.* The Open Dentistry Journal, 2013. **7**: p. 132 - 139.
107. Sasan, D., et al., *Toothbrush selection: A Dilemma?* Indian Journal of Dental Research, 2006. **17**(4): p. 167 - 170.
108. Harrington, J.H. and I.A. Terry, *Automatic and Handbrushing Abrasion Studies.* Journal of American Dental Association, 1964. **68**: p. 43-50.
109. Addy, M., *Tooth Brushing, Tooth Wear and Dentine Hypersensitivity - Are They Associated?* Journal of the Irish Dental Association, 2006. **51**(5): p. 226 -231.
110. Weigand, A., et al., *Impact of Toothpaste Slurry Abrasivity and Toothbrush Filament Stiffness on Abrasion of Eroded Enamel - An In Vitro Study.* Acta Odontologica Scandinavica, 2008. **66**(4): p. 231 - 235.
111. Addy, M. and M.L. Hunter, *Can tooth brushing damage your health? Effects on oral and dental tissues.* International Dental Journal, 2003. **53**(3): p. 177 - 186.
112. Manly, R.S., *Factors Influencing Tests on the Abrasion of Dentin by Brushing with Dentifrices.* Journal of Dental Research, 1944. **23**: p. 59 - 72.
113. Moore, C. and M. Addy, *Wear of Dentine in vitro by Toothpaste Abrasives and Detergents Alone and Combined.* Journal of Clinical Periodontology, 2005. **32**: p. 1242 - 1246.
114. Kumar, S., et al., *Comparision of Surface Abrasion Produced by Bristle Designs: A Profilometric in vitro Study.* Journal of Conservative Dentistry, 2014. **17**(4): p. 369 - 373.
115. Norris, T. *Is It Better to Use an Electric or a Manual Toothbrush?* Electric vs. manual toothbrush 2018 [cited 2018 30/12]; Available from:

https://www.healthline.com/health/dental-and-oral-health/electric-toothbrush-vs-manual#manual-cons.
116. Grover, D., et al., *Toothbrush 'A key to mechanical plaque control'.* Indian Journal of Dental Research, 2012. **3**(2): p. 62-68.
117. Ganss, C., et al., *Effects of Toothbrushing on Eroded Dentine.* European Journal of Oral Sciences, 2007. **115**: p. 390 - 396.
118. Scherge, M., et al., *Dental Tribology at the Microscale.* Wear, 2013. **297**: p. 1040 - 1044.
119. Niemi, M.L., J. Ainamo, and H. Etemadzadeht, *Gingival Abrasion and Plaque Removal with Manual Vs Electric Toothbrushing.* Journal of Clinical Periodontology, 1986. **13**: p. 709 - 714.
120. Asadoorian, J., *CDHA Position Paper on Tooth Brushing.* Canadian Journal of Dental Hygiene, 2006. **40**(5): p. 1 - 14.
121. Breitenmoser, J., W. Mormann, and H.R. Muhlemann, *Damaging Effects of Toothbrush Bristle End Form on Gingiva.* Journal of Periodontology, 1979. **50**(4): p. 212 - 216.
122. Alexander, J.F., A.J. Saffir, and W. Gold, *The measurement of effect of toothbrush on soft tissue abrasion.* Journal of Dental Research, 1977. **56**.
123. Bass, C.C., *An Effective Method of Personal Oral Hygiene.* Journal of Louisiana State Medical Society, 1954. **106**(2): p. 57 - 73.
124. Checchi, L., et al., *Toothbrush Filaments End - Rounding: Stereomicroscope Analysis.* Journal of Clinical Periodontology, 2001. **28**: p. 360 - 364.
125. Bartlett, D.W. and P. Shah, *A Critical Review of Non-Carious Cervical (Wear) Lesions and the Role of Abfraction, Erosion, and Abrasion.* Journal of Dental Research, 2006. **85**(4): p. 306 - 312.
126. Mannerberg, F., *Appreariacne of tooth surface as observed in shadowed replcias in various age groups, in long-term studies, after tooth-brushing, in cases of erosion and after exposure to citrus fruit juice. .* Odontologisk Revy, 1960. **11**: p. 70-86.
127. Lewis, R. and R.S. Dwyer- Joyce, *Interactions Between Toothbrush and Toothpaste Particles During Simulated Abrasive Cleaning.* Journal of Engineering Tribology, 2006. **220**: p. 755 - 765.
128. Armin, S. and E.M. Blackburn, *Dentifrice Abrasion. Report of a case.* Journal of Periodontology, 1961. **32**: p. 43 - 48.
129. Sehmi, H. and R.C. Olley, *The effect of toothbrush abrasion force on dentine hypersensitibity in-vitro.* Journal of Dentistry, 2015. **43**.
130. Padbury, A. and M. Ash, *Abrasion caused by three methods of toothbrushing.* Journal of Periodontology, 1974. **45**(6): p. 434-438.
131. Khocht, A. and P. Person, *Gingival recession in relation to history of hard toothbrush use.* Journal of Periodontology, 1993. **64**(9): p. 900-905.
132. van der Weijden, G.A., et al., *High and Low Brushing Force in Relation to Efficacy and Gingival Abrasion.* Journal of Clinical Periodontology, 2004. **31**: p. 620 -624.
133. Mair, L.H., *Wear in Dentistry- Current Terminology.* Journal of Dentistry, 1992. **20**: p. 140 - 144.
134. Rosema, N.A.M., et al., *Plaque-Removing Efficacy of New and Used Manual Toothbrushes - A Professional Brushing Study.* International Journal of Dental Hygiene, 2013. **11**: p. 237 - 243.
135. Lemesos, P.E. *Tooth abrasion and erosion*. 2007 [cited 2015 18th July]; Available from: http://www.lemesosdental.com/dental-advice/tooth-abrasion-&-erosion/en/6. .
136. Chang, P.P. *Gingival (gum) recession*. 2015 [cited 2015 23rd January]; Available from: http://www.mckinneyperioimplant.com/gingival-gum-related/gingival-gum-recession/.
137. Ozgoz, M., et al., *Relationship between Handedness and Toothbrush-Related Cervical Dental Abrasion in Left and Right Handed Individuals.* Journal of Dental Sciences, 2010. **5**: p. 177 - 182.

138. Zhong-Rong, Z., et al., *Dental Biotribology*. 2013, China: Springer.
139. Grippo, J.O., M. Simring, and S. Schreiner, *Attrition, Abrasion, Corrosion and Abfraction Revisited: A New Perspective on Tooth Surface Lesions.* The Journal of American Dental Association, 2004. **135**: p. 1109 - 1118.
140. Mair, L.H., et al., *Wear: Mechanicms, Manifestations and Measurement. Report of a Workshop.* Journal of Dentistry, 1996. **24**: p. 141 - 148.
141. Harsha, A.P. and U.S. Tewari, *Two-body and three-body abrasive wear behaviour of polyaryletherketone composites.* Polymer testing, 2003. **22**(4): p. 403-418.
142. Challen, J.M. and P.L.B. Oxley, *Plastic deformation of a metal surface in sliding contact with a hard wedge: Its relation to friction and wear.* Proceedings of the Royal Society of London, 1984. **394**: p. 161 -181.
143. Kovarikova, I., et al., *Study and Characteristic of Abrasive Wear Mechanisms.* 2009.
144. Kato, K. and K. Adachi, *Wear Mechanisms* 2001: CRC press.
145. Kovalchenko, A.M. and Y.V. Milman, *On the cracks self-healing mechanism at ductile mode cutting of silicon.* Tribology International, 2014. **80**: p. 166 -171.
146. Mair, L.H., *Effect of Surface Conditioning on the Abrasion Rate of Dental Composites.* Journal of Dentistry, 1991. **19**: p. 100 - 106.
147. Pena, A., et al., *Micro-Abrasion Study of Some Dental Restorative Materials and Enamel.* Journal of Engineering Tribology, 2013. **227**(5): p. 486 - 495.
148. Adachi, K. and I.M. Hutchings, *Wear mode mapping for the micro-scale abrasion test.* Wear, 2003. **255**.
149. Trezona, R.I. and I.M. Hutchings, *Three body abrasive wear testing of soft materials.* Wear, 1999. **233-235**.
150. Gee, M.G.e.a., *Progress towards standardisation of ball cratering.* Wear, 2003. **255**: p. 1-13.
151. Bello, J.O. and R.J.K. Wood, *Micro-abrasion of filled and unfilled polyamide 11 coatings.* Wear, 2005. **258**.
152. Bose, K. and R.J.K. Wood, *Influence of load and speed on rolling micro-abrasion of CVD diamond and other hard coatings.* Wear, 2003. **12**.
153. Hayes, A., S. Sharifi, and M.M. Stack, *Micro-abrasion-corrosion Maps of 316L stainless steel in artifical saliva.* Journal of Bio Tribo Corrosion, 2015. **1**(15).
154. Cozza, R.C., D. Tanaka, K, and R.M. Souza, *Micro-abrasive wear of DC and pulsed DC titanium nitride thin films with different levels of film residual stresses.* Surface and Coatings Technology, 2006. **201**.
155. Trezona, R.I., D.N. Allsop, and I.M. Hutchings, *Transitions between two-body and three-body abrasive wear: influence of test conditions in the microsclae abrasive wear test.* Wear, 1999. **225-29**.
156. Wharton, J.A., P.E. Sinnett-Jones, and R.J.K. Wood, *Micro-abrasion-corrosion of a CoCrMo alloy in simlated artifical hip joint environements.* Wear, 2005. **259**: p. 898-909.
157. Williams, J.A. and A.M. Hyncica, *Abrasiev wear in lubricated contacts.* Journal of Physics, 1992. **25**: p. A81-A90.
158. Zheng, J. and Z. Z.R, *Friction and Wear Behavior of Human Teeth Under Various Wear Conditions.* Tribology International, 2007. **40**: p. 278 - 284.
159. Zheng, J., et al., *On the Friction and Wear Behaviour of Human Tooth Enamel and Dentin.* Wear, 2003. **255**: p. 967 - 974.
160. Fusayama, T., T. Katayori, and S. Nomoto, *Corrosion of gold and amalgam placed in contact with each other.* Journal of Dental Research, 1963. **42**: p. 1183 - 1197.
161. Joiner, A., et al., *The Measurement of Enamel and Dentine Abrasion by Tooth Whitening Products Using an in situ Model.* International Dental Journal, 2005. **55**: p. 194 - 196.
162. Zimmer, S., et al., *Evaluation of Dentin Abrasion During Professional Tooth Cleaning in an in Vitro Model.* Journal of Clinical Periodontology, 2005. **32**: p. 947 - 950.

163. Kaidonis, J.A., et al., *Wear of Human Enamel: A Quantitative in vitro Assessment.* Journal of Dental Research, 1998. **77**(12): p. 1983 - 1990.
164. Eisenburger, M. and M. Addy, *Erosion and Attrition of human Enamel in vitro Part I: Interaction Effects.* Journal of Dentistry, 2002. **30**: p. 341 - 347.
165. Eisenburger, M. and M. Addy, *Erosion and Attrition of Human Enamel in vitro Part II: Influence of Time and Loading.* Journal of Dentistry, 2002. **30**: p. 349 - 352.
166. Condon, J.R. and J.L. Ferracane, *Evaluation of Composite Wear With A New Multi-Mode Oral Wear Simulator.* Dental Materials, 1996. **12**: p. 218 - 226.
167. Torres, C.P., et al., *Surface and Subsurface Erosion of Primary Enamel by Acid Beverages over Time.* Brazilian Dental Journal, 2010. **21**(4): p. 337 - 345.
168. Hemingway, C.A., et al., *Erosion of enamel by non-carbonated soft drinks with and without toothbrushing abrasion.* British Dental Journal, 2006. **201**(7).
169. Wiegand, A., L. Kowing, and T. Attin, *Impact of Brushing Force on Abrasion of Acid-Softened and Sound Enamel.* Archives of Oral Biology, 2007. **52**: p. 1043 - 1047.
170. Lorne, P. *How to avoid Tooth Erosion so Teeth Can Stay Strong and be Sensitivity-free!* Dental Tips 2016 [cited 2018 30th January]; Available from: https://www.lorneparkdental.com/site/practice/5627.
171. Bello, J.O., R.J.K. Wood, and J.A. Wharton, *Synergistic effects of micro-abrasion-corrosion of UNS S30403 S31603 and S32760 stainless steels.* Wear, 2007. **263**.
172. Sharifi, S., et al., *Micro-Abrasion of Y-TZP in Tea.* Wear, 2013. **297**: p. 713 - 721.
173. Andrade, M.F.C., et al., *Influence of the abrasive particles size in the micro- abrasion wear tests of TiAlSiN thin coatings.* Wear, 2008. **12**(114).
174. Stack, M.M., et al., *Some views on the construction of bio-tribo-corrosion maps for titanium alloys in Hank's solution: particle concentration and applied loads effects.* Tribology International, 2011. **44**.
175. Sharifi, S. and M.M. Stack, *A comparison of the tribologival behaviour of Y-TZP in tea and coffee under micro-abrasion conditions.* Journal of Applied Physics, 2013. **46**.
176. Shipway, P.H. and L. Howell, *Microsclae abrasion-corrosion behaviour of WC-Co hardmetals and HVOF sprayed coatings.* Wear, 2005. **258**(1-4).
177. Buchanaan, F.J. and P.H. Shipway, *Micro-abrasion- a simple method to asses surface degradation of UHMPE follwoing sterlization and ageing.* Biomaterials, 2002. **23**.
178. Gant, A.J. and M.J. Gee, *A review of micro-scale abrasion testing.* Journal of Physics, 2011. **44**.
179. Walsh, P.J., C.A. Mitchell, and F.J. Buchanaan, *Wear Evaluation of Dental Restorative Composites*, in *7th world biomaterials congress*. 2004.
180. Kelly, D.A. and I.M. Hutchings, *A new method for measurement of particle abrasivity.* Wear, 2001. **250**(1-12).
181. Shipway, P.H., *The role of test conditions on the microabrasive wear behaviour of soda-lime glass.* Wear, 1999. **233**.
182. Elmer, P., *Nylon 6 – Influence of Water on Mechanical Properties and Tg*, in *Thermal Analysis*. 2007, Perkin Elmer precisely USA. p. 2.
183. Chan, D.C., *The effect of microabrasion on resrotative materials and tooth surface.* Operative dentistry, 1996. **21**(2): p. 63 - 8.
184. Antunes, P.V. and A. Ramalho, *Study of Abrasive Resistance of Composites for Dental Restoration by Ball Cratering.* Wear, 2003. **255**: p. 990 - 998.
185. Manly, R.S., et al., *A Method for Measuremnt of Abrasion of Dentin by Toothbrush and Dentifrice.* Journal of Dental Research, 1965. **44**: p. 533 - 540.
186. Burgett, F.G. and M.M. Ash, *Comparative Study of the Pressure of Brushing with Three Types of Toothbrushes.* Journal of Periodontology, 1974. **45**(6): p. 410 - 413.
187. Plint, T., *TE77 High frequency friction machine*, P.T. Phoenix, Editor. 2017: United Kingdom.

188. Popa, M., et al., *A tribological approach to understand the behaviour of oral-care silica during tooth brushing.* Biotribology, 2016. **6**.
189. Wang, C., et al., *An in vitro screen assay for dental stain cleaning.* BioMed Central Oral Health, 2017. **17**(37): p. 1-10
190. Jardret, V., et al., *Understanding and quantification of elastic and plastic deformation during a scratch test.* Wear, 1998. **218**: p. 8-14.
191. Karacaoglu, F., N.Y. Tuzcel, and M. Akkaya, *A Comperative Evaluation of 3 Different Polishing Methods on Tooth Surface Roughness.* Journal of Biomedical Sciences, 2016. **6**(1).
192. de Melo, T.A.F., et al., *Are bovine teeth a suitable substitute for human teeth in in vitro studies to assess endotoxin load in root canals?* Microbiology, 2015. **29**.
193. Tanaka, K., Y. Uchiyama, and S. Toyooka, *The mechanism of wear of PTFE.* Wear, 1973. **23**.
194. Laurance-Young, P., et al., *A Review of the Structure of Human and Bovine Dental Hard Tissues and their Physicochemical Behaviour in Relation to Erosive Challenge and Remineralisation.* Journal of Dentistry, 2011. **39**: p. 266 - 272.
195. Costa, L.A., *Evaluation of pH, ultimate tensile strength and micro-shear bond strength of two self-adhesive resin cements.* Brazilian Dental Journal, 2014. **28**(1).
196. Rossi-Fedele, G. and A.P. Roberts, *A preliminary study investigation the survival of tetracycline resistant Enteroccoccis faecalis after root canal irrigation with high concentration of tetracycline.* International Endodontic Journal, 2007. **10**: p. 772 - 7.
197. Friroozmand, L.M., J.V. Brandao, and M.P. Fialho, *Influence of Microhybrid Resin and Etching Times on Bleached Enamel for the Bonding of Ceramic Brackets.* Brazilian Dental Journal, 2013. **27**.
198. Fonseca, R.B., et al., *Radiodensity of Enamel and Dentin of Human, Bovine and Swine Teeth.* Archives of Oral Biology, 2004. **49**: p. 919 - 922.
199. Camargo, C.H., et al., *Topographical, diametral, and quantitative analysis of dentine tubules in the root canals of human and bovine teeth.* Journal of Endodontics 2007. **334**: p. 422-6.
200. Tanaka, J.L.O., et al., *Comparative Analysis of Human and Bovine Teeth: Radiographic Density.* Brazilian Dental Journal, 2007. **22**(4): p. 346 - 51.
201. Yassen, G.H., J.A. Platt, and A.T. Hara, *Bovine Teeth as Substitue for Human Teeth in Dental Research: A Review of Literature.* Journal of Oral Science, 2011. **53**(3): p. 273 - 282.
202. Lopes, F.M., et al., *Swine teeth as potential substitues for in vitro studies in tooth adhesion: a SEM observation.* Archives of Oral Biology, 2006. **51**: p. 548-551.
203. Arends, J., et al., *Remineralisation of bovine dentine in vitro. The influence od the F content in solution on mineral distriution.* Caries Research, 1989. **23**: p. 309 - 314.
204. Davidson, C.L., G. Boom, and J. Arends, *Calcium distribution in human and bovine surface enamel.* Caries Research, 1973. **7**: p. 349-359.
205. Tanaka, J.L.O., et al., *Comparative Analysis of Human and Bovine Teeth: Radiographic Density.* Brazilian Oral Research, 2008. **22**(4): p. 346 - 351.
206. Rios, D., et al., *Effect of salivary stimulation on erosion of human and bovine enamel subjected or not to subsequent abrasion: an in situ/ex vivo study.* Caries Research, 2006. **40**.
207. Attin, T., et al., *The potential of deciduous and permanent bovine enamel as substitute for deciduous and permanent human enamel: erosion-abrasion experiments.* Jounral of Dentistry, 2007. **35**.
208. Wegehaupt, F., et al., *Is bovine dentine an appropriate substitute for human dentine in erosion/abrasion tests?* Journal of Oral Rehabilitation, 2008. **35**.
209. Wegehaupt, F.J., R. Widmer, and T. Attin, *Is bovine dentine an appropriate substitute in abrasion studies?* Clinical oral investigation, 2010. **14**.
210. Planinsic, G., *Explore your Toothpaste. Physics Education.* 41, 2006. **4**: p. 6.

211. Adachi, K. and I.M. Hutchings, *Sensitiviy of wear rates in the micro-scale abrasion test to test conditions and material hardness.* Wear, 2005. **258**.
212. Gee, M.G.e.a., et al., *Results from an interlaboratory excerise to validate the micro-scale abrasion test.* Wear, 2005. **259**(1-6).
213. Licausi, M.P., I.A. Munoz, and A.V. Borras, *Tribocorrosion Mechanisms of Ti6Al4V Biomedical Alloys in Artificial Saliva with Different pHs.* Journal of Physics, 2013. **46**: p. 1 - 10.
214. Meyer, J.M., et al., *Corrosion studies on nickel-based casting alloys* American Society for Testing and Materials, 1979. **684**: p. 295-315.
215. Struers, E.C. *About grinding and polishing*. 2016 [cited 2016 20th June].
216. Micrometrics. *Saturn DigiSizer II*. 1996 [cited 2015 23rd January]; Available from: http://www.micromeritics.com/Product-Showcase/Saturn-DigiSizer-II.aspx.
217. Imaging, A. *InfiniteFocus for Form and Roughness Measurement*. 2000 [cited 2015 5th May]; Available from: http://www.alicona.co.uk/home/products/infinitefocus.html.
218. Starink, M.J. and S.C. Wang, *Scanning Electron Microscopy in Chapter 4, Microstructural characterisation course notes.*, U.o. Southampton, Editor. 2008: U.K.
219. Organisation, I.S., *Ultra surface finish parameters*, in *Filters and additional features*. 2015, Taylor Hobson UK.
220. Jameson, M.W., J.A. Hood, and B.G. Tidmarsh, *The effects of dehydration and rehydration on some mechanical properties of human dentine.* Journal of Biomechanics, 1993. **26**(9): p. 1055-65.
221. Service, L.O. *Wild M420 Makroskop*. 2015 [cited 2015 5th May]; Available from: http://scopeoptic.biz/wild-m420-makroskop/.
222. Toolbox, E. *Eulers column formula*. 2012 [cited 2016 15th June]; Available from: https://www.engineeringtoolbox.com/euler-column-formula-d_1813.html
223. Huber. *Speciality Silicas Zeodent 113 Precipitated Silica*. 2011 [cited 2015 22 January]; Available from: http://www.hubermaterials.com/userfiles/files/productfinder/spec/Zeodent%20113%20Precipitated%20Silica.pdf.
224. Drisko, C., R. Henderson, and J. Yancy, *A review of current toothbrush bristle endo-rounding studies.* Compend Contin Education Dentistry, 1995. **16**(7): p. 694 - 696.
225. Ranjitkar, S., et al., *The Effect of Casein Phosphopeptide- Amorphous Calcium Phosphate on Erosive Enamel and Dentine Wear by Toothbrush Abrasion.* Journal of Dentistry, 2009. **37**: p. 250 -254.
226. Shipway, P.H., *A Mechanical model for particle motion in the micro-scale abrasion test.* Wear, 2004. **257**.
227. Technologies, P. *Alumina Polishing Abrasives.* 2006 [cited 2015 23rd January]; Available from: http://www.metallographic.com/Brochures/alumina2.pdf
228. Craig, R.G. and F.A. Peyton, *The Microhardness of Enamel and Dentin.* Journal of Dental Research, 1957. **37**(4): p. 661 - 668.
229. AzoM. *Silica- Silicon Dioxide*. Azo Materials 2001 [cited 2018 17th March]; Available from: https://www.azom.com/article.aspx?ArticleID=1114.
230. AzoM. *Alumina - Aluminium oxide*. Azo Materials 2001 [cited 2018 17th March]; Available from: https://www.azom.com/properties.aspx?ArticleID=52.
231. Speerschneider, C.J. and C.H. Li, *The Role of Filler Geometrical Shape in Wear and Friction of Filled PTFE.* Wear, 1962. **392**.
232. Bai, L., et al., *Influence of third particle on the tribological behaviours of diamond-like carbon films.* Scientific reports, 2016.
233. Luo, D.B., V. Fridrici, and P. Kapsa, *Relationships between the fretting wear behaviour and the ball cratering resistance of solid lubricant coatings.* Surface and Coatings Technology, 2010. **204**: p. 1259 - 1269.

234. da Silva, W.M., R. Binder, and J.D.B. de Mello, *Abrasive wear of steam-treated sintered iron.* Wear, 2005. **258**.
235. Katra, I. and Y. Hezi, *Intensity and degree of segregation in bimodal and multimodal grain size distributions.* Aeolian Research, 2017. **27**: p. 23-34.
236. Gava, G.H.S., et al., *Effect of load partition and particle distribution on micro-abrasive wear mapping of two-phase metal matrix composites.* Wear, 2013. **301**.
237. Stack, M.M. and M. Mathew, *Micro-abrasion transitions of metallic materials.* Wear, 2003. **255**.
238. Klauer, K., et al., *Applciation of functio-oriented roughness parameters using confocal microscopyq.* Engineering Science and Technology, an Internation Journal, 2018. **21**: p. 302 - 313.
239. Xu, H.H.K., et al., *Indentation Damage and Mechanical Propeties of Human Enamel and Dentin.* Journal of Dental Research, 1998. **77**(3): p. 472 - 480.
240. Hacker, C.H., W.C. Wagner, and M.E. Razoog, *An invitro investigation of the wear of enamel on porcelain and gold in silva.* Journal of Prosthetic Dentistry, 1996. **72**.
241. Bely, V., et al., *Friction and wear in polymer-based materials.* Oxford: Pergamon Press, 1982: p. 416.
242. Myshkin, N.K., M. Petrokovets, and A.V. Kovalev, *Tribology of polymers: Adhesion, friction, wear and mass transfer.* Tribology International, 2005. **38**: p. 910 - 921.
243. Fitch, J.C., R. Scott, and L. Leugner, *The practical handbook of machinery lubrication.* 2012.
244. Tung, S.C. and H. Gao, *Tribological characteristics and surface interaction between poston ring coatings and a blend of energy conserving oils and ethanol fuels.* Wear, 2003. **255**(7 - 12): p. 1276 - 1285.
245. Mann, D.J., L. Zhong, and W.L. Hase, *Effect of Surface Stiffness on the Friction of Sliding Model Hydroxylated a-Alumina Surfaces.* Journal of Physics, 2001. **B**(105).
246. Bowden, F.P. and D. Tabor, *Friction and Lubrication of solids.* Oxford: Clarendon press, 1964.
247. Coronado, J.J., *Effect of Abrasive Size on Wear.* Abrasion Resistance of Materials, 2012.
248. Milka, P.C., et al., *Wear perfomrance of alumina-based ceramics - a revierw of the infleunce of microstructure on erosive wear.* Ceramica, 2015. **61**.
249. Kumar, S. and K. Panneerselvam, *Two-body Abrasive Wear Behaviour of Nylon 6 and Glass Fiber Reinforced (GFR) Nylon 6 Composite.* Procedia Technology, 2016. **25**: p. 1129 - 1136.
250. Ghazal, M., et al., *Two-body wear of resin and ceramic denture teeth in comparison to human enamel.* Dental Materials, 2008. **24**.
251. Lambrechts, P., et al., *Qusntitative in vivo Wear of Human Enamel.* Journal of Dental Research, 1989. **68**(12): p. 1752 - 1754.
252. Kim, M.J., et al., *Wear evaluation of the human enamel opposing differnt Y-TZP dental ceramics and other porcelains.* Journal of Dentistry, 2012. **40**.
253. Seghi, R.R., S.F. Rosenstiel, and P. Bauer, *Abrasion of human enamel by differnet dental ceramics in vitro.* Journal of dental research, 1991. **70**.
254. Ghazal, M. and M. Kern, *The influence of antagonistic surface roughness on the wear of human enamel and nono-filled compoisit resin artifical teeth.* Journal of Prosthetic Dentistry, 2009. **101**.
255. Magne, P., et al., *Wear of enamel and veneering ceramics after laboratory and chairside finishing procedures.* Journal of Prosthetic Dentistry, 1999. **82**: p. 669-79.
256. Delong, R., M.R. Pintado, and W.H. Douglas, *The wear of enamel opposing shaded ceramic restorative materials: an in vitro study.* Journal of Prosthetic Dentistry, 1992. **68**.
257. Hiyasat, A.A.S., et al., *Investigation of human enamel wear against four dental ceramics and gold.* Journal of Dentistry, 1998. **26**: p. 487-495.
258. Eichhold, W.A. and D.T. Brown, *Wear rates of various artifical tooth materials: a literture review.* Compend Contin Education Dentistry, 1996. **17**: p. 1074-8.

259. Mondelli, R.F.L., et al., *Wear and surface roughness of bovine enamel submitted to bleaching.* The European journal of estetic dentistry, 2009. **4**(4).
260. Isaacs, R.L., et al., *Maintenance of tooth colour after prophylaxis: compasion of three dentifrices.* Journal of Clinical Dentistry, 2001: p. 51-55.
261. Slop, D., J.F. de Rooij, and J. Arends, *Abrasion of enamel: An in vitro investigation.* Caries Research, 1983. **17**: p. 242-248.
262. Rios, D., et al., *Influence of toothbrushing on enamel softening and abrasive wear of eroded bovine enamel: an in situ study.* Brazilian Dental Journal, 2006. **20**(2): p. 148-54.
263. Lucas, P.W., et al., *Mechanisms and causes of wear in tooth enamel: implications for hominin diets.* Journal of the Royal Society Interface, 2012. **10**.
264. vieira, A.C., et al., *Toothbrush abrasion, simulated tongue friction and attrition of eroded bovine enamel in vitro.* Journal of Dentistry, 2006. **34**.
265. Joiner, A., et al., *The Protective Nature of Pellicle Towards Toothpaste Abrasion on Enamel and Dentine.* Journal of Dentistry, 2008. **36**: p. 360 - 368.
266. Davis, W.B. and P.J. Winter, *The Effect of Abrasion on Enamel and Dentine after Exposure to Dietray Acid.* British Dental Journal, 1980. **148**: p. 253 - 256.
267. Vieira, A.C., et al., *Influence of pH and Corrosion Inhibitors on the Tribocorrosion of Titanium in Artifical Saliva.* Wear, 2006. **261**: p. 994 - 1001.
268. Wiegand, A., et al., *Abrasion of Eroded Dentin Caused by Toothpaste Slurries of Different Abrasivity and Toothbrushes of Different Filament Diameter.* Journal of Dentistry, 2009. **37**(6): p. 480 - 484.
269. Won-suck, O., R. Delong, and J.A. LKenneth, *Factors affecting enamel and ceramic wear: A literature review.* The Journal of prosthetic dentisrty 2002. **87**: p. 451-9.
270. Wojda, S., B. Szoka, and E. Sajewicz, *Tribological characteristics of enamel-dental material contacts investigated in vitro.* Acta of Bioengineering and Biomechanics, 2015. **17**(1).
271. Hilgenberg, S.P., et al., *Physical-chemical Characteristics of Whitening Toothpaste and Evaluation of its Effects on Enamel Roughness.* Brazilian Oral Research, 2011. **25**(4): p. 288 - 294.
272. White, D.J. and K.M. Kozak, *The Pellic Cleaning Ratio Effects of Multibenefit Dentifrices.* International Association for Dental Research, 2002. **4044**: p. 1- 2.
273. Investopedia. *Synergy*. 2018 [cited 2018 03.07.18]; Available from: https://www.investopedia.com/terms/s/synergy.asp#.
274. Jongsma, M.A., et al., *Synergy of brushing mode and antibacterial use on in vivo biofilm formation.* Journal of Dentistry, 2015. **43**.

Appendix

Paper plan

Paper 1:

Title: Wear of enamel during simulated tooth brushing using alumina and silica abrasive slurries

Journal: Wear, pending submission (2018)

Abstract

Toothpastes contain abrasive particles that have the potential to affect tooth enamel, resulting in wear. The aim of this study is to compare the abrasivity of alumina and silica particles in a brushing simulation experiment using a TE77 reciprocating tribometer and to identify the wear mechanisms resulting in removal of enamel. A Talysurf profilometer was used to record the sample topography to enable wear depth comparisons. Post-test scanning electron microscopy (SEM) was used to characterise the wear processes on the enamel surface. Results revealed that both the friction during brushing and the wear rate was higher with alumina particles. A grooving mechanism was identified which resulted in an overall roughening effect of the enamel and a change of profile. The grooving is as a result of a 2-body mechanism where particles are attached and agglomerated at the end of the filament and dragged across the enamel surface.

Paper 2:

Title: The effect of micro-abrasion on enamel using abrasive slurries

Journal: Biotribology, pending submission (2018)

Abstract

Objectives

Wear of enamel during tooth brushing is a complex phenomenon with many variables affecting the level of loss. Toothpastes contain abrasive particles that have the potential to harm the tooth enamel resulting in wear. Toothpastes contain particles in the size range of 4µm - 12µm. Previous studies have found the abrasive wear rate of enamel to be low in the region of 0.0935mm^3/mN using a saliva-SiC slurry. The objective of the current work is to develop an understanding of the magnitude and mechanisms of wear caused by two, three and mixed- mode abrasion using the Plint TE66 micro-abrasion rig and to investigate the effect of size/ combination of sizes and morphology of abrasive particles on the wear rate and mechanisms of enamel tissue.

Methods

Micro-abrasion testing using a Nylon ball, to simulate the toothbrush, was undertaken on hydrated bovine enamel discs using a range of slurry concentrations (5– 20% volume fraction). The slurries consisted of either angular mono-sized silica and alumina abrasive particles or bimodal particles in artificial saliva. Testing was undertaken at loads of 0.1N, 0.2N and 0.5N. The specific wear co-efficient and volume loss are interpreted using severity of contact (S_c) of enamel. Scanning electron microscope (SEM) and surface profilometry was used to determine the wear mechanisms.

Results

At each volume fraction, the bimodal particle tests produced higher wear rates and enamel loss. This could be explained by a change is wear mechanism from grooving to mixed-mode abrasion. Near scar analysis shows an increase in particles causes an increase in groove width. The volume loss of enamel per particle for 9µm alumina (AL_2O_3) was 5x more than 5µm alumina. Mixed- mode abrasion dominated the wear rate for the mono-sized particle tests. The increase in severity of contact (S_c) is associated with reducing the abrasive size. The smallest abrasive particles were the AL_2O_3 particles thus showed the highest severity of contact. The bimodal tests produced larger groove widths for the mixed-mode mechanism compared to 2-body grooving alone due to an increase in particle size.

Conclusions

The 9µm mono-sized particles are more damaging than the small 5µm particles. Grooving abrasion is caused by angular particles micro-chipping the enamel surface. Bimodal particle tests showed the highest wear rate. This is due to the wear mechanism being mixed-mode. Mixed- mode abrasion is caused by a combination of angular particles micro-chipping and fracturing the enamel rods which is causing enamel damage and removal.

Paper 3:

Title: Characterising wear on enamel during simulated tooth brushing using abrasive slurries

Journal: Surface Topography: Metrology and properties

Purpose

The data presented in this paper will focus on characterising wear on the enamel surface using surface profilometry methods and the SEM. The enamel surface will be assessed for damage and the morphology and groove analysis will be studied in detail.